

Transcriptional and post- transcriptional gene regulatory mechanisms in the malaria parasite, *Plasmodium falciparum*

by

Henriëtte Renèe Hobbs

23065215

Submitted in partial fulfilment of the requirements for the degree
Magister Scientiae in the

Department of Biochemistry
Faculty of Natural and Agricultural Sciences
University of Pretoria

March 2010



DECLARATION:

I, **Henriëtte René Hobbs**, declare that this thesis/dissertation, which I hereby submit for the degree *Magister Scientiae* at the University of Pretoria, is my own work and has not previously been submitted by me for a degree at this or any other tertiary institution.

Signature: _____

Date: _____



PLAGIARISM DECLARATION:

UNIVERSITY OF PRETORIA
FACULTY OF NATURAL AND AGRICULTURAL SCIENCES
DEPARTMENT OF BIOCHEMISTRY

Full name: Henriëtte Reneé Hobbs

Student number: 23065215

Title of the work: Transcriptional and post-transcriptional gene regulatory mechanisms of the malaria parasite, *Plasmodium falciparum*.

Declaration

1. I understand what plagiarism entails and am aware of the University's policy in this regard.
2. I declare that this dissertation is my own, original work. Where someone else's work was used (whether from a printed source, the internet or any other source) due acknowledgement was given and reference was made according to departmental requirements.
3. I did not make use of another student's previous work and submit it as my own.
4. I did not allow and will not allow anyone to copy my work with the intention of presenting it as his or her own work.

Signature _____

Date _____



ACKNOWLEDGEMENTS

It is my greatest pleasure to thank those who helped make this dissertation possible.

This dissertation would not have been possible without the loving grace, blessings and courage from God, which enabled me to accomplish the seemingly impossible.

I would like to give the sincerest thanks to my supervisor and co-supervisors for their encouragement, guidance, invaluable advice and support:

To Dr. Lyn-Marie Birkholtz, thank you for your kind and encouraging support throughout my post-graduate studies and for your invaluable assistance as this dissertation evolved.

To Prof. Heinrich Hoppe, I will be forever grateful for your assistance, suggestions and guidance but most of all, thank you for your enthusiastic spirit.

To Prof. Abraham Louw, thank you for your advice and valuable input.

Thank you to the South African Malaria Initiative (SAMI) for funding this project and blessing me with a generous bursary.

Lastly, I offer my regards and blessings to everyone who supported me during the completion of this degree. To my family and friends, thank you for your moral support and kind advice.



TABLE OF CONTENTS

Acknowledgements	i
Table of Contents	ii
Abbreviations.....	vi
List of Tables	xi
List of Figures.....	xii
Summary	1

CHAPTER 1

LITERATURE OVERVIEW

1.1	Introduction	2
1.2	<i>P. falciparum</i> biology.....	6
1.3	General gene regulation.....	8
1.3.1	Transcriptional regulation	8
1.3.2	Post-transcriptional regulation	10
1.3.2.1	<i>mRNA decay</i>	11
1.3.2.2	<i>RNA silencing</i>	13
1.3.3	Translational regulation	16
1.3.4	Epigenetic regulation	17
1.4	Gene regulation in <i>Plasmodia</i>	18
1.4.1	Transcriptional regulation	18
1.4.1.1	<i>Trans-acting regulatory elements</i>	21
1.4.1.2	<i>Cis-regulatory motifs</i>	22
1.4.1.3	<i>Promoters</i>	24
1.4.2	Post-transcriptional regulation	25
1.4.2.1	<i>mRNA decay</i>	25
1.4.2.2	<i>RNA silencing</i>	25
1.4.3	Translational regulation	26
1.4.4	Epigenetic regulation	27
1.4.4.1	<i>Chromatin modification</i>	28
1.4.4.2	<i>Recombination</i>	30
1.4.4.3	<i>Telomere specific silencing</i>	30
1.4.4.4	<i>Heterochromatin gene movement</i>	31
1.4.4.5	<i>Intron interactions</i>	33
1.5	Objectives.....	34



CHAPTER 2

IDENTIFICATION OF *P. FALCIPARUM* NUCLEAR PROTEINS AS REGULATORY TRANSCRIPTION FACTORS

2.1	INTRODUCTION.....	35
2.1.1	<i>var</i> gene regulatory sequences	37
2.1.2	DNA-protein interactions	38
2.2	MATERIALS AND METHODS.....	40
2.2.1	<i>Cis</i> -regulatory elements containing the conserved motifs	40
2.2.2	<i>P. falciparum</i> cell culture	41
2.2.3	Nuclear extraction from cell culture.....	42
2.2.3.1	Nuclear protein extraction (Voss <i>et al</i> , 2003).....	42
2.2.3.2	Commercial protein extraction protocols	43
2.2.3.3	Measurement of protein yield	44
2.2.3.4	SDS-PAGE analysis of nuclear proteins.....	45
2.2.4	Electrophoretic Mobility Shift Assays (EMSA's).....	46
2.2.4.1	Preparation of ³² P-labelled double-stranded motifs	47
2.2.4.2	³² P-based EMSA's.....	48
2.2.4.3	Optimization strategies for ³² P-EMSA	49
2.2.4.3.1	<i>Effectors</i>	49
2.2.4.3.2	<i>Protein origins</i>	49
2.2.4.3.3	<i>EMSA with additional positive controls</i>	50
2.2.4.4	³² P-EMSA of single-stranded oligonucleotides	50
2.3	RESULTS.....	53
2.3.1	<i>P. falciparum</i> cell culture	53
2.3.2	Protein isolation and characterisation.....	53
2.3.3	³² P-EMSA	56
2.3.3.1	Design and labelling of <i>cis</i> -regulatory elements containing the conserved motifs	56
2.3.3.2	Isotopic labelling of oligonucleotides containing the <i>cis</i> -regulatory motifs.....	57
2.3.3.3	³² P-EMSA with positive controls to verify conditions	58
2.3.3.4	Binding reaction and electrophoresis with ³² P-labelled motifs	59



2.3.3.5	³² P-EMSA optimizations	62
2.3.3.5.1	<i>³²P-EMSA with stage-specific nuclear extracts</i>	62
2.3.3.5.2	<i>³²P-EMSA with addition of ATP</i>	64
2.3.3.6	EMSA of single-stranded ³² P-labelled motifs.....	65
2.3.3.6.1	<i>EMSA of single-stranded ³²P-labelled motifs with nuclear extract in either the presence or absence of ATP.....</i>	65
2.3.3.6.2	<i>EMSA of single-stranded ³²P-labelled motifs with specific- and non-specific single-stranded competitors</i>	69
2.4	DISCUSSION	75

CHAPTER 3

RNA INTERFERENCE OF SAMDC/ODC AND SPERMIDINE SYNTHASE

3.1	INTRODUCTION	82
3.1.1	Polyamines.....	82
3.1.2	Polyamine knock-down strategies	84
3.1.2.1	RNA interference	85
3.1.3	Semi-quantitative Real-Time PCR (semi-qPCR).....	86
3.2	METHOD AND MATERIALS	87
3.2.1	Design of RNA interference primers	90
3.2.2	Amplification and purification of genes.....	90
3.2.3	Double-stranded RNA synthesis and purification	91
3.2.4	RNA interference on <i>P. falciparum</i> genes	92
3.2.4.1	Electroporation	92
3.2.4.2	RNA isolation.....	93
3.2.4.2.1	<i>Total RNA isolation using Qiagen kits and Tri reagent..</i>	<i>94</i>
3.2.4.2.2	<i>Total RNA isolation MagMax-96 total RNA isolation kit.....</i>	<i>95</i>
3.2.4.3	Real-Time PCR monitoring of transcript levels.....	96
3.2.4.3.1	<i>cDNA synthesis</i>	<i>96</i>
3.2.4.3.2	<i>Real-Time PCR</i>	<i>96</i>
3.3	RESULTS.....	98



3.3.1	Double-stranded RNA design and synthesis	98
3.3.2	Double-stranded RNA synthesis and purification	102
3.3.3	RNA interference on <i>P. falciparum</i> genes	104
3.3.3.1	Morphology study	104
3.3.4	Semi-qPCR	108
3.3.4.1	Semi-qPCR data	109
3.4	DISCUSSION	117
 <u>CHAPTER 4</u> CONCLUDING DISCUSSION 		
4.1	CONCLUDING CHAPTER	125
	LIST OF REFERENCES	127



Abbreviations:

Accase	Acetyl-CoA carboxylase
ADAR	Adenosine deaminase acting on RNA
AdoDATO	S-adenosyl-1,8-diamino-3-thiooctane
AdoMetDC	S-Adenosylmethionine decarboxylase
ApiAP2	Apicomplexan AP-2 transcription factor
APS	Ammonium persulphate
ARE	AU-rich element
ATP	Adenosine-5'-triphosphate
bp	Base pair
bc1 complex	Cytochrome c oxidoreductase
BRE	TFIIB Recognition Elements
C _q	Threshold cycle
CBP (80, 20)	Cap-binding protein
Ccr4p	Carbon catabolite repression 4
CD36	Cluster determinant 36
CPE	Chromosome-central var gene promoter element
CSA	Chondroitin sulphate A
ddd	Double distilled de-ionized
DDX6	DEAD box polypeptide 6
DFMO	α-difluoromethylornithine
DHFR	Dihydrofolate reductase
DHODH	Dihydro-orotate dehydrogenase
DHPS	Dihydropteroate synthase
DNA	Deoxyribonucleic acid
DNase	Deoxyribonuclease
dNTP (N = A/G/C/T)	Deoxynucleotide triphosphate
DOZI	Development of zygote inhibited - an RNA helicase
DP	DNA-protein complex
DPE	Downstream Promoter Element
DTT	Dithiothreitol
E. coli SSB	<i>E. coli</i> Single-stranded DNA binding protein
E2F	E2 transcription factor

EDTA	Ethylenediaminetetraacetic acid
EGTA	Ethylene glycol-bis-(2-aminoethyl)-N,N,N', N'-tetraacetic acid
eIF	eukaryotic Initiation Factor
eIF4G	eukaryotic Initiation Factor 4G
EMSA	Electrophoretic mobility shift assay
FRET	Foster Resonance Energy Transfer
G-box	<i>Cis</i> -acting DNA regulatory element
GDP	Guanosine diphosphate
GTP	Guanosine-5'-triphosphate
H (3, 4, etc)	Histone (3, 4, etc)
HEPES	4-(2-Hydroxyethyl)piperazine-1-ethanesulfonic acid
HIV	Human Immunodeficiency Virus
h.p.i	Hours post invasion
ICAM	Intercellular adhesion molecule
IDC	Intraerythrocytic developmental cycle
INR	Initiator
iRBC	Infected red blood cell
IRES	Internal ribosome entry sequence
Ka	Association constant/rate
Kd	Dissociation constant/rate
LDH	Lactate dehydrogenase
LNA	Locked nucleic acid
MADIBA	MicroArray Data Interface for Biological Annotation
MCBG	Molecular and Cellular Biology Group
Met-tRNA	Methionine loaded tRNA
MGBG	Methylglyoxal bis-guanylhydrazone
MHC	Major histocompatibility complex
miRNA	micro RNA
MM	Molecular mass marker
MRE	<i>myb</i> regulatory element
mRNA	messenger RNA
mRNP	messenger Ribonucleoprotein particle



MTA	Methylthioadenosine
MTE	Motif Ten Element
MW	Molecular weight
NaOAc	Sodium Acetate
ncRNA	non-coding RNA
NEB	New England Biolabs
NP40	Nonidet P40
Oct2A	Octamer binding factor
ODC	Ornithine decarboxylase
PABP	Poly (A)-binding protein
PACT:	Protein Kinase R Protein Activator
Pan	Poly (A) nuclease
PARN	Poly (A) ribonuclease
PAZ	Piwi/Argonaute/Zwille
PBM	Protein-binding microarray
PCR	Polymerase chain reaction
PEXEL	<i>Plasmodium</i> export element
<i>Pf</i> ATP6	<i>Plasmodium falciparum</i> Calcium-dependent ATPase
<i>Pf</i> CDS	<i>Plasmodium falciparum</i> CDP-diacylglycerol synthase
<i>Pf</i> EMP1	<i>Plasmodium falciparum</i> erythrocyte membrane protein 1
<i>pfg27</i>	<i>Plasmodium falciparum</i> gametocyte-specific gene
<i>Pf</i> HDAC-1	<i>Plasmodium falciparum</i> histone deacetylase
<i>Pf</i> PP1	<i>Plasmodium falciparum</i> Serine/threonine phosphatase I
<i>Pf</i> RPA	<i>Plasmodium falciparum</i> Replication Protein A
<i>Pf</i> Sir2	<i>Plasmodium falciparum</i> silent information regulator
<i>Pf</i> SP1	<i>Plasmodium falciparum</i> signal peptidase 1
<i>Pf</i> TBP	<i>Plasmodium falciparum</i> TATA binding protein
PIWI	P-element induced wimpy testis
PNA	Peptide nucleic acid
PTC	Premature termination codon
PTGS	Post-transcriptional gene silencing
r.p.m	Revolutions per minute
rep20	Subtelomeric repeat element
<i>Rifin</i>	<i>Repetitive interspersed family</i>
RISC	RNA-induced silencing complex

RNA	Ribonucleic acid
RNAi	RNA interference
RNase	Ribonuclease
RPA	Replication protein A
RPMI	Roswell Park Memorial Institute
rRNA	ribosomal RNA
S-AdoMet	S-Adenosylmethionine
SDS-PAGE	Sodium dodecyl sulphate polyacrylamide gel electrophoresis
Semi-qPCR	Semi quantitative real-time polymerase chain reaction
SIR	Silent information regulator
siRNA	small interfering RNA
snoRNA	small nucleolar RNA
snRNA	small nuclear RNA
SPE	Subtelomeric var gene promoter element
<i>Stevor</i>	<i>Subtelomeric variable open reading frame</i>
<i>Surfin</i>	<i>Surface associated interspersed gene</i>
T4 Reg A	Bacteriophage T4 regulatory protein
T4gp32	Gene 32 protein from bacteriophage T4
Ta	Annealing temperature
TAF (1, 2, 6, 9)	TBP-associated factors
TARE	Telomere associated repetitive elements
TAS	Telomere associated sequences
TB	Tuberculosis
TBE	Tris-Borate-EDTA buffer
TBP	TATA binding protein
TEMED	Tetramethylethylenediamine
TFII (A,B,D,E,F,H)	Transcription factor two (A, B, D, E, F, H)
Tm	Melting temperature
TPE	Telomere positioning effect
TRAP	Tryptophan RNA binding attenuation protein
TRBP:	HIV TAR RNA Binding Protein
tRNA	transfer RNA
uORF	upstream open reading frames
UPF	Up-frameshift
UTR	Untranslated region
UV	Ultraviolet

Var

Variant gene family

var2csa

Conserved *var* gene subfamily of *PfEMP1*, primary ligand for CSA



List of Tables:

Table 1.1:	Current anti-malarial therapeutic drugs as described by the World Health Organization and Medicines for Malaria Venture.....	5
Table 1.2:	Examples of current drug discovery projects in malaria	5
Table 1.3:	Four major epigenetic factors associated with <i>var</i> gene regulation in <i>P. falciparum</i>	28
Table 2.1:	Features of the antigenically variant gene families in <i>P. falciparum</i> strain 3D7 ...	37
Table 2.2:	Conserved motifs identified via an <i>in silico</i> search.	38
Table 2.3:	The standard binding reaction set up for ³² P-EMSA's.	48
Table 2.4:	The EMSA set up for the positive controls.	50
Table 2.5:	EMSA reaction set up with single-stranded oligonucleotide, trophozoite and schizont nuclear extract in both the presence and absence of ATP.	51
Table 2.6:	EMSA reaction set up with single-stranded oligonucleotide, trophozoite nuclear extract and 100 fold excess of specific- and non-specific single-stranded competitors.	52
Table 2.7:	The oligonucleotide sequences of the conserved motifs designed and synthesized for EMSA's along with the control oligonucleotides SPE 2 and DIG.	57
Table 3.1:	The RNA interference primers to amplify the AdoMetDC, ODC, Insert and Spermidine synthase targets.	101
Table 3.2:	Real-time PCR primer sets.	109
Table 3.3:	Morphological developmental stage of <i>P. falciparum</i> treated and untreated parasites at time of RNA extraction.	112

List of Figures:

Figure 1.1:	Global distribution of <i>P. falciparum</i> malaria affected areas	2
Figure 1.2:	Morphology of the <i>P. falciparum</i> life cycle stages.	6
Figure 1.3:	Summary of the different levels at which gene regulation can occur within a eukaryotic cell.	8
Figure 1.4:	Eukaryotic transcription initiation machinery.	10
Figure 1.5:	The eukaryotic mRNA structure with its post-transcriptional modifications and the elements that influence translation	10
Figure 1.6:	The two pathways of eukaryotic mRNA decay.	11
Figure 1.7:	Illustration of the regulation of nonsense-mediated mRNA decay in mammalian cells by identifying and distinguishing between normal termination codons and premature termination codons.	12
Figure 1.8:	Illustration of RNA silencing via (a) siRNA- and (b) miRNA-mediated gene silencing.	14
Figure 1.9:	Mechanism of antisense oligonucleotide silencing of mRNA target.	16
Figure 1.10:	Levels of gene regulation in malaria.	18
Figure 1.11:	The phaseogram of the intraerythrocytic developmental cycle of <i>P. falciparum</i>	20
Figure 1.12:	Transcriptional regulation of <i>var</i> genes occur on multiple-levels.	22
Figure 1.13:	The chromosomal location and transcriptional direction of the <i>var</i> gene promoters.	24
Figure 1.14:	Histone marks linked to expression and epigenetic memory of <i>Plasmodium var</i> genes.	29
Figure 1.15:	The <i>P. falciparum</i> telomere ends illustrating the arrangement of variant genes, repetitive elements (rep20) and telomere associated repeat elements (TARE's).	30
Figure 1.16:	Two possible mechanisms of <i>var</i> gene activation and silencing within the parasite nucleus	32
Figure 1.17:	The enhancer-mediated counting mechanism hypothesis of gene switching.	32
Figure 1.18:	Illustration of the strict pairing of a <i>var</i> intron and <i>var</i> promoter required for <i>var</i> gene silencing.	33
Figure 2.1:	Gene families encoding the variant surface molecules exposed on the <i>P. falciparum</i> infected erythrocyte surface.	35
Figure 2.2:	The structure of a <i>var</i> gene.	36
Figure 2.3:	<i>P. falciparum</i> cultures in A) ring, B) early trophozoite, C) late trophozoite and D) schizont stage.	53
Figure 2.4:	BSA standard curve for protein determination in nuclear and cytoplasmic extracts.	53



Figure 2.5:	SDS-PAGE of nuclear and cytoplasmic extracts isolated from <i>P. falciparum</i> trophozoite cultures for comparison of NucBuster, ProteoJet and Voss extraction protocols.	54
Figure 2.6:	SDS-PAGE of stage-specific nuclear and cytoplasmic extracts utilizing Voss's protocol performed on <i>P. falciparum</i> <i>in vitro</i> cultures.	56
Figure 2.7:	Electrophoresis of all double-stranded oligonucleotides containing the conserved <i>cis</i> -regulatory motifs for labelling efficiency with ³² P.	57
Figure 2.8:	EMSA analysis of all control oligonucleotides.	58
Figure 2.9:	Densitometric lane analysis of EMSA results from Figure 2.8	59
Figure 2.10:	EMSA of Motif 2 in the presence and absence of the random single-stranded unlabelled oligonucleotide.	60
Figure 2.11:	Lane analysis utilizing Quantity One Software to verify the shifts obtained by EMSA analysis of Motif 2 in the presence and absence of the random single-stranded DNA.	61
Figure 2.12:	EMSA of Motif 1, Motif 2, Motif 3, Motif 4 and Dyad with trophozoite nuclear extract	62
Figure 2.13:	(A) EMSA of Motif 2 with nuclear extracts from rings, trophozoites and schizonts and (B) densitometric lane analysis of EMSA lane 4, 5 and 6.....	63
Figure 2.14:	EMSA of all five motifs in question with nuclear extracts from rings, trophozoites and schizonts.....	63
Figure 2.15:	(A) EMSA of Motif 1, Motif 2, Motif 3, Motif 4 and Dyad with trophozoite nuclear extract in either the presence or absence of ATP, (B) densitometric lane analysis of Motif 2 with trophozoite nuclear extract in either the presence or absence of ATP	64
Figure 2.16:	(A) EMSA of single-stranded Motif 2 with trophozoite and schizont nuclear extract in the presence and absence of ATP and densitometric lane analysis of single-stranded Motif 2 EMSA with (B) trophozoite nuclear extract and (C) schizont nuclear extract.	66
Figure 2.17:	EMSA of Motif 1, Motif 3, Motif 4 and Dyad in single-stranded state with trophozoite and schizont nuclear extract in the presence and absence of ATP ..	67
Figure 2.18:	Densitometric lane analysis of single-stranded (A) Motif 1, (B) Motif 3, (C) Motif 4 and (D) Dyad with trophozoite nuclear extract in the presence and absence of ATP.....	68
Figure 2.19:	(A) EMSA of single-stranded control Motif 2 with trophozoite nuclear extract in the presence and absence of random single-stranded unlabelled oligonucleotide and (B) densitometric lane analysis of EMSA.....	70
Figure 2.20:	EMSA's (left) of single-stranded motifs with trophozoite nuclear extract with different specific- and non-specific single-stranded competitors, densitometric lane analysis (right) of EMSA's	72

Figure 2.21:	CLUSTALW alignment of the five motifs in question	73
Figure 3.1:	A simplified illustration of the metabolic pathways of polyamine synthesis in <i>P. falciparum</i>	83
Figure 3.2:	Mechanisms of reporters commonly used in semi-qPCR.....	87
Figure 3.3:	(A) The transcript expression profile of Spermidine synthase and AdoMetDC/ODC of <i>P. falciparum</i> 3D7 strain, B) Illustration of the experimental set up for RNA interference in <i>P. falciparum</i> 3D7 strain.	89
Figure 3.4	Illustration of normalizing strategy depicting direct time point comparison and morphological comparison.	98
Figure 3.5:	(A) The protein alignment profile of <i>P. falciparum</i> Spermidine synthase with Spermidine synthase of <i>A. thaliana</i> , <i>T maritime</i> and <i>H. Sapiens</i> and (B) the nucleotide sequence of Spermidine synthase obtained from PlasmDB	99
Figure 3.6:	The amino acid sequence alignments of <i>P. falciparum</i> AdoMetDC/ODC with AdoMetDC or ODC from <i>H. sapiens</i> (Hs), <i>M. musculus</i> (Mm) <i>T. brucei</i> (Tb), <i>L. donovani</i> (Ld) <i>P. bergeri</i> (Pb) and <i>P. yoelii</i> (Py).	100
Figure 3.7:	Large scale purified PCR amplicons of AdoMetDC, ODC, Insert, Spermidine synthase, Section 1, 2, 3 and 4 sequences on a 2% agarose gel.	102
Figure 3.8:	Trial double-stranded RNA synthesis and digestion of AdoMetDC, ODC, Spermidine synthase and Insert.	103
Figure 3.9:	Large scale purified double-stranded RNA of all eight genes.	104
Figure 3.10:	Morphological analysis of Giemsa stained slides illustrating ring stage <i>P. falciparum</i> after 6 and 24 hours incubation with double-stranded RNA.	105
Figure 3.11:	Morphological analysis of Giemsa stained slides illustrating trophozoite stage <i>P. falciparum</i> after 6 and 24 hours incubation with double-stranded RNA.	107
Figure 3.12:	Semi-qPCR product of <i>P. falciparum</i> parasites treated with double-stranded RNA in the ring and trophozoite stage.	109
Figure 3.13:	Representative graphs of semi-qPCR amplification curves (A) and melting peaks (B).	110
Figure 3.14:	LDH expression levels of treated and untreated samples (T/UT) as determined by qBasePlus.....	110.
Figure 3.15:	LDH standard curves for each time point (A) 16, (B) 34, (C) 26 and (D) 44 h.p.i.	111
Figure 3.16:	Average expression ratios of <i>P. falciparum</i> AdoMetDC/ODC transcripts after 6 (16 h.p.i harvested) and 24 hours incubation (34 h.p.i harvested) with double-stranded RNA, starting in the ring stage.....	113
Figure 3.17:	Average expression ratios of <i>P. falciparum</i> Spermidine synthase transcripts after 6 and 24 hours incubation with double-stranded RNA, starting in the ring stage	114



Figure 3.18: Average expression ratios of *P. falciparum* AdoMetDC/ODC transcripts after 6 (26 h.p.i harvested) and 24 hours incubation (44 h.p.i harvested) with double-stranded RNA, starting in the trophozoite stage.115

Figure 3.19: Average expression ratios of *P. falciparum* Spermidine synthase transcripts after 6 and 24 hours incubation with double-stranded RNA, starting in the trophozoite stage.116

Figure 3.20: Parasite-specific inserts within the N- and C-terminal of the bifunctional AdoMetDC/ODC protein of the wild type *P. falciparum* parasite117

Malaria is a devastating disease which affects almost half of the world's population. Since the description of the malaria genome sequence, various aspects of the parasite have been studied, including drug resistance mechanisms, epidemiology and surveillance systems. Alarmingly, very little is known about the basic biological processes such as the regulation of the expression of parasite genes. The parasite, *Plasmodium falciparum*, has developed highly specialized methods of regulating the transcription of genes, starting at the regulation of genes controlling basic cellular processes such as protein synthesis and erythrocyte invasion, followed by the transcriptional regulation of more specialized genes, such as those aiding in immune evasion and pathogenesis. The description of the *P. falciparum* transcriptome by Bozdech *et al.* in 2003 revealed a complex, just-in-time and tightly regulated transcription profile of *P. falciparum* genes. This suggests that the most probable Achilles heel for *Plasmodium* may be its unique mechanisms of regulating gene expression. Various *cis*- and *trans*-regulatory sequences have been identified in *P. falciparum*, along with possible DNA (and RNA) binding proteins. The first part of this research focussed on transcriptional regulatory mechanisms in which an *in silico* search identified *cis*-regulatory sequences in the 5' untranslated region of the antigenically variant *var* gene family. Electrophoretic mobility shift assays (EMSA) were used to identify protein binding partners of these sequences, which could ultimately act as transcription factors in regulating the expression of this essential gene family. The second part of the research investigated the involvement of post-transcriptional regulatory mechanisms in the polyamine biosynthetic pathway of *P. falciparum*. Polyamines have been proven to be crucial for the parasite's development and therefore, an RNA interference knock-down strategy was used to verify the importance of the polyamine biosynthetic enzymes S-Adenosylmethionine decarboxylase (AdoMetDC), Ornithine decarboxylase (ODC) and Spermidine synthase. It is clear that various mechanisms for gene regulation are used by the parasite and that this is critical for the survival of this organism. The results of this study suggest the potential presence of both double-stranded and single-stranded DNA regulatory proteins within *P. falciparum* nuclear extract. As controversial as RNA interference remains in *P. falciparum*, this technique was used as a plausible knock-down strategy of parasite specific genes and certain trends, regarding the visible decreases in gene transcript level after double-stranded RNA treatment, were observed. However, final conclusions as to the feasibility of using RNA interference in *P. falciparum* remain to be elucidated. This study therefore ultimately lends insight into the transcriptional and post-transcriptional levels of *P. falciparum* gene regulation.

CHAPTER 1

LITERATURE OVERVIEW:

1.1 Introduction

Malaria as a growing epidemic has become one of the most threatening human infections of our time. Compared to other infectious diseases such as Human Immunodeficiency Virus (HIV) and Tuberculosis (TB), it is evident that malaria is one of the most important public health challenges as it has become more difficult to prevent and cure, due to frequent genetic changes of *P. falciparum* (Flick *et al.*, 2004). Since the start of the 21st century, approximately 3000 million people live in malaria areas, which translates back to approximately 40% of the world's population being at risk (Figure 1.1) (Aide *et al.*, 2007). It has been estimated that there are between 300 and 500 million clinical malaria cases and 2.7 million deaths annually (Aide *et al.*, 2007). In the sub-Saharan Africa regions, children under 5 years of age account for 90% of all deaths due to malaria (Gardener *et al.*, 2002; Griffith *et al.*, 2007). Moreover, pregnant woman who acquire malaria have a high risk of both maternal and perinatal morbidity and mortality, which could include still birth and spontaneous abortion of the foetus (Griffith *et al.*, 2007). Many communities are crippled by malaria since they simply do not have the resources to treat and prevent the disease, which eventually leads to poor economical growth and the parasite's persisting existence.

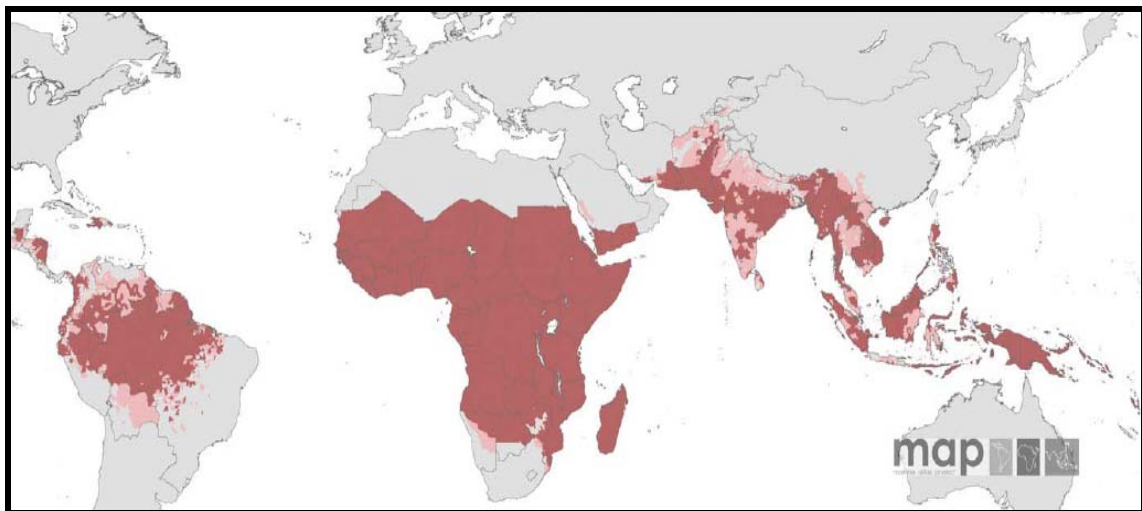


Figure 1.1: Global distribution of *P. falciparum* malaria affected areas (Guerra *et al.*, 2008).
Areas of high incidence (dark red), low incidence (pink) and no risk (light grey).

The malaria parasite is an Apicomplexan from the genus *Plasmodium*. Human malaria is caused by four different species of the *Plasmodium* genus and are known as *P. vivax*, *P. malariae*, *P. ovale* and *P. falciparum* (Griffith *et al.*, 2007). *P. vivax* is most common and is predominantly found in South and Northern Asia, Eastern Europe as well as Central and South

America (Griffith *et al.*, 2007). *P. ovale* on the other hand is most frequently found in West Africa and occasionally occurs in Southeast Asia and Papua New Guinea, while *P. malariae* is the least frequent, occurring in patchy areas worldwide (Griffith *et al.*, 2007). However, *P. falciparum* predominates in sub-Saharan Africa, Hispaniola and Papua New Guinea and is the species that causes the most virulent form of malaria resulting in the most deaths annually compared to any of the other species (Griffith *et al.*, 2007).

The malaria parasite is transmitted to its hosts through the infectious bite of an *Anopheles* mosquito with *A. gambiae* being the most common *P. falciparum* vector. *P. cynomolgi*, *P. inui* and *P. knowlesi* are simian malarial parasites that are known to be transmitted to humans through the bite of an infected *Leucosphyrus* group of anopheline mosquito, such as *A. latens* (Galinski *et al.*, 2009). *P. cynomolgi* is related to *P. vivax*, *P. inui* resembles *P. malariae* and *P. knowlesi* has often been mistaken for *P. malariae* even though its blood stage cycle is 24 hours compared to *P. malariae* which has a cycle of 72 hours (Galinski *et al.*, 2009). Of the three simian malaria parasites capable of infecting humans, *P. knowlesi* infections have become quite prevalent in areas such as Southeast Asia, Southern China, Thailand, Singapore, Malaysia and Taiwan but to date this parasite species cannot be classified as a human malaria species and is rather classified as a zoonosis (Galinski *et al.*, 2009).

The *P. falciparum* parasite's extended and increasing resistance to current anti-malarial drugs and the mosquito's resistance to the various existing insecticides have made this epidemic more difficult to control than ever before (Woodrow *et al.*, 2006). The development of an anti-malarial vaccine has failed due to the parasite's complexity, which is evident throughout its life cycle stages. The parasite has the ability to present a myriad of antigens through a process known as antigenic variation and this phenomenon allows the parasite to effectively escape the host's immune system. To date, an effective malaria vaccine has not yet been developed due to the high cost and length of the process before it can be placed on the market, as well as low returns as a result of affected countries not being able to afford expensive drugs. In addition to this, the effectiveness of the current anti-malarial drugs are challenged by the increasing resistance of the parasites and in turn, has discouraged pharmaceutical companies (Aide *et al.*, 2007).

The main focus of this research is gene regulatory mechanisms in *P. falciparum* and thus the following discussion on anti-malarial drugs for treatment and prophylaxis should be considered as a short summary. Details associated with mechanisms of drug action and resistance mechanisms will not be provided, instead the discussion will focus on the biological processes and intricate parasite biology, particularly as related to gene regulation.

Quinine is an aryl aminoalcohol which originates from the bark of *Cinchona officinalis* (Yeka *et al.*, 2009). To date, Quinine is used as a first-line treatment in severe malaria cases and a second-line treatment in uncomplicated malaria cases (Yeka *et al.*, 2009). Chloroquine was historically the first-line drug used for the treatment and prophylaxis of malaria but due to increased resistance to chloroquine, sulfadoxine-pyrimethamine became the drug of choice. Sulfadoxine-pyrimethamine is a combination of sulphur-based drugs and is part of the antifolate drug family, aimed at inhibiting the *P. falciparum* folate biosynthetic enzymes dihydrofolate reductase (DHFR) and dihydropteroate synthase (DHPS) (Nzila, 2006). However, subsequent resistance and toxicity problems to this drug combination resulted in the need to find new means of treating malaria. Currently, the best form of treatment relies on the combination of two or more blood schizontocidal drugs that have independent modes-of-action (Deen *et al.*, 2008). The WHO recommends the use of Quinine, Artemether and Artesunate for the treatment of severe *P. falciparum* malaria (Yeka *et al.*, 2009).

Artemisinin is a sesquiterpene extracted from *Artemisia annua* and is a strong anti-plasmodial drug with an elimination half-life of 2-5 hours (Balint, 2001). Artemisinin's mode-of-action is unclear and various mechanisms have been proposed, which include the interaction of Artemisinin with heme to subsequently produce carbon-centered free radicals, which ultimately damage the parasite microorganelles and membranes (Balint, 2001) and the interference of Artemisinin with the electron transport chain resulting in dysfunctional mitochondria (Li *et al.*, 2005). Additional studies have verified that Artemisinins are not only localized to the food vacuole but are located throughout the parasite and do not require heme, which led to another theory of Artemisinin anti-malarial action, which proposes the activation of Artemisinin by iron which in turn causes the irreversible inhibition of a metabolic enzyme known as Smooth Endoplasmic Reticulum calcium-dependent ATPase (*Pf*ATP6) (Ridley, 2003). Combination therapy combines derivatives of artemisinin, which reduces the biomass of existing parasites by 95%, with a partner compound which has a longer half-life, such as mefloquine, in order to kill remaining parasites. The combination therapies currently available and in use include Artemether-lumefantrine, Dihydroartemisinin-piperaquine, Artesunate-mefloquine and Artesunate-amodiaquine. Table 1.1 summarises the various other anti-malarial therapeutic drugs currently described by WHO that can be used for both the treatment and prophylaxis of malaria (Deen *et al.*, 2008). Treatment aims at alleviating symptoms, preventing relapses (*P. vivax* and *P. ovale*) and preventing further transmission while prophylaxis drugs aim to prevent the initial malaria infection by effectively killing erythrocytic and/or hepatic stage parasites.

Table 1.1: Current anti-malarial therapeutic drugs as described by the World Health Organization and Medicines for Malaria Venture (Deen *et al.*, 2008; Wells *et al.*, 2009).

Compound	In combination with	Used for the treatment of
Amodiaquine (T)	Artesunate	<i>P. vivax</i> , <i>P. malariae</i> , <i>P. ovale</i>
Artemether (T)	-	Mild to severe malaria
Artemether-lumefantrine (T)	-	Mild to severe malaria
Artesunate (T)	Amodiaquine, mefloquine, pyronaridine, sulfadoxine-pyrimethamine	Mild to severe malaria
Chloroquine (T) + (P)	-	<i>P. vivax</i>
Doxycycline (P)	Quinine	Mild to severe malaria
Mefloquine (T) + (P)	Artesunate	Mild to severe malaria
Primaquine (P)	-	<i>P. vivax</i> , <i>P. ovale</i>
Quinine (T)	Doxycycline	Mild to severe malaria
Sulfadoxine-pyrimethamine (P)	Artesunate	Mild to severe malaria
Dihydroartemisinin-piperaquine	-	Mild to severe malaria

Compounds are categorized for use as (T): treatment and/or (P): prophylaxis

Due to the failure of current anti-malarial drugs and the parasites increasing resistance to the present drugs, new drug targets are being identified and studied for future therapeutic treatments. The various molecular targets currently under clinical trial investigation is summarised in Table 1.2.

Table 1.2: Examples of current drug discovery projects in malaria (Wells *et al.*, 2009).

Molecular target	Function	Key objective of drug development
Dihydrofolate reductase	Folate biosynthesis	Overcome existing resistance
Dihydroorotate dehydrogenase	Pyrimidine synthesis	Show selectivity and potency <i>in vivo</i>
Purine nucleoside phosphorylase	Nucleoside synthesis	Provide clinical proof-of-concept
Adenosine deaminase	Nucleoside synthesis	Show selectivity and potency <i>in vivo</i>
Cytochrome bc1 complex	Mitochondrial respiration	Overcome existing resistance and show selectivity for parasite target
Subtilisin-like protease	Egress from erythrocytes	Lead discovery
Falcpains	Proteolysis of haemoglobin	Show selectivity against host proteases and develop pharmacophores that do not cross-react with host thiols
Fatty acid biosynthesis	Apicoplast lipid synthesis	Lead discovery
Histone deacetylase	DNA replication	Show selectivity for parasite target
Kinases	Signal transduction	Show selectivity for parasite target

Cytochrome bc1 complex: ubiquinol-ferricytochrome *c* oxidoreductase.

It is evident that *P. falciparum* drug-resistance remains a problem and thus research focussed on obtaining a better understanding of how the parasite survives is therefore crucial for the development of more effective, safe and affordable anti-malarial drugs. To develop the next front-line anti-malarial drugs will require a thorough understanding of the parasites biology.



1.2 *P. falciparum* biology

P. falciparum has two life cycles within separate hosts, an asexual life cycle within the human host and a sexual life cycle within female *Anopheles* mosquitoes (Figure 1.2).

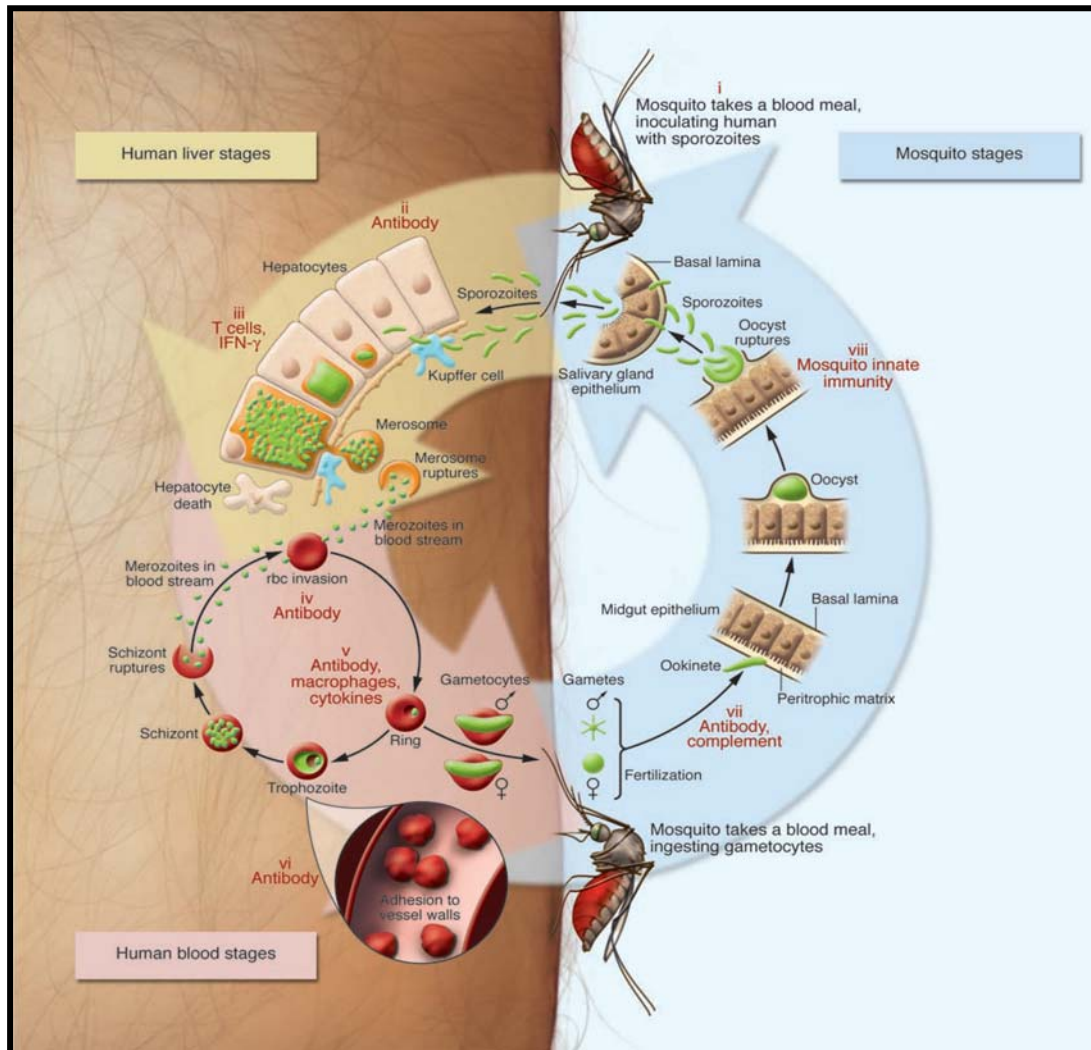


Figure 1.2: Morphology of the *P. falciparum* life cycle stages (Greenwood *et al.*, 2008).

A female *Anopheles* mosquito takes a blood meal from an infected human to obtain the required nutrients for sustaining oogenesis and reproduction (Barillas-Mury *et al.*, 2005). The haploid male and female parasite gametocytes in the blood, enter the mosquito and are transformed into microgametes and macrogametes, respectively. A diploid zygote forms by the fusion of the microgamete with the female macrogamete in the mosquito's midgut and the zygote then transforms into a motile ookinete which needs to survive the harsh conditions inside the mosquito including the ability to cross several barriers and avoid destruction by the mosquito's immune system (Barillas-Mury *et al.*, 2005). Within the next 24 hours, the ookinete secretes chitinases from its apical end to digest the peritrophic matrix consisting of a sheath of chitin and enter the midgut epithelium where it develops into an oocyst (Barillas-Mury *et al.*, 2005; Ghosh *et al.*, 2000). The oocyst progresses through various developmental processes to produce

thousands of sporozoites which are released to invade the salivary gland epithelium cells (Ghosh *et al.*, 2000). Once the sporozoites have invaded the salivary glands they remain in the cytoplasm temporarily, after which they travel to the secretory cavity where they await the next mosquito blood meal (Ghosh *et al.*, 2000).

During feeding, the sporozoites penetrate the secretory duct and enter the vertebrate host where they travel, via the blood stream, to the liver to invade the hepatocytes (Kirk, 2001). After about 7 days, the hepatocyte ruptures to release merozoites which in turn burst to release thousands of merozoites into the circulation of the host where each merozoite quickly invades an erythrocyte (Greenwood *et al.*, 2008). Invasion of the erythrocyte involves the merozoite attaching itself to specific surface receptors on the erythrocyte, re-orientating itself to ensure the apical end of the merozoite is in contact with the erythrocyte, followed by penetration of the membrane (Rasti *et al.*, 2004).

Once in the erythrocyte, the parasite lies relatively dormant in the ring stage until approximately 15 hours post invasion (h.p.i), whereafter both the metabolic and biosynthetic activity within the erythrocyte increases as the parasite progresses into the trophozoite stage (Kirk, 2001). During this stage the parasite lacks a functional citric acid cycle and is therefore wholly reliant on glycolysis for its energy supply (Kirk, 2001). As the parasite grows and matures within the vacuole, the rate of glucose utilization and lactic acid production in the parasitized cell increases and the parasite digests proteins of the host cell, principally hemoglobin, into small peptides that are utilized by the parasite as a source of amino acids (Kirk, 2001). Isoleucine is the one amino acid which is absent from human hemoglobin and thus the parasite obtains this amino acid by exchanging leucine, an amino acid abundant in hemoglobin, for isoleucine from the extracellular medium (Martin *et al.*, 2007). Moreover, the structure of the erythrocyte is altered completely from being smooth and biconcave, to an irregularly shaped cell with its surface covered in small electron-dense protrusions known as knobs, which serve as localization points for parasite derived proteins (Kirk, 2001). The late-stage trophozoite finally enters the schizont stage at about 36 hours after invasion of the erythrocyte where it subdivides to produce ~30 daughter merozoites which are released into the blood stream when the erythrocyte ruptures and each new merozoite invades another erythrocyte, continuing the cycle (Kirk, 2001).

During the transition from trophozoite to schizont, the parasite's metabolic activity increases dramatically as the parasite prepares for cell growth, cell division and immune evasion. In the trophozoite stage of the parasite, regulation of the immune evasion machinery become of utmost importance and the tight control of gene transcription and translation becomes evident. This stage therefore marks the beginning of the intricate mechanisms the parasite utilizes to regulate its genes, as will be discussed in the following sections.

1.3 General gene regulation

The mechanisms involved in eukaryotic gene regulation can only be fully understood when the different stages at which gene expression can be regulated are considered. Figure 1.3 depicts a summary of the different levels within a cell at which gene expression can be regulated and thus the various facets where gene expression can be controlled include the transcriptional level, epigenetically on the chromatin level, post-transcriptionally at the level of RNA processing and stability and finally at the translational level (Meissner *et al.*, 2005).

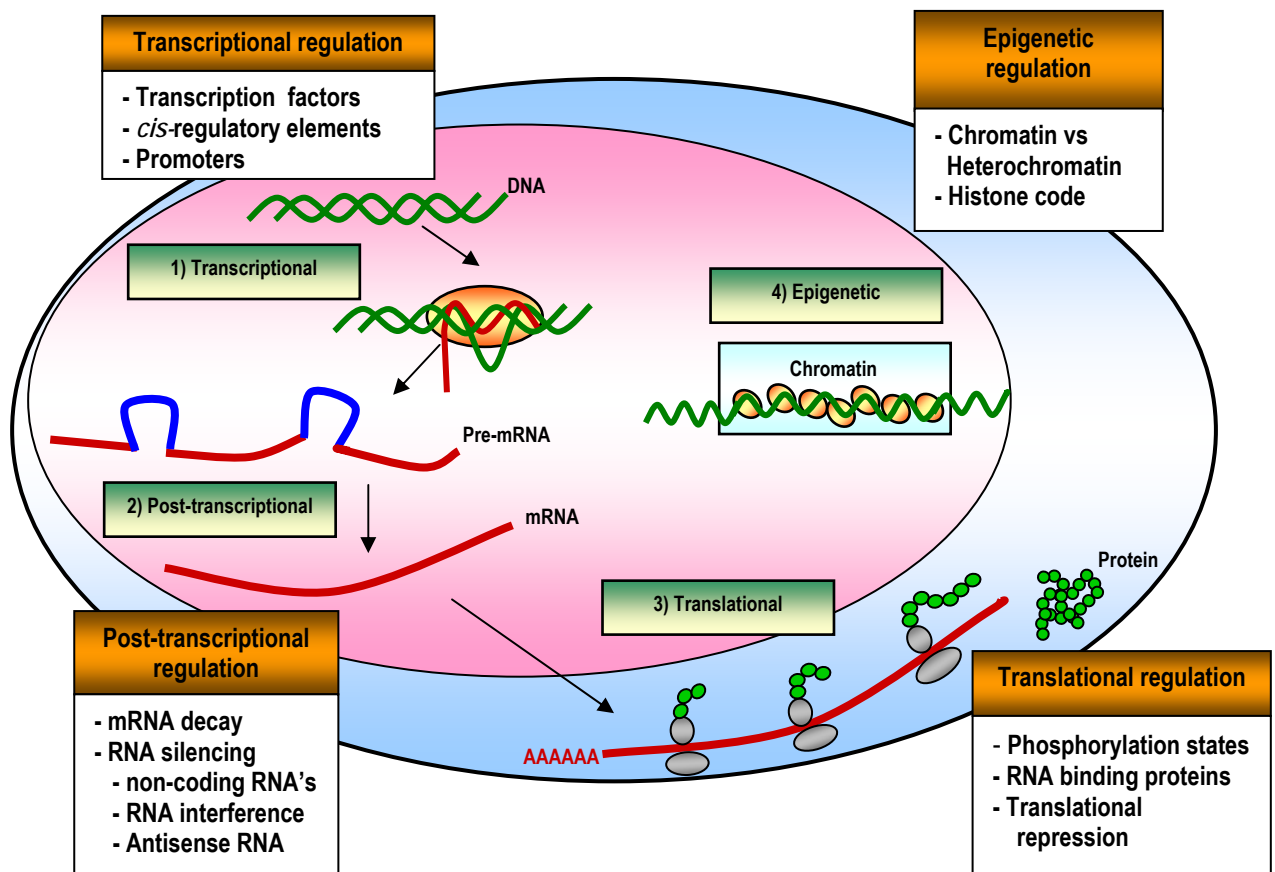


Figure 1.3: Summary of the different levels at which gene regulation can occur within a eukaryotic cell.

1.3.1 Transcriptional regulation

A gene is a sequence of DNA which carries a code required for RNA followed by protein synthesis and this DNA code often contains regulatory regions which aid in regulating both the rate of mRNA synthesis and the rate of activity of genes. Upstream promoter and enhancer regions are referred to as regulatory regions of a gene and contain novel 3-dimensional foldback DNA structures to aid the polymerase enzymes and transcription machinery to recognize specific sites (Maclean, 1989). At the transcriptional level of regulation, the

transcription rate is influenced by the intricate interplay between protein components known as *trans*-acting factors (or transcription factors) localized in the nucleus that interact with *cis*-regulatory DNA elements, to facilitate the correct RNA polymerase to bind to the correct promoter at the right time (Kumar *et al.*, 2004; Meissner *et al.*, 2005). These transcription factors regulate transcription by binding to DNA *cis*-acting elements within enhancers or promoters, which in turn signals chromatin and histone modifying enzymes to alter the nucleosome and make it accessible to the transcription machinery. The DNA is bent thereby exposing previously unseen, or hiding previously seen, binding sites from other transcription factors (Heintzman *et al.*, 2007; Kumar *et al.*, 2004). Studies in organisms ranging from yeast to humans revealed that active promoters are usually marked by several features such as nucleosome depletion and histone H3 and H4 acetylation, which are absent from inactive promoters (Heintzman *et al.*, 2007).

Transcription in eukaryotes is regulated by three different RNA polymerases (RNA polymerase I, II and III) and each RNA polymerase synthesizes a different class of RNA (Sadhale *et al.*, 2007). The transcription initiation complex (Figure 1.4) requires RNA polymerase II, which catalyzes the transcription of all protein coding genes and six transcription factors (TFIIA, TFIIB, TFIID, TFIIIE, TFIIF, TFIIH) which are known to assist the polymerase in its function (Sadhale *et al.*, 2007). TFIID is a primary factor which recruits on the promoter and helps with the assembly of the other transcription factors and the RNA polymerase II to form the pre-initiation complex (PIC). This PIC then recognizes elements of the eukaryotic promoter.

Figure 1.4 below illustrates the typical eukaryotic machinery where a eukaryotic TATA box, which is an AT-rich sequence found between -20 and -30 nucleotides upstream from the transcription start site, is recognized by a TATA binding protein (TBP), Initiator (INR) is recognized by TBP-associated factors (TAF 1 / TAF 2) of TFIID and the Downstream Promoter Element (DPE) is recognized by TAF 6 and TAF 9 of TFIID (Sadhale *et al.*, 2007). TFIIB recognizes two TFIIB Recognition Elements (BRE) and Motif Ten Element (MTE), a consensus sequence known to enhance RNA polymerase II mediated transcription. Several cofactors are also required for transcriptional initiation and these are classified into two classes. The first class of enzymes and proteins is important for modification of chromatin while the second class, often referred to as a mediator complex, are factors important for the interaction with RNA polymerase II and the general transcription factors (Sadhale *et al.*, 2007).

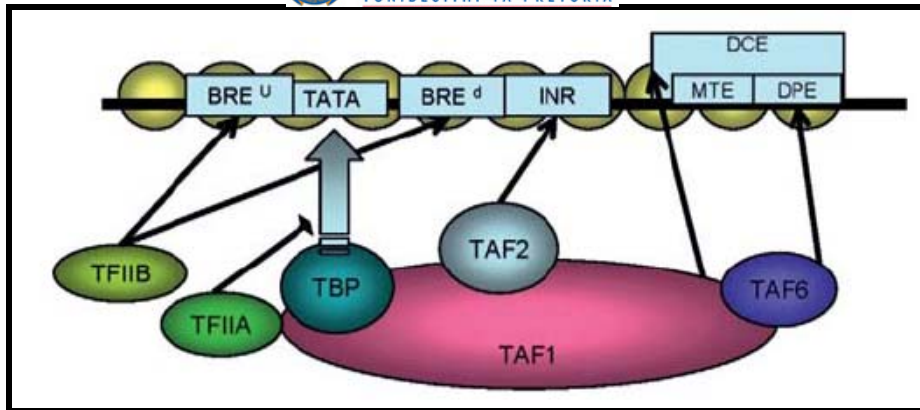


Figure 1.4: Eukaryotic transcription initiation machinery (Sadhale *et al.*, 2007).

Transcription factor binding protein (TBP) identifies the TATA box, TAF 1/TAF2 are TBP-associated factors that recognize the Initiator (INR) while TAF 6 recognizes the downstream promoter element (DPE). TFIIB Recognition Elements (BRE) and Motif Ten Element (MTE) enhance RNA polymerase II transcription.

The central dogma of molecular biology intricately connects the transcription of DNA to RNA and the translation of RNA to protein. After replication of the DNA, RNA polymerase binds to the promoter sequence on the double-stranded DNA which then unwinds to form two single DNA strands. This allows one of the strands to act as the template from which the genetic code will be transcribed. The presence of transcription factors are crucial for RNA polymerase functioning and the binding of transcription factors to their designated *cis*-acting sequences (TATA box or CAAT box) determine whether transcription of a certain gene is initiated. Once the mRNA transcript has been produced, it requires post-transcriptional modifications before translation can continue.

1.3.2 Post-transcriptional regulation

The mRNA becomes modified extensively from its immature to mature forms and each feature and regulatory sequence will determine the final fate of the transcript. The mRNA 5' cap and poly(A) tail represent strong promoters for the initiation of translation while internal ribosome entry sequences (IRES), the upstream open reading frames (uORF) and tertiary RNA structures such as hairpins, all affect translation in some way (Figure 1.5) (Gebauer *et al.*, 2004). Post-transcriptional regulation can be summarised to include mRNA decay, non-coding RNA, antisense RNA and RNA interference.

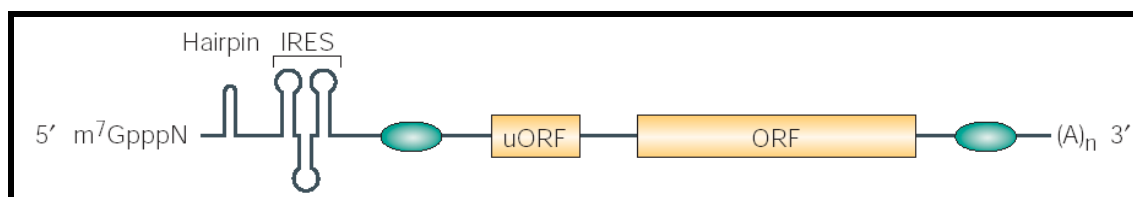


Figure 1.5: The eukaryotic mRNA structure with its post-transcriptional modifications and the elements that influence translation (Gebauer *et al.*, 2004).

IRES (internal ribosome entry sequences), uORF (upstream open reading frame) and green/blue ovals represent binding sites for proteins and RNA regulators.

1.3.2.1 mRNA decay

mRNA decay is an important aspect for regulating the number of transcripts present in the cell and short-lived mRNA's often encode the proteins which are of significant value to the cell (Meyer *et al.*, 2004). The mRNA decay rates differ between various transcripts from a few minutes to over an hour, which implies the mechanisms involved in mRNA decay to be quite complex. The mRNA turnover machinery is important in eliminating possible mutant RNA such as genes containing premature stop codons, which are effectively degraded by nonsense-mediated decay pathways (Wilusz *et al.*, 2001).

mRNA contain a 5' 7-methylguanosine cap structure and a 3' poly(A) tail structure which are determining factors in transport, stability and translation. The poly(A) tail protects the mRNA from degradation by interacting with the poly(A)-binding protein (PABP), forming a ternary complex with eukaryotic initiation factor 4G (eIF4G) and preventing access of decapping and deadenylating enzymes to their targets, thereby stabilizing the mRNA transcript (Wilusz *et al.*, 2001). Two mRNA decay pathways exist in eukaryotes (Figure 1.6), which have different mechanisms of degradation.

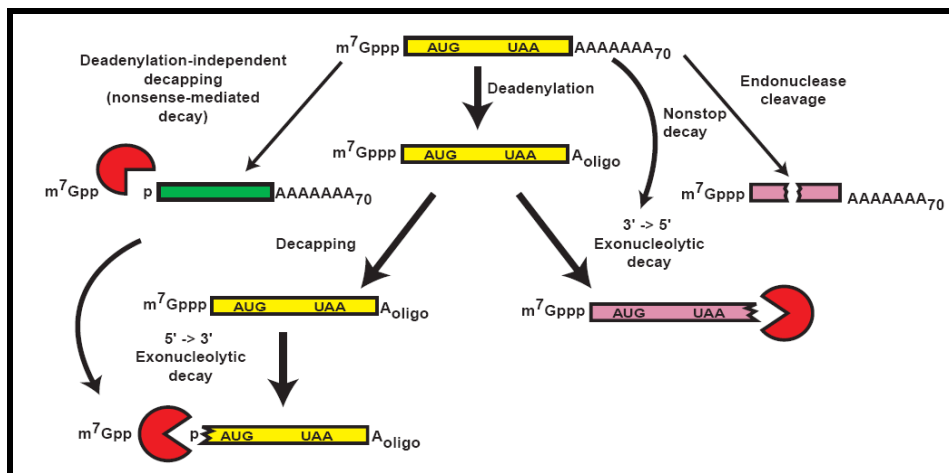


Figure 1.6: The two pathways of eukaryotic mRNA decay (Parker *et al.*, 2004).

In the first pathway the mRNA poly(A) tail is shortened by mRNA deadenylases after which a decapping enzyme hydrolyzes the 5' cap, releasing the m^7GpppN cap and produces an mRNA with an exposed 5' monophosphate which then undergoes exonuclease degradation in the 5'-3' direction (Parker *et al.*, 2004). The exonuclease forms a complex with various other proteins located in cytoplasmic processing structures known as P-bodies and is involved in both normal mRNA decay and nonsense-mediated mRNA decay (Newbury, 2006). P-bodies contain pools of mRNAs that are not engaged in translation since P-bodies do not contain the translational machinery and require mRNA's for their assembly (Valencia-Sanchez *et al.*, 2006). The deadenylating enzymes, decapping proteins and DEAD-box helicase proteins are found in the

P-bodies since these are the sites where mRNAs are specifically deadenylated and decapped (Newbury, 2006). When translation of the mRNA is repressed the RNA transcript is transported to P-bodies where the transcript is either degraded or stored (Newbury, 2006).

The second pathway, known as the 3' decay pathway, involves deadenylation of the poly(A) tail followed by direct degradation in the 3'-5' direction via the cytoplasmic exosome (Parker *et al.*, 2004). The nuclear exosome functions in RNA processing and assists in the turnover of incomplete mRNA while the cytoplasmic exosome assists in non-stop mRNA decay and degradation of the mRNA after deadenylation (Parker *et al.*, 2004). Sequence elements within the UTR of mRNA known as AU-rich elements (ARE) have the ability to regulate the rate of mRNA turnover by playing a role in either promoting rapid deadenylation and mRNA decay or in stabilizing the mRNA transcript (Parker *et al.*, 2004).

mRNA decay can additionally undergo either nonsense-mediated mRNA decay (NMD) or non-stop mRNA decay (Maquat, 2004; Van Hoof *et al.*, 2002). NMD regulates the degradation of mRNA's containing a premature translational stop codon by regulating the endonucleolytic cleavage of the mRNA by a ribosome associated endonuclease (Newbury, 2006). A premature termination codon (PTC) (UAA, UAG, UGA) is often located upstream from the normal site of translation termination, which results in the production of a truncated protein that could function in various deleterious mechanisms (Maquat, 2004). In mammalian cells, various elements allow for the identification of PTC. The intron position within a pre-mRNA is a determinant for NMD since a PTC that is followed by an intron located more than 55 nucleotides downstream is suitable for NMD, while normal termination codons often reside in the last exon or are followed by an exon-exon junction less than 55 nucleotides downstream and are in this way immune to NMD (Figure 1.7) (Maquat, 2004). When the premature termination codon is identified, the mRNA can undergo nonsense-mediated decay via two pathways, the decapping pathway which is followed by 5'-3' decay and the deadenylation pathway which is followed by 3'-5' exosome-mediated decay (Figure 1.7) (Maquat, 2004).

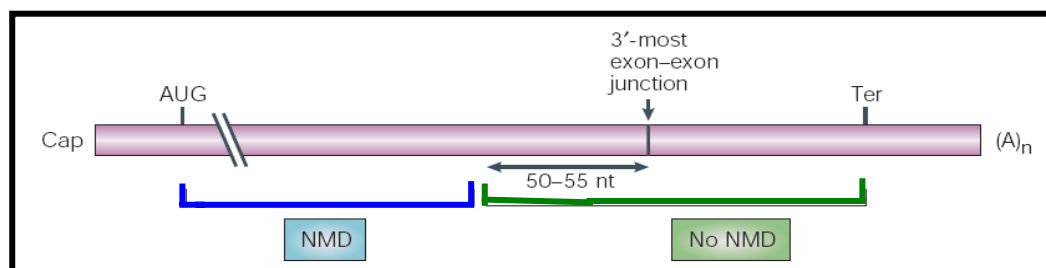


Figure 1.7: Illustration of the regulation of nonsense-mediated mRNA decay in mammalian cells by identifying and distinguishing between normal termination codons and premature termination codons (Maquat, 2004).

If a PTC is located in the blue region, it is followed by an exon-exon junction, which is more than 25 nucleotides away and therefore elicits NMD. If a PTC is located anywhere in the green region, it is within 55 nucleotides from an exon-exon junction and therefore does not elicit NMD. The normal termination codon (Ter) is located in the last exon and therefore doesn't elicit NMD

Non-stop-mediated mRNA decay regulates the degradation of mRNA's that lack a termination codon via the 3'-5' cytoplasmic exosome pathway. The non-stop mRNA decay pathway requires translation of the mRNA which becomes deadenylated and degraded by the exosome in the cytoplasm starting from the 3' end (Van Hoof *et al.*, 2002). The mRNA lacking a termination codon is recognized by two mechanisms. The first requires that the translating ribosome reach the poly(A) tail and the 3' end of the mRNA, therefore indicating that the ribosome has an empty A-site (Van Hoof *et al.*, 2002). The second mechanism involves the COOH and NH₂ terminals of a protein component of the exosome (Van Hoof *et al.*, 2002).

1.3.2.2 *RNA silencing*

RNA silencing refers to a sequence-specific RNA degradation mechanism and includes post-transcriptional gene silencing (PTGS) in plants, gene quelling in fungi and RNA interference in animals (Cottrell *et al.*, 2003).

Non-coding RNA's (ncRNA) are RNA transcripts which are not translated into protein and most of these transcripts do not have any open reading frames (Li *et al.*, 2008). ncRNA's are integral components of ribonucleoprotein complexes that are involved in gene regulation and can be either small non-coding RNA's which include molecules such as microRNA's (miRNA), short interfering RNA's (siRNA), small nucleolar RNA's (snoRNA) and tRNA's, or they can be large non-coding RNA's (Yasgan *et al.*, 2007). In all eukaryotic cells, there appear to be both protein coding and non-coding transcripts. ncRNA found in other eukaryotic organisms have been implicated to be involved in phenomena involving RNA-RNA and RNA-DNA interactions as well as chromatin remodelling such as X-chromosome inactivation in mammals or the postulation that some ncRNA's are implicated in maintaining the methylation status of CpG islands, thereby affecting promoter activities (Mattick, 2001; Yasgan *et al.*, 2007).

miRNA and siRNA are RNA molecules of between 21 and 26 nucleotides in length and have emerged as important regulators of mRNA translation and decay. miRNA and siRNA have the ability to silence cytoplasmic mRNA by one of three mechanisms: either by triggering endonuclease cleavage, by promoting translational repression or by accelerating mRNA decapping (Carthew, 2006; Valencia-Sanchez *et al.*, 2006). miRNA's and siRNA's are distinguished by their mode of biogenesis (Figure 1.8) since miRNA's are produced from transcripts that form stem-loop structures and inhibit translation by interacting with the 3' UTR of the target mRNA (Ullu *et al.*, 2004). siRNA's are produced from long double-stranded RNA which are either endogenously produced or exogenously provided when using RNA interference as a silencing tool (Valencia-Sanchez *et al.*, 2006). In addition, stRNA from *lin-4* and *let-7*, are small temporal RNA molecules that are transcribed from the genome as hairpin precursors and are processed by Dicer to allow the accumulation of one strand only (Hannon, 2002). Perfect

complimentarity between target mRNA and stRNA is not required for silencing and does not induce degradation but instead results in translational inhibition (Hannon, 2002).

RNA interference (Figure 1.8) was first observed by plant biologists in the 1980's but its molecular mechanism was only revealed in the late 1990's (Leung *et al.*, 2005). RNA interference has become a useful molecular tool for the knock-down of gene expression and requires a cytoplasmic ribonuclease III (RNase III)-like protein known as Dicer and a multi-protein complex known as the RNA-induced silencing complex (RISC). A key component of the RISC complex is the Argonaute proteins. The Argonaute family members all contain a PAZ (Piwi/Argonaute/Zwille) domain and a PIWI (P-element induced wimpy testis) domain which functions in slicer activity since it is related to RNase H endonucleases (Valencia-Sanchez *et al.*, 2006). Dicer is active in the cytoplasm and cleaves double-stranded molecules into small RNA duplexes of 19-25 base pairs in length with 3'-dinucleotide overhangs. The small interfering RNA (siRNA) duplex becomes incorporated into RISC where an ATP-dependent helicase unwinds the duplex, allowing one of the two strands to act as the guiding strand to recognize and bind to its mRNA (Leung *et al.*, 2005). The degree of complimentarity between the guiding strand and the target mRNA will determine whether the silencing will be achieved by site-specific cleavage in the region of the siRNA-mRNA duplex. This is followed by degradation of the products by non-specific RNases or via miRNA translational repression with the help of P-bodies.

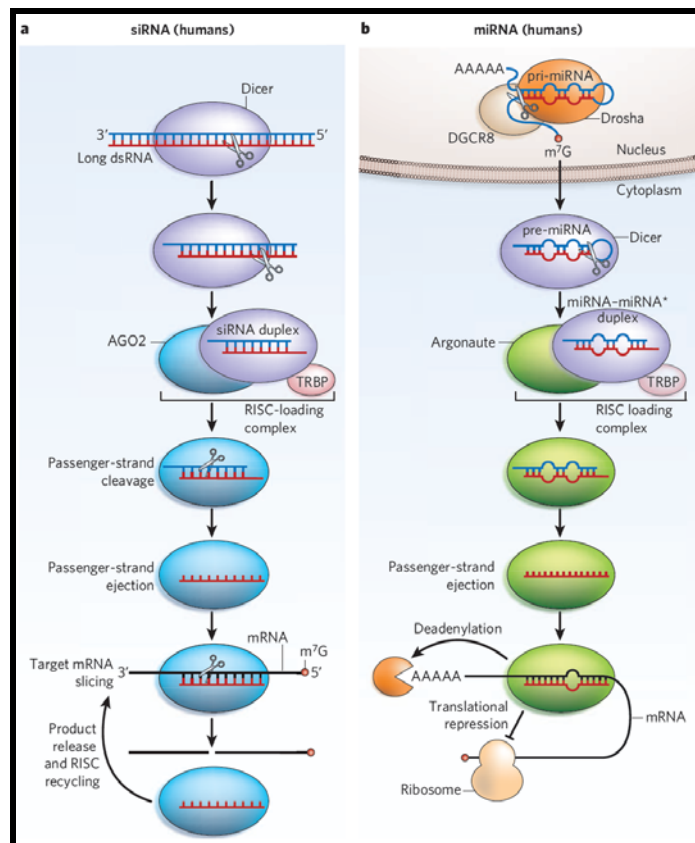


Figure 1.8: Illustration of RNA silencing via (a) siRNA- and (b) miRNA-mediated gene silencing (Jinek *et al.*, 2009).

Processing of miRNA and siRNA are both Dicer-dependent and key principles of their function lie in the interaction between miRNA/siRNA with the mRNA target. The 5' portion of the miRNA is highly conserved and the base pairing between the 5' end of miRNA with the mRNA target establishes the thermal stability of the interaction, while the 3' end of miRNA has been suggested to function as a modulator of suppression (Valencia-Sanchez *et al.*, 2006). For endonuclease cleavage, base pairing between base 10 and 11 is required and thus only one complementary site is needed to direct repression. Translational repression requires multiple complementary sites (Valencia-Sanchez *et al.*, 2006). Endonucleolytic cleavage is favoured by perfect base pairing between the miRNA/siRNA and the target mRNA, however some mismatches are tolerated allowing cleavage to occur. It has been suggested that miRNA's utilize other mechanisms of target degradation such as sequestering the target mRNA to P-bodies where the transcripts are unavailable to the protein synthetic machinery and instead are the substrates for decapping enzymes and degradation nucleases (Carthew, 2006; Valencia-Sanchez *et al.*, 2006). The localization of Argonaute proteins in P-bodies are also functionally important and it has been proven to be important for miRNA gene silencing (Valencia-Sanchez *et al.*, 2006).

The first antisense RNA discovery was made in 1981 in the laboratories of Tomizawas and Nordstroms when they found that copy numbers in *E. coli* plasmids were controlled by small RNA-regulators (Brantl, 2002). Antisense RNA's are small (35-150 nucleotides), highly structured and act via sequence complementarity with target sense strand mRNA's (Brantl, 2002). Antisense RNA's are coded in *cis* by being transcribed from a promoter which is located on the opposite strand of the same DNA molecule. However, some antisense RNA's have been found to be encoded in *trans*, requiring only partial complementarity to their target mRNA and often have more than one mRNA target (Brantl, 2002). The main function of antisense RNA's are the inhibition of target mRNA's, however certain activating antisense RNA's have also been identified (Brantl, 2002). Antisense oligonucleotides are defined as the non-coding complementary sequences that act as an RNA/DNA template to the target mRNA to be degraded. These antisense oligonucleotides have been recognized as naturally occurring gene regulation mechanisms of which very little is known with regards to the mechanism of action (Figure 1.9). Antisense deoxynucleotides are single strands of deoxynucleotide sequences that bind to the target mRNA and activate RNase H, an endogenous enzyme which cleaves the RNA strand of a heteroduplex RNA-DNA complex, ultimately causing the degradation of the targeted transcript (Kang *et al.*, 2008). Various other antisense mechanisms have been observed such as interference with mRNA processing and transport, formation of a triplex with the DNA and modifications of synthetic antisense oligonucleotides to produce morpholino oligomers, peptide nucleic acids (PNA) or locked nucleic acids (LNA) which are all capable of acting in different mechanisms (Rayburn *et al.*, 2008). Antisense oligonucleotides, as a

molecular gene silencing tool, have been used for target validation, gene function studies and gene therapy.

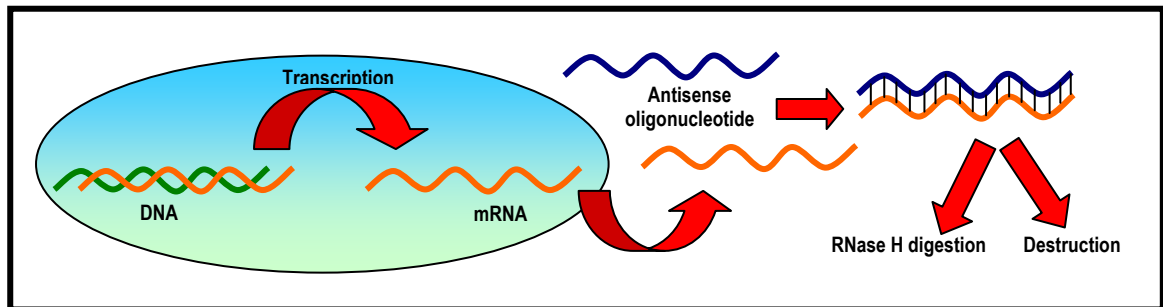


Figure 1.9: Mechanism of antisense oligonucleotide silencing of mRNA target.

1.3.3 Translational regulation

Translation of eukaryotic mRNA determines the relevant protein levels within cells and the times at which the crucial proteins are expressed with regards to the cell cycle. Translational control is critical for eukaryotic cells since it is involved with cell differentiation, proliferation and development (Garcia-Sanz *et al.*, 1998). Translational regulation is characterized by the various mechanisms pre-existing mRNA's are utilized, which include changes in phosphorylation states of translational initiation factors, alterations in translation elongation or poly(A) tail length modulation and initiation rate changes via *trans*-acting factors and *cis*-acting elements (Garcia-Sanz *et al.*, 1998). To understand global regulation and mRNA specific regulation, the mechanism of eukaryotic translation must be considered. Firstly, the small 40S ribosomal subunit binds to the 5' end of the mRNA and scans the mRNA sequence in a 5'-3' direction until it identifies the initiation (AUG) codon (Gebauer *et al.*, 2004). The 60S ribosomal subunit joins the 40S subunit and together, the two subunits form the 80S ribosome (Gebauer *et al.*, 2004). The ribosomal units contain eukaryotic initiation factors (eIF) that help control the translation of the mRNA.

Global control/regulation of a protein is accompanied by changes in phosphorylation states of either the initiation factors or the regulators that interact with the initiation factors (Gebauer *et al.*, 2004). A prime example is the translational inhibition which occurs when one of the eIF2 subunits are phosphorylated. During translation initiation, when the AUG codon is recognized, the GTP-bound eIF2 is hydrolyzed to GDP-bound eIF2 which is catalyzed by eIF2B (Gebauer *et al.*, 2004). The eIF2 consists of three subunits (α, β, γ) and when the α -subunit is phosphorylated, the GTP-GDP exchange is blocked since the dissociation rate of eIF2 from eIF2B is slowed down and therefore the catalytic activity of eIF2B is unavailable, ultimately resulting in translational inhibition (Gebauer *et al.*, 2004). The cap-binding protein eIF4E is another factor which affects the translation rate since it interacts with the scaffold protein eIF4G

(Gebauer *et al.*, 2004). The eIF4E associates with a domain in the eIF4G, however when 4E-binding proteins become hypophosphorylated, they bind to eIF4E which prevents eIF4E from interacting with eIF4G and the small ribosomal subunit fails to associate with the mRNA, which ultimately results in translational repression (Gebauer *et al.*, 2004).

Reinitiation is another mechanism of translational regulation in eukaryotes and occurs when the termination codon is reached and the 60S ribosome dissociates from the 40S ribosome, but the 40S ribosome still remains attached to the mRNA and continues scanning until it reaches yet another start codon (AUG) and initiates translation downstream (Kozak, 2005). Reinitiation in eukaryotes can only occur if the scanning 40S ribosomal subunit has enough time to pick up another methionine loaded tRNA (Met-tRNA) before it arrives at the next start codon (Kozak, 2005). Since the loading of the Met-tRNA to the ribosome requires GTP and eIF2, the reinitiation mechanism can be regulated by manipulating the eIF2-GTP levels, which allows the 40S ribosome to bypass certain start codons while scanning since the Met-tRNA has not yet been loaded onto the ribosome (Kozak, 2005).

mRNA-specific regulation refers to the regulation of specific mRNA's through the interaction of RNA binding proteins (Gebauer *et al.*, 2004). RNA binding proteins act through three different mechanisms, either by sterically hindering the binding site of the small ribosomal subunit on the mRNA, interfering with the formation of the eIF4F complex (cap-binding complex necessary for translation initiation) or by cap-independent inhibition which interferes with ribosome scanning from the cap structure (Gebauer *et al.*, 2004).

1.3.4 Epigenetic regulation

Epigenetic gene regulation refers to alterations in gene expression and gene transcriptional states which are not as a result of changes in the DNA sequence but rather due to changes in DNA modifications or chromatin structure, such as histone methylation and acetylation (Deitsch *et al.*, 1999). The concept of epigenetics was first established in the 1940's and is a mechanism of gene regulation which generates diversity and helps maintain cell integrity and stability (Cheung *et al.*, 2005). Epigenetic changes are heritable and reversible, usually involving DNA methylation and chromatin modifications (Cheung *et al.*, 2005).

Eukaryotic genomes are packaged into the DNA-protein complex, chromatin, which consists of nucleosome repeating units wrapped around a core histone (Rando *et al.*, 2007). Chromatin is known to affect the transcription of genes since the nucleosome position can serve as either an activator or repressor of gene expression. In eukaryotes, the state of chromatin can be altered by enzymes which either acetylate lysine residues of histones (histone acetyltransferases),

causing relaxation of chromatin and therefore transcriptional activation, or enzymes that deacetylate lysine residues (histone deacetylases) inducing chromatin condensation which leads to transcriptional repression (Hakimi *et al.*, 2007). Other histone modifying enzymes can also methylate (methyltransferase) or demethylate (demethylase) the histone lysines often resulting in transcriptional repression and activation, respectively, albeit certain exceptions exist (Cheung *et al.*, 2005).

CpG islands are frequent C-G dinucleotide sequences present in short stretches of DNA and are often located around promoters of housekeeping genes, designating them as active. Approximately 80% of CpG islands present in the mammalian genome are inactivated by methylation at C⁵ of cytosine (Cheung *et al.*, 2005). Multi-cellular organisms utilize histone methylation and acetylation marks to generate transcriptional memory, whereby the cell types can remember their genetic program throughout the developmental cycle (Comeaux *et al.*, 2007). These histone modifications present a probable mechanism by which a virulence gene program can be maintained over many life cycles and is known as the histone code (Comeaux *et al.*, 2007).

1.4 Gene regulation in *Plasmodia*

Gene regulation in *P. falciparum* can occur at various levels including transcriptional, post-transcriptional, translational and epigenetic as depicted in Figure 1.10. The mechanisms behind epigenetic gene regulation in *Plasmodia* have been investigated to a greater extent and will therefore form a more extensive discussion.

Transcriptional regulation	Post-transcriptional regulation	Translational regulation	Epigenetic regulation
<ul style="list-style-type: none"> - Transcription factors - <i>cis</i>-regulatory elements - Promoters 	<ul style="list-style-type: none"> - mRNA decay - RNA silencing <ul style="list-style-type: none"> - non-coding RNA's - RNA interference - Antisense 	<ul style="list-style-type: none"> - Histone tails - Translational repression - Gametocyte 	<ul style="list-style-type: none"> - Chromatin - Recombination - Telomeres - Heterochromatin - Introns

Figure 1.10: Levels of gene regulation in malaria.

1.4.1 Transcriptional regulation

The transcriptional machinery of *P. falciparum* is very similar to those found in other eukaryotes which includes RNA polymerases (I, II, III), RNA processing (capping and splicing), promoter regions and some transcription factors. However, differences were observed with regards to the *cis*-acting elements, which indicates no homology to standard regulatory sequences found in

eukaryotes and suggests the possible impact of evolution on the parasites mechanisms of gene regulation (Kumar *et al.*, 2004).

In *P. falciparum*, transcription is carried out by RNA polymerase II and is monocistronic which means that the resulting mRNA sequence contains the genetic information to translate only a single protein. This therefore suggests that transcription depends on discrete intergenic sequences to manage transcriptional initiation and termination (Horrocks *et al.*, 2009). Transcription in *P. falciparum* depends on the interaction of various nuclear *trans*-acting factors with their cognate sequences upstream of the transcription start site, which is correlated with promoter activity and is thus also associated with the sequential steady-state accumulation of mRNA and protein (Horrocks *et al.*, 2009). The *Pf*TBP shares a typical higher order structure with other TATA box binding proteins, resulting in the formation of a “saddle-like” tertiary structure that sits over the TATA box. The location of the TATA box of *P. falciparum* appears to be situated much further upstream from the transcriptional start site than in most eukaryotes and this suggest that the parasite utilizes a scanning mechanism, in order to correctly identify the transcription start site (Coleman *et al.*, 2008; Horrocks *et al.*, 2009). Due to the AT-richness of the parasite genome, the specificity of the *Pf*TBP interaction with its *cis*-acting DNA element also suggest that other components of the parasite PIC may recognise additional core promoter sequences, in order to correctly select the specific transcription start site (Horrocks *et al.*, 2009). However, our understanding of transcription remains limited since a well described transcription start site in the parasite remains to be elucidated.

P. falciparum has an intricate life cycle and in order to ensure that its survival, pathogenesis and transmission between hosts remain successful, several complicated yet unique regulatory mechanisms must be in place. The discovery of the intra-erythrocytic transcriptome profile of *P. falciparum* by Bozdech *et al.* (2003) revealed that this parasite possesses an extremely well regulated, phase-like mechanism of transcription that involves the up- and down-regulation of specific genes in a stage- and time-specific manner (Figure 1.11). These trends observed in the phaseogram lead to the “just-in-time” hypothesis which states that the induction of any gene occurs only when that gene is required. The transcription of a gene is often immediately proceeded by the translation of the gene into a mature protein product however, in *P. falciparum* a delay in protein production is observed with the majority of the genes (Le Roch *et al.*, 2004). This feature is unique to *P. falciparum* alone and suggests that there is indeed a hard-wired transcriptome and thus allows the mechanisms controlling the regulation of transcription to be one of the most sought after discoveries to date (Ganesan *et al.*, 2008).

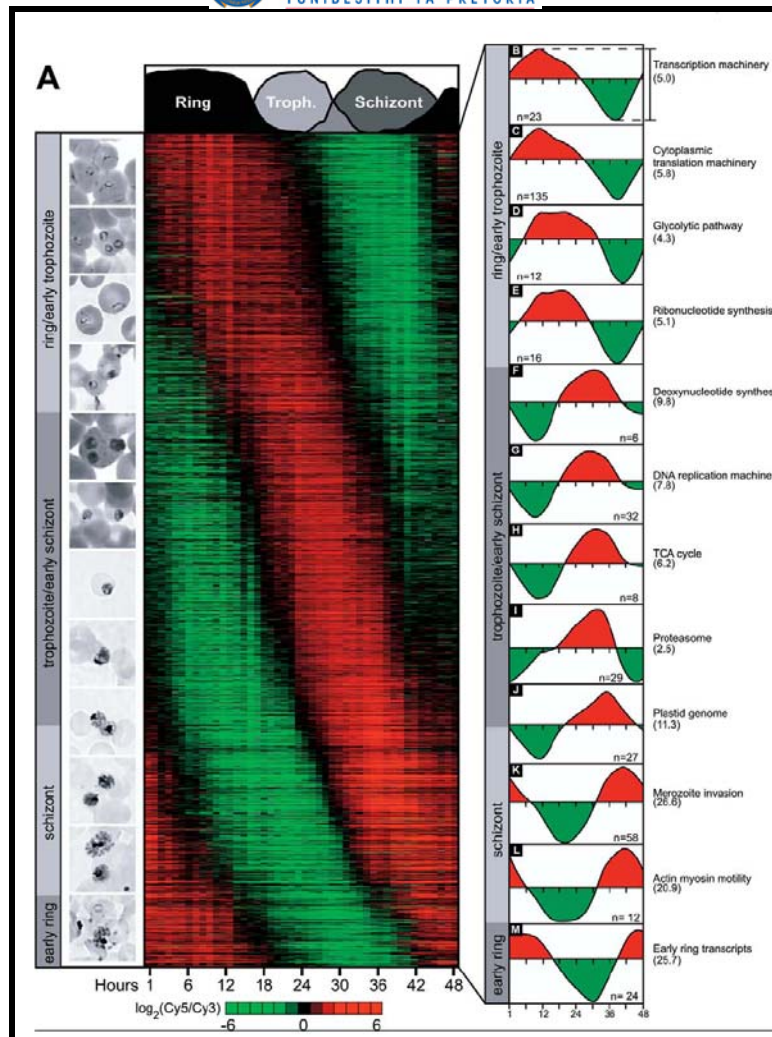


Figure 1.11: The phaseogram of the intra-erythrocytic developmental cycle of *P. falciparum* (Bozdech *et al.*, 2003).

Green represents down-regulated expression while red represents up-regulated expression. Mean peak-to-trough amplitude indicated in parentheses

Genes involved in general eukaryotic cellular functions, such as ribonucleotide synthesis and glycolysis, are abundant in the first half of the intra-erythrocytic developmental cycle (IDC) with high levels of expression representing the genes involved in the transcriptional and translational machinery, such as RNA polymerases, transcription factors and elongation factors (Figure 1.11) (Bozdech *et al.*, 2003). The expression profile of these genes decrease as the parasite progresses through into the trophozoite and schizont stage while the genes abundantly expressed during these stages of the parasite life cycle are those related to specialized parasite functions, such as cytoadherence and DNA replication, as well as those genes involved in membrane transport of host cell nutrients such as hemoglobin which is degraded into hemozoin (Bozdech *et al.*, 2003).

Hall *et al.* (2005) performed a microarray and proteomic study where they analyzed the transcriptome and proteome profile of *P. berghei* at different time points during the ring, trophozoite, schizont and gametocyte stages and identified four categories of gene expression

as follows: (i) housekeeping, (ii) host-related expression, (iii) strategy-specific expression, and (iv) stage-specific expression (Hall *et al.*, 2005). These categories and their respective proteins correlate well with the findings of Bozdech *et al.* (2003) since the host-related genes up-regulated in the gametocytes were associated with mitochondrial proteins while the strategy-specific genes involved in invasion, asexual replication and sexual development were up-regulated in the merozoite and sporozoite stages, again confirming the presence of a “just-in-time” regulation mechanism of the transcriptome (Hall *et al.*, 2005).

P. falciparum has developed mechanisms to control the levels of gene expression under various external perturbations where there appears to be tight control between transcript production and expression level. The effect of gene up- and down-regulation as a result of either drug-induction, polyamine depletion or thermoregulation are only a few examples of studies performed to determine how the parasite reacts to external perturbations and adjusts its gene expression levels accordingly, once again providing support for the tightly controlled mechanism of gene regulation within this parasite (Birkholtz *et al.*, 2008; Clark *et al.*, 2008; Gunasekera *et al.*, 2007a; Gunasekera *et al.*, 2003; Oakley *et al.*, 2007; Van Brummelen *et al.*, 2009).

1.4.1.1 *Trans-acting regulatory elements*

Several known transcription factors have been identified in the *P. falciparum* genome and the importance of transcription factors were intensely studied to reveal a complex, yet very intriguing mode-of-action as will be discussed here. Apicomplexans possess additional transcription factors in their proteome despite the presence of the expected general transcription factors (Balaji *et al.*, 2005). Analysis of the apicomplexan genomes revealed the presence of C2H2 type Zn-finger and E2F domains in proteins but the genomes seem to lack the conserved DNA binding domains found across eukaryote crown groups, such as the basic leucine zipper and basic helix-loop-helix domains (Balaji *et al.*, 2005).

Myb proteins in eukaryotes have been shown to bind DNA in a sequence-specific manner and *PfMyb*, the first non-basal transcription factor identified in *P. falciparum*, was shown to interact with the *myb* regulatory element (MRE) (Gissot *et al.*, 2005). To determine the importance of this protein, RNA interference studies were performed and the results of knocking down the gene expressing this protein caused growth inhibition *in vitro*. These results revealed the importance of *PfMyb* for growth and development of the parasite, further supporting the role of this protein as a transcription factor (Gissot *et al.*, 2005).

Studies of the apicomplexan nuclear proteins revealed the presence of a novel apicomplexan DNA binding protein known as Apicomplexan AP-2 transcription factor (ApiAP2) (De Silva *et al.*,

2008). A closer look at ApiAP2 revealed that 22 of the 26 genes encoding ApiAP2 proteins are expressed in different stages of the IDC and thus suggests that they could mediate the regulation of stage-specific genes (Figure 1.12) (Balaji *et al.*, 2005; Coleman *et al.*, 2008; De Silva *et al.*, 2008). The role of ApiAP2 proteins as transcription factors regulating transcription remain uncertain however, it has been suggested that ApiAP2 proteins interact with each other and the chromatin remodelling factors which in turn recruit these complexes to specific locations to interact with the core transcription machinery (De Silva *et al.*, 2008). It still remains unclear how individual antigenically variant genes such as the *var* genes, which are present in euchromatin, are expressed while neighbouring genes remain in a silenced state and it is assumed that this process involves specific histone modifications (which will be discussed later) or that repression is as a result of ApiAP2 protein binding (Coleman *et al.*, 2008). Voss *et al.* (2003) describe the identification of a schizont expressed binding protein which binds in a highly specific and tight manner to the subtelomeric promoter element (SPE) 2 sequence and recently, this binding protein has been identified to be a member of the ApiAP2 family of transcription factors however, its role in regulating *var* gene transcription remains to be elucidated (Flueck *et al.*, 2008).

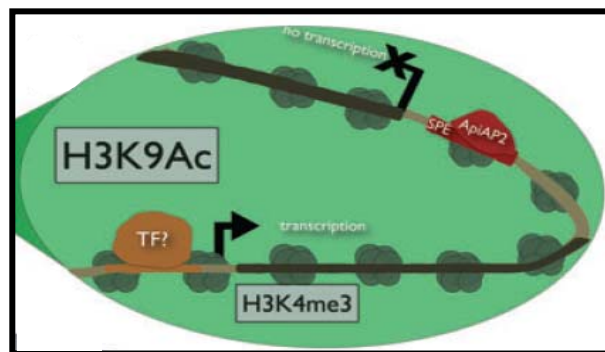


Figure 1.12: Transcriptional regulation of *var* genes occur on multiple-levels (Coleman *et al.*, 2008). The process of *var* gene silencing remains elusive and the process is likely to involve either specific histone modifications (such as histone marks H3K4me3 and H3K9Ac which designate *var* genes as active), repression via ApiAP2 binding proteins to an SPE promoter or transcription factor (TF) binding which activates specific genes.

1.4.1.2 *Cis-regulatory motifs*

Regulatory elements in *P. falciparum* have been identified using bioinformatic approaches and one of the best-defined regulatory elements in *Plasmodium* is the G-box element sequence. The G-box element is conserved throughout *Plasmodia* and was identified in the heat shock protein family to bind nuclear proteins (Militello *et al.*, 2004). The conservation of the G-box element among different *Plasmodium* species suggests that this G-box might be involved in the regulation of gene expression, however the mechanisms involved are still speculative (Militello *et al.*, 2004).

Voss *et al.* (2003) identified three nuclear proteins that bound specifically to different conserved promoter fragments termed CPE (chromosome-central *var* gene promoter element), SPE 1 and SPE 2 (subtelomeric *var* gene promoter element) (Voss *et al.*, 2003). Antigenically variant gene

families such as the *var* gene family, undergo mutually exclusive expression with *var* gene transcription occurring between 18-27 hours post invasion. The expression of SPE 1 and CPE binding proteins in the trophozoite and schizont stages suggest their role in *var* gene repression which was later confirmed with deletion studies (Voss *et al.*, 2003). It seems feasible that the binding of the regulatory protein to its cognate *cis*-regulatory sequence is associated with silencing of *var* genes and thus illustrate the possible role of nuclear proteins, with distinct promoter elements, in regulating transcription of antigenically variant genes, such as the *var* genes (Voss *et al.*, 2003).

Two distinct DNA elements were identified in the antigenic variant *rif* gene family and are believed to be associated with *rif* gene repression (Tham *et al.*, 2007). These elements (CGCACAACAC and TATGCAATGATT) also appear to bind to nuclear proteins that are expressed during different stages of the parasite life cycle while mutation and deletion of these elements in reporter gene constructs enhanced expression of the reporter gene (Tham *et al.*, 2007). An interesting finding during this study was that the one *rif* gene element (CGCACAACAC) and the *var* gene element (SPE 2) discovered by Voss *et al.* (2003) were bound by the same protein, which could imply co-regulation of repression between these two antigenically variant gene families (Tham *et al.*, 2007).

The *P. falciparum* CDP-diacylglycerol synthase (*PfCDS*) is a rate-limiting enzyme and catalyzes the conversion of phosphatidic acid to CDP-diacylglycerol (Osta *et al.*, 2002). Similar to the *var* genes, the CDS gene is expressed in a stage-specific manner with its expression peaking at the trophozoite and schizont stage (Osta *et al.*, 2002). Deletion mapping of this *PfCDS* promoter led to the identification of a 44 base pair element known as sequence B which interacts specifically with nuclear proteins isolated from trophozoite stage parasites and appears to be essential for promoter activity (Osta *et al.*, 2002). Sequence B was identified to be a *cis*-acting sequence which activates transcription when it co-operatively interacts with additional *cis*-acting elements present in the enhancer region and within sequence B there exists a 24 bp *cis*-acting element crucial for CDS promoter activity (Coleman *et al.*, 2008; Osta *et al.*, 2002).

The gametocyte specific gene *pfg27* promoter in *P. falciparum* was previously shown to be inactive during the asexual stages of the parasite life cycle but active at the start of gametocytogenesis, only to become down-regulated during gametocyte maturation (Olivieri *et al.*, 2008). Upstream of the *pfg27* gene is an element known as box C which is adjacent to a GC-rich element while box C in reverse orientation is also present downstream of the GC-rich element, followed by a poly-dA/poly-dT tract referred to as the poly A+T element (Olivieri *et al.*, 2008). Deletion of these elements in the *pfg27* promoter revealed the importance of the poly A+T element alone. This 140 base pair A+T element was able to retain the promoter in an inactive state in asexual stages and switch on the transcription of the promoter at the start of

gametocytogenesis, demonstrating the positive and negative control of a promoter through the information present in the genetic elements adjacent to it (Olivieri *et al.*, 2008). The identification of these elements suggests the presence of possible parasite-specific factors that could bind to these elements and further regulate transcription of parasitic genes.

1.4.1.3 Promoters

Promoters are regions on a DNA sequence that facilitate gene transcription and are commonly found a few nucleotides upstream from the gene they regulate. The most common promoter element found in Eukaryotic genes is the TATA box. The *var* genes of 3D7 *P. falciparum* are classified into six types according to the promoter sequence location on the chromosome and the orientation of gene transcription (Figure 1.13) (Kraemer *et al.*, 2006).

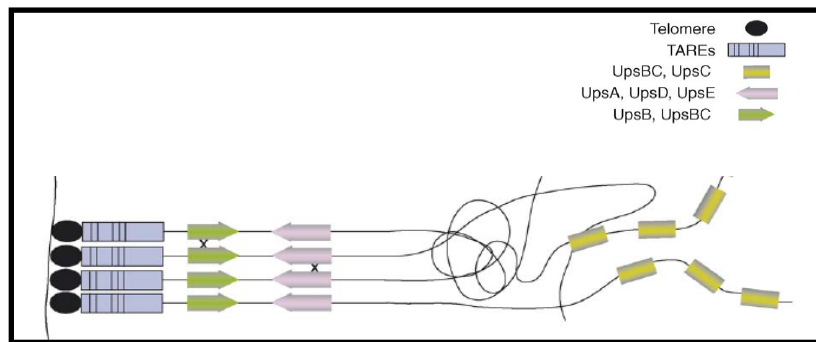


Figure 1.13: The chromosomal location and transcriptional direction of the *var* gene promoters (Kraemer *et al.*, 2006).

The UpsA, UpsD and UpsE *var* genes are located in the subtelomere and transcribed toward the telomere. UpsB *var* genes are located in the subtelomere transcribed towards the centromere. UpsC and UpsBC *var* genes are exclusively found in the chromosome internal clusters (central).

Studies on the UpsB promoter resulted in the discovery that silencing of the UpsB promoter was not dependent on the presence of the intron and that activation was dominant over silencing, while further investigations revealed the importance of the chromatin environment on gene activation and silencing (Voss *et al.*, 2007). Studies on UpsC revealed that the presence of the intron and rep20 element had no effect on UpsC promoter silencing but that the intron prevented the spread of the promoter activation, suggesting a role of the intron in preventing *var* genes found in the chromosome-central clusters from activation by an adjacent active gene (Voss *et al.*, 2006). It could be concluded that the UpsC promoter maintains the chromosome central *var* genes in a silenced state and that UpsB promoter could play a similar role in subtelomeric *var* gene silencing (Voss *et al.*, 2006). It is evident from the studies performed by Voss *et al.* (2006) that the activation of a *var* promoter is crucial in mutually exclusive expression of *var* genes and the proposed mechanism for mono-allelic *var* expression is similar to the mechanism described for *Trypanosoma brucei* which involves a perinuclear compartment, responsible for the transcription of a single *var* locus (Voss *et al.*, 2006).

1.4.2 Post-transcriptional regulation

1.4.2.1 *mRNA decay*

Orthologs of the mRNA decay components found in humans and *S. cerevisiae* have been identified in *P. falciparum*, however due to the AT-richness of the genome and the uncharacterized UTR's, identification of putative decay motifs have been very challenging (Shock *et al.*, 2007). Several proteins with similarity to RNA binding proteins, especially CCCH-type zinc finger motifs, have been discovered and are assumed to play roles in mRNA stability (Shock *et al.*, 2007).

mRNA half-lives gradually lengthen during the IDC with ring parasites having mean mRNA half-lives of 9.5 minutes, 20.5 minutes for trophozoites and increasing to 65.4 minutes for late schizonts (Shock *et al.*, 2007). The mechanisms involved in the observed mRNA half-life increase are still unknown but may include a decrease in deadenylation, decapping and exonuclease activity in later stages of the parasite life cycle (Shock *et al.*, 2007). One interesting observation was that the decay rates of genes functioning in the same pathway or process are similar, an observation also seen in yeast and mammals (Shock *et al.*, 2007).

1.4.2.2 *RNA silencing*

In *P. falciparum*, the role of nuclear non-coding RNA's (ncRNA's) are assumed to be different from their role in other eukaryotes since many of the components associated with the RNA interference machinery usually found in eukaryotes, have not been identified in *Plasmodium*. However, this suggests that ncRNA's found in *P. falciparum* might play pivotal roles in cellular processes (Li *et al.*, 2008). ncRNA's have been identified in *P. falciparum* and associate with centromeric chromatin, most likely via a protein interaction (Li *et al.*, 2008). These ncRNA's are transcribed from centromere sequences and have discrete sizes. This indicate that these transcripts are processed, most probably via a unique mechanism other than the mechanisms involved in miRNA or RNA interference (Li *et al.*, 2008). The possible role of these ncRNA's have been speculated to include organization, maintenance and function of centromeric chromatin (Li *et al.*, 2008).

The existence of RNA interference in *Plasmodium* remains controversial since database mining using the consensus sequences for Dicer, Piwi, PAZ and RdRp failed to reveal the presence of these RNA orthologs in any *Plasmodium* species. It seems that the existence of a classical RNA interference pathway is not supported by the genetic make-up of these parasites or that other mechanisms exist (Ullu *et al.*, 2004). It should however be kept in mind that RNA interference in

T. brucei has been proven to exist even though database mining failed to identify a putative Dicer homologue. This indicates that these organisms may be so divergent that protein homologues are not bioinformatically recognized (Ullu *et al.*, 2004).

Antisense oligonucleotides can reduce target mRNA transcripts in the absence of RNA interference machinery. Antisense knock-down has been performed in *Plasmodium* with great success and thus it is possible that the resulting decrease in mRNA transcripts observed in previous RNA interference studies, could be due to antisense mechanisms, rather than RNA interference (Gardiner *et al.*, 2000; Noonpakdee *et al.*, 2003; Wanidworanun *et al.*, 1999).

1.4.3 Translational regulation

Translational repression of the *Plasmodium* mRNA transcript is of utmost importance during gametocytogenesis and sexual differentiation, since this mechanism controls the expression of certain protein cascades and directs the location of translation within a cell (Mair *et al.*, 2006). The translational repression mechanism in metazoans appear to involve the interaction between RNA binding proteins (Puf) and certain sequences located in the 5' and 3' UTR of transcripts. A similar mechanism is suggested to occur in *P. falciparum* (Braks *et al.*, 2007).

The *Plasmodium* p25 and p28 genes encode proteins that play crucial roles in both zygote development and midgut invasion of the mosquito. These transcripts remain in a translationally repressed state until their translation is initiated by the ingestion of gametocytes by the mosquito (Mair *et al.*, 2006). Studies have shown that certain mRNA transcripts are packaged together with proteins into quiescent messenger ribonucleoprotein particles (mRNPs) and are stored for translation at a later stage (Mair *et al.*, 2006). In *P. bergeri* the p25 and p28 mRNA transcripts in the female gametocytes remain untranslated and associate with an RNA helicase homologue of DDX6 (DOZI) which seems to have a central role in silencing of gametocyte-specific transcripts. It additionally appears to aid in the development of functional zygotes by storing and stabilizing the mRNA in female gametocytes (Mair *et al.*, 2006).

Braks *et al.* (2007) analyzed repressed transcripts of p25 and p28 in *P. bergeri* and identified the importance of the UTR's in translational repression of these genes (Braks *et al.*, 2007). The translational repression was determined to be both stage- and sex-specific and a 47 nucleotide U-rich element, previously identified to be involved in translational repression, was eventually identified in the 3' UTR of p28, confirming its role in translational repression (Braks *et al.*, 2007).

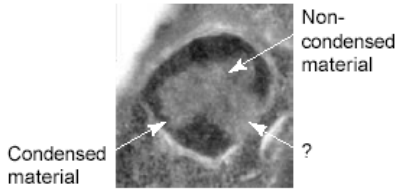
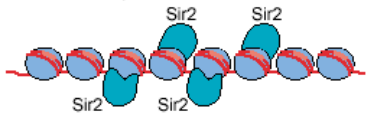
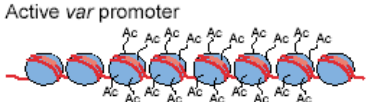
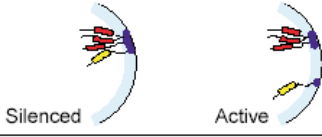
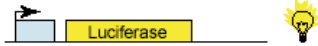

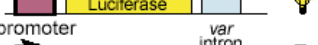
1.4.4 Epigenetic gene regulation

P. falciparum is thought to utilise various epigenetic gene regulation mechanisms to direct the tight, “just-in-time” transcription of the genes when the parasite needs them most. The *P. falciparum* *var* genes will be used as an example of epigenetic regulation due to the following evidence: mutually exclusive gene expression is evident in the trophozoite stage of *P. falciparum* when only a single *var* gene and its corresponding PfEMP1 protein is expressed at any given time, allowing the other *var* genes which were active during the ring stage, to be transcriptionally silent. Moreover, the chromosomal position and DNA sequence between an active and a silent *var* gene does not change, which implies that the difference in the transcriptional states could be due to chromatin structural changes (Deitsch *et al.*, 2004). It has been proposed that each individual *var* gene can exist in one of three different states, either transcriptionally active, transcriptionally silent or transcriptionally inactive with the ability to become active (Frank *et al.*, 2006a). The following discussions therefore focus on the different mechanisms of epigenetic variation proposed to exist in *P. falciparum*, with *var* genes as examples throughout.

Ralph *et al.* (2005) have identified four major epigenetic factors that are associated with antigenic variation of *var* genes in *P. falciparum* which include chromatin modifications and promoter interactions (Table 1.3). With reference to Table 1.3, evidence exists for the presence of epigenetic gene regulation mechanisms in *Plasmodium*. These epigenetic mechanisms include chromatin modifications such as ectopic recombination due to chromosomal end clustering (Deitsch *et al.*, 2004; Freitas-Junior *et al.*, 2000; Freitas-Junior *et al.*, 2005); the telomere positioning effect regulated by the *P. falciparum* silent information regulator (PfSir2) protein, which designates genes as either inactive or active in the presence or absence of this protein respectively (Duraisingh *et al.*, 2005; Freitas-Junior *et al.*, 2005; Ralph *et al.*, 2005b; Scherf *et al.*, 2008); the maintenance of centromeric chromatin via non-coding RNA's (Li *et al.*, 2008); heterochromatin gene movement involving the movement of active genes away from telomere clusters (Marty *et al.*, 2006; Ralph *et al.*, 2005a) and differential histone marks present on otherwise identical *var* genes (Scherf *et al.*, 2008). These epigenetic mechanisms will be discussed shortly.

Table 1.3: Four major epigenetic factors associated with *var* gene regulation in *P. falciparum* (Ralph *et al.*, 2005b).

var gene activation and silencing are assumed to be regulated by four main epigenetic mechanisms.

Epigenetic factor	Silencing of <i>var</i> genes	Activation of <i>var</i> genes	
Perinuclear heterochromatin	Unknown	Unknown	 <p>Non-condensed material Condensed material</p>
Chromatin remodeling at <i>var</i> promoters	✓	✓	<p>Silenced <i>var</i> promoter</p>  <p>Active <i>var</i> promoter</p> 
Perinuclear movement of <i>var</i> locus		✓	 <p>Silenced Active</p>
<i>var</i> intron	✓	Unknown	<p><i>var</i> promoter</p>  <p><i>hrpII</i> promoter <i>var</i> intron</p>  <p><i>var</i> promoter <i>var</i> intron</p> 

1.4.4.1 Chromatin modification

The apicomplexan genome contains three effector modules that are distributed within the parasite's histone acetyltransferase and histone deacetylase enzymes and are known to direct the folding of condensed chromatin (Hakimi *et al.*, 2007). The bromodomain binds to acetylated histone tails, the chromodomain binds to methyl-lysine and acts as a chromatin regulator and the plant homeodomain binds to the epigenetic mark H3K4me3 (Histone H3 trimethylated at lysine 4) (Hakimi *et al.*, 2007).

A single active *var* gene in *P. falciparum* is defined by histone marks as either active (H3K4me2/3) or repressive (H3K9me3) (Figure 1.14) (Issar *et al.*, 2009; Scherf *et al.*, 2008). Histone marks in eukaryotes are hypothesized to mark genes for targeting to specific transcription factories while the marks observed for *P. falciparum* have not been analyzed with regards to their nuclear spatial distribution, although it seems as though the H3K9me3 mark results in a unique sub-nuclear pattern (Issar *et al.*, 2009). Studies on *var2csa*, a member of the *var* gene repertoire known to mediate adhesion to placental chondroitin sulphate A, support the notion of the histone code. Studies showed that H3K4me2 and H3K4me3 are highly enriched in

the 5' flanking region of *var2csa* when it is actively transcribed in the ring stage but in later developmental stages of the cycle, this histone enrichment remains significant even though the *var* gene is no longer being transcribed (refer to Figure 1.14). This histone enrichment presumably acts as a bookmark for expression of this gene for the next asexual life cycle (Comeaux *et al.*, 2007).

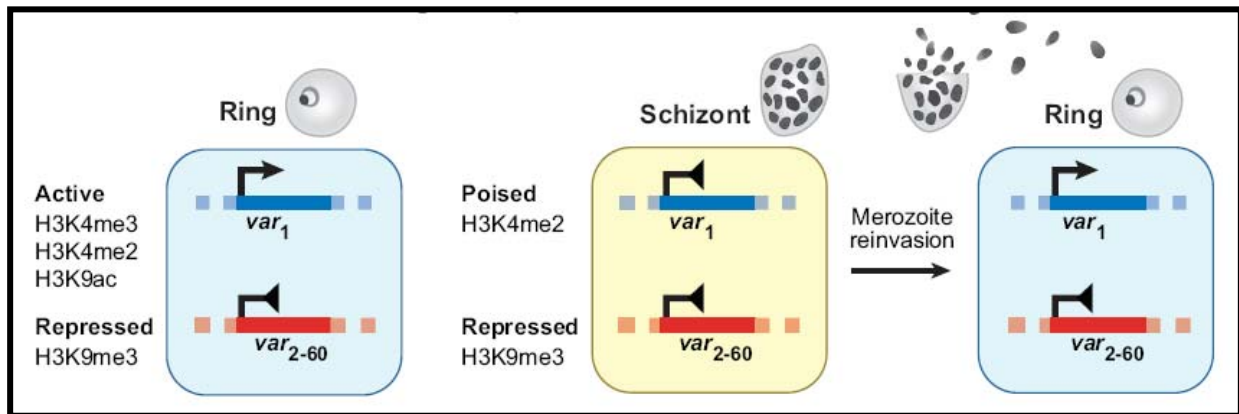


Figure 1.14: Histone marks linked to expression and epigenetic memory of *Plasmodium var* genes (Scherf *et al.*, 2008).

Three different transcriptional states of *var* genes are proposed: Actively transcribed *var* genes in ring stages (blue). The previously active gene is poised/silenced in the trophozoite/schizont stage but maintains the H3K4me2 enrichments which are assumed to transmit memory of the active *var* gene during cell division. H3K9me3 enrichment maintains stably silenced *var* genes throughout the asexual life cycle.

In contrast to this finding, H3K9me3 is enriched in the 5' flanking and coding regions of a *var* gene which is silent throughout the asexual life cycle lending further insight into the possible mechanisms the parasite utilizes to generate memory of the expression profiles of its genes through numerous generations (Comeaux *et al.*, 2007).

Histone methylation seems to be only one part of a larger "histone code" enriched at active, poised or silenced *var* gene loci (Comeaux *et al.*, 2007). Modifications such as those discussed above could work in concert with other modifications to generate a "barcode" which could signify exactly which *var* gene locus should be transcribed (Comeaux *et al.*, 2007). The ultimate significance of identifying a histone mark associated with activation, rather than silencing, implies that the absence of a silencing modification (H3K9me3) does not designate a *var* locus as active but that other activators recruited at one specific *var* locus out of the approximate 60 present in a single genome, could lead to its transcription (Comeaux *et al.*, 2007).

The question has been raised as to whether it is possible for these histone marks to denote transcriptional activation and silencing only of the *var* gene loci unique to *var* genes, or whether these marks are more universal, relating to the whole *P. falciparum* genome.

Chromosome-end clustering has been observed in budding yeast and is assumed to be associated with transcriptional silencing of telomeres (Smith *et al.*, 2001). The function of chromosomal end clustering at the telomeres of *P. falciparum* is not fully understood but it appears as though it could aid in ectopic (non-allelic) recombination events, which allow *var* genes to become aligned and in this way mediate antigenic variation (Deitsch *et al.*, 2004; Freitas-Junior *et al.*, 2005). Since the parasite lacks the telomere binding Ku complex, which is known to suppress recombination between sister telomeres in eukaryotic cells, the utilization of this form of regulation by the parasite seems to be quite possible. When two identical *P. falciparum* parental strains were crossed, the resulting progeny contained a new *var* form as a result of telomere clustering and gene recombination events (Freitas-Junior *et al.*, 2000). Gene conversion is promoted as a mechanism for this recombination since the chromosomal inheritance pattern of progeny presenting ectopic rearrangements showed that duplication of a specific fragment was common (Freitas-Junior *et al.*, 2000). An important feature for recombination in the *P. falciparum* telomere-associated sequence is the telomere-associated gene conversion events, which involves sequences located on different chromosomal ends to produce new *var* assortments (Freitas-Junior *et al.*, 2000). This therefore implies that ectopic recombination events are associated with antigenic variation to rapidly generate sequence diversity in the subtelomeric virulence genes of *P. falciparum* (Freitas-Junior *et al.*, 2000).

1.4.4.3 *Telomere specific silencing*

Variant gene families are arranged on the telomeres of chromosomes among telomeric repeats (Figure 1.15). The chromosome ends consists of telomeres which are followed by telomere associated sequences (TAS) consisting of six different blocks of telomere associated repetitive elements (TARE) (Figueiredo *et al.*, 2005). The telomere and centromere chromatin are highly condensed and can vary with modifications of histones (hyper/hypo-acetylation) which in turn cause an alteration in the gene's accessibility to regulatory elements (Freitas-Junior *et al.*, 2005; Ralph *et al.*, 2005b).

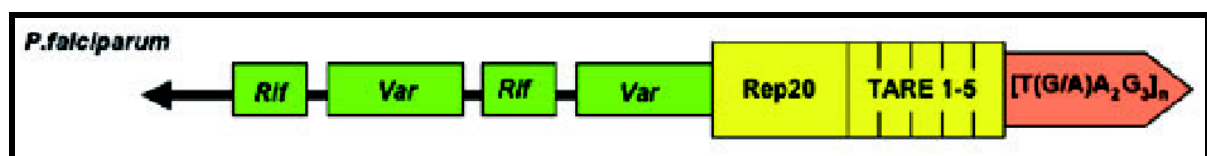


Figure 1.15: The *P. falciparum* telomere ends illustrating the arrangement of variant genes, repetitive elements (rep20) and telomere associated repeat elements (TARE's) (Merrick *et al.*, 2006).

One possible mechanism of regulating antigenic variation at the telomere is known as the telomere positioning effect (TPE). The *PfSir2* protein is a homolog of the *S. cerevisiae* histone

deacetylase SIR2 protein and is involved in the transcriptional repression of telomeric genes by producing hypoacetylated histones (Duffy *et al.*, 2007). Studies on the *var* gene UpsE promoters indicated that when the promoter was in complex with *PfSir2*, the gene transcribed by this promoter was inactive, while the dissociation of *PfSir2* from this promoter designated this gene as active (Freitas-Junior *et al.*, 2005). The silencing effect created by *PfSir2* seemed to spread into the chromosome, affecting the transcriptional state of *var* genes located up to 50kb away from the telomere (Ralph *et al.*, 2005b). The *PfSir2* protein doesn't form a complex with the UpsC promoter which suggests that the central promoters are repressed in a *PfSir2* independent manner, perhaps via the *var* intron (Duraisingh *et al.*, 2005; Freitas-Junior *et al.*, 2005).

1.4.4.4 *Heterochromatin gene movement*

Ralph *et al.* (2005) revealed that a silent subtelomeric *var* gene was associated with the telomere cluster but the activation of this gene required movement of the *var* gene away from the telomere, thus suggesting that silencing proteins such as *PfSir2* are concentrated in the telomere (Ralph *et al.*, 2005a). *var* genes are therefore required to move away from the telomere to enter the euchromatic region of the nuclear periphery which in turn will allow the transcription machinery to freely access this gene and designate it as active (Figure 1.16 [A]) (Ralph *et al.*, 2005a). There appears to be no co-localization between the telomeric clusters and the central *var* genes, supporting the speculation that other factors, such as the intron, might play a role in the silencing of central genes (Ralph *et al.*, 2005a).

Marty *et al.* (2006) discovered that the subtelomeric *var* gene co-localizes with heterologous chromosome ends within the telomere clusters, regardless of the gene being in a silent or active transcriptional state (Marty *et al.*, 2006). The mechanism of activation and silencing of the *var* genes is assumed to involve active and silent "clusters" where an activated gene is either located within the "active cluster" before its activation, or the gene is relocated from a "silent cluster" to an "active cluster" for its activation (Figure 1.16 [B]) (Marty *et al.*, 2006). The movement of chromosome ends between telomere clusters have been observed previously and therefore the possibility of chromosome ends moving to active zones within the nuclear periphery and adjusting the transcriptional states of genes, does seem to be an attractive notion (Marty *et al.*, 2006).

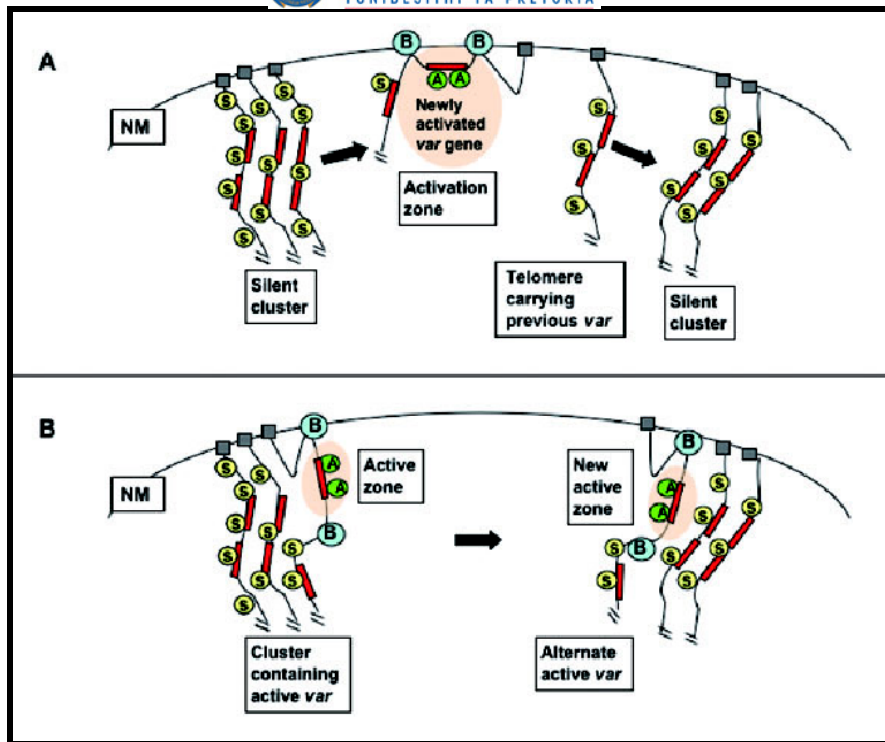


Figure 1.16: Two possible mechanisms of *var* gene activation and silencing within the parasite nucleus (Merrick *et al.*, 2006).

A) Silent *var* genes are clustered on telomeres and are associated with silencing factors while upon activation, one telomere is predicted to move into an “active zone” while the adjacent genes remain silenced. The previously active *var* gene rejoins a telomere cluster and becomes silenced.

B) A selected *var* gene becomes active while remaining in a “silenced-cluster” and is isolated from the adjacent silent genes by boundary elements. A different gene within a cluster can become active while the previously active gene becomes switched off. S: silencer, A: transactivator, NM: nuclear membrane, B: Boundary element.

More recently, an attractive hypothesis was proposed by Lopez-Rubio *et al.* (2007) in which a regulatory element, such as an enhancer, could localize within an active compartment and enhance transcription of different genes from a single promoter. This is known as the “counting mechanism” and is assumed to be used by different parasites to achieve phenotypic variation (Figure 1.17) (Lopez-Rubio *et al.*, 2007). It suggests that a single enhancer is required to activate gene members present on different chromosomes and thus interact with promoter elements of another member of the gene family, designating it as active (Lopez-Rubio *et al.*, 2007).

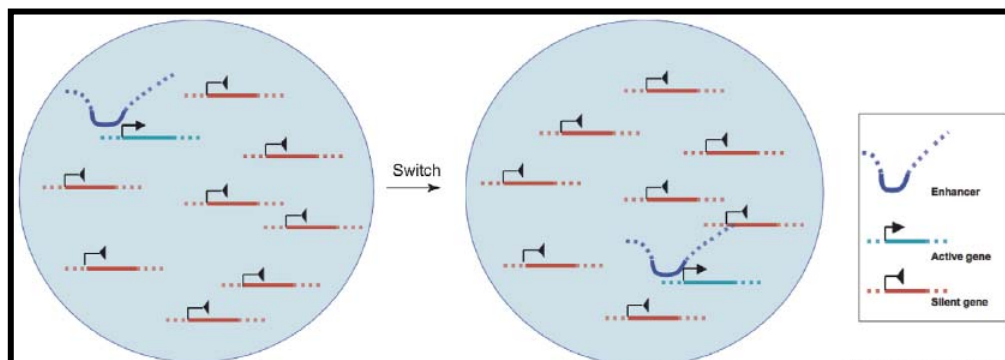


Figure 1.17: The enhancer-mediated counting mechanism hypothesis of gene switching (Lopez-Rubio *et al.*, 2007).

A unique enhancer could activate in *cis* or in *trans* gene members that are dispersed on different chromosomes.

1.4.4.5 *Intron interactions*

The intron of a *var* gene exerts a silencing effect on the promoter in a selective manner, suggesting that the intron enhances repression of the *var* promoter (Deitsch *et al.*, 2001a; Scherf, 2006). The *var* genes all contain two functional promoters, one located within the intron and the other located upstream from *var* exon I (Calderwood *et al.*, 2003). The function of the *var* intron on gene silencing is apparently through its region 2, which exerts a greater repression on the expressed gene than either region 1 or region 3 or a combination of both region 1 and 3 while deletion of region 2 was shown to cause the activation of a previously silenced promoter (Calderwood *et al.*, 2003; Gannoun-Zaki *et al.*, 2005). Moreover, a *var* promoter paired with an intron is silenced and dissociation of the promoter from the intron results in the activation of the promoter (Figure 1.18) (Frank *et al.*, 2006b).

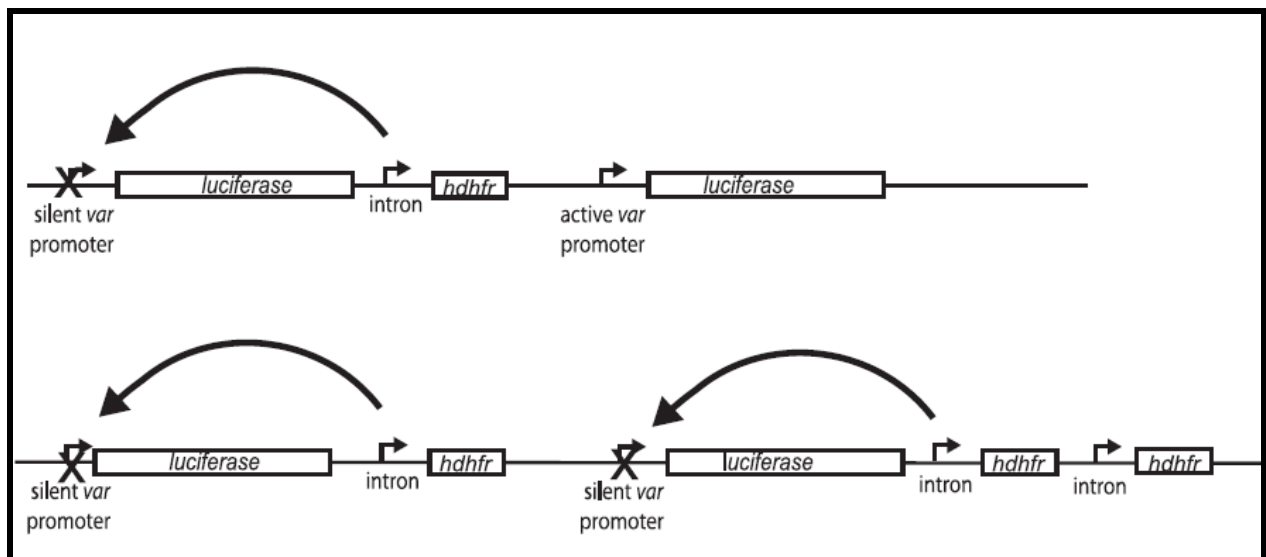


Figure 1.18: Illustration of the strict pairing of a *var* intron and *var* promoter required for *var* gene silencing (Frank *et al.*, 2006b).

In the top figure, a *var* promoter and *var* intron is paired resulting in the promoter being silenced however, the unpaired *var* promoter remains active, allowing active expression to take place. This demonstrates that a single *var* intron can only silence one *var* promoter, even if several *var* promoters are in close proximity. In the bottom figure, *var* promoters are paired with their *var* introns resulting in silenced promoters, while the unpaired *var* intron, with intrinsic promoter activity, results in active expression.

After analysing the complex nature of its existence, it is quite clear that the malaria parasite *P. falciparum* has various facets in its life cycle that need thorough regulation, from surviving in the mosquito host, to penetrating various cells and finally to remain outside the immune radar of the human host. The various mechanisms involved in gene regulation is therefore of major interest since the design and synthesis of drugs against the transcriptional and translational machinery of the parasite, could aid in complete elimination of the parasite.

This study will therefore attempt to investigate gene regulatory mechanisms in *P. falciparum* by focussing on the transcriptional and post-transcriptional levels of regulation.



1.5 OBJECTIVES AND AIMS

The main objective of this research was to investigate transcriptional and post-transcriptional mechanisms of gene regulation in *P. falciparum*. As such, Chapter 2 aimed to investigate the transcriptional level of regulation and involved analyzing the importance of five conserved motifs, previously identified in the 5' UTR of *P. falciparum var* genes, in the binding to regulatory protein binding partners.

In Chapter 3, the post-transcriptional level of regulation was studied by exploiting the polyamine biosynthetic pathway of *P. falciparum* with the use of RNA interference. RNA interference was performed on the polyamine biosynthetic enzymes Spermidine synthase and S-Adenosylmethionine decarboxylase/Ornithine decarboxylase, to characterize these as anti-malarial drug targets.

The results described in this dissertation have been presented at the following conference:

- 2007: Molecular and Cellular Biology Group (MCBG) Conference
Title: *Cis*-regulatory motifs contribute towards the regulation of gene expression and antigenic variation in the malaria parasite *Plasmodium falciparum*.

CHAPTER 2

IDENTIFICATION OF *P. FALCIPARUM* NUCLEAR PROTEINS AS REGULATORY TRANSCRIPTION FACTORS IN TRANSCRIPTIONAL REGULATION

2.1 INTRODUCTION

P. falciparum resides in the mature host erythrocyte, an ideal home for this parasite since erythrocytes do not differentiate, do not possess any protein synthesis or trafficking machinery and do not express any of the major histocompatibility complex (MHC) molecules such as MHC class I or II on its surface (Deutsch *et al.*, 1997; Newbold, 1999; Scherf *et al.*, 2008). *P. falciparum* utilizes the resources within the erythrocyte to synthesize parasite-specific proteins, which are then exported to the surface of the erythrocyte (located in so-called knobs) and mediate the binding of the parasitized erythrocyte to other endothelial surfaces (cytoadherence) and in this way avoid non-specific clearance from the spleen (Fernandez *et al.*, 1999; Newbold, 1999; Sherman *et al.*, 2003). These parasite-specific proteins include PfEMP1, rifin, stevor, PfMC-2TM and surfin (Figure 2.1) (Lavazec *et al.*, 2007; Trenholme *et al.*, 2004).

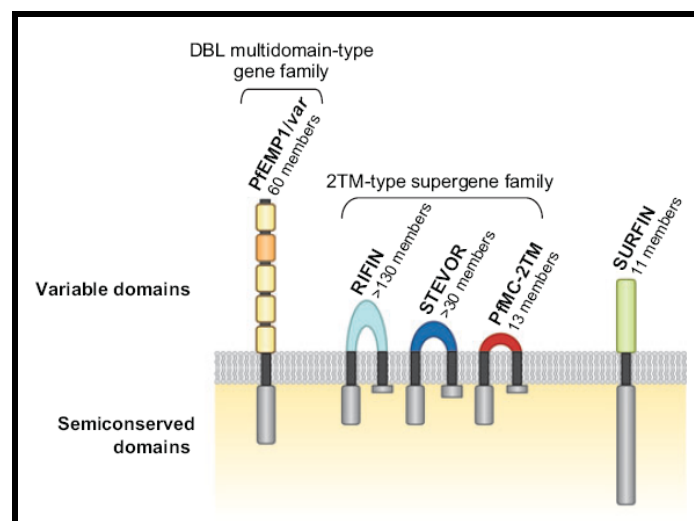


Figure 2.1: Gene families encoding the variant surface molecules exposed on the *P. falciparum* infected erythrocyte surface (Scherf *et al.*, 2008).

In addition to preventing clearance by the spleen, the above-mentioned proteins provide the major advantage to the parasite of immune system evasion through a process called antigenic variation. Antigenic variation has been used by numerous microbes other than *P. falciparum* such as *T. brucei*, *Neisseria meningitidis*, *N. gonorrhoea* and *Haemophilus influenzae*, with the rate of antigenic variation in *P. falciparum* parasite being approximately 2% per generation. This is extremely important since the rate needs to be fast enough to prevent complete elimination from the host immune system and slow enough to ensure that the entire repertoire of antigens

are not expressed too quickly (Frank *et al.*, 2006a). The switch rates of antigens are believed to be an intrinsic property of each individual gene and this in turn suggests that the activation and silencing of a particular gene could be controlled by the surrounding DNA (Deitsch *et al.*, 2004).

The *var* gene family, discovered in 1995, encodes the antigenically variant protein *PfEMP1*, which is exposed on the surface of infected erythrocytes and has the ability to mediate the binding of the infected erythrocyte to other surfaces (Voss *et al.*, 2000). *PfEMP1* is a high molecular weight protein (~250 kDa) which recognizes various receptors such as intercellular adhesion molecule-1 (ICAM), cluster determinant 36 (CD36) and chondroitin sulphate A (CSA) (Dzikowski *et al.*, 2006; Keys *et al.*, 2007; Smith *et al.*, 2001). There are approximately 59 highly diverse *var* genes per haploid *P. falciparum* genome and these genes are predominantly found in the subtelomeric regions of all 14 chromosomes, except chromosome 14 (Trenholme *et al.*, 2004). The 5' exon of the *var* gene encodes the extra-cellular portion of the *PfEMP1* protein while the short 3' exon encodes the cytoplasmic tail and remains conserved between the *var* genes (Figure 2.2) (Ralph *et al.*, 2005b). The transcription of the *var* genes starts at around 12 hours post invasion, after which the transcription becomes tightly regulated where transcription of only a single *var* gene dominates during the trophozoite stage (Voss *et al.*, 2000)

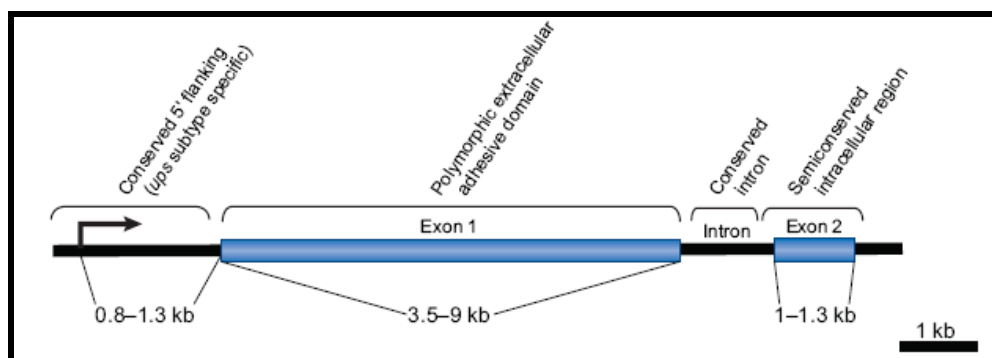


Figure 2.2: The structure of a *var* gene (Scherf *et al.*, 2008).

The *rifin* (repetitive interspersed family) gene family code for immunogenic proteins that are expressed on the infected erythrocyte surface and function in antigenic variation (Table 2.1). The *rif* genes are located in close proximity to the *var* genes and are assumed to be associated with rosetting. The *rif*, *stevor* and *Pfmc-2TM* genes all share a common two transmembrane structure consisting of a short first exon encoding a signal peptide sequence, a long exon which encodes the rest of the gene and a short variant loop of amino acids exposed at the surface of the erythrocyte (Dzikowski *et al.*, 2006). Rifins are abundantly found in sporozoites, merozoites and gametocytes to allow A-type rifins to be exported to Maurer's cleft and the erythrocyte surface, while the B-type rifins reside within the parasite (Joannin *et al.*, 2008).

Approximately 30-40 *stevor* genes encode *stevor* proteins (~30-40 kDa) located subtelomerically on all 14 chromosomes of *P. falciparum* (Blythe *et al.*, 2004). Transcription of

these *stevor* genes within *P. falciparum* 3D7 was shown to occur between 22 and 32 hours post invasion, with peak transcription occurring at 28 hours post invasion (Blythe *et al.*, 2004). A selected subset of *stevor* is transcribed at any given point and *stevor* migrates to Maurer's cleft to protect the components within the Maurer's cleft during the schizont stage when naturally occurring antibodies can freely pass through the erythrocyte membrane (Blythe *et al.*, 2004). During the asexual stage of the parasite's life cycle, the *stevor* proteins are expressed after *PfEMP1* and *rifin* which suggests an important function of *stevor* proteins in late stage parasites, perhaps aiding in cytoadherence (Blythe *et al.*, 2004).

The *Pfmc-2TM* gene family encodes the *Pfmc-2TM* proteins and are localized to the Maurer's cleft while the *surfin* (surface associated interspersed genes) multi-gene family encodes *surfin* proteins exported to the erythrocyte surface (Dzikowski *et al.*, 2006). The ultimate roles of these proteins have yet to be discovered and it remains unknown if gene expression switching occurs (Scherf *et al.*, 2008).

Table 2.1: Features of the antigenically variant gene families in *P. falciparum* strain 3D7 [adapted from (Dzikowski *et al.*, 2006; Rasti *et al.*, 2004; Scherf *et al.*, 2008; Winter *et al.*, 2005).

Feature	<i>var</i>	<i>rif</i>	<i>stevor</i>	<i>PfMC-2TM</i>	<i>Surf</i>
Functions	Cytoadherence Immune escape Immunomodulation	Unknown	Unknown	Unknown	Unknown
Subcellular location	Maurer's cleft/ Infected erythrocyte surface	Maurer's cleft/Parasitophorous vacuole/Merozoite	Maurer's cleft/Parasitophorous vacuole/Merozoite	Maurer's cleft/Parasitophorous vacuole	Maurer's cleft/Parasitophorous vacuole/Infected erythrocyte surface/Merozoite
Protein size	200-350 kDa	30-45 kDa	30-40 kDa	27 kDa	280-300 kDa
Gene copies	~60	~150	~28-40	~13	~10
Variant antigen	<i>PfEMP1</i>	<i>rifin</i>	<i>stevor</i>	<i>Pfmc-2TM</i>	<i>surfin</i>
mRNA expression (h.p.i)	3-18	12-27	22-32	18-30	<6-40

h.p.i: Hours post invasion.

2.1.1 *var* gene regulatory sequences

Bioinformatics has proven to be a reliable technique to identify conserved motifs with probable functions in gene regulation. An *in silico* search for conserved motifs was performed previously with the use of the MADIBA web server (MicroArray Data Interface for Biological Annotation), which was developed to facilitate the interpretation of the biological significance of gene clusters (Law *et al.*, 2008) (Claudel-Renard, Unpublished work). The complete genome was analysed for over-represented DNA sequences, a similar strategy to that used by Tompa *et al.* (2005) and reviewed by Walhout *et al.* (2006) (Tompa *et al.*, 2005; Walhout, 2006). Subsequently, an additional analysis was performed to determine how many of these genome wide "hits" were

present in the antigenically variant genes. This resulted in the identification of conserved motifs in the upstream regions of antigenically variant genes, including *var*, *rif*, and *stevor* (Table 2.2). The motifs identified are sequence motifs consisting of a nucleotide pattern in a DNA sequence, while the Dyad consists of two sets of four conserved nucleotides separated by two random nucleotides (assigned as N) (Table 2.2) (Claudel-Renard, C. unpublished work).

Table 2.2: Conserved motifs identified via an *in silico* search.

Motif name	Sequence	Important genes in the genome	Important <i>PfEMP1</i> or <i>var</i>	Interesting genes	Motif position
Dyad	ACATNNTGTC	156	44	1 <i>stevor</i> , 4 <i>rif</i>	-40-50 nt
Motif 1	CTCCATAAC	34	29	3 <i>rif</i>	-100 nt
Motif 2	TCGGTACTG	15	15		-600 nt
Motif 3	GCCTCTGTTG	16	14	1 <i>rif</i>	-1100 nt
Motif 4	CGAAATCGTG	21	21		-1150 nt

Significant findings are highlighted in bold since the *in silico* search indicated Motif 2 and Motif 4 sequences are exclusively located in the *var* gene family.

As discussed in this chapter, *var* genes have various levels of regulation which include regulatory sequences. These *cis*-acting regulatory elements are bound by proteins and thus this chapter aimed to identify the protein binding partners to the *cis*-motifs with the use of the following techniques.

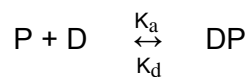
2.1.2 DNA-protein interactions

DNA binding proteins are categorized as either functional or structural and these features should enable the protein to access the nucleotide bases through either the major or minor groove. The major groove is generally the site of direct information readout while the minor groove is an important target for proteins that expand the major groove upon binding (Neidle, 2002). Minor groove interactions assist in DNA-protein stabilization and commonly prefer AT base pairs. DNA bending may also be required to reveal residues that were previously unseen and in this way, optimize interactions by producing favourable protein contacts (Neidle, 2002). Regulatory proteins can control gene transcription by binding to double-stranded DNA in a highly specific manner, or it can initiate transcription by binding to a particular sequence such as the 5' TATA sequence (Neidle, 2002). Other DNA binding proteins serve functions such as cleavage proteins (DNase I) which have structural selectivity and little sequence specificity, repair proteins, structural proteins such as histones which maintain integrity of packaged DNA, DNA topoisomerases which function to resolve topological problems and processing proteins typified by DNA and RNA polymerases (Neidle, 2002).

There are a limited number of ways in which proteins can recognise double-stranded DNA and typical recognition motifs include the helix-turn-helix, helix-loop-helix, Zinc-finger, Zipper motifs, β -sheets and β -hairpins (Neidle, 2002). Helix-turn-helix motifs are major groove binding motifs

and consists of 20 amino acid residues while Zinc-fingers form the largest family of DNA-binding motifs and involve sequence-specific recognition, by recognizing a 3 bp site in the major groove of B-DNA (Neidle, 2002). Leucine zippers are long, continuous, almost straight α -helices with regularly repeating leucine residues and form a coiled coil structure when two helices interact (Lilley, 1995; Neidle, 2002).

Direct DNA-protein contacts involve the formation of hydrogen bonds between amino acid side chains and the nucleotide while long range electrostatic interactions occur between the ionized phosphate group of the nucleic acid and the guanidium or imidazole group of arginine and histidine respectively (Lilley, 1995). Simple kinetic analysis can explain the interaction and the issues underlying the interaction between protein and DNA. When a univalent protein (P) binds to its site on the DNA molecule (D) it will form a complex (DP) which is in equilibrium with the free components, where K_a is the association constant and K_d the rate of dissociation (Moss, 2001)



A strong DNA-protein interaction will have a K_a larger than K_d and two distinct bands corresponding to the complex (DP) and the free DNA (D) will be observed during the gel run. However, during electrophoresis, dissociation is expected and it is impossible for the released DNA to ever catch up with the free DNA therefore causing a slight smear in the resulting gel (Moss, 2001). If the interaction is weak, where K_a is smaller than K_d , a faint band representing the complex (DP) will be visible as a more obvious smear (Moss, 2001).

To understand gene expression at the molecular level requires analyzing the interaction of nucleic acids with various regulatory proteins (Ahmed, 2005). The regulation of various genes relies on the interaction of a specific protein with a DNA sequence and a technique which is central to studying this interaction is known as an electrophoretic mobility shift assay (EMSA). Electrophoretic mobility shift assays are utilized to detect DNA-binding factors by assessing the degree to which the binding protein affects the electrophoretic mobility of specific DNA sequences through a non-denaturing polyacrylamide gel (Walker, 2002). The principle behind EMSA's is that proteins with different molecular weights, charge and size will differ in their electrophoretic mobility in a non-denaturing polyacrylamide gel and thus, DNA in complex with such a protein, will have a different mobility in a non-denaturing gel than a free DNA segment (Moss, 2001). The major advantage of an EMSA is that the protein used in the DNA-protein assay does not necessarily need to be from a purified sample and may be from a crude nuclear protein extract. This assay also provides information on the number and type of binding proteins. If a sequence is bound by multiple proteins or if multiple forms of a protein (eg.

phosphorylation states) bind to a sequence, these complexes can be resolved and characterized.

In this study, EMSA's were utilized to identify protein binding partners to conserved motifs in *var* gene UTR since EMSA's provide a sensitive method to study DNA-protein interactions and transcriptional regulators. In order to detect any DNA-protein complexes, the DNA fragment can be labelled with either radioactive labels such as ^{32}P , covalent or non-covalent fluorophores, non-radioactive biotin or hapten labels and detected via autoradiography, fluorescence imaging, chemiluminescent imaging or chromophore deposition (Hellman *et al.*, 2007).

2.2 MATERIALS AND METHODS

2.2.1 *Cis*-regulatory elements containing the conserved motifs

The conserved motifs identified via an *in silico* approach in the upstream UTR of the *var* genes were used to design oligonucleotides to be used in EMSA procedures (Table 2.2). The conserved motifs consist of ~10 nucleotides each, which were too short for gel analysis. Therefore, the *var* gene sequences were analyzed and approximately 10-15 conserved nucleotides were added to either side of the conserved motif to produce oligonucleotides with a final length of ~40 nucleotides. The conserved motifs and their flanking regions were obtained from GeneDB (www.genedb.org) and since each conserved motif appeared on more than one chromosome, the flanking regions varied. A multiple alignment was performed with each motif where the various flanking regions associated with the conserved sequence was aligned using CLUSTALW (www.ebi.ac.uk/clustalw) to obtain consensus sequences for the motifs.

Lyophilized oligonucleotides (IDT, Germany) were resuspended in Tris buffer (10 mM Tris-HCl, pH 8) to obtain a final concentration of 100 mM of each oligonucleotide by rotation (120 r.p.m) at 4°C, overnight (Rotator HAG, Korea). Oligonucleotide concentrations were determined spectrophotometrically by determining absorbance at 230 nm, 260 nm, 280 nm and 320 nm with a Genequant Pro Spectrophotometer (Amersham Biosciences). The $A_{260}:A_{280}$ ratios for all the oligonucleotides ranged between 1.7 and 2.2 indicating that the oligonucleotides were pure. The oligonucleotide molar concentrations were determined using the formula:

$$\text{pmol}/\mu\text{l} = (\text{ng}/\mu\text{l}) / \text{MW}_{\text{oligonucleotide}} \times \text{dilution factor}$$

2.2.2 *P. falciparum* cell culture

All media and solutions utilized in the culturing procedure were prepared under sterile conditions with the use of sterile double distilled, de-ionized (ddd) water and were sterilized either by autoclaving or filtration (0.22 µm filters). General ethical clearance for all *in vitro P. falciparum* culturing has been obtained from the ethical committee of the Faculty of Natural and Agricultural Sciences (investigator Prof L. Birkholtz).

Blood (O⁺) from consenting volunteers were collected in vacutainer tubes containing Ethylenediaminetetraacetic acid (EDTA) as anticoagulant and centrifuged for 5 minutes at 2500xg (Hermle Z 320, Hermle Labortechnik GmbH, Germany). The serum, platelets and white blood cells were removed and the pelleted erythrocytes were resuspended in one pellet volume of incomplete culture media (1.04% w/v RPMI (Sigma), 0.022 M glucose (Sigma), 0.025 M HEPES (Sigma), 0.005% w/v Hypoxanthine (Sigma), 0.096% v/v Gentamicin (Sigma) and 0.25 M Bicarbonate (Merck) pH 7.4), mixed and centrifuged as before. This wash step was repeated three times after which the pelleted erythrocytes were resuspended in one pellet volume of incomplete culture medium to obtain a hematocrit of 50%. The erythrocytes were stored at 4°C and washed every two days by centrifugation and resuspension in fresh incomplete culture media.

P. falciparum strain 3D7 was thawed from cryopreservation in liquid nitrogen (-190 °C) in a 37°C water bath for 3 minutes. The thawed parasite suspension (~1 ml) was transferred under sterile conditions to 10 ml tubes (Corning, Sigma-Aldrich) and 0.2 ml sterile 12% (w/v) NaCl was slowly added, followed by mixing the suspension with gentle pipetting. Subsequently, 1.8 ml sterile 1.6% (w/v) NaCl was added to the suspension, mixed by pipetting and centrifuged for 5 minutes at 2500xg. The supernatant was aspirated and 1 ml washed erythrocytes were added to the parasite pellet and mixed by gentle pipetting. The suspension of cells was transferred to 75 cm³ Lasec tissue culture flasks and 10 ml of pre-warmed (37 °C) complete culture medium (incomplete culture medium with 0.5% w/v Albumax II (Invitrogen)) was added to obtain a final hematocrit of 5%. The culture was gassed with a gas mixture (Afrox, South Africa) consisting of 5% oxygen, 5% carbon dioxide and 90% nitrogen, sealed airtight and incubated at 37 °C in a NAPCO CO₂ incubator (Precision Scientific).

The parasites were maintained in culture with modification of the original method of Trager and Jensen (Trager *et al.*, 1976) with daily microscopic monitoring of Giemsa-stained thin smears (Nikon AFXDX microscope equipped with a camera), adding fresh culture media and gassing. Parasitemia and hematocrit values of the parasite cultures were calculated and adjusted

accordingly to ensure a parasitemia of 5-10% and hematocrit of ~5% throughout the culturing period.

P. falciparum cultures were synchronized with the addition of filtered 5% w/v D-Sorbitol when the parasites were predominantly in the ring stage. Sorbitol is used to convert an asynchronous mixed stage parasite culture to a synchronous culture by eliminating trophozoite and schizont stage parasites since trophozoite and schizont infected erythrocytes are osmotically intolerant to sorbitol while ring stage parasites remain intact and unaffected. Parasites were pelleted by centrifugation for 5 minutes at 2500xg after which 5 pellet volumes of sterile, pre-warmed (37 °C) 5% w/v D-Sorbitol was added to the parasite pellet and mixed by gentle pipetting. After incubation at 37°C for 10 minutes, the parasite suspension was centrifuged for 5 minutes at 2500xg and the pellet washed twice by addition of one pellet volume of complete culture medium and centrifuged as above. Finally, the parasites were resuspended in complete culture media and fresh erythrocytes were added to obtain a final hematocrit of 5%, after which the flasks were gassed and placed in an incubator (37°C).

2.2.3 Nuclear extraction from cell culture

2.2.3.1 Nuclear protein extraction (Voss *et al*, 2003)

Sixteen flasks of 30 ml *P. falciparum* cultures with ~7% parasitemia and 5% hematocrit were transferred to 50 ml centrifuge tubes and centrifuged at 2500xg. The supernatant was aspirated and 5 pellet volumes of a 0.05% w/v saponin in PBS (10 mM Na₂HPO₄, 1.4 mM KH₂PO₄, 137 mM NaCl and 2 mM KCl, pH 7.4) was added to the pellet, the suspension was mixed well and placed on ice for 10 minutes to allow cell lysis to occur. Saponin forms a complex with the cholesterol in erythrocytes and thus forms pores in the cell membrane bilayer, ultimately leading to erythrocyte lysis. The lysed parasites were centrifuged for 5 minutes at 2500xg after which the supernatant was aspirated and the pellet washed by the addition of one pellet volume of ice-cold 1xPBS and subsequently centrifuged at 4°C for 2 minutes at 11 000xg. The pellet was washed twice more with 1xPBS as described previously, until the supernatant appeared clear.

The supernatant was aspirated and 1.5 ml ice cold lysis buffer (20 mM Hepes, pH 7.8, 10 mM KCl, 1 mM EDTA, 1 mM EGTA, 1mM DTT, 1 x Protease inhibitor cocktail (Roche), 0.65% v/v NP40)) was added to the pellet, mixed well and incubated on ice for 5 minutes. The protease inhibitor cocktail consists of various protease inhibitors such as the serine protease inhibitors Chymotrypsin and Trypsin, the cysteine protease inhibitor Papain and the metalloprotease inhibitor Thermolysin, which provide reliable protection against proteases which are released during different extraction procedures. Non-ionic detergents such as Tween20 and Triton X-100

have uncharged hydrophilic head groups with a poly-oxyethylene polar region and are often used for the isolation and solubilisation of functional proteins (Hellman *et al.*, 2007). Nonidet P40 (NP40) is a non-ionic, non-denaturing detergent, used for solubilizing the membrane proteins during this isolation procedure. The pellet was centrifuged for 5 minutes at 2500xg and the supernatant containing the cytoplasmic proteins was carefully transferred to an Eppendorf tube. The pellet was resuspended in 1.5 ml ice cold lysis buffer, incubated on ice for 5 minutes and centrifuged as before. The supernatant was removed and combined with the previous supernatant to be stored at -70°C.

The nuclear pellet was washed three more times with 1 ml lysis buffer until the supernatant was clear. The nuclear pellet was resuspended in 1 pellet volume of nuclear extraction buffer (20 mM Hepes, pH 7.8, 800 mM KCl, 1 mM EDTA, 1 mM EGTA, 1 mM DTT, 1x complete protease inhibitor cocktail (Roche)) and vortexed at a high speed (Heidolph vortex, Reax 2000, Germany) for 30 minutes at 4 °C. The suspension was subsequently centrifuged for 3 minutes at 13 000xg at 4°C (Eppendorf centrifuge 5415R, Eppendorf, Germany) and the supernatant containing the nuclear proteins were transferred to a new Eppendorf tube. The supernatant was centrifuged for 30 minutes at 13 000xg at 4°C after which the supernatant was transferred to a new tube and one pellet volume of dilution buffer (20 mM Hepes, pH 7.8, 1 mM EDTA, 1 mM EGTA, 1 mM DTT, 30% v/v glycerol) was added to the nuclear extract pellet and stored at -70°C.

2.2.3.2 Commercial protein extraction protocols

The protein yield of nuclear and cytoplasmic extracts from two kits, the NucBuster kit from Novagen and the ProteoJet kit from Fermentas, were compared to each other and the Voss extraction protocol. To do this, one 45 ml flask of *P. falciparum* culture was gently mixed to obtain an evenly dispersed suspension of erythrocytes, infected erythrocytes and culture medium. The flask was split into three 15 ml volumes and centrifuged at 2500xg for 5 minutes. Saponin lysis was performed as in section 2.2.3.1. One 15 ml volume of culture was used to extract nuclear and cytoplasmic proteins with the Voss protocol as described in section 2.2.3.1. All centrifugation steps to follow were performed at 4 °C and all reagents and reactions were placed on ice throughout the entire extraction procedure.

For the NucBuster extraction protocol, the instructions were followed as described by the manufacturer. First, the 40 µl *P. falciparum* parasite pellet obtained after saponin lysis, was resuspended in 150 µl proprietary reagent 1 and vortexed at maximum speed for 15 seconds. The reaction was incubated on ice for 5 minutes after which it was vortexed again at maximum speed for 15 seconds and centrifuged at 16 000xg for 5 minutes, 4 °C. The supernatant, which contains the cytoplasmic proteins, was transferred to a new Eppendorf tube and stored at -70

°C. The pellet was washed with 500 µl ice cold 1xPBS, centrifuged at 16 000xg for 5 minutes to remove the excess cytoplasmic proteins and the supernatant discarded. The pellet was resuspended in 75 µl proprietary reagent 2, supplemented with 1 µl (100 x) protease inhibitor cocktail supplied by the NucBuster kit and 1 µl 100 mM DTT. The suspension was vortexed at maximum speed for 15 seconds, incubated on ice for 5 minutes, vortexed a second time and centrifuged at 16 000xg for 5 minutes. The supernatant, containing the nuclear proteins, was transferred to a new Eppendorf tube and stored at -70°C.

The ProteoJet extraction procedure was also followed as described by the manufacturer. The 40 µl *P. falciparum* parasite pellet obtained after saponin lysis was resuspended in 500 µl proprietary cell lysis buffer supplemented with 20 µl (25 x) complete protease inhibitor cocktail (Roche) and 5 µl 100 mM DTT. The suspension was vortexed for 10 seconds, incubated on ice for 10 minutes, vortexed again for 10 seconds and centrifuged for 7 minutes at 500xg. The supernatant containing the cytoplasmic proteins was transferred to a new Eppendorf tube and the pellet was placed on ice. The supernatant was centrifuged at 16 000xg for 20 minutes and the supernatant was transferred to a clean Eppendorf tube and stored at -70°C. The nuclei pellet was washed with 500 µl proprietary wash buffer supplemented with 20 µl (25 x) protease inhibitor cocktail and 15 µl 100 mM DTT, vortexed briefly, incubated on ice for 2 minutes and centrifuged at 500xg for 7 minutes. This wash step was repeated once more after which the supernatant containing some cytoplasmic proteins was transferred to a clean Eppendorf tube and stored at -70°C. The pellet was resuspended in 150 µl proprietary storage buffer supplemented with 6 µl (25 x) protease inhibitor cocktail and 7.5 µl 100 mM DTT, followed by the addition of 15 µl proprietary lysis buffer to the nuclei pellet, vortexed at 4°C at moderate speed for 15 minutes and centrifuged at 16 000xg for 10 minutes. The supernatant containing the nuclear proteins was transferred to a clean Eppendorf tube and stored at -70 °C.

2.2.3.3 Measurement of protein yield

Due to the presence of many interfering substances such as detergents, reductants and ampholytes in the extraction buffers used, careful consideration regarding the method of quantitation was required. Both the Bradford assay and the Micro BCA Protein assay kit (Pierce) gave inaccurate results (not shown) and thus the 2-D Quant kit (Amersham Biosciences) was used to accurately quantify the protein present in extract samples. The 2-D Quant kit works by quantitatively precipitating proteins while the interfering substances remain in solution. The precipitated proteins are then resuspended in a copper containing solution, which allows the cupric ions to bind to polypeptide backbones present in proteins. The unbound copper is measured with a colorimetric reagent. The absorbency of the reactions is measured at 492 nm and the intensity of the colour is inversely proportional to the protein concentration.

Standard curves were set up as described in the 2-D Quant kit manual. For the standard curve, six tubes were set up, each containing increasing amounts (0 µg – 50 µg) of the BSA (2 mg/ml) standard solution provided with the kit. Three tubes containing 10 µl, 20 µl and 30 µl of the nuclear extract were set up and identical reactions were set up for the cytoplasmic extract. The proprietary colorimetric working reagent was prepared fresh as described by the kit.

First, 500µl of proprietary precipitant from the kit was added to each tube and each tube was vortexed briefly, incubated at room temperature for 3 minutes after which 500 µl of proprietary co-precipitant was added and vortexed briefly. Each tube was inverted prior to centrifugation at 16 000xg for 3 minutes at 4°C. The supernatant was decanted and the tubes containing white precipitate were centrifuged at 16 000xg for 3 minutes at 4°C, after which the remaining supernatant was carefully removed, followed by the addition of 100 µl proprietary copper solution and 400 µl ddd water. The tubes were vortexed to dissolve the precipitate and 1 ml of the freshly prepared colorimetric working reagent was added to each tube, immediately inverted and incubated at room temperature for 20 minutes after which 300 µl from each tube was transferred to an ELISA plate in triplicate and the absorbance was read at 492 nm.

2.2.3.4 SDS-PAGE analysis of nuclear proteins

To analyze and compare the protein profiles of the nuclear and cytoplasmic extracts of *P. falciparum*, sodium dodecyl sulphate polyacrylamide gel electrophoresis (SDS-PAGE) and silver staining was performed. SDS-PAGE is a technique widely used to separate proteins based on size, since the non-ionic detergent SDS allows all the proteins in the sample to be negatively charged. The SDS-polyacrylamide gel consisted of a 4% stacking gel and a 10% separating gel. The 10% separating gel (39% v/v ddd H₂O, 25% v/v 1.5 M Tris-HCl, pH 8.8, 1% v/v 10% SDS, 32% v/v acrylamide/bisacrylamide) was prepared and degassed for 10 minutes after which 0.05% v/v tetramethylethylenediamine (TEMED) and 0.5% v/v of a 10% w/v ammonium persulphate (APS) solution were added. TEMED is used in conjunction with APS which is a strong oxidizing agent since TEMED catalyzes the decomposition of the APS ion to create free radicals and allow polymerization of the acrylamide gel. The separating gel was poured between two glass plates (0.5 mm separating distance) and immediately covered with a thin layer of 20% ethanol to prevent drying. The gel was allowed to polymerize for approximately 30 minutes after which a 4% stacking gel (61% v/v ddd H₂O, 25% v/v 0.5 M Tris-HCl, pH 6.8, 1% v/v 10% SDS, 13% v/v acrylamide/bisacrylamide) was prepared and degassed for 10 minutes, followed by the addition of 0.1% v/v TEMED and 0.5% v/v of a 10% w/v APS solution. The ethanol was carefully removed with Whatman Paper and the stacking gel was poured on top of the separating gel and allowed to polymerize at room temperature overnight.

Nuclear and cytoplasmic extract (0.5 µg each) from various samples were mixed with 4 µl SDS-sample buffer (50% v/v water, 12.5% v/v 0.5 M Tris-HCl, pH 6.8, 10% v/v glycerol, 20% v/v of 10% w/v SDS, 5% β-mercaptoethanol and 2.5% w/v of 0.05% w/v bromophenol blue) in a final volume of 15 µl, boiled for 5 minutes and loaded onto the SDS-polyacrylamide gel. The gel was run at 35 V for 30 minutes while the samples travelled through the stacking gel, followed by 85 V for approximately 2 hours for separation. The gels were placed in a fixing solution (30% v/v EtOH, 10% v/v Acetic acid) overnight for subsequent silver staining.

To detect and visualise the protein within the nuclear and cytoplasmic extracts, the SDS-polyacrylamide gel was stained with silver staining, which is highly sensitive with a detection limit of 0.2 ng (Switzer *et al.*, 1979). All incubation steps were performed with shaking at 19 r.p.m at room temperature on a shaking platform (HIR 10M Rotating hybridization oven, Grant Boekel). The gels were incubated in a sensitizing solution (30% v/v ethanol, 0.5 M sodium acetate, 0.5% v/v glutaraldehyde, 0.2% w/v sodium thiosulphate) for 30 minutes. Sodium thiosulphate keeps the silver ions in solution and minimizes background staining while glutaraldehyde allows reduction of the silver ions during the staining procedure. The solution was decanted and the gels were incubated in distilled water for 10 minutes. The water was decanted and the previous water wash step was repeated three times. The gels were incubated for 30 minutes in 0.1% w/v AgNO₃ and 0.25% v/v formaldehyde, washed briefly with distilled water and placed in the developing solution (2.5% Na₂CO₃, 0.01% formaldehyde) until the protein bands were clear. The silver nitrate solution provides silver ions and the low formaldehyde concentration during the fixing step allows impregnation of the silver ions. The higher concentration of formaldehyde in the developing step creates a moderate reducing environment which reduces the silver ions to elemental silver, which is then visible as black spots. The silver reaction was stopped with the addition of 0.05 M EDTA.

2.2.4 Electrophoretic Mobility Shift Assays (EMSA's)

Non-denaturing PAGE, also known as native PAGE, can be used to separate native proteins depending on factors such as size, shape and native charge and is the technique of choice in EMSA's (Ahmed, 2005). Since mobility relies on both charge and molecular size, a buffer with a high pH is often used since the majority of proteins are thus negatively charged and migrate towards the anode (Ahmed, 2005). Various factors could interfere with the DNA-protein binding reaction in EMSA's and thus prior to loading the reactions onto the gel, it is necessary to wash the wells with 0.5 x TBE running buffer to remove APS, Urea and residual polyacrylamide.

For optimal DNA-protein binding reactions investigated by EMSA, various reagents can be added. This includes poly L-lysine (small polypeptide of L-lysine) to improve the binding of the

protein to its oligonucleotide partner. Poly [d(I-C)] binds to non-specific DNA binding proteins reducing non-specific binding with the motifs in question and effectively eliminates false-positive shifts. Divalent cations such as Zn^{2+} and Mg^{2+} may act as co-factors in the binding reaction between protein and DNA while glycerol acts as a stabilizing factor for the protein in the nuclear extracts.

Once shifts are obtained, unlabelled competitors (100 fold excess) can be included in competitor assays. Non-specific, unlabelled competitor, with a different nucleotide sequence to the motif in question, will not compete with the labelled oligonucleotide for the binding protein and the shift should remain intact. However, a specific, unlabelled competitor with identical sequence to the oligonucleotide will compete for the binding protein and the shift should thus disappear. The use of such specific or non-specific competitors will provide insight into the specificity, or lack thereof, of the DNA-protein interaction.

2.2.4.1 Preparation of ^{32}P -labelled double-stranded motifs

Complimentary single-stranded sense and antisense oligonucleotides were annealed to form double-stranded oligonucleotides at 1 pmol/ μ l working solutions as follows: 100 pmol of each sense and antisense strand were incubated at 95°C for 5 minutes in 1x NEB restriction buffer 3 (100 mM NaCl, 50 mM Tris-HCl, 10 mM $MgCl_2$, 1 mM DTT, pH 7.9). The reactions were subsequently allowed to slowly cool to room temperature (~1 hour) and stored at -20 °C.

The double-stranded oligonucleotides were labelled with α - ^{32}P dATP (250 μ Ci, 3000 Ci/mmol (Perkin Elmer)). ^{32}P dATP is incorporated to the 3' end of oligonucleotides using Klenow fragment, a DNA polymerase lacking 5'-3' exonuclease activity but still has 5'-3' polymerase activity. The labelling reaction was performed at room temperature for 20 minutes and contained 1 pmol double-stranded oligonucleotide, 6.6 pmol ^{32}P dATP (3000 Ci/mmol), 50 μ M each of dCTP, dGTP and dTTP, 1 x Klenow buffer (500mM Tris-HCl (pH 7.2), 100mM $MgSO_4$ and 1mM DTT) and 1 Unit Klenow fragment (Promega) in a volume of 20 μ l. The reaction was stopped with the addition of 10 mM EDTA.

The ^{32}P -labelled double-stranded oligonucleotides were subsequently purified from single-stranded oligonucleotides and dNTP's using CentriSep size exclusion spin columns (Applied Biosystems) according to the manufacturer's instructions. Briefly, 800 μ l ddd water was added to the columns and hydrated overnight at 4 °C. The column was equilibrated to room temperature for 2 hours, drained by gravity and dried by centrifugation at 750xg for 2 minutes. The ^{32}P -labelled double-stranded oligonucleotide reaction was transferred to the centre of the column and centrifuged at 750xg for 2 minutes after which an additional wash step with 30 μ l

ddd water was included and centrifuged as above. The eluate consisting of the purified ^{32}P -labelled double-stranded oligonucleotides were stored at -20°C until use.

2.2.4.2 ^{32}P -based EMSA

The binding reaction (20 μl) between the ^{32}P -labelled double-stranded oligonucleotides and the nuclear extract (from section 2.2.3.1) was set up on ice as described by Voss *et al.* (2003) and summarized in Table 2.3 (Voss *et al.*, 2003). The 4 x EMSA buffer consist of 80 mM HEPES, pH7.9, 240 mM KCl, 8 mM MgCl_2 , 0.1 mM ZnCl_2 , 2 mM EDTA, 8 mM DTT 0.4% Triton X-100 and 40% glycerol. The reactions were incubated on ice for 10 minutes after which ^{32}P -labelled oligonucleotide was added to a final concentration of 2 fmol/20 μl reaction and was incubated at room temperature for 15 minutes. The samples were cross-linked by exposing the reactions to UV light for 3 minutes and then loaded onto a pre-run 6% native polyacrylamide gel without loading dye since the 4 x EMSA buffer already contains glycerol. DNA-protein complexes could dissociate during the gel run if the interaction between the protein and DNA is weak and thus UV cross-linking is included to fix these interactions by forming covalent bonds between amino acids and proteins. The gel was run for 90 minutes at 115 V and exposed to a phosphor imager for 20 minutes, after which the results were analyzed with Quantity One Software (BioRad).

Table 2.3: The standard binding reaction set up for ^{32}P -EMSA's.

Reagent	Motif	Motif + Nuclear extract	Motif + Nuclear extract + competitor
EMSA buffer	1 x	1 x	1 x
DTT (mM)	2	2	2
Nuclear extract (μg)	-	0.42	0.42
Poly (dl-dC) (μg)	0.05	0.05	0.05
Single-stranded competitor (fmol)	10.5	10.5	10.5
Protease inhibitor cocktail	1 x	1 x	1 x
Unlabelled double-stranded specific competitor (fmol)	-	-	100
Total volume (μl)	19	19	19

Table represents final concentrations of reagents in 19 μl final reaction volume.

The phosphor screen (Bio-Rad) is composed of a barium fluorobromide matrix which is doped with europium (BaFBr:Eu) and is sensitive to particles such as β -particles and X-rays. This enables detection of radioisotopic emitters such as ^{32}P , ^{33}P and ^{35}S . The glass plates were separated and the wet gel remaining on the single plate was wrapped with plastic wrap (glad wrap) and placed on the phosphor screen. The leak-proof plastic wrapped gel was placed in a sample exposure cassette to ensure close contact between the sample and the imaging screen for optimum exposure. The gel was removed and the screen was placed in a laser scanner

where the results were analyzed with Quantity One software (BioRad Laboratories). The image was obtained when the radioactive emission strikes the phosphor screen and phosphor oxidation occurs forming a high-energy active site which, when illuminated with wavelengths of visible light, undergoes a reduction reaction and the trapped energy is released as photons, that are captured by the photomultiplier tube which in turn produces a quantitative image to analyze. The darkness of each pixel in the image represents the signal intensity of the sample and thus the bands and their approximate positions can be detected.

2.2.4.3 Optimization strategies for ^{32}P -EMSA

^{32}P -EMSA's were optimized by including positive controls, by determining the effect of added ATP and lastly by determining the stage-specificity of nuclear proteins.

2.2.4.3.1 *Effectors*

Since some DNA-protein interactions require additional co-factors such as specific ions (Mg^{2+}) or ATP, 1 mM ATP (Sigma Aldrich) was added to the tubes prior to the 10 minute ice incubation step. The 4 x EMSA buffer contains various ions (Mg^{2+} and ZnCl_2^{2+}) which could affect binding however, since this buffer has successfully been used in previous EMSA reactions in *P. falciparum* (Voss *et al.*, 2003), it was not optimized further. The reactions were set up as in Table 2.3.

2.2.4.3.2 *Protein origins*

The nuclear protein of interest is assumed to be expressed in the trophozoite stage of the *P. falciparum* life cycle since this is the developmental stage where all but a single selected *var* gene is transcribed. To eliminate the possibility of this nuclear protein being present in any of the other two life cycle stages and to verify the nuclear protein's production in the trophozoite stage, stage-specific nuclear extraction from subsequent life cycle stages of *P. falciparum* were performed. Additionally, schizont stage nuclear extracts are required for control reactions using SPE 2 which is a sequence identified by Voss *et al.* (2003). For the stage-specific binding reactions, the reaction set up was as described in Table 2.4 except the nuclear extracts used were from specific stages of the parasite life cycle.

In addition, to verify that any shifts observed were due to protein expressed in the nuclear extract, EMSA's were performed with cytoplasmic extracts (0.42 μg) and total protein extracts (0.47 μg) obtained from *P. falciparum*, instead of nuclear extracts. EMSA reactions were set up as described previously in Table 2.3.

2.2.4.3.3 EMSA with additional positive controls

Two additional positive controls were introduced to verify EMSA binding conditions. The first is the inclusion of the SPE 2 sequence identified by Voss *et al.* (2003), which was found to strongly bind a nuclear protein specifically expressed in the schizont stage of *P. falciparum*. The second control is an unlabelled oligonucleotide from a DIG gel shift kit (Second Generation, Roche), which was radioactively labelled. DIG oligonucleotide is known to specifically bind a control protein, Oct2A, and should thus provide a clear and definite shift if EMSA conditions are optimal. For comparison purposes EMSA's were performed with the DIG protocol (described by the kit manual) and the Voss protocol (Table 2.4).

Table 2.4: The EMSA set up for the positive controls.

	Motif 2 (similar to SPE 1)			SPE 2 oligonucleotide			DIG oligonucleotide (Voss binding reaction)		
EMSA buffer	1 x	1 x	1 x	1 x	1 x	1 x	1 x	1 x	1 x
DTT (mM)	2	2	2	2	2	2	2	2	2
Nuclear extract (µg)	-	0.42 _T	0.42 _T	-	0.42 _S	0.42 _S	-	-	-
Oct2A factor (ng)	-	-	-	-	-	-	-	~2.6	~2.6
Poly (dl-dC) (µg)	0.05	0.05	0.05	0.05	0.05	0.05	0.05	0.05	0.05
Single-stranded competitor (fmol)	10.5	10.5	10.5	10.5	10.5	10.5	10.5	10.5	10.5
Protease inhibitor cocktail	1 x	1 x	1 x	1 x	1 x	1 x	1 x	1 x	1 x
Unlabelled double-stranded specific competitor (fmol)	-	-	100	-	-	100	-	-	100
Total volume (µl)	19	19	19	19	19	19	19	19	19

The nuclear extract used for the EMSA reactions were obtained from either trophozoite_T stages or schizont_S stages of the parasite life cycle.

After the 10 minute ice incubation step, 2 fmol P³²-labelled double-stranded oligonucleotides was added in a final volume of 20 µl and treated as described in section 2.2.4.2.

2.2.4.4 ³²P-EMSA of single-stranded oligonucleotides

Evidence for the existence of some single-stranded RNA binding proteins in *P. falciparum* that bind to DNA (or RNA) sequences exists (Gunasekera *et al.*, 2007b). To determine whether the motifs in question bind proteins when in single-stranded state, the ³²P- labelled double-stranded oligonucleotides were denatured to their single-stranded forms by incubating 10 pmol of each double-stranded oligonucleotide at 95°C for 1 minute and snap cooling the oligonucleotides on ice for 10 minutes.

The EMSA reactions were set up as in Table 2.5 using nuclear extracts from trophozoite and schizont *P. falciparum* stages respectively, in either the presence or absence of added ATP.

Table 2.5: EMSA reaction set up with single-stranded oligonucleotide, trophozoite and schizont nuclear extract in both the presence and absence of ATP.

	Motifs (1,2,3,4,Dyad)						
EMSA buffer	1 x	1 x	1 x	1 x	1 x	1 x	1 x
DTT (mM)	2	2	2	2	2	2	2
Nuclear extract (µg)	-	0.42 _T	0.42 _T	0.42 _T	0.42 _S	0.42 _S	0.42 _S
ATP (mM)	-	-	1	1	-	1	1
Poly (dl-dC) (µg)	0.05	0.05	0.05	0.05	0.05	0.05	0.05
Single-stranded competitor (fmol)	10.5	10.5	10.5	10.5	10.5	10.5	10.5
Protease inhibitor cocktail	1 x	1 x	1 x	1 x	1 x	1 x	1 x
Unlabelled single-stranded sense competitor (fmol)	-	-	-	100	-	-	100
Total volume (µl)	19	19	19	19	19	19	19

The nuclear extract used for the EMSA reactions were obtained from either trophozoite_(T) stages or schizont_(S) stages of the parasite life cycle.

The reactions were incubated on ice for 10 minutes after which 2 fmol ³²P-labelled single-stranded oligonucleotides were added and reactions were subsequently treated as described in section 2.2.4.2.

To verify the repeatability of shifts and the specificity of the binding, reactions were set up as described in Table 2.6 with 100-fold excess of numerous specific- and non-specific, single-stranded oligonucleotides. A single-stranded random competitor oligonucleotide, which has been shown to prevent non-specific shifts by binding to the single-stranded binding protein *PfRPA*, previously identified by Voss *et al.* (2002) as *P. falciparum* replication protein A, which is present in *P. falciparum* nuclear extract (Voss *et al.*, 2002), was also included. This should indicate if the observed shifts are due to the random, non-specific binding of *PfRPA* to the oligonucleotide under investigation. Sheared salmon sperm DNA replaced Poly (dl-dC) in these reactions to bind to non-specific proteins.



Table 2.6: EMSA reaction set up with single-stranded oligonucleotide, trophozoite nuclear extract and 100 fold excess of specific- and non-specific single-stranded competitors.

	Motifs (1,2,3,4,Dyad)						
EMSA buffer	1 x	1 x	1 x	1 x	1 x	1 x	1 x
DTT (mM)	2	2	2	2	2	2	2
Nuclear extract (µg)	-	0.42 _T	0.42 _T	0.42 _T	0.42 _T	0.42 _T	0.42 _T
Sheared salmon sperm DNA (2 µg/µl)	0.05	0.05	0.05	0.05	0.05	0.05	0.05
Single-stranded competitor (fmol)	10.5	-	10.5	10.5	10.5	10.5	10.5
Protease inhibitor cocktail	1 x	1 x	1 x	1 x	1 x	1 x	1 x
Unlabelled single-stranded competitor (fmol)	-	-	-	100 _A	100 _B	100 _C	100 _D
Total volume (µl)	19	19	19	19	19	19	19

- 100 fold excess single-stranded competitors used are as follows:
 - (A): Mixture of single-stranded sense and antisense unlabelled oligonucleotide specific to the ³²P-labelled oligonucleotide
 - (B): Single-stranded sense unlabelled oligonucleotide specific to the ³²P-labelled oligonucleotide
 - (C): Single-stranded antisense unlabelled oligonucleotide specific to the ³²P-labelled oligonucleotide
 - (D): Mixture of single-stranded sense and antisense unlabelled oligonucleotide non-specific to the ³²P-labelled oligonucleotide

After the 10 minute ice incubation, 2 fmol ³²P-labelled single-stranded oligonucleotides were added and reactions were treated as described in section 2.2.4.2.

2.3 RESULTS

2.3.1 *P. falciparum* cell culture

The *P. falciparum* cultures were maintained *in vitro* and the complete life cycle comprising of ring, early trophozoite, late trophozoite and schizont stages could be visualized by light microscopy (Figure 2.3). The *P. falciparum* parasites showed no signs of stress throughout the culturing period and the rate of parasite multiplication (3-7 fold) during the culture period confirmed that the culture was well maintained. Subsequent protein extractions were performed on the parasite cultures during the ring, late trophozoite and schizont stages for EMSA studies.

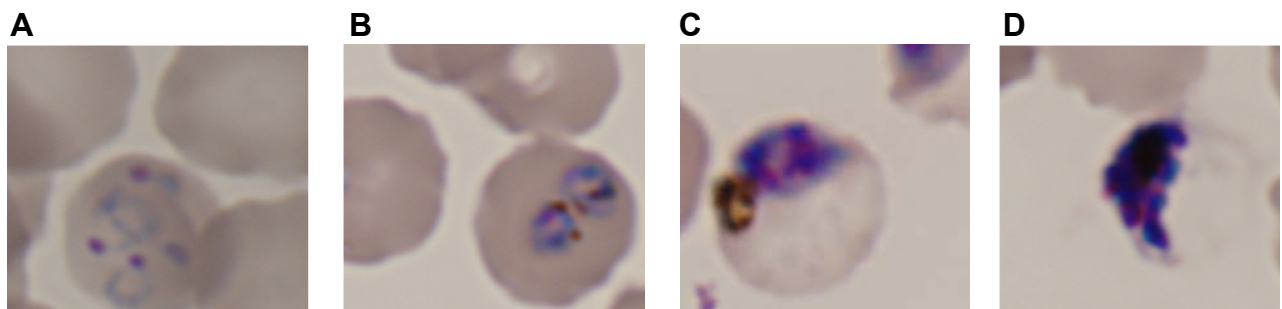


Figure 2.3: *P. falciparum* cultures in A) ring, B) early trophozoite, C) late trophozoite and D) schizont stage.

2.3.2 Protein isolation and characterisation

A BSA standard curve was used to determine the concentration of proteins isolated from *P. falciparum* nuclear and cytoplasmic extracts. A standard curve was constructed for each extraction procedure and Figure 2.4 is a representative of such a standard curve. R^2 values of all the curves ranged between 0.973 and 0.997, which allowed accurate concentration deductions to be made.

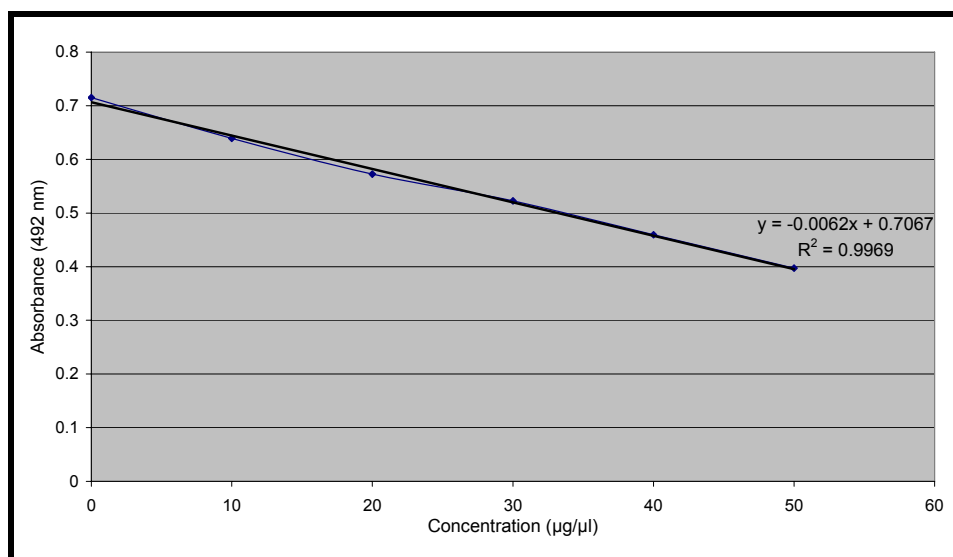


Figure 2.4: BSA standard curve for protein determination in nuclear and cytoplasmic extracts.

Proteins isolated from either *P. falciparum* nuclear or cytoplasmic extracts with the Voss protocol (Voss *et al.*, 2003) ranged in yield from 120 µg (0.3 µg/µl) to maximally 720 µg (1.8 µg/µl). The protein concentrations present in the cytoplasmic extracts were 2-fold higher than the protein concentration of the nuclear extracts for both the commercial products NucBuster and ProteoJet. The nuclear extract obtained from the Voss protocol however, contained a greater concentration (280 µg) of proteins compared to the residual cytoplasmic extract (200 µg) indicating the optimized nature of this protocol for the extraction of nuclear protein from *P. falciparum*.

The general trend observed was that the concentration of the isolated proteins increases as the parasite progresses through its life cycle with the least amount of nuclear protein present in extracts from the ring stage (120 µg) and the highest concentration of proteins being present in extracts from schizont stages (320 µg). This trend in protein production was expected since the parasite's metabolic activity increases as it passes from the ring stage through the trophozoite stage into the schizont stage.

In order to analyze and detect proteins within the *P. falciparum* nuclear and cytoplasmic extracts, SDS-PAGE was performed and proteins visualized with silver staining (Figure 2.5).

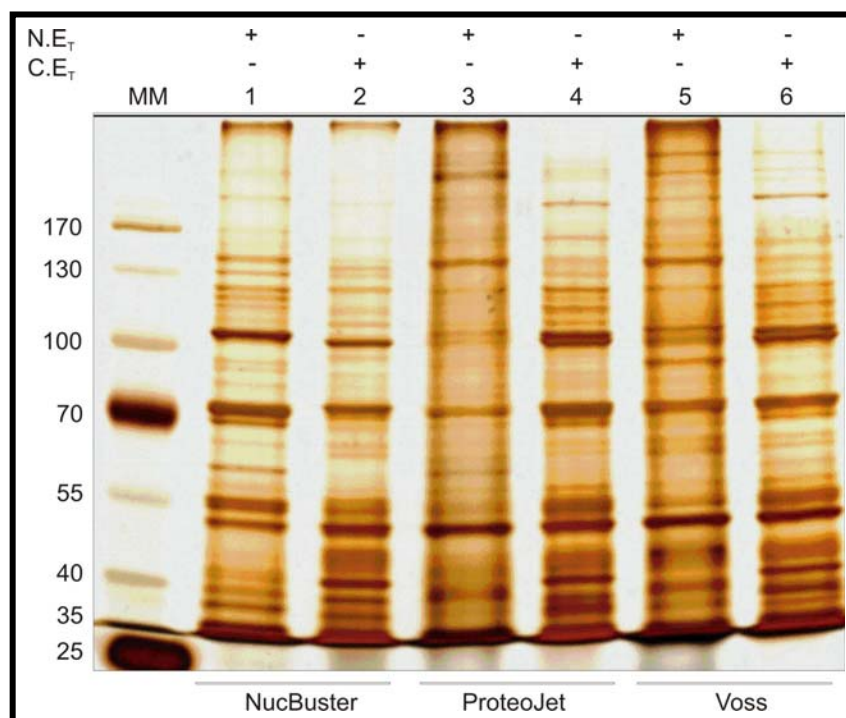


Figure 2.5: SDS-PAGE of nuclear and cytoplasmic extracts isolated from *P. falciparum* trophozoite cultures for comparison of NucBuster, ProteoJet and Voss extraction protocols.

MM: Protein marker, N.E: Nuclear extract, C.E: Cytoplasmic extract, (+) and (-) indicates reagent was added and omitted respectively.

Nuclear and cytoplasmic extracts were obtained from *P. falciparum* cultures using three different extraction procedures for comparison purposes. The commercial NucBuster and ProteoJet kits were compared to the extraction protocol described by Voss *et al.* (2003). From Figure 2.5, it can be seen that with the NucBuster protocol, the cytoplasmic and nuclear extracts contain similar sized proteins including those at ~35-40 kDa, ~55 kDa, ~60-70 kDa, 100 kDa and a selected set of proteins between 100 and 170 kDa. Protein differences are also clear for proteins present at ~40-45 kDa, ~65 kDa and ~110 kDa in the cytoplasmic extract while proteins at ~60-70 kDa, ~80-90 kDa and ~110-170 kDa are present only in nuclear extract. The extraction profiles of the ProteoJet and Voss protocols produced very similar results when both the cytoplasmic and nuclear extracts are analyzed. Protein similarities between nuclear and cytoplasmic extracts obtained with the ProteoJet kit are observed (~55 kDa, ~70 kDa, ~100 kDa and ~120-170 kDa) while protein differences are also evident (~30-45 kDa, ~55-60 kDa, 110-170 kDa and above 170 kDa). The protein bands present at ~38 kDa, 68 kDa and greater than 170 kDa are present in the nuclear extract and absent in the cytoplasmic extract of ProteoJet samples. For the Voss protocol, numerous similarities (~38 kDa, ~40-45 kDa, 55 kDa, ~60-70 kDa, 100-170 kDa and above 170 kDa) and differences (~35-45 kDa, ~60 kDa, ~68 kDa, ~38 kDa, 100-130 kDa and 170 kDa) are observed between the nuclear extract and cytoplasmic extract. All extracts share a common protein of 55 kDa.

The ultimate aim here was to isolate clean, clear nuclear extract for subsequent EMSA reactions. Analysis of the nuclear extract protein profile obtained via the Voss protocol clearly reveal the presence of proteins exclusively present in this nuclear extract which are absent in either or both the NucBuster and ProteoJet extract. As can be seen in Figure 2.5, it appears as though the Voss procedure provides a clearer, cleaner protein and a greater abundance of nuclear proteins when compared to the commercial kits used here. Therefore, for all extraction procedures to follow, the Voss protocol was utilized.

Nuclear extracts from ring, trophozoite and schizont stages of *P. falciparum* were subsequently prepared using the Voss protocol (Figure 2.6) (Voss *et al.*, 2003). The results obtained in Figure 2.6 reveals the intricate expression profiles of *P. falciparum* proteins during various stages of the parasite's life cycle. As expected, there are numerous similarities and differences between the proteins present in the nuclear and cytoplasmic extracts.

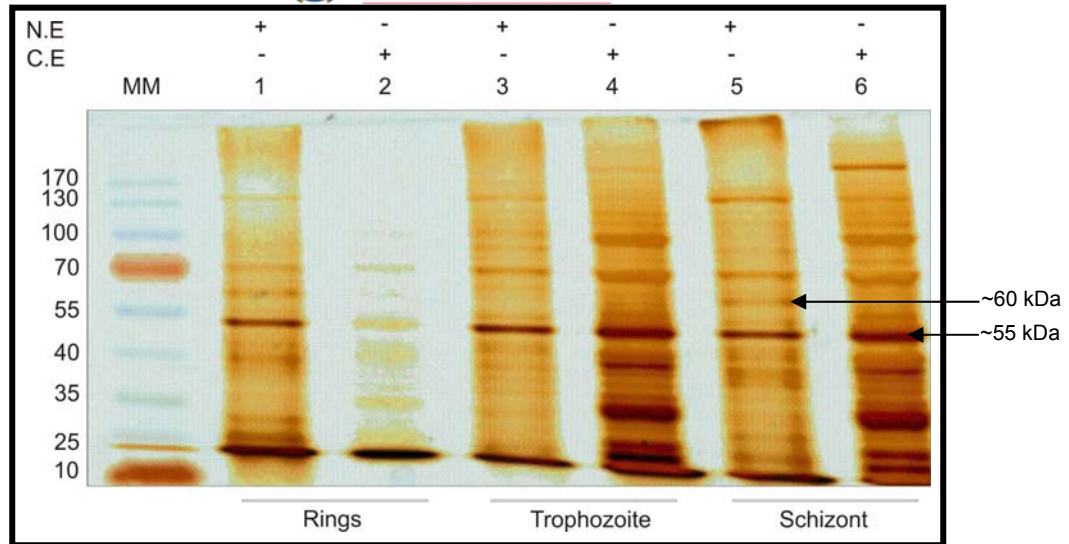


Figure 2.6: SDS-PAGE of stage-specific nuclear and cytoplasmic extracts utilizing Voss's protocol performed on *P. falciparum* *in vitro* cultures.

MM: Protein marker, N.E: Nuclear extract, C.E: Cytoplasmic extract, (+) and (-) indicates reagent was added and omitted respectively.

Figure 2.6 shows a common protein at ~55 kDa present throughout all the extracts regardless of the life stage or compartment at which the extracts were obtained. An interesting observation however, is the presence of a protein, approximately 60 kDa, present in both the ring and schizont stage nuclear extract but absent in the trophozoite stage nuclear extract.

It remains evident in Figure 2.5 and Figure 2.6 that the Voss extraction protocol (Voss *et al.*, 2003) from trophozoite stage *P. falciparum* parasites provides sufficient nuclear proteins for future EMSA reactions with the conserved motifs in question.

2.3.3 ³²P-EMSA

2.3.3.1 Design and labelling of *cis*-regulatory elements containing the conserved motifs.

The conserved motifs previously identified *in silico* (Clausel-Renard, unpublished results) were converted into 39-44 oligonucleotides with the conserved motif represented in bold in the centre of these oligonucleotides (Table 2.7). The oligonucleotides, each containing the specific conserved motifs will be referred to in text as Motif 1, 2, 3, 4 and Dyad. The oligonucleotide concentrations were determined using absorbance readings on a GeneQuant Pro and the $A_{260}:A_{280}$ ratios of all the oligonucleotides were between 1.8 and 2.2, which indicated good purity. These oligonucleotides were subsequently isotopically labelled with ³²P and used in the EMSA studies.

Table 2.7: The oligonucleotide sequences of the conserved motifs designed and synthesized for EMSA's along with the control oligonucleotides SPE 2 and DIG.

Oligonucleotide name	Oligonucleotide sequence (5'-3')	Size	Ta
Motif 1 sense	ACCATATCACA ACTCCCATA ACATAACATAACATACA	39	60.3
Motif 1 antisense	TGTATGTTATGTTAT GTTATGGGAG TATTGTGATATGGT	39	60.3
Motif 2 sense	TATATATAATAATTCT CGGTTACTGC ATGTGTCCGTGCAC	40	63.4
Motif 2 antisense	GTGCACGGACACAT GCAGTAACCG AAGATTATTATATATA	40	63.4
Motif 3 sense	CGGAAGAAGATATTT GCCTCTGTTG TATCTCTAAAATAT	40	61.4
Motif 3 antisense	ATATTTTAGAGATA ACAACAGAGGC AAATATCTTCTTCCG	40	61.4
Motif 4 sense	AGATACCCAAAAAAT CGAAATCGTGC ACGGACACATGCAG	40	66.5
Motif 4 antisense	CTGCATGTGTCCGT GCACGATTTG ATTTTTGGGTATCT	40	66.5
Dyad sense	CATTTATATATTATATATT ACATTATGTC ATTTATTAATAAATA	44	53.3
Dyad antisense	TATTTATTAATAAAT GACATAATGTA ATATATAATATAAATG	44	53.3
SPE 2 sense	GTGCGACTTTATT GTGCATAGTGGT GCGAATTATACTTTGG	42	65.4
SPE 2 antisense	CCAAAGTATAAATT CGCACC ACTATGCACAATAAAGTCGCAC	42	65.4
DIG sense	GTACGGAGTATCCAGCTCCGTAG CATGCAA ATCCTCTGG	39	69.7
DIG antisense	TCGACCAGAGG ATTTGCATG CTACGGAGCTGGATACTCC	39	69.7

Conserved sequences are in bold. Ta symbolizes annealing temperature which is calculated by subtracting 5 °C from the melting temperature (Tm).

$$T_m = 69.3^\circ\text{C} + (0.41 \times \text{GC}\%) - 650/\text{primer length (Rychlik et al., 1990)}$$

2.3.3.2 Isotopic labelling of oligonucleotides containing the *cis*-regulatory motifs

Previous EMSA results using a DIG-labelled form of Motif 2 oligonucleotide, containing the conserved motif, was shown to be unreliable and not reproducible (results not shown). For this reason, ³²P was used as the labelling system for the subsequent EMSA's. Klenow fragment was used to catalyze the isotopic labelling of the above oligonucleotides containing the *cis*-regulatory motifs. The ³²P-labelled double-stranded oligonucleotides were analyzed for labelling efficiency by native polyacrylamide gel electrophoresis and exposed to a phosphor imager for detection. In Figure 2.7, it is clear that the labelling and spin column purification of the oligonucleotides were sufficient since a strong radioactive signal can be detected, allowing subsequent EMSA reactions to be performed.

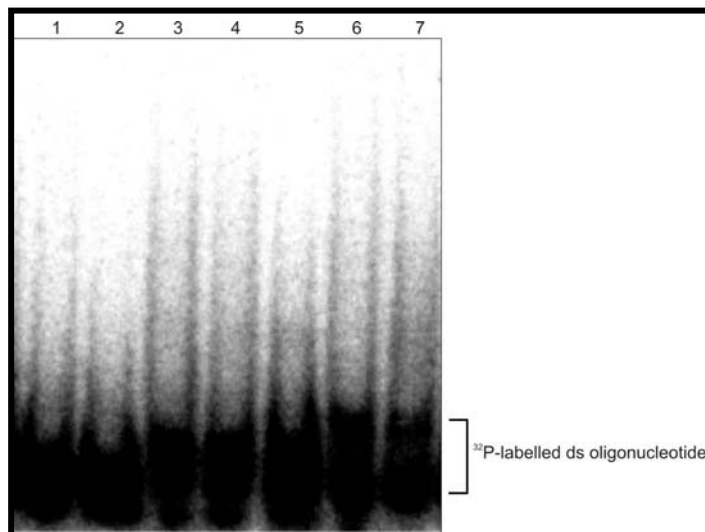


Figure 2.7: Electrophoresis of all double-stranded oligonucleotides containing the conserved *cis*-regulatory motifs for labelling efficiency with ³²P.

Lane 1: Motif 1; Lane 2: Motif 2; Lane 3: Motif 3; Lane 4: Motif 4; Lane 5: Dyad; Lane 6: SPE 2; Lane 7: DIG.

2.3.3.3 ³²P-EMSA with positive controls to verify conditions

Motif 2 (similar to the previously described motif involved in *var* gene regulation, SPE 1 (Voss *et al.*, 2003)) was used throughout this study as a positive control. EMSA reactions performed by Voss *et al.* (2003) included the addition of a random single-stranded unlabelled oligonucleotide to remove any shifts that could be caused by the non-specific binding of *Pf*RPA.

The SPE 2 motif is a regulatory element discovered by Voss *et al.* (2003) and was proven to bind a protein expressed in the schizont stage of *P. falciparum* in a highly specific manner. The DIG gel shift kit used previously provides an unlabelled oligonucleotide (DIG) which was labelled isotopically with ³²P and used as a control to bind Oct2A. The ³²P-labelled control oligonucleotides Motif 1 (similar to SPE 1), SPE 2 and DIG were therefore used in EMSA reactions with their respective nuclear extracts or binding proteins according to the Voss protocol (Figure 2.8). For comparative purposes, the DIG EMSA reaction was set up as described by the kit, utilizing the kit binding buffer and reagents. As can be seen in Figure 2.8, the EMSA reaction, with conditions described by the Voss protocol, provided clear shifts with all three controls (lanes 2, 5 and 8) in the presence of the respective binding protein. Competitor reactions, using 100-fold excess unlabelled oligonucleotide specific to each motif, were set up to determine the specificity of the reaction. Introduction of the double-stranded unlabelled competitors eliminated the previously observed shift (Figure 2.8, lanes 3, 6, 9 and 12), indicating that the DNA-protein interactions observed were specific.

The binding reaction of the DIG oligonucleotide set up as described by the kit did not produce as clear a shift as compared to the Voss protocol (lane 11). Thus, all future EMSA reactions, including the controls, were set up as described by the Voss protocol.

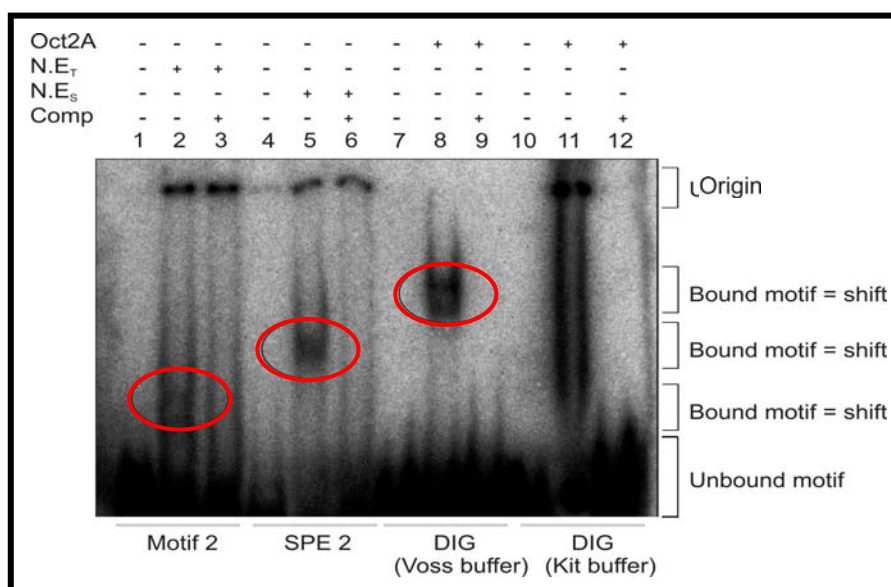


Figure 2.8: EMSA analysis of all control oligonucleotides.

Oct2A: DIG binding factor; N.E_{T/S}: Nuclear extract from (T) trophozoites or (S) schizonts; Comp: 100 fold excess double-stranded unlabelled specific competitor oligonucleotide.

To verify the presence of the shifts observed in the EMSA (Figure 2.8), a densitometric lane analysis was performed using Quantity One Software (BioRad), to analyze each lane of the gel individually by calculating the intensity of pixels which are representative of the ^{32}P radioactive signal. Densitometric lane analysis (Figure 2.9) confirms a shift observed at an Rf of ~ 0.6 for Motif 2, ~ 0.43 for SPE 2 and ~ 0.35 for DIG. Lane analysis confirmed the absence of shifts with the DIG motif set up using the kit binding reactions (Figure 2.9 (D)).

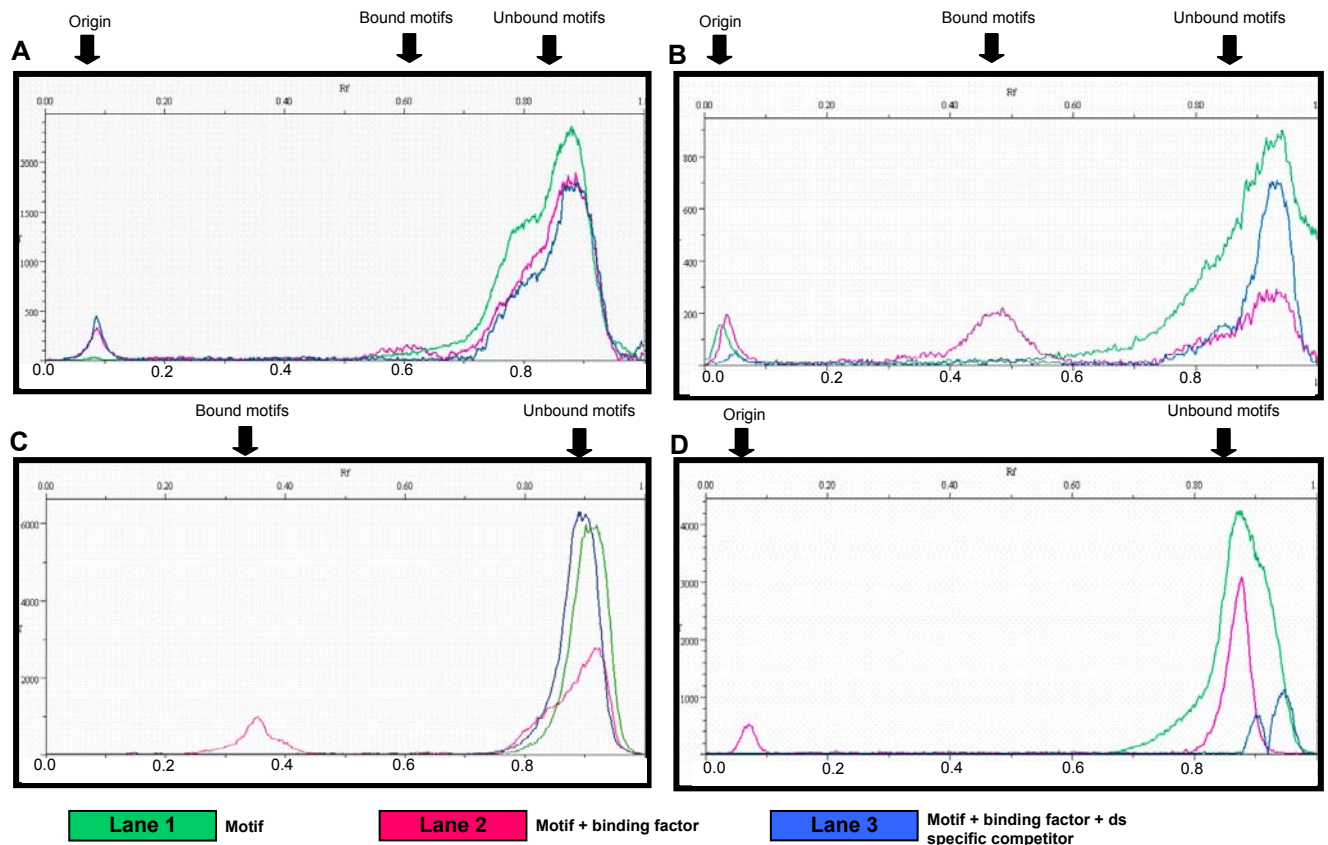


Figure 2.9: Densitometric lane analysis of EMSA results from Figure 2.8.

(A) Motif 2; (B) SPE 2; (C) DIG (Voss binding reaction) and (D) DIG (kit binding reaction) control oligonucleotides to verify the shifts observed in the EMSA gel.

Compared to EMSA results in literature (Voss *et al.* 2003, Lanzer *et al.* 1992), the shifts observed in Figure 2.8, regardless of the motif under study, are similar to the EMSA shifts obtained by the authors mentioned. These EMSA results confirm that the Voss protocol is optimal for the EMSA analyses in *P. falciparum* and the EMSA conditions allowed shifts that were verified by densitometric lane analysis (Figure 2.9).

2.3.3.4 Binding reaction and electrophoresis with ^{32}P -labelled motifs

The EMSA reactions thus far confirmed that Motif 2, in the presence of trophozoite nuclear extract, clearly provides shifts representing DNA-protein interactions and can thus be used as a control. A random single-stranded unlabelled oligonucleotide should be added to the EMSA reactions to remove shifts that could be caused by the non-specific binding of *PfRPA* (Voss *et*

al., 2002). Subsequent analysis of binding to ^{32}P -labelled Motif 2 was performed in the presence and absence of this random unlabelled single-stranded oligonucleotide (Figure 2.10).

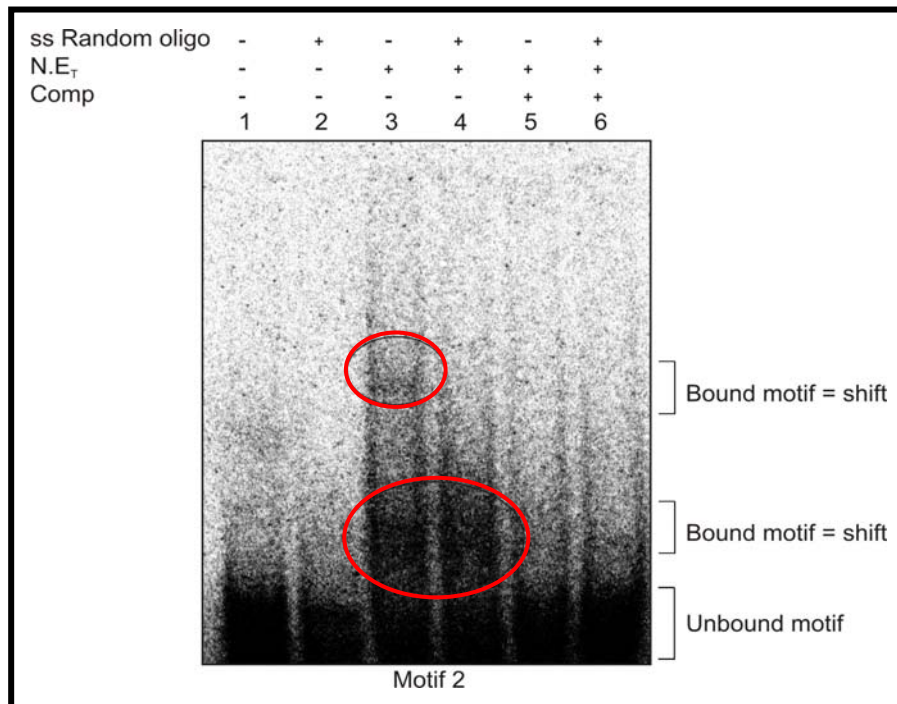


Figure 2.10: EMSA of Motif 2 in the presence and absence of the random single-stranded unlabelled oligonucleotide.

Ss Random oligo: random single-stranded unlabelled oligonucleotide (50 fold excess); N.E._T: Nuclear extract from trophozoites; Comp: 100 fold excess double-stranded unlabelled specific competitor oligonucleotide.

In Figure 2.10, as expected, no shifts are observed when Motif 2, without nuclear extract, is in the presence or absence of the random single-stranded unlabelled oligonucleotide (lanes 1 and 2). Shifts are however visible when the ^{32}P -labelled Motif 2 was incubated with nuclear extract (lanes 3 and 4). Two shifts are observed in the absence of the random single-stranded unlabelled oligonucleotide (lane 3), however in the presence of the random single-stranded unlabelled oligonucleotide, only one clear shift was observed (lane 4). The two shifts present in the absence of the random single-stranded unlabelled oligonucleotide are therefore assumed to originate from a nuclear extract protein partner binding specifically to Motif 2 and in addition, *PfRPA* is thought to bind non-specifically to single- and/or double-stranded ^{32}P -labelled Motif 2. When random single-stranded unlabelled oligonucleotide is added, it competes for binding to the non-specific binding protein *PfRPA* and only one shift remains visible after electrophoresis. This shift (lane 4) correlates in position ($R_f \sim 0.63$, Figure 2.11) to that observed for Motif 2 in Figure 2.8 (lane 2) and is therefore assumed to be as a result of a protein present in the *P. falciparum* nuclear extract binding specifically to Motif 2.

Competitor reactions containing nuclear extract with excess double-stranded unlabelled Motif 2 specific oligonucleotide lack shifts in both the presence and absence of the random single-stranded unlabelled oligonucleotide (lanes 5 and 6). This result was expected since a 100-fold

excess of this double-stranded unlabelled competitor would compete with ^{32}P -labelled Motif 2 for the binding protein of interest present in the *P. falciparum* nuclear extract.

The presence of the shifts in the above EMSA (Figure 2.10) was verified with densitometric lane analysis (Figure 2.11). In the presence of ^{32}P -labelled Motif 2 and *P. falciparum* nuclear extract (lane 3), two peaks are observed, one at an Rf of ~ 0.39 assumed to be as a result of the PfRPA protein binding to the labelled Motif 2 and a second peak at an Rf of ~ 0.63 , assumed to be as a result of the nuclear protein binding to Motif 2.

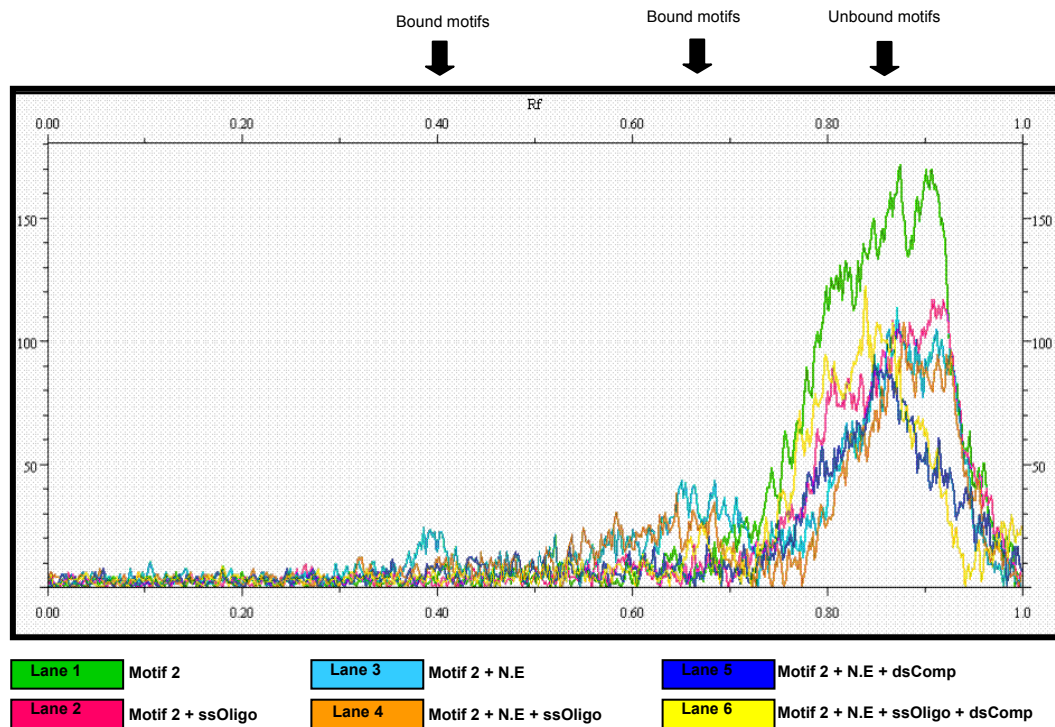


Figure 2.11: Lane analysis utilizing Quantity One Software to verify the shifts obtained by EMSA analysis of Motif 2 in the presence and absence of the random single-stranded DNA.

Lane numbers correspond to the lanes used in the EMSA in Figure 2.10

In the presence of random single-stranded oligonucleotide (lane 4), only a single shift at an Rf of ~ 0.63 was observed (Figure 2.11), confirming the result of the nuclear binding protein present in the *P. falciparum* nuclear extract binding to Motif 2 (Figure 2.10). Comparing the Rf values obtained in Figure 2.11 lanes 3 and 4 (Rf ~ 0.63) to the Rf value of Motif 2 with trophozoite nuclear extract (lane 2) of Figure 2.9 A (Rf ~ 0.6), the Rf values are very similar and thus confirms the specific binding of a protein present in this *P. falciparum* nuclear extract to ^{32}P -labelled Motif 2.

Since shifts were observed with ^{32}P -labelled Motif 2 and the importance of the random single-stranded unlabelled oligonucleotide was determined, all EMSA's performed hereafter contained the random single-stranded unlabelled oligonucleotide unless otherwise stated. In the case where a double-stranded unlabelled competitor was used, the competitor was specific to each

motif unless otherwise stated. EMSA reactions were set up for the remaining four ^{32}P -labelled motifs in question using the *P. falciparum* trophozoite nuclear extract as a source for binding proteins and Motif 2 as internal control (Figure 2.12).

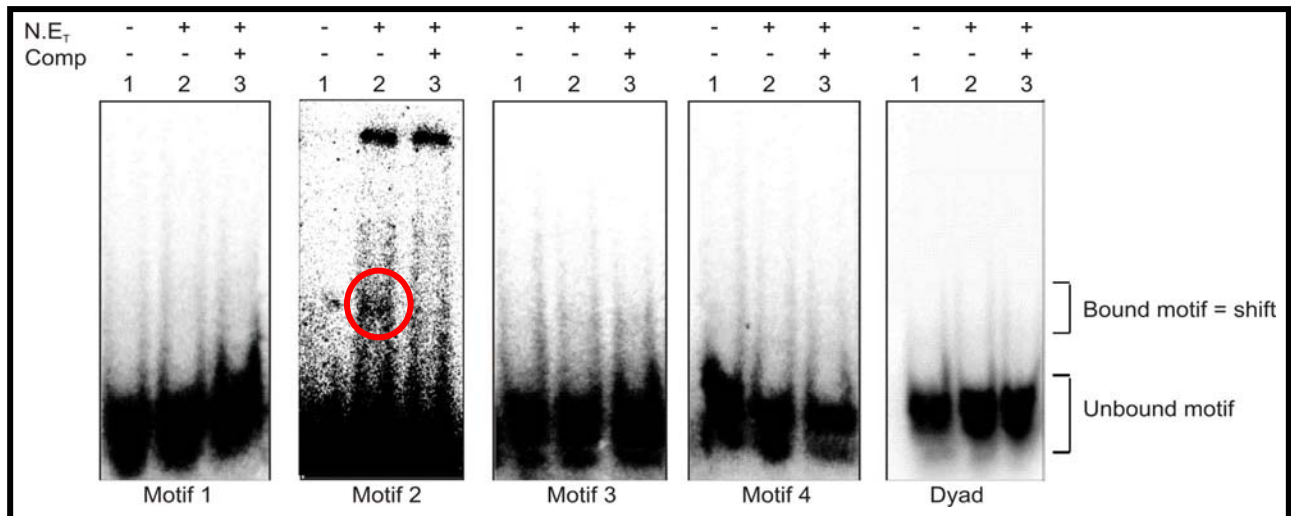


Figure 2.12: EMSA of Motif 1, Motif 2, Motif 3, Motif 4 and Dyad with trophozoite nuclear extract.

N.E.: Nuclear extract from trophozoites; Comp: 100 fold excess double-stranded unlabelled specific competitor oligonucleotide.

It appears as though no shifts are present in any of the EMSA's performed with Motif 1, Motif 3, Motif 4 or the Dyad while the internal control Motif 2 resulted in the expected shift. Densitometric lane analysis was also utilized to confirm the observations (results not shown) and indeed it was confirmed that no shifts or DNA-protein complexes were present for the motifs but that the shift observed for Motif 2 was comparable to earlier results, again with an Rf of ~0.61.

2.3.3.5 ^{32}P -EMSA optimizations

2.3.3.5.1 ^{32}P -EMSA with stage-specific nuclear extracts.

Nuclear extracts were prepared from *P. falciparum* cultures in the ring, trophozoite and schizont stages to determine if the motifs in question have binding proteins which are expressed during specific stages of the parasite life cycle only. The EMSA was firstly performed with ^{32}P -labelled Motif 2 as internal control. Increasing amounts (3 μg , 6 μg , and 9 μg) of nuclear extracts isolated from three life cycle stages of *P. falciparum* were added to Motif 2 to determine the minimum amount of protein required to produce a shift. As can be seen in Figure 2.13 (A), the addition of the *P. falciparum* ring and schizont nuclear extracts did not result in shifts. However, shifts were only observed with the addition of the *P. falciparum* trophozoite nuclear extract (lanes 5 and 6). These results confirm that the binding protein for Motif 2 remains solely expressed in the trophozoite stage. Densitometric lane analysis (Figure 2.13 (B)) confirms the presence of shifts, again at an Rf of ~0.6 and these results additionally confirm that shifts become more evident when nuclear extracts exceeding 6 μg are used.

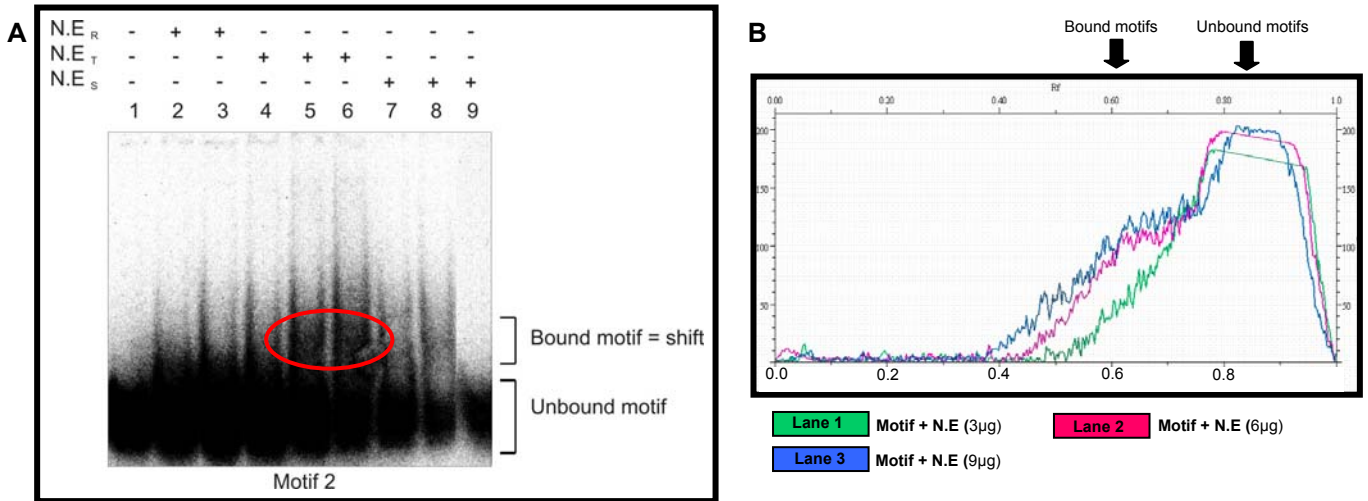


Figure 2.13: (A) EMSA of Motif 2 with nuclear extracts from rings, trophozoites and schizonts and (B) densitometric lane analysis of EMSA lane 4, 5 and 6.

N.E_{R/T/S}: Nuclear extract from (R) rings, (T) trophozoites, (S) schizonts; Comp: 100 fold excess double-stranded unlabelled specific competitor oligonucleotide.

EMSA reactions with nuclear extracts from ring, trophozoite and schizont stage *P. falciparum* were subsequently performed on the remaining four motifs in question. As can be seen in Figure 2.14, no shifts were observed with any of the nuclear extracts, for any of the motifs, other than Motif 2 in the presence of trophozoite nuclear extract and these observations were confirmed by densitometric lane analysis (results not shown). It could thus be assumed that either the conditions are not optimal for binding, that the binding protein for these motifs are not expressed in any of these stages or that none of these motifs have regulatory functions in the double-stranded form.

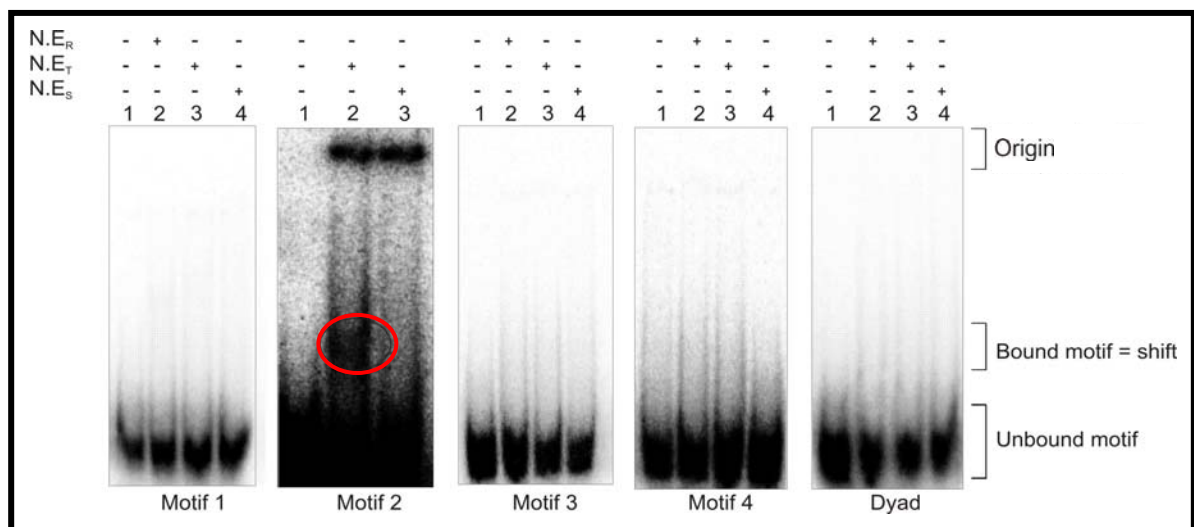


Figure 2.14: EMSA of all five motifs in question with nuclear extracts from rings, trophozoites and schizonts.

N.E_{R/T/S}: Nuclear extract from (R) rings, (T) trophozoites, (S) schizonts.

Due to the success of previous *P. falciparum* EMSA's by Voss *et al.* (Voss *et al.*, 2003), as well as with Motif 2 observed here, cation and salt concentrations seemed optimal for the EMSA's performed in this study. Previous DNA-protein studies discovered that the addition of ATP could increase the affinity of the nuclear protein for the regulatory motif (Menetski *et al.*, 1985) and thus ATP optimization was considered next.

2.3.3.5.2 ³²P-EMSA with addition of ATP.

EMSA reactions for the five ³²P-labelled motifs in question were set up in both the presence and absence of ATP to determine if DNA-protein interactions could be improved (Figure 2.15).

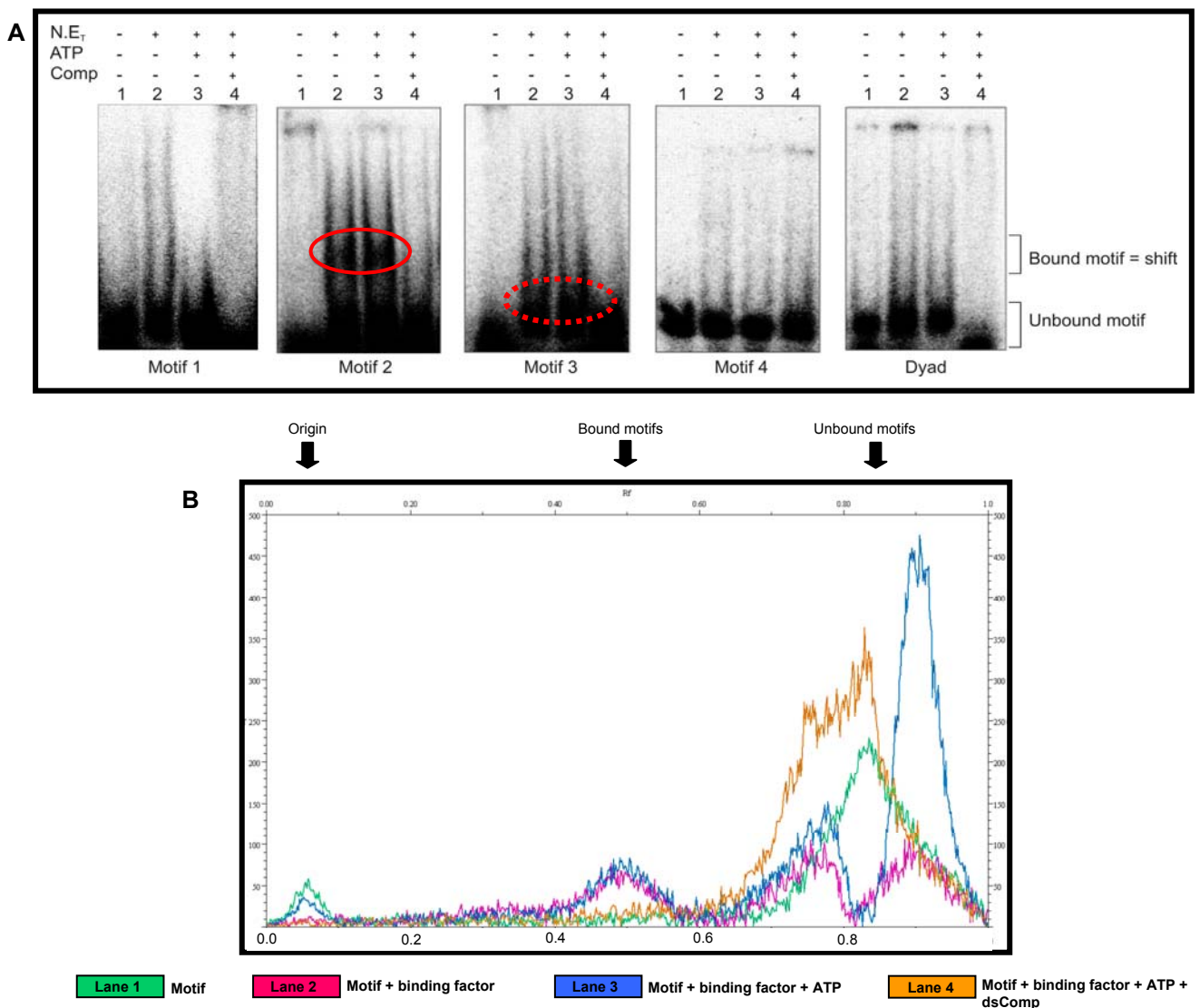


Figure 2.15: (A) EMSA of Motif 1, Motif 2, Motif 3, Motif 4 and Dyad with trophozoite nuclear extract in either the presence or absence of ATP, (B) densitometric lane analysis of Motif 2 with trophozoite nuclear extract in either the presence or absence of ATP.

N.E_T: Nuclear extract from trophozoites; ATP: Adenosine triphosphate; Comp: 100 fold excess double-stranded unlabelled specific competitor oligonucleotide.

In Figure 2.15 (A) no shifts were observed for Motif 1, 4 or the Dyad in either the presence or absence of ATP (lanes 2 and 3) and densitometric lane analysis (not shown) confirmed the absence of shifts for these three motifs. A possible shift appeared to be present for Motif 3 in the presence and absence of ATP (lanes 2 and 3) however, densitometric lane analysis could not confirm shifts associated with this motif. An apparent shift was observed for Motif 2 in the absence and presence of ATP (lanes 2 and 3) and densitometric lane analysis of Motif 2 (Figure 2.15 (B)) revealed identical shifts of Rf values ~ 0.5 , irrespective of the presence or absence of ATP.

2.3.3.6 EMSA of single-stranded ^{32}P -labelled motifs

The motifs in question, except Motif 2, appear to not be regulatory in their double-stranded state. Since some regulatory proteins bind to both single- and double-stranded DNA and RNA (Babitzke *et al.*, 2009; Lilley, 1995; Nimonkar *et al.*, 2003) and RNA binding proteins have been identified in *P. falciparum* (Cui *et al.*, 2002; Gunasekera *et al.*, 2007b), EMSA reactions were performed on single-stranded ^{32}P -labelled *cis*-regulatory oligonucleotides to determine if the motifs in question are perhaps regulatory in the single-stranded state.

2.3.3.6.1 EMSA of single-stranded ^{32}P -labelled motifs with nuclear extract in either the presence or absence of ATP

The ^{32}P -labelled single-stranded versions of the oligonucleotides for each motif were used in EMSA reactions in the presence and absence of ATP. Nuclear extracts from both trophozoite and schizont stage *P. falciparum* were used to determine if the single-stranded motifs in question have binding proteins expressed in these life cycle stages of *P. falciparum*. The random single-stranded unlabelled competitor (to bind *PfRPA*) was included in all reactions and competitor reactions were performed with excess specific, unlabelled single-stranded sense oligonucleotides.

The motifs were denatured to 95.0°C and snap cooled on ice and therefore the majority of each motif was expected to be in the single-stranded state. Figure 2.16 (A) illustrates the EMSA result of Motif 2 in its single-stranded form and a clear shift is observed in the presence of trophozoite nuclear extract, both in the presence and absence of ATP (lanes 2 and 3). There also appears to be a second shift present in both lanes 2 and 3 and possibly also lanes 5 and 6.

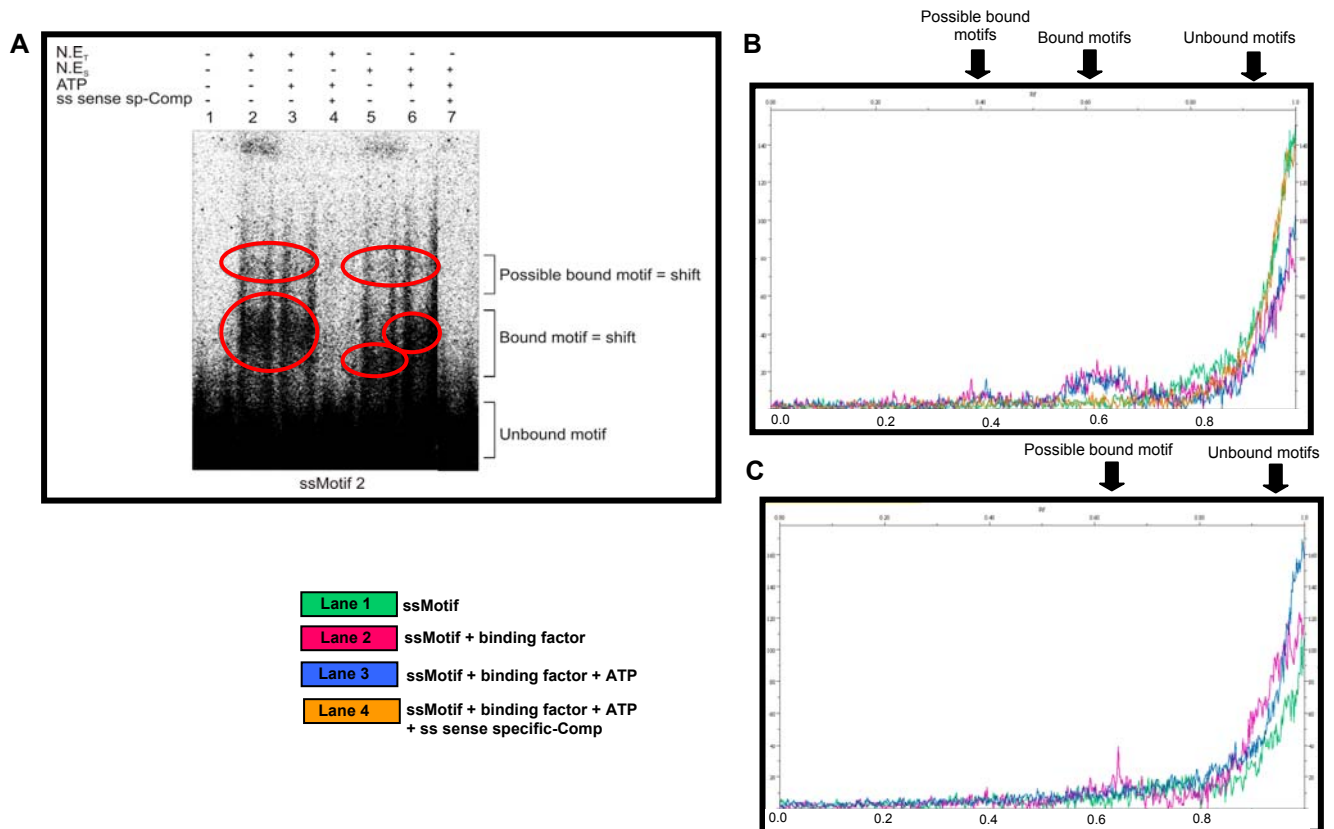


Figure 2.16: (A) EMSA of single-stranded Motif 2 with trophozoite and schizont nuclear extract in the presence and absence of ATP and densitometric lane analysis of single-stranded Motif 2 EMSA with (B) trophozoite nuclear extract and (C) schizont nuclear extract.

Ss: single-stranded; N.E_{T/S}: Nuclear extract from trophozoites (T) schizonts (S); ATP: Adenosine triphosphate; ss sense sp-Comp: 100 fold excess single-stranded unlabelled sense specific competitor oligonucleotide.

Densitometric inspection of the shifts obtained with trophozoite nuclear extract (lanes 2 and 3) confirmed the presence of two shifts, one at an Rf of ~0.39 and a second shift at an Rf of ~0.61 (Figure 2.16 B) for single-stranded Motif 2. The addition of ATP had no effect on DNA-protein complex formation. With the addition of the single-stranded, unlabelled specific-competitor oligonucleotide, the shift is eliminated due to competition reactions with the binding protein. This indicates the specificity of both DNA-protein binding reactions. Previously, the shift obtained at an Rf of ~0.39 was suggested to be *PfRPA* since this binding protein binds non-specifically to single-stranded DNA and inclusion of the random single-stranded unlabelled competitor oligonucleotide eliminated the shift associated with this protein. In these EMSA reactions, the random single-stranded unlabelled competitor oligonucleotide was included and it did not eliminate the binding protein, causing a shift at an Rf of ~0.39. Instead, only single-stranded unlabelled specific competitor eliminated both shifts (Rf ~0.61 and Rf ~0.39), suggesting that the observed shifts in these EMSA reactions are as a result of *P. falciparum* nuclear extract proteins binding specifically to Motif 2.

Similar shifts were obtained when single-stranded Motif 2 was incubated with schizont nuclear extract in the presence of ATP (Figure 2.16 (A), lanes 5 and 6), however Rf values from

densitometric lane analysis (Figure 2.16 (C)) confirms that a single shift at $R_f \sim 0.63$ is present with schizont nuclear extract, only in the absence of ATP (lane 5). No other shifts were confirmed with densitometric lane analysis.

The EMSA experiment for single-stranded forms of Motif 1, Motif 3, Motif 4 and Dyad was subsequently performed in parallel with Motif 2 (Figure 2.16). In Figure 2.17, shifts are observed for all the motifs when incubated with *P. falciparum* trophozoite nuclear extract (lanes 2 and 3). However, only Motif 3, Motif 4 and the Dyad resulted in possible shifts when incubated with *P. falciparum* schizont nuclear extracts as well (lanes 5 and 6).

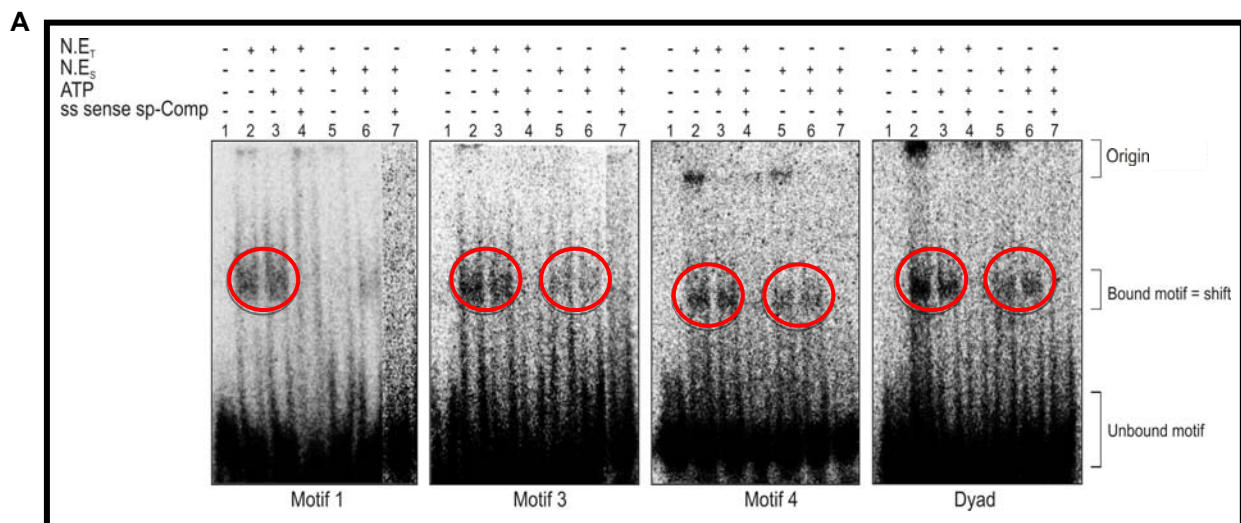


Figure 2.17: EMSA of Motif 1, Motif 3, Motif 4 and Dyad in single-stranded state with trophozoite and schizont nuclear extract in the presence and absence of ATP.

N.E_{T/S}: Nuclear extract from trophozoites (T) or schizonts (S); ATP: Adenosine triphosphate; ss sense sp-Comp: 100 fold excess single-stranded unlabelled sense specific competitor oligonucleotide.

Shifts were obtained with all single-stranded oligonucleotides in the presence of both the trophozoite and schizont nuclear extract, except for Motif 1 which resulted in a shift with trophozoite nuclear extract only. Densitometric lane analysis was performed on the motifs incubated with *P. falciparum* trophozoite and schizont nuclear extract, however no shifts were confirmed for any of the motifs incubated with the schizont nuclear extract (results not shown) while shifts were confirmed with trophozoite nuclear extract (Figure 2.18 (A-D)).

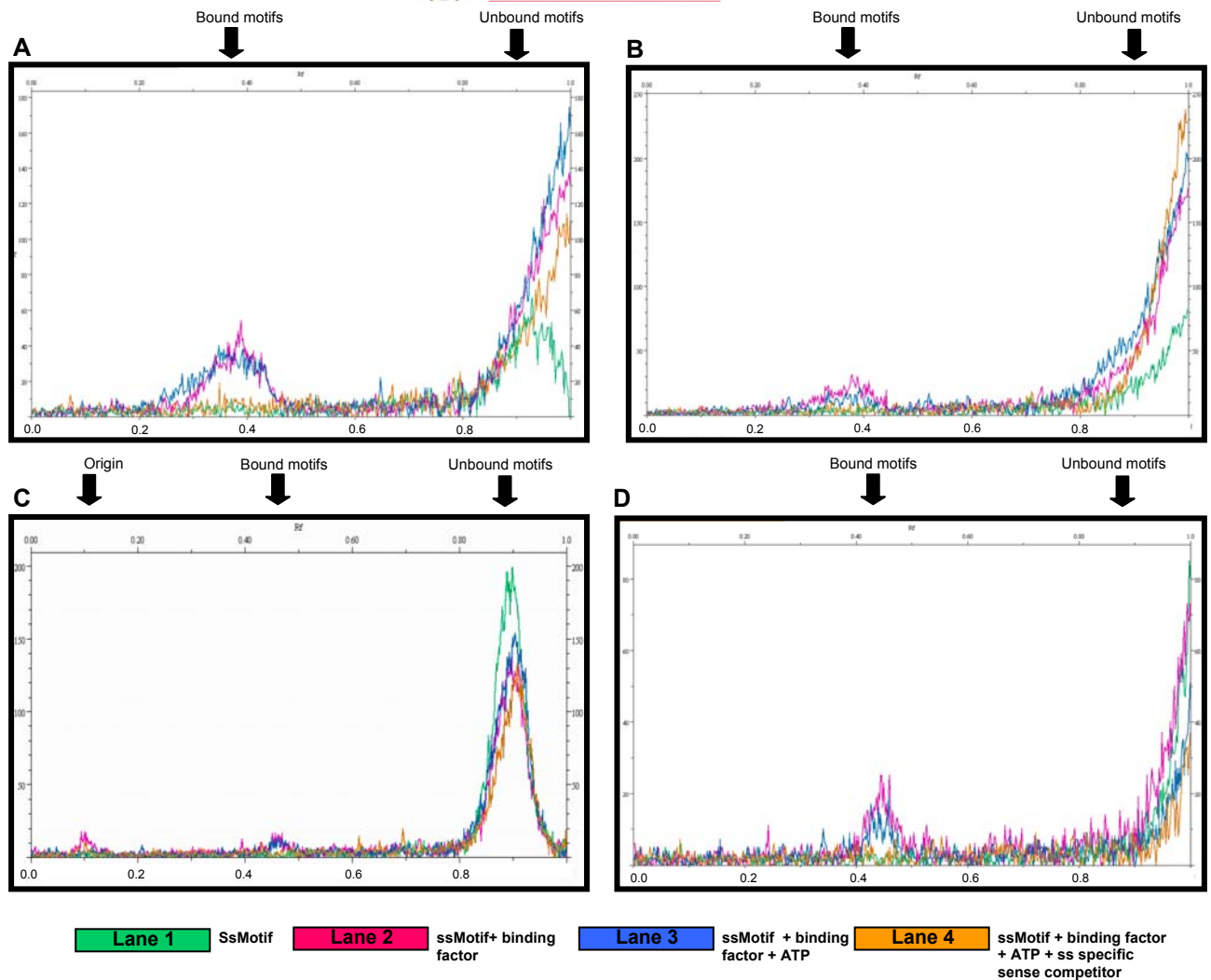


Figure 2.18: Densitometric lane analysis of single-stranded (A) Motif 1, (B) Motif 3, (C) Motif 4 and (D) Dyad with trophozoite nuclear extract in the presence and absence of ATP.

The shifts observed for these motifs with *P. falciparum* trophozoite nuclear extract also seem to be similar with regards to the degree of retardation (Figure 2.18 (A-D)) since Motif 1 and Motif 3 have similar Rf values of ~0.39, while Motif 4 and the Dyad have similar Rf values of ~0.44, in both the presence and absence of ATP. These results convey the possibility that Motif 1 and Motif 3 share the same binding protein or same sized protein while Motif 4 and the Dyad appear to share the same or similar sized protein.

Competitor reactions of single-stranded ³²P-labelled motifs with single-stranded unlabelled sense competitor oligonucleotides, specific to each motif, eliminated the observed shifts, indicating thus far that the binding between the motif and protein is sense oligonucleotide specific. This however was investigated further by additional competitor studies which are described in the following section.

2.3.3.6.2 EMSA of single-stranded ³²P-labelled motifs with specific- and non-specific single-stranded competitors.

The binding of proteins present in *P. falciparum* nuclear extract to ³²P-labelled single-stranded oligonucleotides were studied with various specific- and non-specific single-stranded competitors to determine the specificity of the observed DNA-protein interactions. EMSA reactions were performed with *P. falciparum* trophozoite nuclear extract and both specific and non-specific single-stranded sense and antisense competitors were added to compete for the binding protein. The unlabelled single-stranded motif pool of each motif was used as the non-specific competitor for every other motif. In other words, the unlabelled single-stranded non-specific competitor used for Motif 1 was unlabelled single-stranded Motif 3, and so forth. Therefore, assuming the single-stranded oligonucleotides remain unhybridized, it is possible to determine which single-stranded oligonucleotide is being identified by the binding protein. To do this, both sense and antisense specific unlabelled single-stranded oligonucleotides were added to the competitor reactions in 100-fold excess. Thus, if the DNA-protein binding interaction is sense strand-specific, then only the sense-specific unlabelled single-stranded competitor sequence should eliminate the shift, and the same scenario is predicted for the antisense-specific competitor.

Motif 2 was studied as a control and as can be seen in Figure 2.19 (A), a shift is produced with the addition of the *P. falciparum* trophozoite nuclear extract. This shift remains in the absence and presence of the random single-stranded oligonucleotide (lane 2 and 3). In the absence of the random single-stranded oligonucleotide, a shift of high intensity is observed (lane 2) at an Rf of ~0.39 and a faint shift is observed slightly lower in the same lane (Rf ~0.6, lane 2). The addition of the random single-stranded oligonucleotide resulted in a fainter shift (lane 3) at an identical Rf of ~0.39 in the gel.

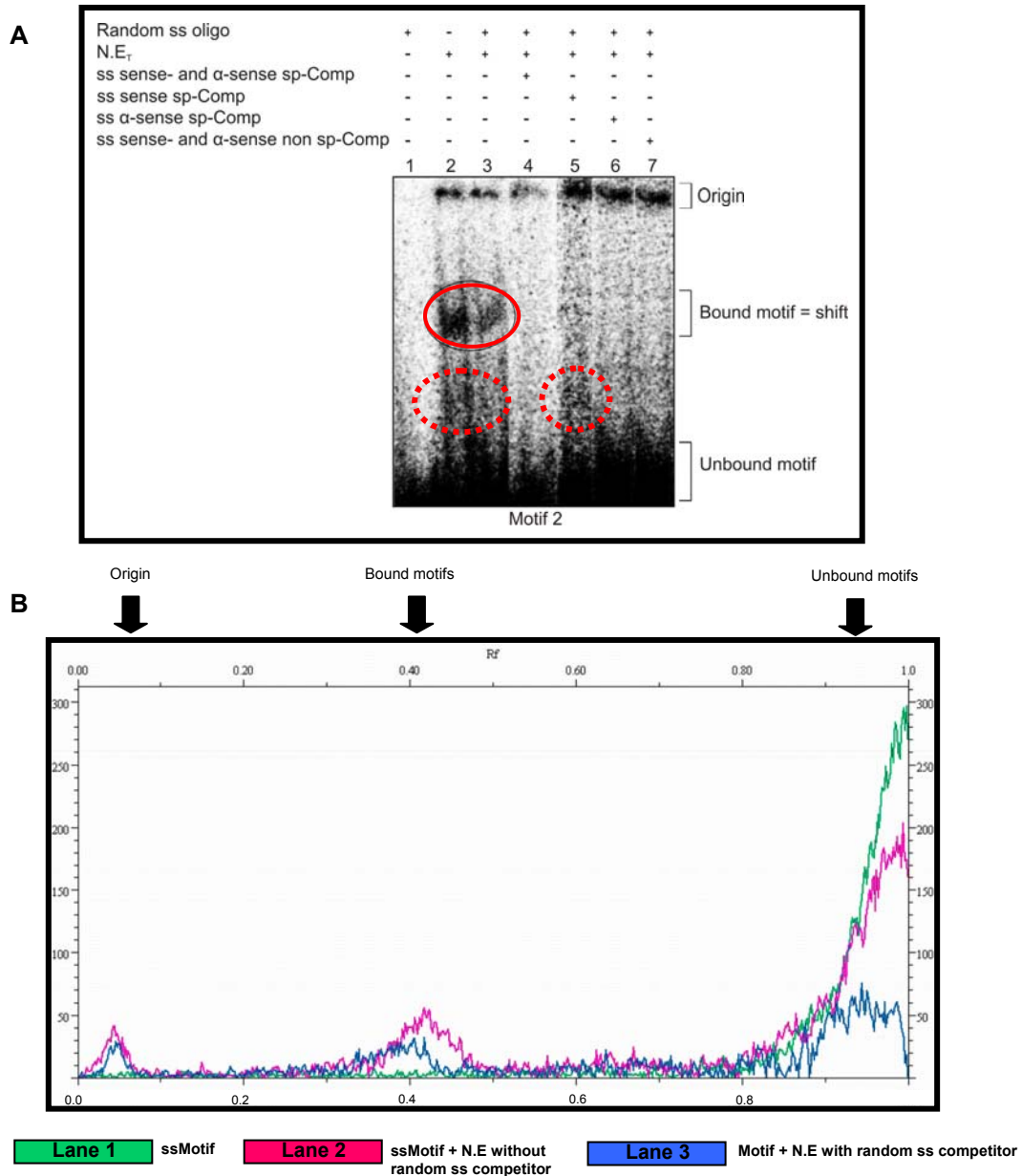


Figure 2.19: (A) EMSA of single-stranded control Motif 2 with trophozoite nuclear extract in the presence and absence of random single-stranded unlabelled oligonucleotide and (B) densitometric lane analysis of EMSA.

Dashed circles represents possible shifts however, densitometric lane analysis concluded that these were not shifts. Random ss oligo: Random single-stranded unlabelled oligonucleotide (50 fold excess); N.E_T: Nuclear extract from trophozoites; ss sense and α -sense sp-Comp: 100 fold excess single-stranded sense and antisense unlabelled specific oligonucleotide; ss sense sp-Comp: 100 fold excess single-stranded sense unlabelled specific oligonucleotide; ss α -sense sp-Comp: 100 fold excess single-stranded antisense unlabelled specific oligonucleotide; ss sense and α -sense non sp-Comp: 100 fold excess single-stranded sense and antisense unlabelled non-specific oligonucleotide

Densitometric lane analysis (Figure 2.19 (B)) confirms the presence of identical shifts with Rf values of ~0.4 in both the presence and absence of the random single-stranded oligonucleotide. The absence of the shift at Rf ~0.6 is unexpected since the EMSA results illustrated in Figure 2.16 of single-stranded Motif 2 in the presence of the random single-stranded competitor (and absence of ATP) did result in two shifts, one at an Rf of ~0.39 and the other at Rf ~0.6.

Since the ^{32}P -labelled motifs are in single-stranded form, it could thus be possible that the shift observed here is as a result of two proteins of similar size binding to different fractions of the ^{32}P -labelled single-stranded motif. The addition of the random single-stranded unlabelled oligonucleotide out-competes for what is thought to be *PfRPA* and subsequently causes a decrease in the amount of protein bound to the ^{32}P -labelled single-stranded motif, which is observed in the EMSA as a less prominent band (lane 3), while the *P. falciparum* nuclear protein remains bound to the labelled motif. It therefore remains plausible that a *P. falciparum* nuclear protein, of similar size to *PfRPA*, binds specifically to a fraction of the ^{32}P -labelled single-stranded motifs while *PfRPA* binds non-specifically to another fraction of the ^{32}P -labelled single-stranded motifs, causing identical shifts (lane 2 and 3). Only *PfRPA* is then out-competed with the random single-stranded oligonucleotide. Again, the shift at $R_f \sim 0.39$ was completely eliminated/out-competed with unlabelled single-stranded specific, and non-specific, oligonucleotide competitors in Figure 2.19 (A) (lanes 4, 5, 6 and 7).

The same EMSA experiment was performed with the remaining four ^{32}P -labelled single-stranded motifs (Motif 1, Motif 3, Motif 4 and Dyad) and again additional competition reactions were set up using non-specific unlabelled single-stranded sense and antisense competitor oligonucleotides to verify the specificity, non-specificity, or sequence-specificity of the DNA-protein interaction. Figure 2.20 represents the EMSA results obtained for Motif 1, 3, 4 and Dyad in single-stranded state with different competitors.

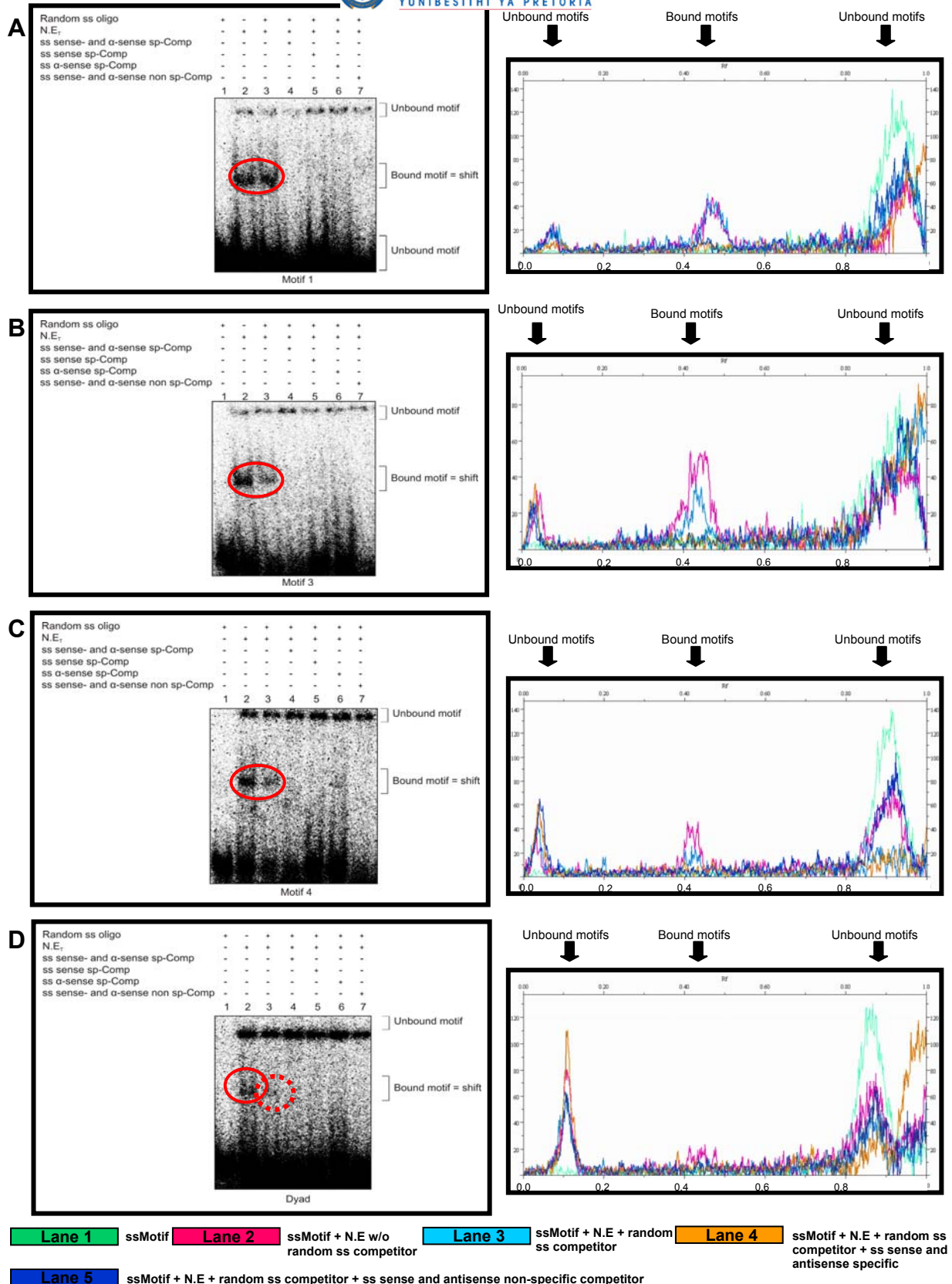


Figure 2.20: EMSA's (left) of single-stranded motifs with trophozoite nuclear extract with different specific- and non-specific single-stranded competitors, densitometric lane analysis (right) of EMSA's.

Dashed circle represents a possible shift. Random ss oligo: Random single-stranded unlabelled oligonucleotide (50 fold excess); N.E.: Nuclear extract from trophozoites; ss sense and α -sense sp-Comp: 100 fold excess single-stranded sense and antisense unlabelled specific oligonucleotide; ss sense sp-Comp: 100 fold excess single-stranded sense unlabelled specific oligonucleotide; ss α -sense sp-Comp: 100 fold excess single-stranded antisense unlabelled specific oligonucleotide; ss sense and α -sense non sp-Comp: 100 fold excess single-stranded sense and antisense unlabelled non-specific oligonucleotide.

In Figure 2.20 (A), Motif 1 resulted in identical shifts at $R_f \sim 0.46$ when the random single-stranded unlabelled oligonucleotide was both absent and present (lane 2 and 3). For Motif 3 and Motif 4, shifts with identical R_f values (0.42) were observed in the presence and absence of the random single-stranded unlabelled oligonucleotide while the addition of the random single-stranded unlabelled oligonucleotide appeared to have caused decrease signal intensities. The Dyad EMSA resulted in a shift at an R_f of ~ 0.43 in the absence of the random single-stranded unlabelled oligonucleotide (lane 2, Figure 2.20 (D)) which was eliminated with the addition of the random single-stranded unlabelled oligonucleotide (lane 3). This result however deviates from the observation in Figure 2.17 (lane 2) where the Dyad EMSA clearly resulted in shifts in the presence of the random single-stranded competitor and in the absence of ATP. The reason for this deviation is uncertain and this result suggests that exact EMSA repeatability is experimentally challenging due to the intricacy of DNA-protein interactions.

All the shifts observed in Figure 2.20 (lanes 2 and 3) were eliminated with the addition of excess motif specific- and non-specific single-stranded competitor oligonucleotides (lanes 4, 5, 6 and 7), regardless as to whether the competitor sequence was sense or antisense. Literature results (Voss *et al*, 2003) of competitor studies illustrated that any added competitor which competes with the sequence of interest for the binding protein, will eliminate the shift completely. This is what was observed in lanes 4, 5, 6 and 7 of Figure 2.20 and thus allow us to conclude that the DNA-protein interaction remaining after addition of random single-stranded competitor oligonucleotide, presumably originates from a *P. falciparum* nuclear protein, and may be sequence-specific.

To address the sequence-specificity of the DNA-protein interaction, a multiple sequence alignment (www.ebi.ac.uk/Tools/clustalw2/index.html) was performed with all five motifs in question, to determine whether there are regions conserved in similarity that may have functional significance in protein binding. The alignment of the motifs is illustrated in Figure 2.21.

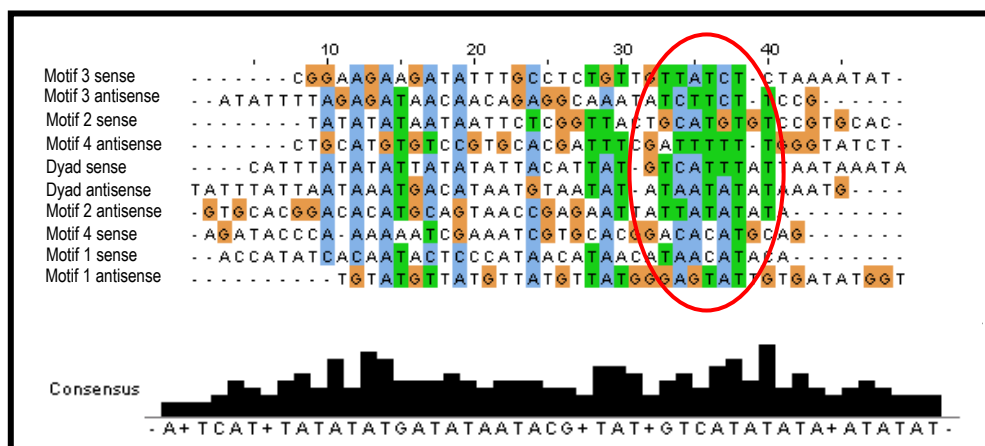


Figure 2.21: CLUSTALW alignment of the five motifs in question.
Red circle represents areas with high similarity among the motifs.

The consensus sequence in Figure 2.21 illustrates the nucleotides most common between all motifs and it appears as though there are small stretches of nucleotides that are very similar among the motifs. However, definite similarities are observed between specific pairs of motifs, especially the nucleotide sequences found between 30 – 40 nucleotides, represented by a red circle.

The alignment verified that Motif 2 and Motif 4 sequences are very similar (45%) and in conjunction with the EMSA results (Figure 2.20), the proteins bound to Motif 2 and Motif 4 are assumed to be similar. Motif 3 shares some similarity with both Motif 4 (30%) and the Dyad (32%), however the Dyad shares greater similarity with Motif 1 (38%). Motif 3 is therefore assumed to share sequence similarity with both Motif 2 and Motif 4. These results allow the assumption that all these motifs share either the same binding protein or similar binding proteins (example: *PfRPA* and the *P. falciparum* nuclear extract specific protein) however, the protein affinities for the sequences may vary and therefore be affected by competition assays.

2.4 DISCUSSION:

The parasite *P. falciparum* has proven to be a complex parasite and a mastermind at escaping the host immune system. In order to eradicate this parasite, new drug targets and gene intervention strategies, aimed at targeting the mechanisms utilized by the parasite to evade the immune system, are required. *P. falciparum* resides within the erythrocyte of its host and utilizes antigenic variation to escape the host immune system. The erythrocyte is an ideal home for the parasite since it does not differentiate and does not hold any trafficking machinery. Antigenic variation in *P. falciparum* is controlled by the *var* gene family and requires regulatory proteins to determine the transcriptional state of the antigenically variant genes. Several conserved *cis*-regulatory sequences were identified in *P. falciparum* using an *in silico* strategy and the aim of this study was to determine whether these sequences are regulated by parasite derived specific proteins.

The structure of the parasite within the erythrocyte is extremely complex, consisting of numerous membranes and residing within a parasitophorous vacuole. This complex structure makes isolation of parasite specific proteins very challenging and special extraction methods were required. In this study, a specialized *P. falciparum* extraction method (Voss *et al.* 2003) was compared to commercial extraction kits and the results obtained revealed that the commercial kits were not as functional and successful in extracting parasite proteins, as was the specialized protocol from Voss *et al.* (2003). Within the erythrocyte, the parasite's metabolic activity increases as it progresses through one life cycle stage to the next and the nuclear extracts from each cycle also revealed the significant increase in protein levels as the parasite proceeded from the ring stage through to the trophozoite stage and into the schizont stage. Although there were extensive similarities and differences between the protein profiles of the different parasite life cycle stages, the up- and down-regulation of certain genes, and the just-in-time transcription of genes proposed by Bozdech *et al.* (2003) become noticeable with certain proteins being present in certain life cycle stages and absent in others. The presence and absence of proteins may also be due to post-transcriptional regulation such as mRNA degradation, as suggested by Shock *et al.* (2007), in addition to the more conventional transcriptional regulation.

Voss *et al.* (2002) identified a protein present in *P. falciparum* nuclear extract to bind in a non-specific manner, but with high affinity to single-stranded DNA and with a lower affinity to double-stranded DNA (Voss *et al.*, 2002). This protein was affinity purified and identified with mass spectrophotometry to be *PfRPA*, a 55 kDa protein which play major roles in DNA metabolism, including DNA replication, recombination and repair (Voss *et al.*, 2002). *PfRPA* activity was found to be present in both nuclear and cytoplasmic extracts and the expression profile of

PfRPA revealed that this protein is expressed in all life cycle stages of *P. falciparum* except mid rings (8-15 h.p.i) (Voss *et al.*, 2002). It is therefore possible that the common 55 kDa band present in both the nuclear and cytoplasmic extract and in all three asexual life cycle stages of the parasite, is *PfRPA*. Analysis of the transcript and proteome profile (Bozdech *et al.*, 2003; Lasonder *et al.*, 2002; Le Roch *et al.*, 2004) clearly indicate the expression of proteins in each stage is related to the protein function and location in that specific life cycle stage. It can be assumed that the presence of the 60 kDa protein in both the ring and schizont stage could be due to the similarity in function of this protein in both stages, for example it may be required for erythrocyte invasion.

Regulatory sequences can be found upstream, downstream or in some cases far from the transcription start site and can be classified as either proximal, such as promoter elements which are close to the 5' end of a gene, or distal, such as enhancers and *cis*-regulatory motifs which are elements located far upstream or downstream from the target gene (Abnizova *et al.*, 2006). *Cis*-regulatory sequences are in general very difficult to recognize since they lack specific transcription signals such as CAAT boxes and TAAAT start site consensus sequences (Abnizova *et al.*, 2006). Furthermore, identification of regulatory sequences in an AT rich genome such as *P. falciparum* can prove to be even more challenging. There are numerous computational methods and algorithms to enable the statistical recognition of regulatory regions. However, the information obtained is often biased since it does not take into account the complicated, irregular structure of regulatory regions (Abnizova *et al.*, 2006). The five potential regulatory motifs in this study were identified using an unsupervised (*ab initio*) interactive computational approach, by searching the *P. falciparum* genome for recurring, over-represented motifs without any prior knowledge of transcription factor binding sites (Claudel-Renard, unpublished results). From the hits obtained, an additional analysis was performed to determine the presence of these conserved gene clusters within antigenically variant gene families and subsequently, the five motifs in this study were identified as presumable *cis*-regulatory sequences.

Various *in vitro* techniques are available to study DNA-protein complex formation, such as methylation interference, protein-binding microarrays (PBM), nitrocellulose binding assays, DNase 1 footprinting, reporter gene constructs and EMSA's. Due to ease, simplicity and inexpensive method of detection, as well as the availability of a specialized *P. falciparum* protocol, EMSA's were the method of choice to study the DNA-protein complex formation between the five motifs under question and *P. falciparum* nuclear proteins. *PfRPA* preferentially binds to AT-rich sequences of double-stranded DNA and since the *P. falciparum* genome is highly AT-rich, it was strongly recommended that a 50-fold excess unlabelled single-stranded oligonucleotide be included in all EMSA reactions associated with *P. falciparum* (Voss *et al.*, 2002). Once the ideal EMSA conditions were determined with the positive controls, the

importance of adding the random single-stranded competitor to out-compete *Pf*RPA was determined. The nuclear extract profiles indicated the presence of a 55 kDa protein present in nuclear extracts from all three life cycle stages of the parasite and the EMSA's indicated the possible presence of this protein in the nuclear extract. The EMSA reactions with double-stranded motifs proved to be challenging at first and optimization strategies were performed with very little success of obtaining double-stranded shifts, other than the shifts obtained with the internal positive control, Motif 2. Motif 2 appeared to be bound by a *P. falciparum* nuclear protein which was out-competed with excess double-stranded unlabelled competitor specific to the target sequence. Nuclear extracts from all three life cycle stages of the parasite were studied to determine if the regulatory proteins for the remaining motifs were expressed in other stages. The EMSA's failed at providing shifts for all the motifs except for Motif 2 whose protein was solely expressed in the trophozoite stage. This result supports the stage specificity and "just-in-time" expression of *P. falciparum* proteins and further suggests the possible regulatory role of the Motif 2 binding protein.

EMSA's were also performed with the addition of *P. falciparum* cytoplasmic extract as well as *P. falciparum* total protein extract (results not shown), instead of nuclear extract, to determine if the binding proteins for the motifs were perhaps expressed and actively present in another cellular compartment. However, no shifts were observed in any of these reactions confirming the absence of binding proteins to these motifs in either cytoplasmic or total protein extract of *P. falciparum*. These results indicated that optimizations of EMSA conditions for each individual Motif is necessary. It should be considered that each motif in general is unique with regards to its sequence and the respective protein-binding partner and thus the optimal binding conditions for each motif may differ. Several studies have shown that the addition of co-factors such as ATP and Mg^{2+} can aid the protein binding to its cognate DNA sequence (De *et al.*, 1998; Jazwinski, 1987; Mcentee *et al.*, 1981; Menetski *et al.*, 1985) while other studies have shown that added ATP could adversely interfere with the DNA-protein interaction (Jovanovic *et al.*, 2006). The results obtained suggest that ATP does not increase the *P. falciparum* protein affinity for the five probable regulatory sequences in this study, regardless of whether the sequences are in the single- or double-stranded state.

The binding buffer is of extreme importance since this buffer contains divalent cations such as Mg^{+2} and Zn^{+2} , non-ionic detergent Triton X-100 and various chelating reagents and it was assumed that the 4 x EMSA buffer recommended by Voss *et al.* (2003) was optimized. The use of poly (dI-dC) to eliminate non-specific binding proteins are advisable in EMSA's but studies performed by Larouche *et al.* (1996) have shown that excessive amounts of poly (dI-dC) can impair and even prevent the DNA-protein complex formation (Larouche *et al.*, 1996). It was recommended by Voss *et al.* (2003) to use between 0.1-2 μ g poly (dI-dC) for *P. falciparum*

EMSA's and thus 1 μg poly (dI-dC) was used in the present study. However, the lack of clear EMSA shifts obtained for most of the putative regulatory sequences suggests that some optimization of poly (dI-dC) concentration may have been required. Some DNA-protein interactions require optimum NaCl and KCl concentrations and excess salt has been proven to decrease DNA-protein complex stability (Jazwinski, 1987). The optimum molar concentrations of Mg^{2+} was found to be ~ 10 mM and the 4 x EMSA buffer contained 8 mM MgCl_2 and 240 mM KCl respectively. The difficulty of obtaining shifts in these EMSA's may therefore indicate that future optimisation of the 4 x EMSA buffer for application to the oligonucleotides used in this study may be necessary.

No DNA-protein complexes were observed with double-stranded Motif 1, Motif 3, Motif 4 or the Dyad in the presence of ring, trophozoite or schizont nuclear extract. As seen with Cro proteins, the sequence of a gene is of utmost importance for specific protein binding since changing the DNA sequence from ATAT to AGCT decreases the binding affinity of the Cro protein 60-fold (Lilley, 1995). When designing the motifs under question in this study, the flanking regions were designed by sequence alignment and choosing conserved residues. This could have resulted in small changes in the overall regulatory sequence identified by the cognate binding protein, ultimately resulting in a decrease of affinity. Co-operativity is also a common finding amongst DNA-binding proteins where the binding proteins are arranged in such a way to be a functional pair and synergistically activate or repress promoter activity. The regulatory sequences in this study were all approximately 40 nucleotide bases in length while Voss *et al.* (Voss *et al.*, 2003) used motifs of up to 80 nucleotide bases. It could thus be possible that the sequences used here were too short for co-operative binding to occur if the protein binding partner of interest to the motifs in question were indeed co-operative and required a second protein for the initial DNA recognition. The majority of DNA-protein interactions involve Guanine base recognition, and identification of binding proteins in *P. falciparum* is difficult due to the fact that Adenine bases are less frequently recognized by binding proteins, compared to Guanine bases (Neidle, 2002). The sequences of the regulatory motifs identified in this study are by default AT-rich and thus could have complicated protein recognition.

Certain proteins have the ability to bind both double- and/or single-stranded regulatory sequences (Stark *et al.*, 1992). The final study was to determine if the motifs in question have single-stranded binding proteins. In these single-stranded EMSA's it appears as though a protein of similar size to *PfRPA* binds to all the conserved motifs and that single-stranded Motif 2 has two binding proteins. The ^{32}P -labelled single-stranded oligonucleotides were in a one to one ratio of sense and antisense and could also anneal to form double-stranded oligonucleotides. The annealing temperatures of these oligonucleotides are higher than room temperature and thus, the formation of double-stranded motifs after denaturation may be

favourable. This suggests that the shifts observed could be due to the nuclear protein binding to either the sense or antisense or even the double-stranded oligonucleotide sequence. The shifts with identical Rf values obtained with every motif occurred in the presence of the random single-stranded competitor and was eliminated with unlabelled single-stranded competitors derived from the motifs themselves, suggesting that the shifts observed were as a result of a *P. falciparum* nuclear protein, with sequence specificity, binding to either the sense or antisense strand of the motifs. The elimination of the shift with motif derived competitor could, however, also be as a result of excess (100 fold) competitor as apposed to the 50 fold random competitor. Since the single-stranded EMSA reaction contained excess single-stranded motifs, perhaps a greater fold competitor (100 fold) was needed to out compete for the binding protein, which in this case could then be *PfRPA*. After competitor studies in the presence and absence of the random single-stranded competitor and sequence alignment, it appeared that these motifs share some sequence similarity and that another protein, in addition to *PfRPA*, may be binding to the motifs with different degrees of affinity. It appears as though all the motifs in question have single-stranded regulatory proteins and the identity and function of these remain to be elucidated.

An interesting alignment finding was the great degree of sequence similarity shared between Motif 2 and Motif 4 and the similar EMSA results obtained with these single-stranded motifs. The *in silico* approach used to identify these motifs (Table 2.2), classified these two motifs as important findings, since all repeats of these two motifs reside within antigenically variant gene families. This result therefore further suggests that Motif 2, previously identified by Voss *et al.* (2003) as SPE 1, is a potential double-stranded, and to a lesser extent single-stranded, regulatory gene and that Motif 4 could be a potential single-stranded regulatory sequence, important for regulating *P. falciparum* antigenic variation.

A fundamental part of any EMSA is the presence and integrity of the protein binding partner within the nuclear extract. The quality of the nuclear extract and the final protein concentration correlated well with literature values (Voss *et al.* 2003). In this study it has become apparent that EMSA experiments with *P. falciparum* proteins remain challenging with regards to repeatability of shifts and emphasizes the importance of using an optimized protocol. EMSA reactions performed with the modified protocol by Voss *et al.* (2003) proved promising and the importance of including the random single-stranded unlabelled oligonucleotide to eliminate non-specific shifts caused by *PfRPA* was confirmed.

It would have been beneficial to this study to determine the fraction of radioactively labelled DNA which is in double- and single-stranded form, prior to the EMSA's, since this would have assisted with the subsequent EMSA analysis of the results. The single- and/or double-stranded

state of the oligonucleotides after denaturation can be determined via either hydroxyapatite chromatography, S1 nuclease hydrolysis of single-stranded DNA, DNA Quant assays or capillary electrophoresis (Drabovich *et al.*, 2004; Durre, 2005; Kinney *et al.*, 1999; Schroder *et al.*, 2003). The hydroxyapatite chromatography utilizes high molarity buffers to elute the bound double-stranded DNA while S1 nuclease digestion specifically digests single-stranded DNA allowing the remaining double-stranded DNA to be precipitated (Schroder *et al.*, 2003). The DNAQuant assay (Promega) uses coupled enzyme reactions to produce ATP which is proportional to the amount of the double-stranded DNA present in the sample, while the single-stranded binding protein (SSB) capillary electrophoresis technique allows the separation of single-stranded and double-stranded DNA via the change in electrophoretic mobility of single-stranded DNA, which is bound by SSB (Drabovich *et al.*, 2004; Kinney *et al.*, 1999). In addition, Colorimetric detection of single-stranded DNA using colloidal gold nanoparticles can be used to determine the presence and fraction of single-stranded DNA in a solution containing double-stranded DNA and single-stranded DNA (Rho *et al.*, 2009). An easier alternative would have been to label each sense- and antisense-strand separately with ^{32}P and use them independently in the EMSA reactions. These techniques were however not utilized at the time of study since the requirement to distinguish which fractions of the motif pool were single- or double-stranded were unclear at that stage.

It would be of great interest to this study to analyse the DNA-protein interaction observed with the five motifs further but utilizing additional *in vitro* techniques such as Nitocellulose binding assays, DNase 1 footprinting, DNA protein crosslinking and Chromatin Immunoprecipitation (ChIP) (Abnizova *et al.*, 2006). Double-stranded microarray studies of the DNA-protein interaction can help to explore the sequence specificity of DNA-protein binding to ultimately indicate the relative affinity of the binding proteins (Abnizova *et al.*, 2006). Protein-binding microarrays (PBM) can also be used to determine *in vitro* binding specificities of transcription factors by assaying the sequence-specific binding of individual transcription factors to double-stranded DNA microarrays containing numerous potential DNA binding sites (Mukherjee *et al.*, 2004). In addition to this, X-ray crystallography and NMR spectroscopy data can be utilized to study the structural details of the DNA-protein interaction, to ultimately add data to both the protein data bank and the nucleic acid database.

Single-stranded binding proteins such as eukaryotic RPA function in numerous eukaryotic processes including replication, repair and recombination. Homology searches for the presence of other well known single-stranded and double-stranded DNA binding proteins in *P. falciparum* resulted in no significant hits. Thus, future perspectives for this study would include finding a means to accurately identify and characterize the binding proteins. Antibodies against RPA exist and therefore supershift assays can be performed to verify if the shifts observed are due to PfRPA or due to another protein. Tryptic digestion of UV crosslinked EMSA reactions can be

analyzed via SDS-PAGE, to determine the various positions at which these binding proteins bind, since this will give further insight as to whether these proteins identify and bind identical sites on the DNA motif. Finally, it would be ideal to isolate the binding proteins via affinity purification by using streptavidin-coated magnetic beads with the tethered biotinylated motif of interest. The bound proteins can be eluted after several wash steps and fractions can be analyzed by SDS-PAGE and silver staining. Thereafter the purified protein eluates can be combined, run on an SDS-PAGE and the band of interest excised, trypsin digested and analyzed with mass spectrophotometry. Database searches with the fragmentation spectra obtained via MS/MS from the tryptic peptides could ultimately identify the DNA binding protein. Once these regulatory binding proteins have been identified and characterized, more specific anti-malarial drugs can be designed to mimic these regulatory proteins and ultimately abolish antigenic variation in *P. falciparum*.

CHAPTER 3

POST-TRANSCRIPTIONAL MECHANISMS OF REGULATION FOCUSING ON POLYAMINE PATHWAY ENZYMES S-ADENOZYMETHIONINE DECARBOXYLASE/ORNITHINE DECARBOXYLASE AND SPERMIDINE SYNTHASE

3.1 INTRODUCTION

3.1.1 Polyamines

Polyamines are a group of organic cations that are present in all cells and although their roles have not yet been fully elucidated, studies have made it clear that they are involved in cellular processes such as transcription, replication, translation and even apoptosis and are thus crucial factors in cell proliferation and differentiation (Thomas *et al.*, 2003). Polyamines are positively charged molecules which allow electrostatic interactions (via cationic amino groups) and hydrophobic interactions (via methylene bridging groups) to be dominant, allowing polyamines to interact with anionic compounds such as DNA, RNA and mitotic chromosomes or act as ligands on DNA, RNA, proteins and phospholipids (Thomas *et al.*, 2003). Polyamines have the ability to promote DNA conformational changes where DNA bending can be provoked by micromolar concentrations of polyamines, which in turn lead to regulation of gene expression (Thomas *et al.*, 2003). Polyamines also have the ability to enhance the binding of several gene-regulatory proteins to specific regulatory sequences (Thomas *et al.*, 2003).

Due to their multiple functions, intracellular levels of polyamines are tightly controlled through biosynthetic, catabolic and transport mechanisms (Loikkanen, 2005). The levels of the polyamines, putrescine (a diamine), spermidine (a triamine) and spermine (a tetra-amine) are controlled by enzymes which are either biosynthetic or catabolic (Figure 3.1) (Thomas *et al.*, 2003). Biosynthetic enzymes of the polyamine pathways include Ornithine decarboxylase (ODC), S-Adenosylmethionine decarboxylase (AdoMetDC), Spermidine synthase and Spermine synthase while the catabolic enzymes are spermine/spermidine acetyltransferase, flavin containing polyamine oxidase and copper containing diamine oxidase (Thomas *et al.*, 2003). The transport of polyamines are carrier-mediated, involving transporters, which suggests that the uptake of polyamines are relatively saturable and a energy-mediated process (Loikkanen, 2005). Studies performed by Jänne *et al.* (1975) illustrated that polyamines participate in protein synthesis by enhancing the synthesis and activity of RNA polymerases, in addition to stimulating the synthesis of specific proteins and decreasing amino acid misincorporation during polypeptide synthesis (Jänne *et al.*, 1975; Loikkanen, 2005). Polyamine accumulation and

deprivation respectively stimulate and inhibit synthesis of DNA, RNA and proteins and thus their intracellular levels require tight regulation (Loikkanen, 2005).

Polyamine synthesis involves two amino acids; L-arginine and L-Methionine (Loikkanen, 2005). L-ornithine is cleaved from L-arginine by arginase II and decarboxylated by ODC to release putrescine (Loikkanen, 2005). Methionine adenosyltransferase converts L-Methionine to S-adenosylmethionine (S-AdoMet) which is decarboxylated by AdoMetDC. An aminopropyl moiety is transferred from decarboxylated S-AdoMet to putrescine by Spermidine synthase forming spermidine (Loikkanen, 2005). In mammals, Spermine synthase converts spermidine to spermine. The metabolic pathway in *P. falciparum* is more simplified such that Spermidine synthase catalyzes the production of spermine and no interconversion pathway exists (Figure 3.1) (Haider *et al.*, 2005). ODC and AdoMetDC have very fast turnover rates with half-lives less than one hour and are said to be the rate limiting enzymes (Loikkanen, 2005).

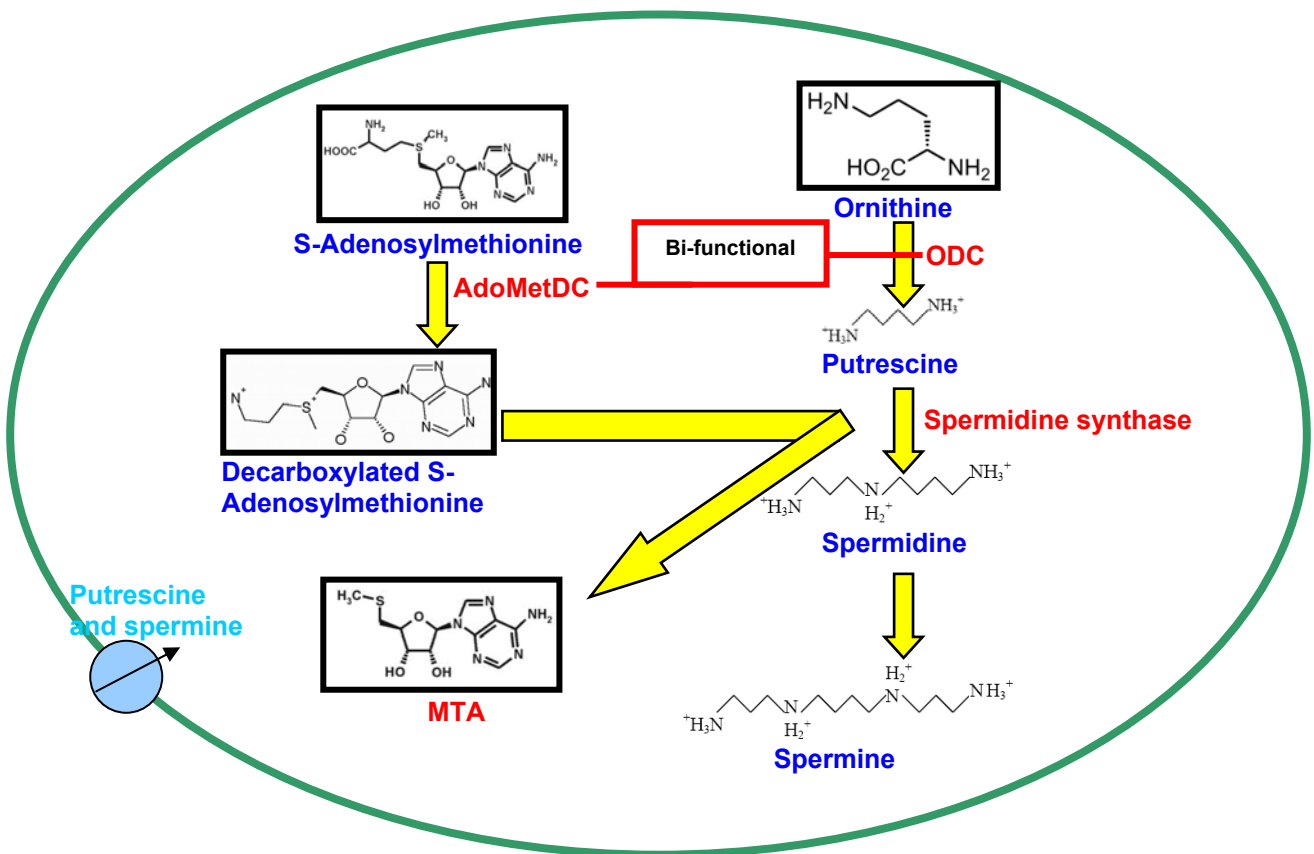


Figure 3.1: A simplified illustration of the metabolic pathways of polyamine synthesis in *P. falciparum*.

ODC (Ornithine decarboxylase), AdoMetDC (S-Adenosylmethionine decarboxylase), MTA (methylthioadenosine)

ODC and AdoMetDC are usually produced by separate genes and are monofunctional homomeric and heterotetrameric structures, respectively (Wrenger *et al.*, 2001). In *P. falciparum* however, ODC and AdoMetDC have been described as a heterotetrameric bifunctional enzyme since a single polypeptide bears both AdoMetDC and ODC activities which are separated by a

hinge region (Birkholtz *et al.*, 2004). This protein has an approximate molecular mass of 330 kDa with AdoMetDC activity on the N-terminus while ODC activity resides in the C-terminus (Birkholtz *et al.*, 2004). During rapid cellular growth, the activity and quantity of the biosynthetic enzymes AdoMetDC and ODC increase, in addition to an increase in the polyamine levels, which makes these enzymes involved in polyamine biosynthesis very intriguing drug targets (Reguera *et al.*, 2005).

Spermidine synthase catalyzes the production of spermidine which increases DNA-polymerase activity and is of great importance for modifying and activating the eukaryotic translation initiation factor eIF5A (Burger *et al.*, 2007).

Since polyamines are important factors in cell proliferation and growth, they have been extensively studied and therapeutically used in the treatment of certain cancers and have additionally been studied as drug targets against *P. falciparum*. Various inhibitors of AdoMetDC, ODC and Spermidine synthase have been developed to block the parasite polyamine pathway, including MGBG (methylglyoxal bis-guanylhydrazone), DFMO (α -difluoromethylornithine) and AdoDATO (S-adenosyl-1, 8-diamino-3-thiooctane), respectively. Both MGBG and DFMO have been used efficiently in the treatment of certain leukaemias and lymphomas but MGBG's use as an anticancer drug was limited due its extreme cytotoxicity and anti-mitochondrial activity (Loikkanen, 2005). DFMO was originally designed as an anti-cancer agent but has become established as an effective agent in the treatment of African sleeping sickness, caused by the protozoan *Trypanosoma brucei gambiense* (Wrenger *et al.*, 2001). DFMO has been used in *P. falciparum* culture and was found to block the erythrocytic schizogony of the parasite. However, due to its cytostatic versus cytocidal effect, it has not been used effectively as a therapeutic agent against *P. falciparum* (Burger *et al.*, 2007).

3.1.2 Polyamine knock-down strategies

Transfection studies provides a valuable tool for analyzing gene function in various organisms and provide greater information on gene function when animal models are available. Transfection in parasites can become challenging since only circular plasmid DNA can be used and the drugs commonly used to select transformed parasites within host cells may result in killing of the host cells (Crabb, 2002). Stable transfection in *P. falciparum* has been developed and makes use of mutant dihydrofolate reductase–thymidylate synthase genes as selectable markers in transfection plasmids (Crabb, 2002). Current techniques employed for gene knock-down include morpholino oligonucleotides, siRNA, transfection and allelic exchange which have been successfully used in *Plasmodium* (Kocken *et al.*, 2002; Nkrumah *et al.*, 2009; Russo *et al.*, 2009; Triglia *et al.*, 1998; Waller *et al.*, 2003).

Several gene knock-out and knock-down strategies that are aimed at polyamine metabolism have been employed in both *T. brucei* and *Leishmania* and thus provide evidence for the importance of polyamine biosynthetic enzymes in cell growth. Knock-outs of AdoMetDC, ODC and Spermidine synthase in *L. donovani* have allowed functional characterization and determination of the importance of these enzymes. Both AdoMetDC and ODC knock-out studies resulted in parasites incapable of growing in medium not supplemented with polyamines. However, addition of spermidine to the medium rescued the deletion mutant parasites (Jiang *et al.*, 1999; Roberts *et al.*, 2001; Roberts *et al.*, 2002).

The mechanism of polyamine regulation has been studied in *T. brucei* with the use of RNA interference, where the effect of AdoMetDC and prozyme knock-down on cell growth was studied (Willert *et al.*, 2008). AdoMetDC is activated when a prozyme, which is a catalytically dead homolog, binds to it and forms a heterodimer (Willert *et al.*, 2008). RNA interference was utilized to knock-down AdoMetDC and prozyme and the results revealed a decrease in spermidine and trypanothione levels, which ultimately lead to cell death (Willert *et al.*, 2008). Trypanothione is unique to Trypanosomatids and is produced when spermidine becomes conjugated to glutathione (Willert *et al.*, 2008). It is evident through inhibitor studies that interference of polyamine production in *P. falciparum* is detrimental to the parasite and the importance of the AdoMetDC/ODC bifunctional gene and Spermidine synthase gene for polyamine production and cell proliferation, has been demonstrated (Assaraf *et al.*, 1984; Clark *et al.*, 2008; Dasgupta *et al.*, 2005; Muller *et al.*, 2008; Van Brummelen *et al.*, 2009). Knocking-out of *P. falciparum* essential genes may prove to be challenging, leading to sudden parasite death and inconclusive results, whereas gene knock-down studies of parasite essential genes maintain parasites in a viable state and may provide a greater understanding of gene regulation.

3.1.2.1 RNA interference

Several studies claim the success of using RNA interference as a gene knock-down tool in *Plasmodium*. Double-stranded RNA has been used against dihydro-orotate dehydrogenase (DHODH), cysteine proteases (falcipain-1, falcipain-2 and falcipain-3), signal peptidase (*PfSP1*), Serine/threonine phosphatase (*PfPP1*) and several pathogenic genes (Dasaradhi *et al.*, 2005; Kumar *et al.*, 2002; Malhotra *et al.*, 2002; Mcrobert *et al.*, 2002; Siau *et al.*, 2007; Tuteja *et al.*, 2008). The mechanism associated with the decreased transcript levels observed in the studies mentioned above remain to be elucidated since a RISC-mediated degradation mechanism has not yet been demonstrated in *P. falciparum*.

Recently Baum *et al.* (2009) performed various studies to determine the viability of RNA interference in *Plasmodium* by utilizing *in silico* homology searches and a variety of biological

investigating techniques, such as introducing siRNA into parasite lines and designing double-stranded RNA hairpin constructs to knock-down certain genes under study (Baum *et al.*, 2009). Their final results lead them to conclude that RNA interference is not possible in *Plasmodium* but that antisense mechanisms should be investigated further. In addition, Siau *et al.* (2007) hypothesized that *P. falciparum* may utilize its existing antisense machinery to process double-stranded RNA, which would ultimately result in gene knock-down (Siau *et al.*, 2007).

Advantages of using RNA interference as a knock-down tool is the efficiency and specificity of the degradation. RNA interference often results in the partial knock-down of a gene and thus leads to the production of a range of phenotypes with differing severity, which in turn facilitates the study of essential genes (Small, 2007). RNA interference can be controlled in a time-dependent manner and several related genes can be targeted to determine gene functions. Disadvantages of RNA interference include off-target effects, since the expression of genes not targeted by the double-stranded RNA may be affected. RNA interference provides the ability to analyze the effect of reduced gene expression while at the same time allowing the parasite to survive and thus this technique was used to attempt knock-down of *P. falciparum* AdoMetDC/ODC and Spermidine synthase with the aim of further exploring the significance of these biosynthetic enzymes in parasite growth and survival.

3.1.3 Semi-quantitative Real-Time PCR (semi-qPCR)

The original polymerase chain reaction (PCR) reaction allows the amplification of any nucleic acid sequence by using a cyclic process to generate multiple copies, which are then analyzed with electrophoresis (Kubista *et al.*, 2006). Quantification is a serious limitation of PCR since end-point analysis of the PCR product only reveals that the same amount of product forms, independent of the amount of template in the original sample (Kubista *et al.*, 2006). End-point analysis thus would provide both qualitative results, to confirm the presence or absence of a target, and semi-quantitative results, since the analysis is performed once the reaction is exhausted and has reached a plateau phase (Kubista *et al.*, 2006). End-point analysis is the only analysis option available for standard PCR, while it is not essential in semi-qPCR, but can be useful to determine the presence of any primer-dimers (Kubista *et al.*, 2006). Due to the limitations of the original PCR, semi-qPCR was developed to use a fluorescent reporter which binds to the product formed during the reaction and in this way, the fluorescent signal is directly proportional to the amount of product (Kubista *et al.*, 2006). The fluorescent signal is weak at first but as the amount of product accumulates during the PCR run, the signal increases exponentially and eventually levels off and saturates, usually due to the reaction being depleted of critical components such as primers, dNTP's or reporter. In the log phase of the reaction, the response curves become separated and the difference in the initial amounts of template

molecules that were present, can be determined by comparing the number of amplification cycles that were required for the response curve of the sample to reach a certain fluorescent threshold signal, known as the sample's threshold cycle (C_T) value, here known as the C_q point (Kubista *et al.*, 2006; Lefever *et al.*, 2009).

Semi-qPCR makes use of different types of probes and dyes to detect the product. Taqman probes and molecular beacons depend on FRET (Foster Resonance Energy Transfer) while SYBR Green is a fluorescent dye which emits a strong signal once it is bound to double-stranded DNA (Figure 3.2) (Dharmaraj, Applied Biosystems). SYBR Green is the simplest, most economical and inexpensive fluorescent method to use in semi-qPCR and is both sensitive and easy-to use, however the disadvantage is that it can bind to any double-stranded DNA sequence, including primer-dimers (Dharmaraj, Applied Biosystems).

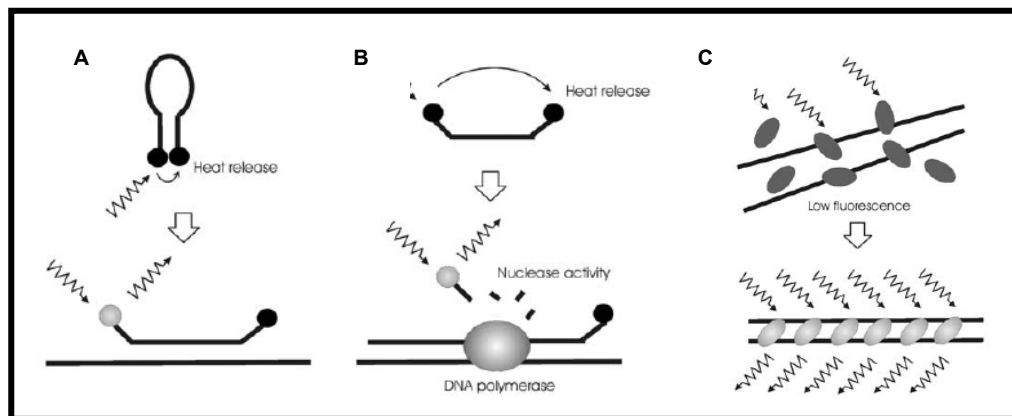


Figure 3.2: Mechanisms of reporters commonly used in semi-qPCR (adapted from (Kubista *et al.*, 2006).

(A) Molecular beacon: Hybridization of molecular beacon to the target, separates the fluor and the quencher resulting in fluorescent light upon radiation. (B) Taqman probe: The 5' nuclease activity of DNA polymerase cleaves the Taqman probe resulting in the decoupling of the probe and quencher and fluorescent signal is detected. (C) SYBR Green: Binding of SYBR green to double-stranded DNA causes bright fluorescence and thus fluorescence signal increases proportionally as semi-qPCR product accumulates.

In this study, semi-qPCR was employed to monitor the transcript levels of *P. falciparum* AdoMetDC/ODC and Spermidine synthase after double-stranded RNA knock-down of these genes.

3.2 MATERIALS AND METHODS

Keeping the expression profiles in mind, double-stranded RNA treatment time points and RNA extraction time points were carefully considered. For the RNA interference study, *P. falciparum* parasites were treated in both the ring stage (~10 h.p.i) and in the early trophozoite stage (~20 h.p.i) (Figure 3.3). Treating parasites in the ring stage required electroporation to introduce the double-stranded RNA into the cell (Waterkeyn *et al.*, 1999). Electroporation allows foreign material to enter the cell since, once an electric potential is applied and the critical field is

achieved, there is a rapid rearrangement of lipids which result in the formations of a pore, which then allows the movement of molecules into the cell. Transcription of AdoMetDC/ODC and Spermidine synthase is between 8-38 h.p.i (Figure 3.3 (A)). Treating parasites at 10 h.p.i allows double-stranded RNA to be introduced in the ring stage, at the start of the AdoMetDC/ODC and Spermidine synthase transcript production in *P. falciparum*. *P. falciparum* parasites were harvested at 16 h.p.i, a time point which falls before and during peak production of AdoMetDC/ODC and Spermidine synthase transcript, respectively. Cultures are again harvested at 34 h.p.i, after peak transcription of both AdoMetDC/ODC and Spermidine synthase has been reached. At 16 h.p.i the transcripts for AdoMetDC/ODC and Spermidine synthase are still actively being transcribed and thus the RNA interference effect at this time point will be expected to be minimal due to possible saturation. However, due to the “just-in-time” hypothesis, mRNA transcripts are often immediately translated into protein and thus the most effective transcript interference may occur when the transcript is being actively transcribed. At 34 h.p.i however, the parasites will be metabolically active in the trophozoite stage and transcripts would have reached maximum expression. Therefore, the double-stranded RNA introduced into the cells are assumed to adversely affect the remaining mRNA transcript levels and the RNA interference effect may be more noticeable at this time point.

P. falciparum cultures were also treated in the early trophozoite stage (~20 h.p.i). Introduction of double-stranded RNA in this developmental stage does not require electroporation and instead, requires simple incubation since it is believed that parasites at this stage are highly metabolically active and have a modified erythrocyte membrane which can freely take up compounds from the surrounding medium (Adisa *et al.*, 2007; Elford, 1986). Treating parasites at ~20 h.p.i again introduces the double-stranded RNA when the transcripts of AdoMetDC/ODC and Spermidine synthase are being produced. Parasite cultures are harvested at 26 h.p.i., a time point where AdoMetDC/ODC transcript production is at its peak while Spermidine synthase transcript production is on a gradual decline. At this time point the RNA interference effect may be expected to be significant for Spermidine synthase since the available transcripts of Spermidine synthase will be available for degradation, assuming a RISC-mediated degradation mechanism exists in *P. falciparum*. The RNA interference effect on AdoMetDC/ODC may once again be significant at 26 h.p.i, due to the effective interference the introduced double-stranded RNA may have on the transcripts during peak transcription. The cultures are also harvested at 44 h.p.i. when the transcript production of both AdoMetDC/ODC and Spermidine synthase have come to a halt. Therefore, at 44 h.p.i, the RNA interference effect is expected to be noticeable for all double-stranded RNA treatments since AdoMetDC/ODC and Spermidine synthase transcripts are expected to be adversely affected and the pronounced effect of RNA interference on parasite growth can be studied.

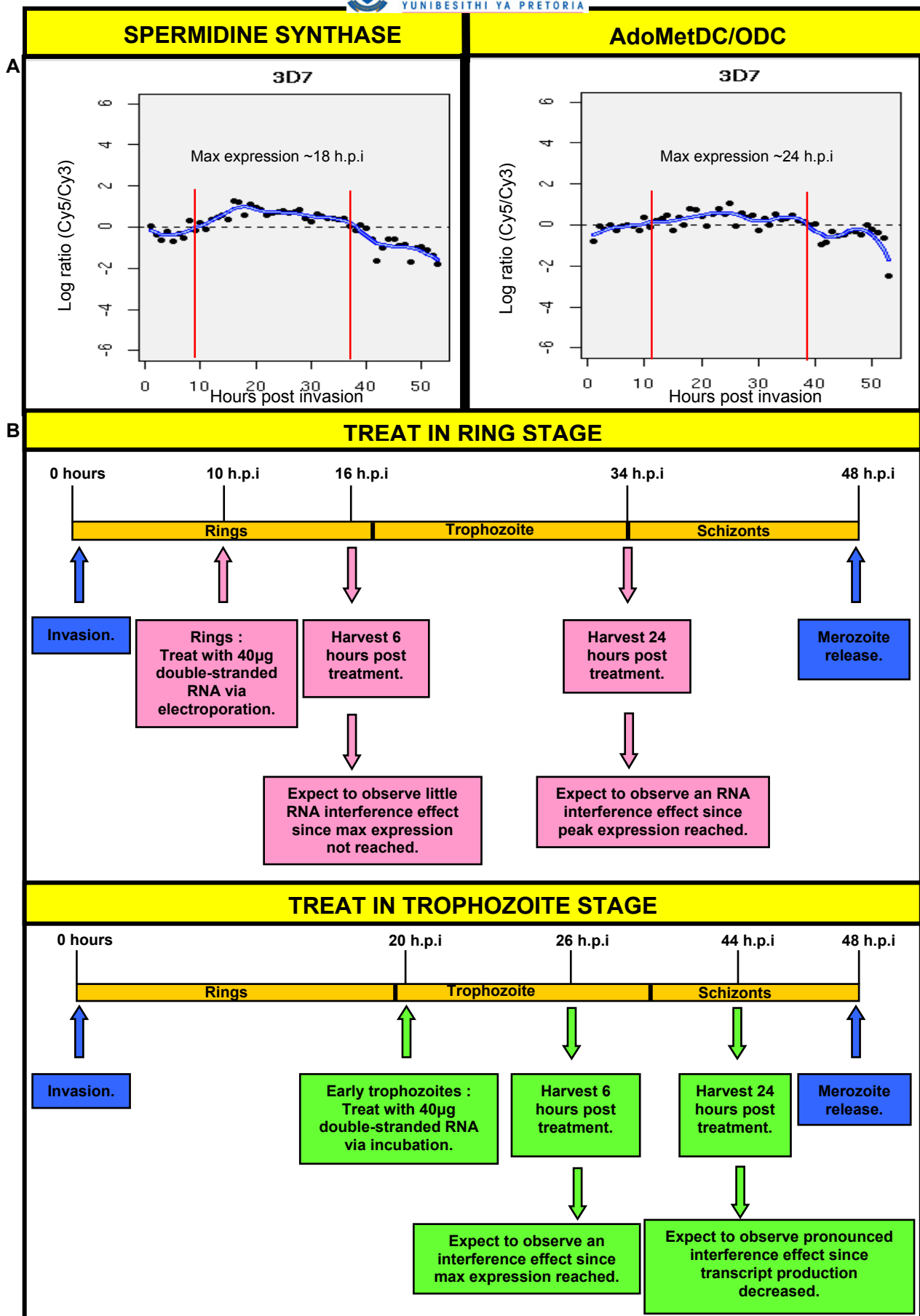


Figure 3.3: (A) The transcript expression profile of Spermidine synthase and AdoMetDC/ODC of *P. falciparum* 3D7 strain (DiRisi lab at <http://malaria.ucsf.edu>), B) Illustration of the experimental set up for RNA interference in *P. falciparum* 3D7 strain.

(A): Red lines indicate start and end of transcript production.

3.2.1 Design of RNA interference primers

The entire gene sequence of AdoMetDC/ODC (Accession number PF10_0322) and Spermidine synthase (Accession number PF11_0301) was obtained from PlasmoDB and subsequently analyzed. The most conserved sequence within each gene region was used for sequence-specific primer design, utilizing primer designing software Oligo (Version 6, MBI). Parameters were set to reduce the formation of hairpin loops and primer-dimers and thus primers requiring less than -5 kcal/mol for dimer or hairpin formation were omitted. Primers were designed to amplify the conserved regions of each gene from plasmids, to subsequently be converted to RNA for the RNA interference study. The T7 promoter sequence was added to the 5' end of both forward and reverse primers to produce final primer lengths of ~40 nucleotides. The T7 RNA polymerase promoter is required at the 5' end of both DNA sequence strands since the T7 RNA polymerase enzyme is extremely promoter specific and catalyzes the formation of RNA in the 5'-3' direction. Longer sections of the AdoMetDC/ODC gene were also considered for RNA interference and thus the AdoMetDC/ODC gene (greater than 4000 nucleotides) was split into four sections of roughly 1000 nucleotides each and primers were subsequently designed with a T7 promoter sequence at the 5' end of both the forward and the reverse primers, as described previously. The primers were used in subsequent PCR reactions to amplify the sections of the genes under investigation.

The lyophilized primers were reconstituted as described in section 2.2.1. The $A_{260}:A_{280}$ ratios for all the oligonucleotides ranged between 1.9 and 2.4 indicating that the oligonucleotides were pure.

3.2.2 Amplification and purification of genes

The genes of interest, previously cloned into expression plasmids (kind gift from Professor Rolf Walter at the Bernhard Nocht Institute) were amplified for use as templates in double-stranded RNA synthesis. The PCR reactions contained 50% (v/v) Kapa Taq polymerase ready mix, 1 pmol of each forward and reverse primer and 11 ng (110 ng/ μ l) plasmid DNA. The annealing temperature for all the primers in the optimized PCR were identical, however the amount of cycles used for the extension and amplification differed. Amplification of AdoMetDC, Insert, Section 1, Section 2 and Section 4 required 27 cycles while ODC, Spermidine synthase and Section 3 required 29 cycles for successful amplification. PCR reactions were performed in a PCR thermal cycler (GeneAmp PCR System 9700, Perkin Elmer) at 94°C for 3 minutes, followed by the respective amount of cycles at 94°C for 30 seconds, primer annealing at 60°C for 30 seconds and primer extension at 65°C for 4.5 minutes. The PCR cycles were completed after a single incubation step at 65°C for 7 minutes. After large scale PCR reactions were

complete, 10 µl of each amplicon was analyzed on a 2% w/v agarose gel prepared in 1 x TAE (0.04 M Tris, 0.02 M Acetic acid, 0.001 M EDTA, pH 7.6), run at 8 V/cm in a Hoefer HE 33 electrophoresis gel system (Amersham Biosciences) and stained with ethidium bromide.

PCR products were purified at room temperature with the E.Z.N.A cycle-pure kit (PeqLab, Perkin Elmer) as described by the manufacturer. The E.Z.N.A kit purifies DNA ranging in size from 100 bp - 10 kb and assures the elimination of oligonucleotides, nucleotides and polymerases which are present in the PCR reactions. For the gene fragments smaller than 200 bp (AdoMetDC, ODC, Insert and Spermidine synthase), two volumes of proprietary Buffer XP1 were added while only one volume of proprietary Buffer XP1 was added to the gene fragments larger than 200 bp (Sections 1, 2, 3 and 4). The samples were vortexed thoroughly for 5 seconds to evenly resuspend the DNA in the buffer, loaded onto the HiBind DNA spin column, inserted into a 2 ml collection tube and centrifuged at 10 000xg for 1 minute (Eppendorf mini-spin plus, Merck, Germany). The column was subsequently washed twice by adding 750 µl proprietary SPW buffer and centrifuged as described previously. The column was subsequently dried with centrifugation at 10 000xg for 2 minutes and the DNA was eluted with 40 µl ddd water and centrifuged as above.

The concentrations of the purified DNA products were determined spectrophotometrically as in section 2.2.1. All DNA yields were above 100 ng/µl and all $A_{260}:A_{280}$ ratios were between 1.85 and 2.0.

3.2.3 Double-stranded RNA synthesis and purification

To synthesize double-stranded RNA from the PCR-generated DNA templates, the T7 RiboMax Express RNA interference system (Promega) was utilized. The optimum conditions for double-stranded RNA synthesis were determined by increasing the 37°C incubating time incrementally from 2 hours to 6 hours. Sufficient product for the RNA interference study was obtained with 3 hour 37°C incubation. The efficiency of DNase and RNase digestion was determined by comparing the undigested double-stranded RNA product with RNase and DNase digested products. Once the optimum conditions for RNA synthesis were determined, double-stranded RNA was produced on a large scale for all genes in question. Reactions contained 1 x proprietary RiboMAX 2x buffer, 6 µg purified DNA template and 8 µl proprietary T7 Express enzyme mix. Reactions were incubated at 37°C for 3 hours in a PCR thermal cycler (Perkin Elmer), followed by enzyme inactivation at 65°C for 5 minutes. The reactions were allowed to cool to room temperature for 5 minutes after which the reactions were again incubated at 70°C for 10 minutes and allowed to cool to room temperature for 20 minutes to anneal complementary RNA's.

The double-stranded RNA reactions were treated with both a proprietary RQ1 RNase-free DNase and a proprietary RNase1 solution, obtained from the T7 RiboMax Express RNA interference system, to eliminate any remaining contaminating DNA and single-stranded RNA respectively. A 1/200 dilution of the RNase solution provided by the kit was prepared fresh for each digestion. For the double-stranded RNA digestion reaction, 4 µl of proprietary DNase and 4 µl diluted proprietary RNase was added to each 80 µl double-stranded RNA product and incubated at 37°C for 30 minutes and placed on ice. For the large double-stranded RNA sections (Section 1, 2, 3 and 4) it was necessary to perform the RNase/DNase digestion step at 37°C for 2 hours to degrade the majority of contaminating nucleic acids.

In order to purify the double-stranded RNA from the digested RNA reactions, sodium acetate-ethanol precipitation was performed as described by the T7 RiboMax Express RNA interference system. To each reaction, 0.1 volumes of a 3M NaOAc (pH 5.2) and 2.5 volumes of ice cold 95% ethanol was added, mixed and incubated on ice for 5 minutes. The cloudy reactions were centrifuged at 4°C for 10 minutes at 16 100xg (Eppendorf centrifuge 5415R, Eppendorf, Germany) after which the supernatant was carefully removed and the white pellet was washed with 500 µl ice cold 70% ethanol. All the ethanol was carefully removed and the pellet air dried for approximately 20 minutes. The RNA pellet was resuspended in 3 volumes nuclease-free water and stored at -70°C.

The RNA concentrations of double-stranded RNA samples were determined spectrophotometrically with a NanoDrop (Thermo Scientific) by measuring the absorbance at 260 nm and 280 nm. The $A_{260}:A_{280}$ ratios were between 2.0 and 2.3 and the double-stranded RNA yields were between 1.7 µg/µl and 2.6 µg/µl. The double-stranded RNA product was also analyzed on an agarose gel by loading 25 µl of a 1/100 double-stranded RNA dilution onto a 2% w/v agarose gel prepared in 1 x TAE, as described in section 3.2.2.

3.2.4 RNA interference on *P. falciparum* genes

3.2.4.1 Electroporation

According to literature, RNA interference in *P. falciparum* is achieved at double-stranded RNA concentrations of 40 µg (Malhotra *et al.*, 2002). For the RNA interference study, *P. falciparum* parasite cultures were treated with each individual double-stranded RNA in triplicate.

Parasite pellets were obtained from 3 x 30 ml 3D7 *P. falciparum* culture of approximately 8-10% parasitemia, maintained as described in section 2.2. For treatment in the ring stage (~10 h.p.i), parasites were centrifuged at 2500xg for 5 minutes, washed once with 10 ml sterile cytomix

transfection buffer (120 mM KCl, 0.15 mM CaCl₂, 5 mM MgCl₂, 2 mM EDTA , 25 mM Hepes, 10 mM KH₂PO₄, pH 7.6) and centrifuged as above. Upon electroporation, cells are sensitive to the osmolarity and ionic composition of the medium and thus the cytomix electroporation buffer is used in transfection reactions since it resembles the intracellular ionic composition of cells and thus cells are more likely to survive the harsh conditions of electroporation when suspended in cytomix (Van Den Hoff *et al.*, 1992). The transfection reactions consisted of 200 µl cytomix buffer containing 40 µg double-stranded RNA added to 200 µl washed parasite pellet which was incubated on ice for 10 minutes. The electroporator (BioRad Gene Pulser II with capacitance extender) was set at a voltage of 0.31 kV, capacitance set to 950 µF and electroporation occurred in 0.2 cm electroporation cuvettes (BioRad). After electroporation, 600 µl complete culture medium was added to each cuvette, mixed by pipetting and incubated on ice for 5 minutes. After this, 300 µl of each transfected reaction was aliquoted in triplicate into the wells of a 24 well plate, containing 1.5 ml pre-warmed complete culture medium, to produce a total volume of 1.8 ml double-stranded RNA treated culture of 8-10% parasitemia and ~3.3% hematocrit. The plate was incubated in an incubation chamber which was sealed airtight and gassed for 3 minutes, followed by incubation at 37°C for either 6 or 24 hours. Three triplicate biological replicates were each transfected and aliquoted into a 48-well plate in triplicate.

For treatment in the trophozoite stage (~20 h.p.i), parasites were centrifuged at 2500xg for 5 minutes and 200 µl infected erythrocyte pellet was added to Eppendorf tubes containing 800 µl complete culture media supplemented with 40 µg double-stranded RNA. 300 µl of each transfected reaction was aliquoted in triplicate into the wells of a 24 well plate, containing 1.5 ml pre-warmed complete culture medium to produce a total volume of 1.8 ml double-stranded RNA treated culture of ~8% parasitemia and ~4% hematocrit. The 24 well plate was incubated in an incubation chamber which was sealed airtight and gassed for 3 minutes, followed by incubation at 37°C for either 6 or 24 hours.

Prior to harvesting, Giemsa stained slides were prepared from each treatment for morphological monitoring. Since the parasites have not completed a full developmental cycle, the parasitemia did not change. The pellets were harvested by transferring the culture to Eppendorf tubes, centrifugation for 5 minutes at 16 000xg, removing the supernatant followed by flash freezing the pellet quickly in liquid nitrogen and stored at -70°C for RNA isolation.

3.2.4.2 RNA isolation

RNA isolation was performed at ~16 h.p.i, ~26 h.p.i, ~34 h.p.i and ~44 h.p.i. Two separate RNA isolation techniques were utilized, one protocol utilizes three Qiagen kits and Tri-reagent and this procedure was used for isolating RNA from the negative control samples, while the other

protocol utilizes the MagMax-96 total RNA isolation kit (AEC Amersham) for large scale RNA isolation from the samples treated with the eight double-stranded RNA sequences in question.

3.2.4.2.1 *Total RNA isolation using Qiagen kits and Tri-reagent*

This RNA isolation procedure requires reagents from the following kits: RNeasy kit (Qiagen), TRI-Reagent (Sigma), RNase free DNase1 set (Qiagen), and QIA-Shredder (Qiagen). Triple autoclaved Eppendorf tubes and RNase free and DNase free tips were used throughout the isolation procedure.

Frozen treated pellets were thawed on ice and 600 µl proprietary Lysis buffer (RLT from RNeasy kit) was added, vortexed at maximum speed for 5 seconds, pipetted onto a QIA-Shredder column (Qiagen) and centrifuged at 15 700xg for 2 minutes. This was followed by addition of 600 µl TRI-Reagent (Sigma), vortexing as before and incubating the reactions at room temperature for 5 minutes. TRI-Reagent is a mixture of phenol and guanidine isothiocyanate which is used in RNA isolation procedures since it effectively disrupts cells and breaks down cellular components, while maintaining the integrity of the RNA. Addition of 400 µl of chloroform to each reaction followed by vigorous vortexing for 15 seconds, incubation at room temperature for 10 minutes and centrifugation at 15 700xg for 15 minutes, separates the solution into an aqueous and organic phase. The colourless aqueous phase of each reaction, containing the RNA, was transferred to a clean Eppendorf tube. One volume of 70% ethanol was added to each tube, mixed by inversion, loaded onto RNeasy columns (Qiagen) and centrifuged for 15 seconds at 8000xg. The column was washed by adding 350 µl of proprietary wash buffer RW1, centrifugation at 8000xg for 15 seconds and discarding the flow-through.

For on column DNase digestion, 70 µl of proprietary Buffer RDD was added to a 10 µl aliquot of DNase 1, mixed gently by inversion and this 80 µl DNase1 mixture was pipetted directly onto the membrane of the column and incubated at room temperature for 15 minutes. The column was washed by adding 350 µl proprietary Buffer RW1, centrifuging the column at 8000xg for 15 seconds and subsequently washed twice with 500 µl proprietary wash buffer RPE and centrifuged as above. The RNeasy column was placed into a new 2 ml collection tube and centrifuged at 15 700xg for 1 minute to ensure that the membrane was completely dry. RNA was eluted in 30 µl of RNase free water at room temperature for 5 minutes, centrifuged at 8000xg for 1 minute and stored at -70°C. The RNA concentrations were determined with the NanoDrop as described in section 3.2.3 and the $A_{260}:A_{280}$ ratios were all between 1.9 and 2.2 with RNA yields between 25 ng/µl and 218 ng/µl.

3.2.4.2.2 *Total RNA isolation using MagMax-96 total RNA isolation kit*

The MagMax-96 total RNA isolation kit (AEC Amersham) was used for large scale RNA isolation. This kit disrupts the cells in the samples in a guanidinium thiocyanate-based solution to solubilise cellular membranes and inactivate nucleases. After homogenization, the samples are mixed with magnetic beads coated with a nucleic acid binding surface. The beads with the bound nucleic acids are captured on a magnetic stand and washed to remove cell debris, protein and any other contaminants, after which the samples are treated with DNase to remove contaminating DNA and the RNA is eluted in a low salt buffer.

The bead mix was prepared by vortexing the magnetic beads, provided by the kit, at a moderate speed for 10 seconds to ensure a uniform suspension. Each RNA isolation reaction requires 20 µl bead mix and thus the required volume of RNA magnetic beads were aliquoted into a clean Eppendorf tube and the same volume of proprietary Lysis/Binding Enhancer solution was added and placed on ice. The thawed parasite pellets were resuspended in 30 µl ice cold 1xPBS and 140 µl of proprietary Lysis Binding solution, mixed well and passed through a 25-gauge needle to aid in breaking open the cells. The samples were transferred to the wells of the 96-well plate and incubated with shaking at 200 r.p.m for 1 minute. The bead mix was gently vortexed for 5 seconds and 20 µl bead mix was added to each well, followed by incubation with shaking at 200 r.p.m for 5 minutes. The plate was placed on the magnetic stand for 5 minutes to allow the beads to pellet, after which the supernatant was carefully removed and discarded. The plate was removed from the magnetic stand and 150 µl of proprietary Wash solution 1 was added to each well, incubated with shaking for 1 minute at 200 r.p.m, placed on the magnetic stand for 5 minutes and the supernatant removed and discarded. The plate was removed from the stand and 150 µl proprietary Wash solution 2 was added to each well, incubated with shaking as described previously and placed on the magnetic stand for 5 minutes. The supernatant was discarded and the plate was removed from the stand and 50 µl of proprietary diluted TURBO DNase was added to each well and incubated with shaking for 15 minutes at 200 r.p.m. Subsequently, 100 µl proprietary RNA Rebinding solution was added and incubated with shaking at 200 r.p.m for 3 minutes. The DNase solution releases nucleic acids from the beads and degrades genomic DNA while the RNA Rebinding solution allows the RNA in the solution to rebind to the binding beads. The plate was placed on the magnetic stand for 5 minutes and the supernatant was discarded. The plate was removed from the stand and the beads were washed twice by adding 150 µl proprietary Wash solution 2 to each well, incubation with shaking at 200 r.p.m for 1 minute, capturing the beads on the magnetic stand for 5 minutes and discarding the supernatant. The beads were dried by incubating the plate with shaking at 320 r.p.m for 2 minutes. RNA was eluted with the addition of 50 µl proprietary Elution Buffer, incubation with shaking at 300 r.p.m for 3 minutes and subsequently placing the plate on the magnetic stand.

The supernatant containing the RNA was carefully transferred to clean Eppendorf tubes and stored at -70°C . RNA concentrations were determined with the NanoDrop as described in section 3.2.3 and the $A_{260}:A_{280}$ ratios were all between 1.7 and 2.4 with RNA yields between 10 ng/ μl and 158 ng/ μl .

3.2.4.3 Real-Time PCR monitoring of transcript levels

3.2.4.3.1 *cDNA synthesis*

RNA obtained from double-stranded RNA treated *P. falciparum* parasites (section 3.2.4.2) were reverse transcribed using Superscript III reverse transcriptase (Invitrogen) which contains a modified *pol* gene of the Moloney Murine Leukemia Virus. For cDNA synthesis, 500 ng RNA template was mixed with 10 pmol ddPoly-T₂₅ (Integrated DNA technologies, Iowa, USA) and incubated at 70°C for 10 minutes in a PCR thermal cycler (Perkin Elmer), followed by incubation on ice for 5 minutes. Subsequently, 2 μl of a proprietary 5 x First strand buffer was added along with 1 mM DTT and 2 mM dNTP mix (Promega) and incubated at 45°C for 2 minutes. Superscript III was added (200 units) and the reactions were incubated at 45°C for 1 hour. Enzyme was inactivated at 95°C for 3 minutes, reactions were cooled on ice and the cDNA were stored at -70°C .

3.2.4.3.2 *Real-Time PCR*

Semi-qPCR reactions (10 μl) contained 5 μl SYBR Fast LightCycler 480 Ready Mix (KAPA Biosystems, South Africa), 10 pmol of each forward and reverse primer and 1 μl (1/20 dilution) cDNA in a 384 well RT-PCR plate, which was subsequently sealed, spun down at 1000xg for 3 minutes and immediately placed in the LightCycler 480 (Roche). The PCR program for the 10 μl reaction volumes comprised one pre-incubation step at 95°C for 10 minutes followed by 45 cycles of 95°C for 10 seconds, 55°C for 5 seconds and 72°C for 7 seconds. Subsequently, one melting curve cycle at 95°C for 5 seconds, 65°C for 5 seconds and 95°C (increased at a continuous rate of $0.1^{\circ}\text{C}/\text{second}$) was followed by a final cooling cycle at 40°C for 30 seconds. Each cDNA sample was treated separately and each semi-qPCR reaction was performed in duplicate. Three primer pairs (with similar T_m temperatures and same sized amplicons) were used in the semi-qPCR reactions to amplify certain sections of the target genes, to ultimately determine the mRNA level of expression after RNA interference. The semi-qPCR products were analyzed on a 2% w/v agarose prepared in 1 x TAE, run at 8 V/cm in a MaxiCell EC360M electrophoresis gel system (E-C Apparatus Corporation) and stained with ethidium bromide.

Comparison of gene expression levels after different double-stranded RNA treatments required normalization to internal reference genes, which compensates for the expression variances in each sample. It is however challenging to find internal reference genes with constant expression among several known reference (housekeeping) genes, since expression of referencing genes can vary considerably depending on experimental conditions (Li *et al.*, 2009; Thellin *et al.*, 1999). To normalize the semi-qPCR results, a gene whose mRNA transcript is unaffected throughout the RNA interference experiment was needed. The mRNA levels of Lactate dehydrogenase (LDH) were the most constant between treated and untreated parasite cultures and thus LDH was used as a referencing gene for the semi-qPCR normalization (refer to Figure 3.14, page 110).

Two methods can be used to convert the C_q values into normalized relative quantities. The standard curve method assumes 100 % PCR efficiency and uses a single reference gene for normalization while the delta- C_q quantification method calculates the difference in quantification cycle between two samples and transforms it into relative quantities, using an exponential function with the PCR efficiency (E) value as its base (Hellemans *et al.*, 2007). For normalization, LDH standard curves were first constructed using a dilution series of cDNA template and LDH semi-qPCR primers. The average amount of template is directly proportional to the amount of mRNA transcript/expression in each sample and thus the LDH transcript expression between treated (T) and untreated (UT) samples is expected to be very similar, resulting in a T/UT ratio close to 1.0. There may be slight deviations from 1.0 for LDH and thus the factor used to bring the T/UT ratio of LDH to 1.0 is known as the normalizing factor. The normalizing factor was calculated by the flexible and open source program for semi-qPCR data management and analysis known as qBasePlus (Biogazelle), version 1.2 (Hellemans *et al.*, 2007). qBasePlus uses the delta- C_q method to calculate the relative quantities and ultimately give an indication of mRNA expression of AdoMetDC/ODC and Spermidine synthase after double-stranded RNA treatment, at the different time points. Each time point was considered separately. Generally, each respective time point LDH normalizing factor is used to normalize the treated samples at the same time point, known as time point comparison (Figure 3.4). However, according to the morphology study (Figure 3.10 and Figure 3.11), several double-stranded RNA treatments resulted in delayed parasite development and thus normalization was performed using morphological comparisons and not time point comparisons (Figure 3.4).

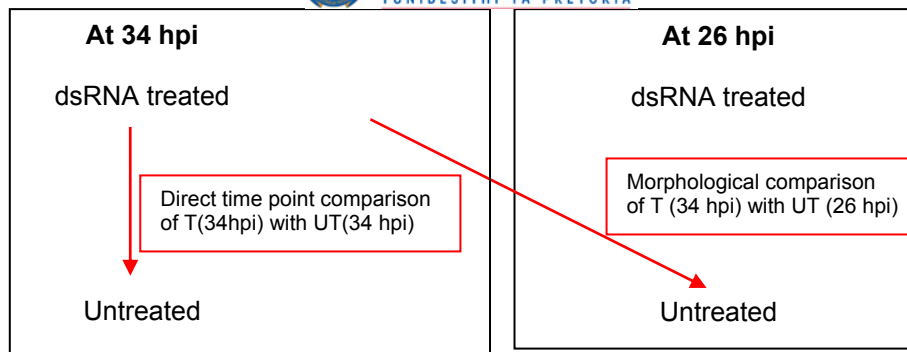


Figure 3.4: Illustration of normalizing strategy depicting direct time point comparison and morphological comparisons.

T: treated; UT: untreated

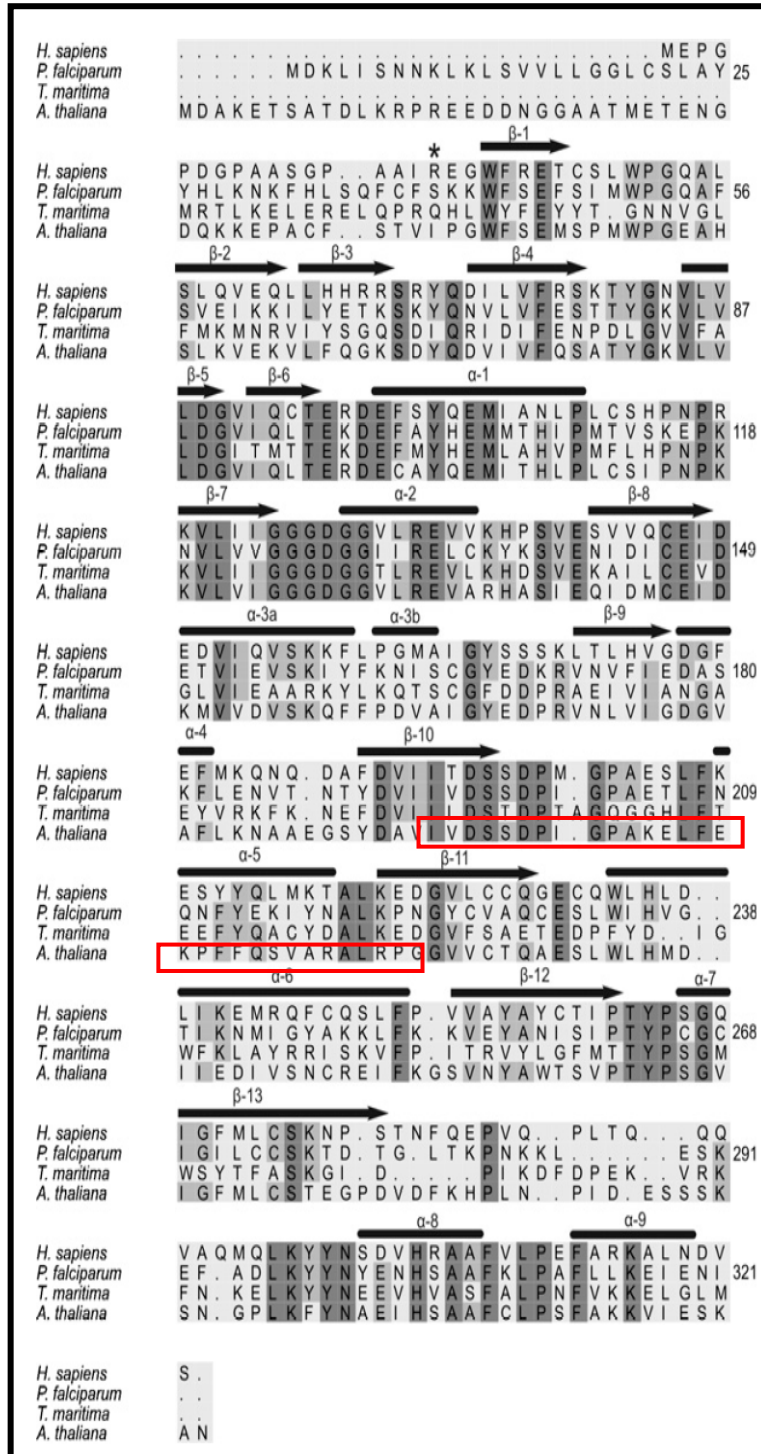
The treated parasites were normalized with the normalizing factor calculated for LDH of the untreated parasites, whose development at the RNA extraction time point was identical/similar to the treated parasites development. In other words, exact life cycle stages were compared with each other such that the treated parasites, whose development was at the late trophozoite stage (while its experimental untreated control was at the middle-schizont stage) was normalized with the LDH values of an untreated parasite also in the late-trophozoite developmental stage, enabling proper comparison of mRNA levels in conjunction with the “just-in-time” expression of transcripts, as proposed by Bozdech *et al.* (2003).

3.3 RESULTS

3.3.1 Double-stranded RNA design and synthesis

RNA interference was aimed at knocking down the *P. falciparum* AdoMetDC/ODC and Spermidine synthase genes. Conserved motifs in these genes were identified and were amplified for subsequent double-stranded RNA synthesis (Figure 3.5 and Figure 3.6). For Spermidine synthase, an area of ~30 amino acids (amino acid 194 – 223) that were conserved was identified (Figure 3.5).

A



B

Nt: ATCGTAGATAGTTTCAGATCCAATAGGACCAGCAGAAACATTATT
 AA: I V D S S D P I G P A E T L F

 AATCAAAATTTTATGAAAAATTTACAACGCCCTAAAGCCTAAC
 N Q N F Y E K I Y N A L K P N

Figure 3.5: (A) The protein alignment profile of *P. falciparum* Spermidine synthase with Spermidine synthase of *A. thaliana*, *T. maritima* and *H. Sapiens* (Burger *et al.*, 2007) and (B) the nucleotide sequence of Spermidine synthase obtained from PlasmoDB (www.plasmodb.org).

Red box/letters represent the conserved sequence within *Pf*Spermidine synthase which was used as template for double-stranded RNA synthesis. The solid black cylinders indicate α -helices while solid black arrows indicate β -sheets. Amino acids shaded light grey have conservation of 50-80% and dark grey have conservation of >80%. Nt: Nucleotide sequence, AA: Amino acid sequence.



For AdoMetDC/ODC, because of its bifunctional nature and size (greater than 4000 bases), various areas were targeted (Figure 3.6).

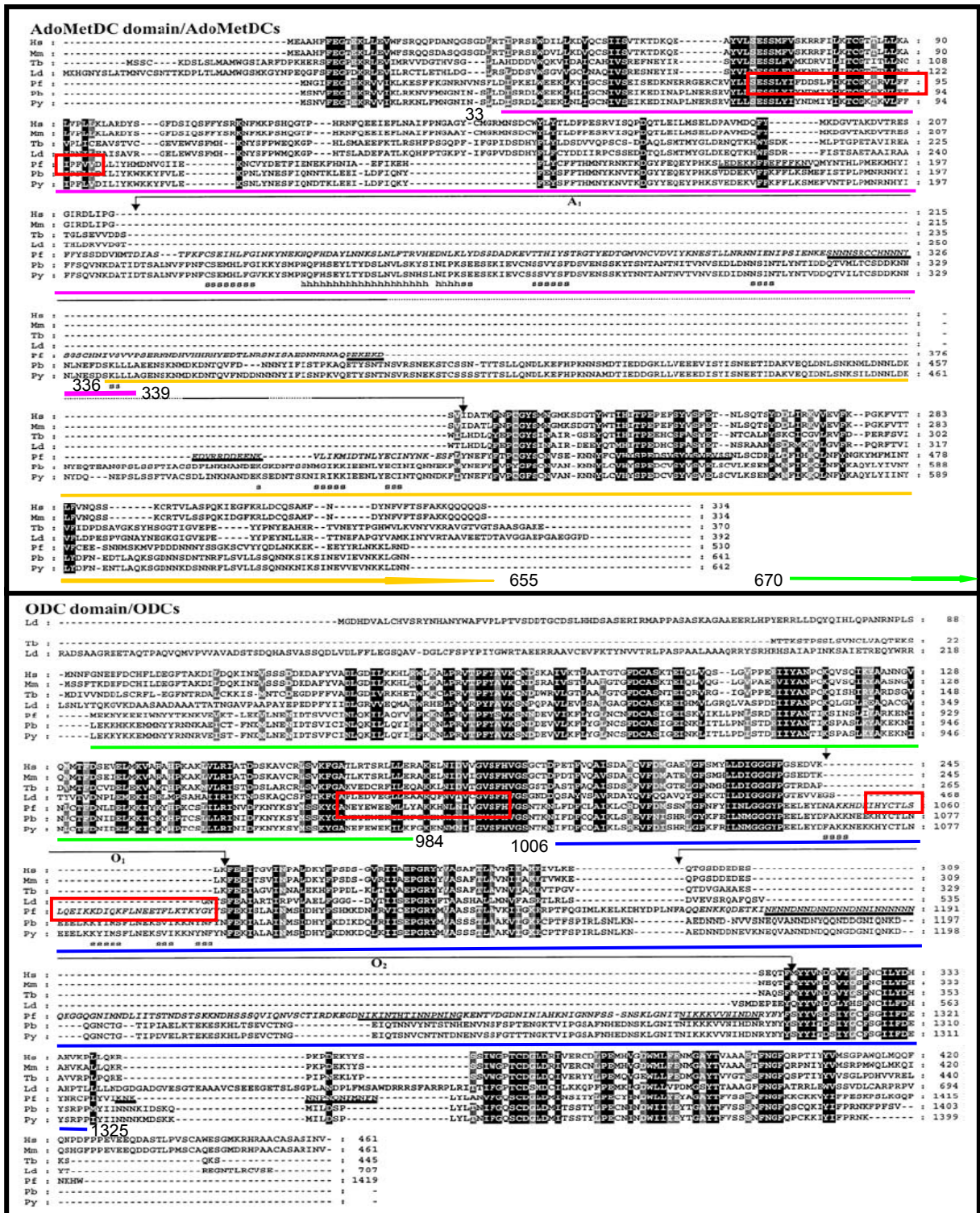


Figure 3.6: The amino acid sequence alignments of *P. falciparum* AdoMetDC/ODC with AdoMetDC or ODC from *H. sapiens* (Hs), *M. musculus* (Mm), *T. brucei* (Tb), *L. donovani* (Ld), *P. bergi* (Pb) and *P. yoelii* (Py) (Modified from (Birkholtz *et al.*, 2004).

Red boxes represent the conserved sequence within *Pf*AdoMetDC/ODC which were used as templates for double-stranded RNA synthesis of small sections. The coloured lines represent the sequences used as templates for the larger sections (Pink: Section 1, Yellow: Section 2, Green: Section 3 and Blue: Section 4). The *Pf*AdoMetDC, hinge and *Pf*ODC domains are indicated. Parasite-specific inserts are in italics with A1 (214-410), H (573-752), O1 (1047-1085) and O2 (1156-1302) while the predicted secondary structures are indicated as s: (β -sheets) and h: (α -helices). Amino acids shaded light grey have conservation of >60% and black have conservation of >80%. Black underlined sequences indicate low-complexity areas.

The first conserved sequence is 93 nucleotides in length (amino acid 71 - 101, Figure 3.6) and is localized in the N-terminal of the AdoMetDC/ODC bifunctional protein, within the AdoMetDC domain (called AdoMetDC). The second conserved sequence corresponds to a region in the ODC domain (amino acid 985 - 1010) and is 78 nucleotides in length, (called ODC). Lastly, an insert of 96 nucleotides (amino acids 1068-1099) has been identified in *P. falciparum* to cause a profound decrease in AdoMetDC/ODC activity, when deleted (Birkholtz *et al.*, 2004) and this was also targeted. Beyond these areas, the complete AdoMetDC/ODC gene was divided into four sections (Section 1: amino acid 33 – 339, Section 2: amino acid 336 – 655, Section 3: amino acid 670 – 984 and Section 4: amino acid 1006 – 1325) to provide full coverage of the gene. The nucleotide lengths for Sections 1, 2, 3 and 4 are 923, 960, 942 and 957 bp respectively.

Primers were designed to amplify the areas of the genes described above. The T7 promoter sequence was included at the 5' end of both the forward and reverse primer (Table 3.1) and the target sequences were subsequently amplified from plasmids containing the full length AdoMetDC/ODC or Spermidine synthase gene.

Table 3.1: The RNA interference primers to amplify the AdoMetDC, ODC, Insert and Spermidine synthase targets.

Gene	Primer	Sequence (5'-3')	Calculated T _m (°C)	Product size (including primers)
AdoMetDC	Forward	<i>TAATACGACTCACTATAGGGTCAGAGAGTTCTTTATAC</i>	67.3	131
	Reverse	<i>TAATACGACTCACTATAGGATCAACCACAAACGGTATG</i>	68.4	
ODC	Forward	<i>TAATACGACTCACTATAGGCTAATGAATATGAATGGGAAGAAAT</i>	67.6	116
	Reverse	<i>TAATACGACTCACTATAGGATGAAATGATACACCTACAATA</i>	66.5	
INSERT	Forward	<i>TAATACGACTCACTATAGGTCATTATTGACTTTAAGTCT</i>	65.4	134
	Reverse	<i>TAATACGACTCACTATAGGATCCATATTTTCGTCTTGAGAA</i>	67.4	
SPD SYNTH	Forward	<i>TAATACGACTCACTATAGGATCGTAGATAGTTCAGATCCA</i>	68.4	128
	Reverse	<i>TAATACGACTCACTATAGGGTTAGGCTTTAGGGCGTTGTAAT</i>	70.3	
Section 1	Forward	<i>TAATACGACTCACTATAGGATATACCTAAAGAATTATGGGA</i>	66.5	961
	Reverse	<i>TAATACGACTCACTATAGGGGAAGGAACAACACTCAC</i>	69.4	
Section 2	Forward	<i>TAATACGACTCACTATAGGGTTGTTCTTCCGAAAGA</i>	68.3	998
	Reverse	<i>TAATACGACTCACTATAGGTGTTTGTACTTTTCAAGTTTT</i>	66.5	
Section 3	Forward	<i>TAATACGACTCACTATAGGGGGTAATAATGAATTGAG</i>	67.3	980
	Reverse	<i>TAATACGACTCACTATAGGTCCATATTTGAAGACATATAA</i>	65.4	
Section 4	Forward	<i>TAATACGACTCACTATAGGTGTATCATTTTCATGTTGG</i>	66.1	995
	Reverse	<i>TAATACGACTCACTATAGGATACTATCGCTTACATAATATG</i>	66.5	

T7 promoter sequence in italics. Product size represents final product length including the primers (36 nucleotides).

$T_m = 69.3^{\circ}\text{C} + (0.41 \times \text{GC}\%) - 650/\text{primer length}$ (Rychlik *et al.*, 1990).

The expected PCR product length of the amplified targets (amplicons) can be found in Table 3.1. As can be seen in Figure 3.7, PCR products of expected sizes were successfully amplified for all the fragments, with no primer dimers or over-amplification. These PCR products were

subsequently purified and used as templates for double-stranded RNA synthesis as described in section 3.3.2.

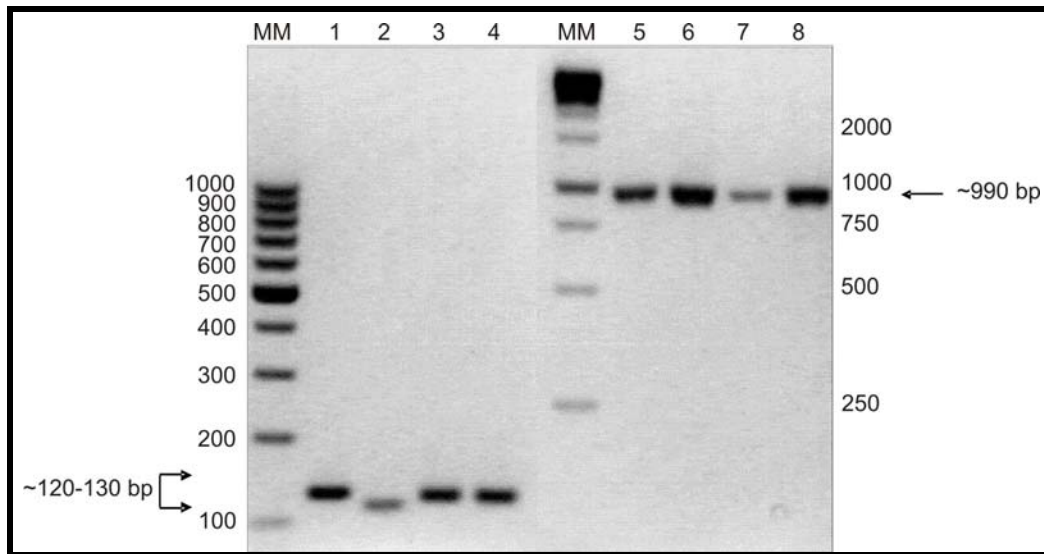


Figure 3.7: Large scale purified PCR amplicons of AdoMetDC, ODC, Insert, Spermidine synthase, Section 1, 2, 3 and 4 sequences on a 2% agarose gel.

MM: DNA ladder; Lane 1: AdoMetDC amplicon; Lane 2: ODC amplicon; Lane 3: Insert amplicon; Lane 4: Spermidine synthase amplicon; Lane 5: Section 1 amplicon; Lane 6: Section 2 amplicon; Lane 7: Section 3 amplicon; Lane 8: Section 4 amplicon.

3.3.2 Double-stranded RNA synthesis and purification

The T7 RiboMax Express RNA interference system was subsequently used to synthesize double-stranded RNA from all template amplicons obtained. RNA samples are often analyzed on an RNase free agarose gel which has been prepared with 3-(N-morpholino) propanesulfonic acid (MOPS) running buffer and contains Formamide to prevent the RNA samples from being degraded. Single-stranded RNA can fold upon itself and form strong secondary structures, which pose a problem when RNA needs to be quantified and analyzed for quality. In such instances, the RNA is denatured prior to loading on an RNA gel and electrophoresed with MOPS as the running buffer. Double-stranded RNA however, is stable and resistant to RNase degradation and since the aim of this step was to verify the presence and correct size of the double-stranded RNA product, an agarose gel was used. The final double-stranded RNA product before and after DNase and RNase digestion was therefore analyzed on a 2% DNA agarose gel (Figure 3.8).

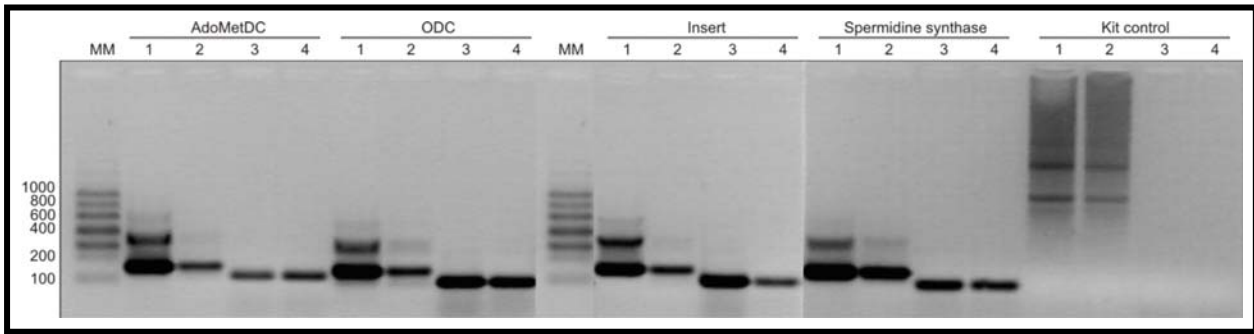


Figure 3.8: Trial double-stranded RNA synthesis and digestion of AdoMetDC, ODC, Spermidine synthase and Insert.

MM: Low range RNA ladder; Lane 1: Undigested and unpurified; Lane 2: Undigested and purified; Lane 3: RNase digested and purified; Lane 4: RNase and DNase digested and purified.

As can be seen in Figure 3.8, analysis of the RNA product with electrophoresis without RNase digestion, DNase digestion or ethanol-purification reveals the presence of two bands (Lane 1 of each). The top lighter band is assumed to be due to the formation of concatamers, where the two T7 promoter sequences anneal, resulting in a band of approximately double the size (~ 240) while the lower darker band may be a mixture of perfectly annealed RNA strands and imperfectly annealed RNA strands, with resulting single-stranded over-hangs (Figure 3.8).

After the RNA product was purified with ethanol precipitation (lane 2 of each), the size of the band remained the same (~130 bp) but the intensity of the band decreased, most likely due to loss of some double-stranded RNA product during the precipitation step. The purified undigested RNA product is assumed to contain a mixture of perfectly annealed double-stranded RNA strands and imperfectly annealed RNA strands with single-stranded RNA over-hangs. Since the RNA samples are electrophoresed on a DNA agarose gel, the RNase's in the environment are expected to degrade any contaminating single-stranded RNA products. RNase digestion followed by precipitation (lane 3) produced a product which was slightly smaller in size than the previous undigested products. Agarose separates nucleic acids based on size and this RNase digested product produced a band which migrated slightly further in the gel and it was therefore assumed that this RNase digested product was marginally smaller in size (~120 bp). This is most likely due to the RNase digesting the remaining single-stranded RNA of the imperfectly annealed RNA strands. RNase digestion followed by DNase digestion and precipitation (lane 4) produced a band similar in size to the RNase digested band since DNases removed the contaminating DNA template. RNase and DNase digestion followed by ethanol precipitation provided a clear, purified double-stranded RNA product. The kit control reactions were used to verify that the DNA template was converted to RNA. The kit provides two linear DNA templates which are used to produce two non-complimentary linear single-stranded RNA transcripts. These single-stranded RNA sequences remained intact in the DNA agarose gel without any prior RNase free treatment. RNase digestion of these RNA transcripts (lane 3, kit control) immediately eliminated them from the product pool as can be seen in Figure 3.8.

The double-stranded RNA synthesis protocol seemed to be sufficient for synthesizing double-stranded RNA and thus large scale double-stranded RNA synthesis of all eight genes in question were performed. As can be seen in Figure 3.9, RNase and DNase digestion produced clean double-stranded RNA product for AdoMetDC, ODC, Insert and Spermidine synthase. For the larger sections, however there appeared to be more than just one double-stranded RNA product, even after RNase and DNase digestion, indicating possible mispriming during RNA synthesis, resulting in additional double-stranded RNA. The ultimate aim was to knock-down larger sections of AdoMetDC/ODC and thus these double-stranded RNA sequences, illustrated in Figure 3.9, were used in the RNA interference study.

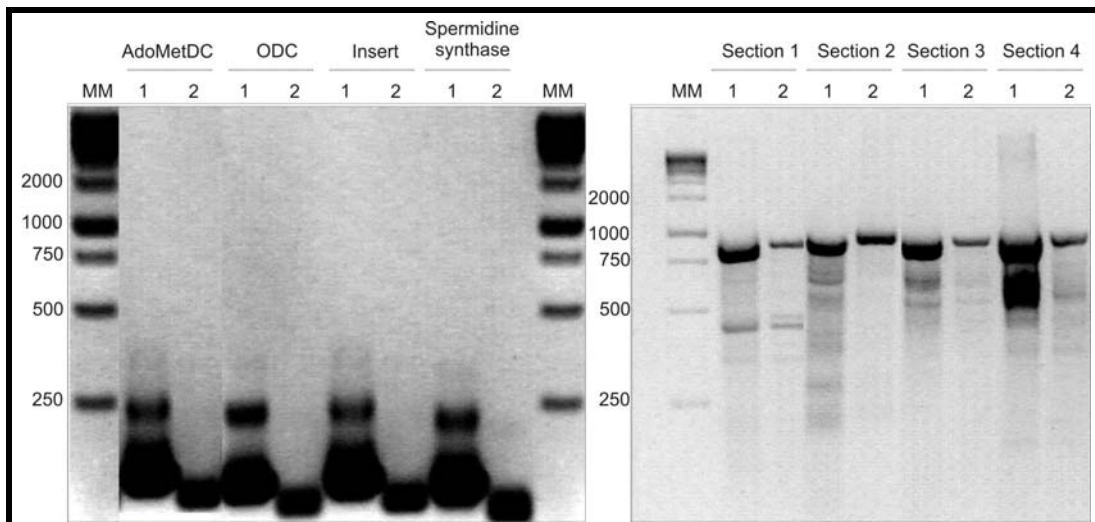


Figure 3.9: Large scale purified double-stranded RNA of all eight genes.

MM: 1 Kb DNA ladder; Lane 1: Undigested and purified RNA; Lane 2: RNase and DNase digested purified double-stranded RNA.

3.3.3 RNA interference on *P. falciparum* genes

3.3.3.1 Morphology study

The expression profiles of AdoMetDC/ODC and Spermidine synthase throughout the IDC of *P. falciparum* was obtained from the DeRisi Laboratory Malaria Transcriptome Database (<http://malaria.ucsf.edu>) as is illustrated in Figure 3.3. Parasite pellets were harvested for RNA isolation and Figure 3.10 and Figure 3.11 show Giemsa stained thin blood smears of *P. falciparum* parasites at ~16 h.p.i, ~26 h.p.i, ~34 h.p.i and ~44 h.p.i.

In Figure 3.10 (A) it can be seen that at the time of treatment, the parasites were in the ring stage and parasites grew without any signs of stress. After 6 hours incubation with the double-stranded RNA, the parasites were in the early trophozoite stage. At this stage, the parasites treated with Insert and ODC double-stranded RNA appeared similar in morphology to the

untreated parasites, while the parasites treated with AdoMetDC and Spermidine synthase double-stranded RNA seemed smaller and their development appeared to be slightly retarded (~14-16 h.p.i). After 24 hours, the RNA interference effect seemed more evident morphologically. The untreated parasites were at approximately 34 h.p.i and as shown in Figure 3.10 (A), the parasites were in the mature trophozoite-early schizont developmental stage. The parasite occupied almost the entire erythrocyte volume and hemozoin deposits were evident, indicating that the parasites were not under stress. When compared to the untreated parasites, the AdoMetDC, Insert and Spermidine synthase treated parasites were much smaller in size, had less hemozoin deposits, the parasites occupied less than half the erythrocyte volume and appeared to be in the middle-trophozoite developmental stage (~28-30 h.p.i). The ODC treated parasites showed signs of stress since these parasites were very small and morphologically appeared to be in the early to middle-trophozoite developmental stage (~26-28 h.p.i).

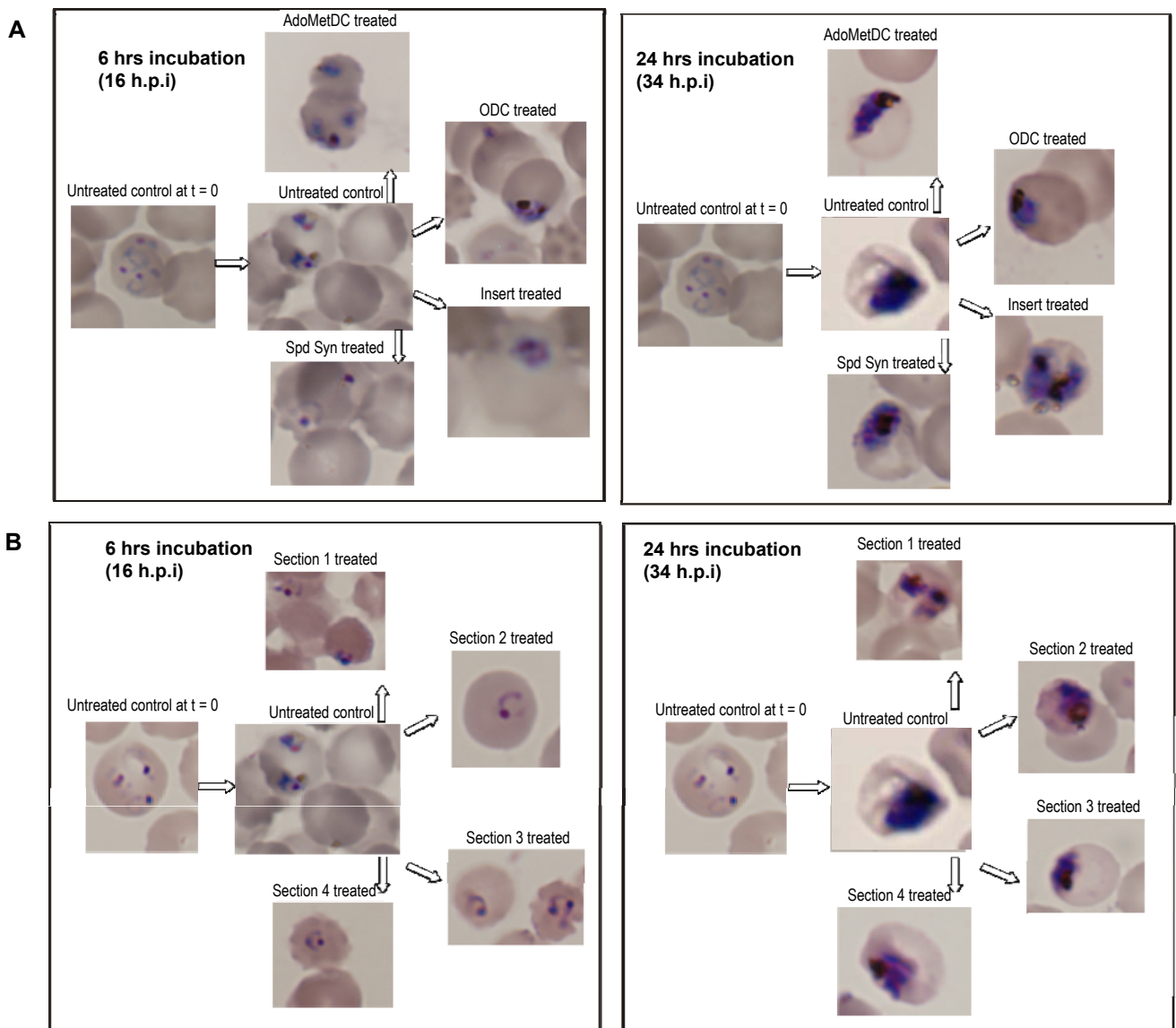


Figure 3.10: Morphological analysis of Giemsa stained slides illustrating ring stage *P. falciparum* after 6 and 24 hours incubation with double-stranded RNA.

Oil immersion microscopy was performed at a 100 x magnification. (A) AdoMetDC, ODC, Insert and Spermidine synthase, (B) Section 1, 2, 3 and 4.

The parasites shown in Figure 3.10 (B) were treated in the ring stage with double-stranded RNA from Section 1, 2, 3, and 4. At 16 h.p.i, the untreated parasites seemed to be in the late ring stage and had started to move into the early-trophozoite stage since the parasite ring appeared denser. After 6 hours incubation with double-stranded RNA, all the treated parasites at 16 h.p.i revealed retarded development (~14 h.p.i) since the parasite structure was not as dense as seen in the untreated parasites at the same time point. The parasites however, did not seem to be under overt stress. At 34 h.p.i the untreated parasites were in the mature trophozoite-early schizont stage since the parasites were larger and took up the majority of the erythrocyte volume. After 24 hours incubation, the parasites treated with Section 1 and Section 3 double-stranded RNA appeared small, pyknotic and concentrated at the edge of the erythrocyte membrane while the parasites treated with Section 2 and Section 4 double-stranded RNA were slightly bigger but not as fully developed as the untreated parasites. This slight growth inhibition is indicative that the parasites were starting to stress. Morphologically, the parasites treated with Section 1 and Section 3 double-stranded RNA appeared to be in the early/middle-trophozoite stage (~26-28 h.p.i) while the parasites treated with Section 2 and Section 4 appeared to be at the middle-trophozoite stage (~30-32 h.p.i)

Figure 3.11 represents Giemsa stained thin blood smears of the parasites treated in the early-trophozoite development stage. Double-stranded RNA was added to the culture medium at ~20 h.p.i and parasites were incubated at 37°C for either 6 or 24 hours.

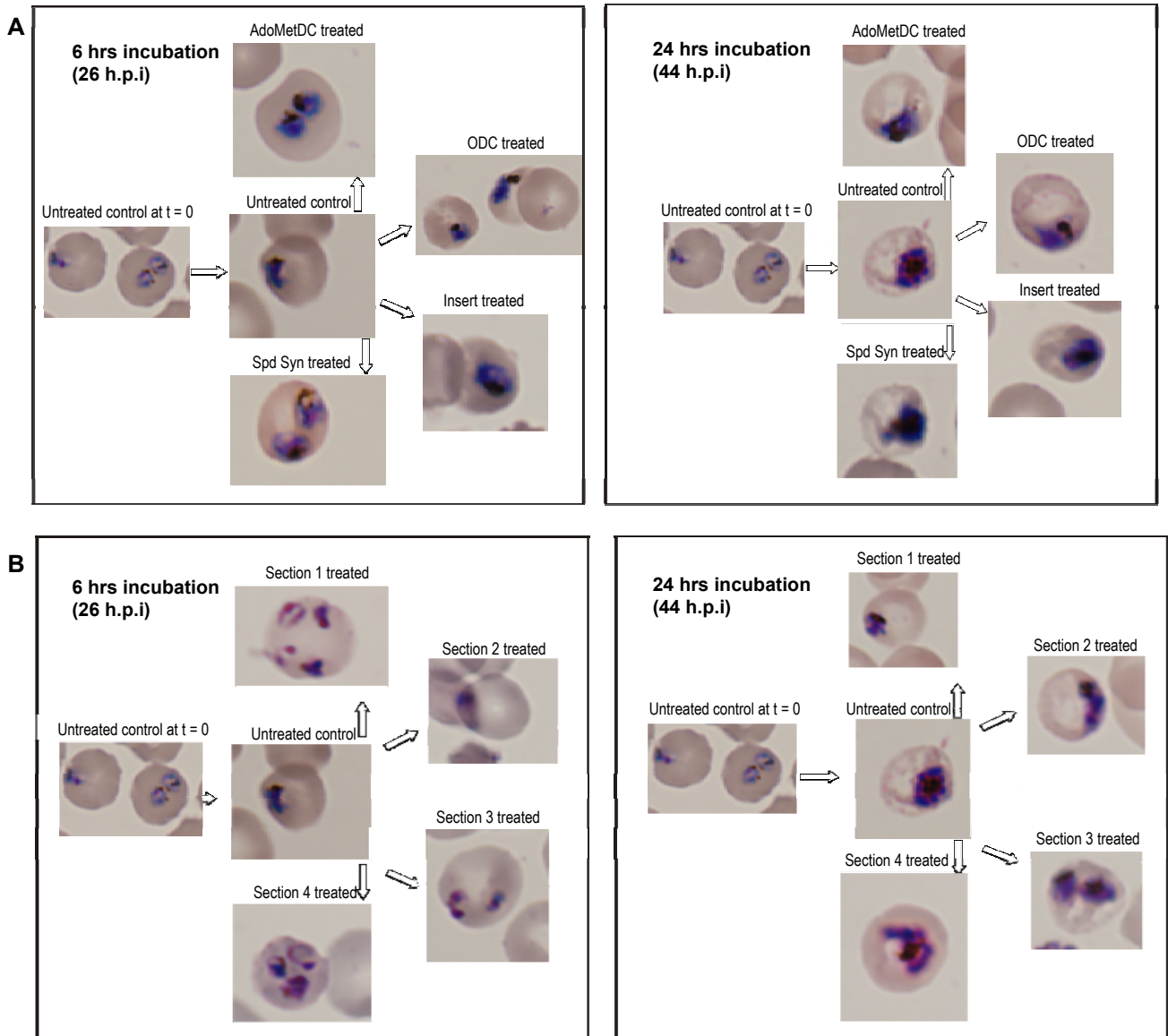


Figure 3.11: Morphological analysis of Giemsa stained slides illustrating trophozoite stage *P. falciparum* after 6 and 24 hours incubation with double-stranded RNA.

Oil immersion microscopy was performed at a 100 x magnification. (A) AdoMetDC, ODC, Insert and Spermidine synthase, (B) Section 1, 2, 3 and 4.

Figure 3.11 (A) represents the parasites treated with AdoMetDC, ODC, Insert and Spermidine synthase double-stranded RNA at ~20 h.p.i. At ~26 h.p.i, the untreated parasites had started to develop into the early/middle-trophozoite developmental stage where the parasite structure was dense and there were signs of hemozoin. After 6 hours incubation with double-stranded RNA, the parasites treated with AdoMetDC and ODC double-stranded RNA appeared to be at the same developmental stage as the untreated parasites, while the parasites treated with double-stranded RNA from Spermidine synthase and Insert appeared to be marginally larger than the untreated parasites with development at ~28 h.p.i. At 44 h.p.i, the untreated parasites had entered the schizont stage as can be seen by the array of nuclei. After 24 hours incubation with double-stranded RNA, it appeared as though the development of treated parasites were slightly behind that of the untreated parasites, since the treated parasites all seemed to be in the

mature-trophozoite developmental stage (~34-36 h.p.i) indicating the parasites were under stress and thus under developed.

Figure 3.11 (B) represents the morphology of the parasites treated with double-stranded RNA from Section 1, 2, 3 and 4 at ~20 h.p.i. The untreated parasites at 26 h.p.i were in the early/middle-trophozoite development stage while 6 hours incubation with Section 1 and Section 4 double-stranded RNA resulted in the treated parasites being in the very early-trophozoite developmental stage (~21 h.p.i). The treated parasites were small and still resembled a ring, indicating the parasites were under stress. The parasites treated with Section 2 and Section 3 double-stranded RNA had slightly retarded development (~24 h.p.i). At 44 h.p.i, the untreated parasites entered the schizont stage and after 24 hours incubation with double-stranded RNA, the treated parasites appeared to have been under stress since the parasites were much smaller in comparison to the untreated parasites. The parasites treated with Section 1 and 2 double-stranded RNA had extremely retarded development, ~27-30 h.p.i, while the parasites treated with Section 3 and Section 4 double-stranded RNA also had retarded development, morphologically based at ~30-32 h.p.i.

The results represented in Figure 3.10 and Figure 3.11 indicate that the incorporation of double-stranded RNA into cells at the ring stage appeared to be more effective, since inhibitory effects were visible after 6 hours of double-stranded RNA incubation for all double-stranded RNA treatments and this inhibitory effect became more evident after 24 hours incubation. However, morphology studies are very subjective and thus to verify the loss of gene function after double-stranded RNA treatment, total RNA was isolated and semi-qPCR was performed as described in section 3.2.4.4 to determine the effect of double-stranded RNA incorporation on selected *P. falciparum* transcript levels.

3.3.4 Semi-qPCR

RNA was isolated from the treated and untreated parasite cultures, cDNA was synthesized from the RNA template and semi-qPCR was performed to determine the mRNA levels of the genes targeted by RNA interference. Three primer sets aimed at amplifying LDH, AdoMetDC/ODC and Spermidine synthase gene fragments were used in the semi-qPCR reaction (Table 3.2). During optimization, it was found that a 1/20 dilution of the cDNA template was optimal and thus this dilution factor was used for the cDNA template throughout the semi-qRT-PCR experiments.



Table 3.2: Real-time PCR primer sets

Gene	Primer	MW (g/mol)	T _m	Product size (bp)	Sequence (5'-3')
Spermidine synthase	Forward	6024.0	57	70	ACAACGCCCTAAAGCCTAAC
	Reverse	6372.2	58		ATTGTTCCCACGTGTATCCAG
AdoMetDC/ODC	Forward	7286.8	58	165	AATCAATTCCATGACGCTTATCTG
	Reverse	7197.7	58		ACAATTCACCATTCTGTATCTTC
LDH	Forward	6541.3	58	169	GATTTGGCTGGAGCAGATGTA
	Reverse	7988.3	55		CAACAATAATAAAAGCATTGGACAA

$$T_m = 69.3^{\circ}\text{C} + (0.41 \times \text{GC}\%) - 650/\text{primer length (Rychlik et al., 1990)}$$

Figure 3.12 represents the end-point analysis of the semi-qPCR product in duplicate, run on an agarose gel. The semi-qPCR was successful since bands of the expected sizes were obtained (refer to Table 3.2) indicating adequate amplification of the cDNA template by all the primer sets.

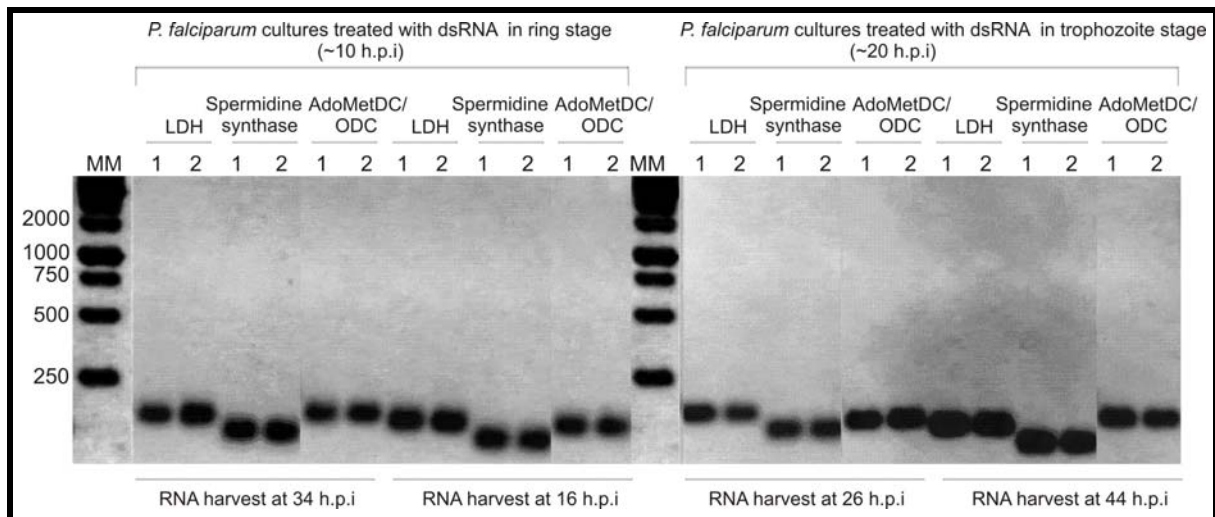


Figure 3.12: Semi-qPCR product of *P. falciparum* parasites treated with double-stranded RNA in the ring and trophozoite stage.

MM: Molecular marker; LDH: Lactate dehydrogenase; AdoMetDC/ODC: S-adenosylmethionine decarboxylase/Ornithine decarboxylase.

3.3.4.1 Semi-qPCR data

Figure 3.13 (A) and (B) represents the amplification and melting curves obtained from the semi-qPCR results from *P. falciparum* parasites treated with double-stranded RNA. As mentioned previously, three sets of primers were used to amplify the cDNA of each gene of interest (AdoMetDC/ODC, Spermidine synthase and LDH). Figure 3.13 (A) represents amplification curves of each gene (with the C_q values indicated). Figure 3.13 (B) illustrates the melting peaks and verifies the absence of primer-dimers, giving an indication of the efficiency of the primer pairs in amplifying the genes of interest. The amplification curves indicate that all the genes were amplified successfully and in the melting peak, three peaks are observed, each corresponding to the genes that were amplified with the three different primer sets used. The

plateau seen in Figure 3.13 A, represented by the red box, illustrates that the semi-qPCR reaction had been exhausted of reagents after ~27 cycles.

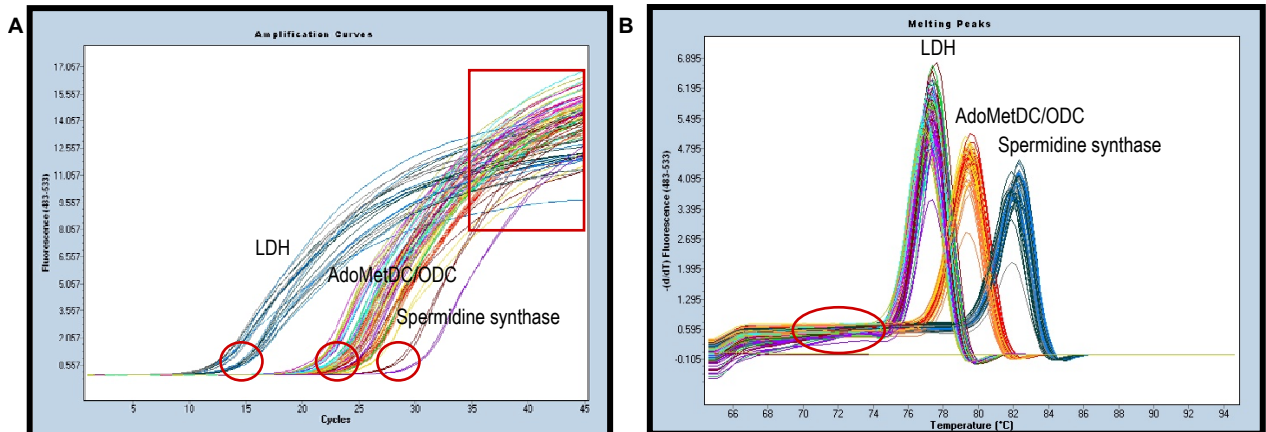


Figure 3.13: Representative graphs of semi-qPCR amplification curves (A) and melting peaks (B). Red circles represent C_q points of the genes being amplified, the red box indicates the plateau/saturation point of the PCR reaction and the red oval indicates that no primer-dimers formed during the reaction.

By using the delta-C_q values (qBasePlus), the relative expression of LDH gene was analysed between treated and untreated samples. The expression levels of LDH were relatively constant (~ 1.0) between treated and untreated samples, as illustrated in Figure 3.14, and thus LDH was verified as a reference gene for this study.

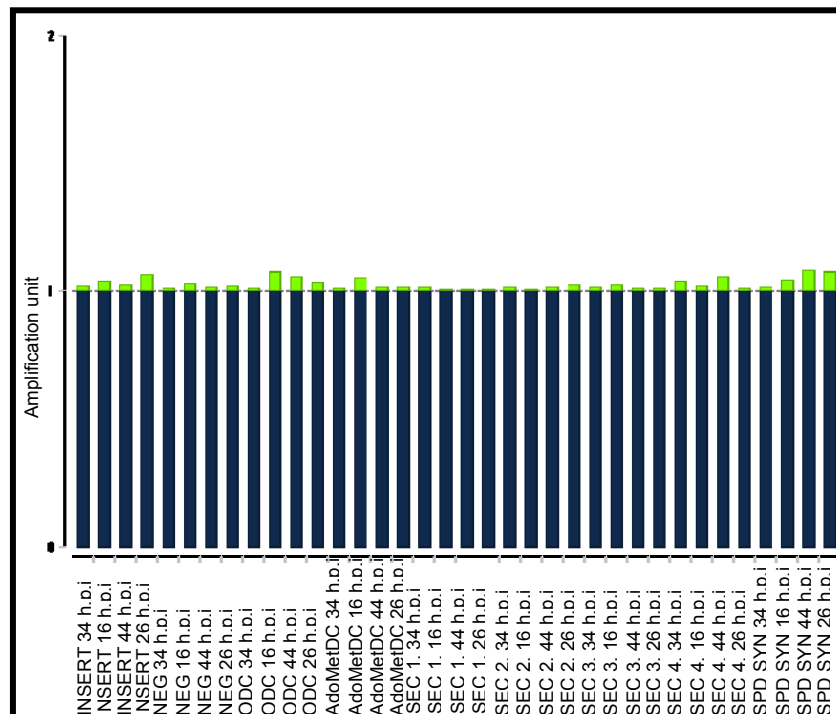


Figure 3.14: LDH expression levels of treated and untreated samples (T/UT) as determined by qBasePlus.

Green bars represent the deviance of LDH expression between treated and untreated samples after various double-stranded RNA treatments.

Once LDH was verified as a reasonably good reference gene, the LDH standard curves were constructed using a dilution series of untreated cDNA obtained from each of the four time points. The four resulting standard curves constructed by qBasePlus are shown in Figure 3.15. The standard curves all have correlation coefficients (R^2 values) close to or equal to 1.0, suggesting a good “fit” resembling the relationship between the X and Y variables. The standard deviations are all less than 0.01 and the efficiency of the PCR reaction is assumed to be 100% since the E values are all above 1.0 (100%).

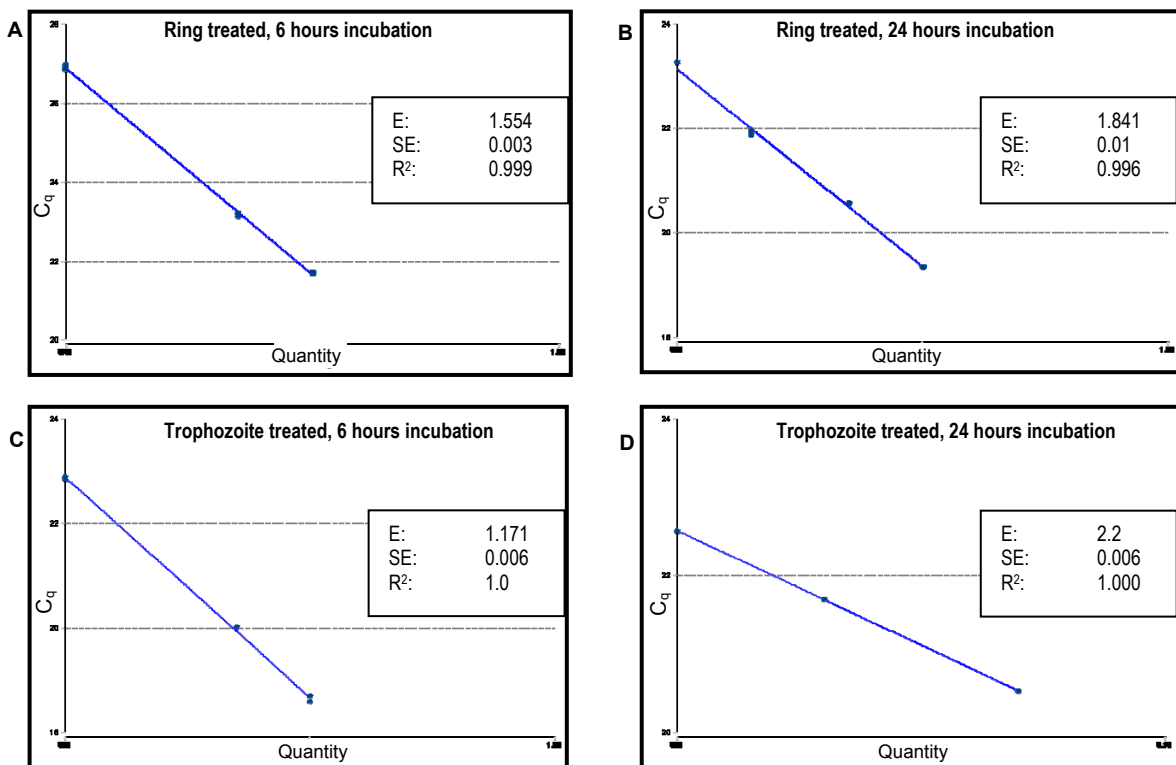


Figure 3.15: LDH standard curves for each time point (A) 16, (B) 34, (C) 26 and (D) 44 h.p.i.

E: Efficiency value, SE: Standard error, R²: Correlation coefficient, C_q: Quantification cycle, Quantity: Starting quantity of template.

The following results represent the transcript levels of Spermidine synthase and AdoMetDC/ODC after treatment with the eight different double-stranded RNA sequences. The relative quantities of each gene in each sample were determined with qBasePlus. The treated samples were normalized using either direct time point comparisons or morphological comparisons. According to the morphology of the parasites (Figure 3.10 and Figure 3.11), Table 3.3 illustrates the developmental time point of the untreated sample which correlates best with the respective developmental time point of the treated samples. The parasite extraction time point and morphological time points were very similar 6 hours after treatment, irrespective of whether parasites were treated at ~10 or ~20 h.p.i, while major morphological changes only became apparent after 24 hours incubation. Table 3.3 therefore illustrates the time point LDH normalizing factor which was used to normalize each treated sample, to obtain the figures to follow.



Table 3.3: Morphological developmental stage of *P. falciparum* treated and untreated parasites at the time of RNA extraction.

Double-stranded RNA treatment:	AdoMetDC	ODC	Insert	Spd Syn	Sec. 1	Sec. 2	Sec. 3	Sec. 4
Morphological parasite developmental stage similar to UT sample at extraction time point:								
Extraction time point: 16 h.p.i	16 h.p.i	16 h.p.i	16 h.p.i	16 h.p.i	16 h.p.i	16 h.p.i	16 h.p.i	16 h.p.i
* Extraction time point: 34 h.p.i	26 h.p.i	26 h.p.i	26 h.p.i	26 h.p.i	26 h.p.i	26 h.p.i	26 h.p.i	26 h.p.i
Extraction time point: 26 h.p.i	26 h.p.i	26 h.p.i	26 h.p.i	26 h.p.i	26 h.p.i	26 h.p.i	26 h.p.i	26 h.p.i
* Extraction time point: 44 h.p.i	34 h.p.i	34 h.p.i	34 h.p.i	34 h.p.i	34 h.p.i	34 h.p.i	34 h.p.i	34 h.p.i

* Represents the samples that were normalized by comparing morphological time points.

The following bar graphs represent the transcript levels of AdoMetDC/ODC and Spermidine synthase after both 6 and 24 hours of incubation with double-stranded RNA. The expression levels of the genes were normalized with the LDH normalizing factor using either morphological time point comparison or the direct time point comparison, as discussed above. The effect of double-stranded RNA on transcript production of AdoMetDC/ODC and Spermidine synthase will be discussed separately for treatment in the ring stage and for treatment in the trophozoite stage.

Figure 3.16 represents the transcript levels of AdoMetDC/ODC obtained from parasites treated with double-stranded RNA in the ring stages and harvested after 6 and 24 incubation. After 6 hours incubation (~16 h.p.i), the untreated parasites were in the late-ring, early-trophozoite stage while the treated parasites all appeared to be at a similar developmental time point (~14-16 h.p.i) and did not present any signs of stress (refer to Figure 3.10). AdoMetDC/ODC transcript production at ~16 h.p.i is at a steady increase (Figure 3.3 (A)) and thus available transcripts were expected to act as substrates for double-stranded RNA interference. As can be seen in Figure 3.16, at 16 h.p.i, the majority of double-stranded RNA treatments caused a reduction in AdoMetDC/ODC transcript levels, except for AdoMetDC and Section 1 derived double-stranded RNA sequences.

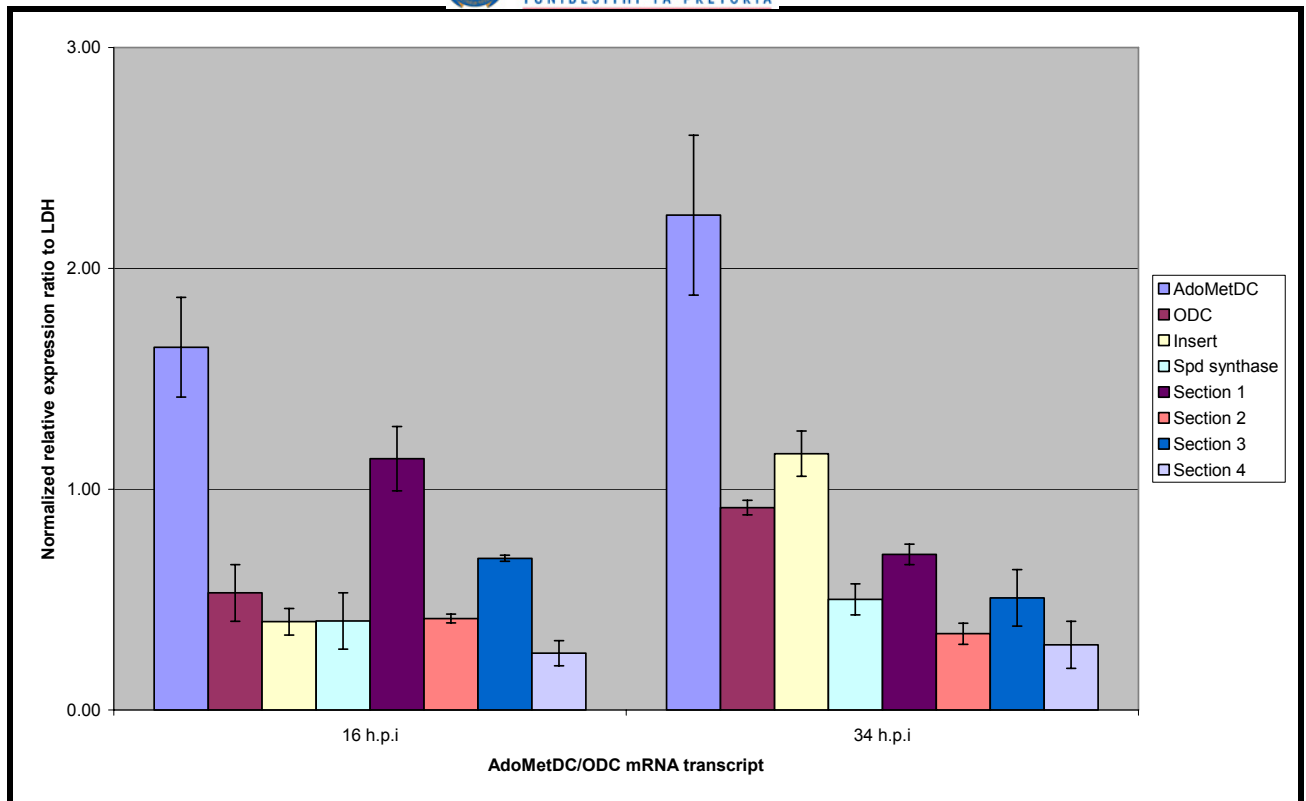


Figure 3.16: Average expression ratios of *P. falciparum* AdoMetDC/ODC transcripts after 6 (16 h.p.i harvested) and 24 hours incubation (34 h.p.i harvested) with double-stranded RNA, starting in the ring stage.

Error bars indicate standard deviations. Double-stranded RNA treatments shown in right hand panel.

After 24 hours incubation (~34 h.p.i), the untreated parasites were mature-trophozoites/early-schizonts while the treated parasites all appeared to have delayed development (between ~26-31 h.p.i (refer to Figure 3.10)). At 34 h.p.i the AdoMetDC/ODC transcript levels were at a steady decline (Figure 3.3 (A)). The double-stranded RNA of Spermidine synthase, Section 2, Section 3 and Section 4 caused a decrease of AdoMetDC/ODC transcript levels at 16 h.p.i and this effect appears to be long lasting, causing a continuous decrease even at 24 h.p.i. The decrease in AdoMetDC/ODC transcript levels with Section 1 becomes apparent with extended incubation while ODC and Insert double-stranded RNA appear to have caused minimal changes in transcript levels. AdoMetDC double-stranded RNA again caused an increase in AdoMetDC/ODC transcript levels, even with extended incubation times.

Double-stranded RNA treatment with shorter sequences (ODC, Insert) (refer to Figure 3.16) previously observed to cause a decrease in AdoMetDC/ODC transcript levels (16 h.p.i), resulted in no significant effect on AdoMetDC/ODC transcript levels when incubation times were extended (34 h.p.i), suggesting the possibility that the RNA interference activity/efficiency of short double-stranded sequences decreases with time. The decrease in transcript levels caused by the larger double-stranded RNA sequences (Section 2, Section 3 and Section 4) all maintained their RNA interference activity after 24 hours and Section 1, which previously caused a slight increase of AdoMetDC/ODC transcript levels, caused a decrease of

AdoMetDC/ODC transcript, with extended double-stranded RNA incubation. However, Spermidine synthase double-stranded RNA appears to also have a long lasting knock-down effect on AdoMetDC/ODC transcript levels which may indicate non-specific effects. The effect of double-stranded RNA interference on Spermidine synthase transcript levels was therefore analyzed next.

Figure 3.17 illustrates the expression levels of Spermidine synthase transcripts after parasites were treated in the ring stage with double-stranded RNA for 6 and 24 hours.

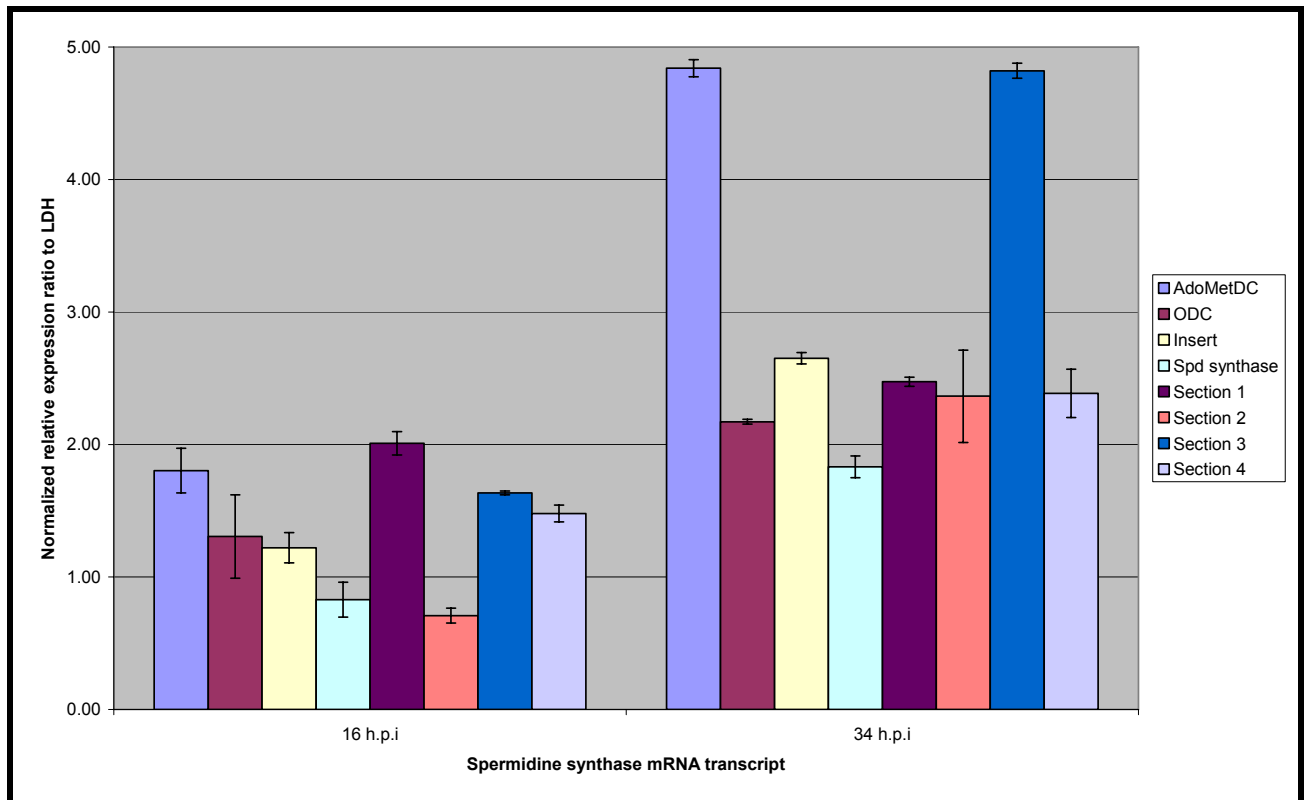


Figure 3.17: Average expression ratios of *P. falciparum* Spermidine synthase transcripts after 6 and 24 hours incubation with double-stranded RNA, starting in the ring stage.

Error bars indicate standard deviations. Double-stranded RNA treatments shown in right hand panel.

At 16 h.p.i, Spermidine synthase transcript production is almost at its maximum (refer to Figure 3.3 (A)). Double-stranded RNA treatments resulted in the increase of Spermidine synthase transcript levels (AdoMetDC, ODC, Insert, Section 1, Section 3 and Section 4) while only Spermidine synthase and Section 2 double-stranded RNA treatment caused a decrease in Spermidine synthase transcript levels. At 34 h.p.i the double-stranded RNA treatments with all eight sequences resulted in the increase of Spermidine synthase transcript levels, again most likely due to non-specific effects.

Figure 3.16 and Figure 3.17 illustrate the effect double-stranded RNA treatment had on AdoMetDC/ODC and Spermidine synthase transcript levels when parasites were treated in the

ring developmental stage. Figure 3.18 and Figure 3.19 represent the transcript levels of AdoMetDC/ODC and Spermidine synthase transcripts after parasites were treated in the early trophozoite developmental stage. Previous RNA interference studies by Sriwilaijaroen *et al.* (2009) involved the addition of double-stranded RNA to the medium of ring stage parasites and inhibition was observed after 24 and 36 hours of incubation (Sriwilaijaroen *et al.*, 2009). The double-stranded RNA which was added to the culture medium was therefore expected to be spontaneously taken up by *P. falciparum* housed within the erythrocyte.

Figure 3.18 illustrates the transcript levels of AdoMetDC/ODC after double-stranded RNA incubation for 6 and 24 hours. At 26 h.p.i, the untreated parasites were in the early/middle-trophozoite developmental stage while the double-stranded RNA treated parasites were morphologically either similar to (~26 h.p.i) or slightly ahead (~28 h.p.i) of the untreated parasites. At 26 h.p.i AdoMetDC/ODC transcript production is at its peak (refer to Figure 3.3 (A)).

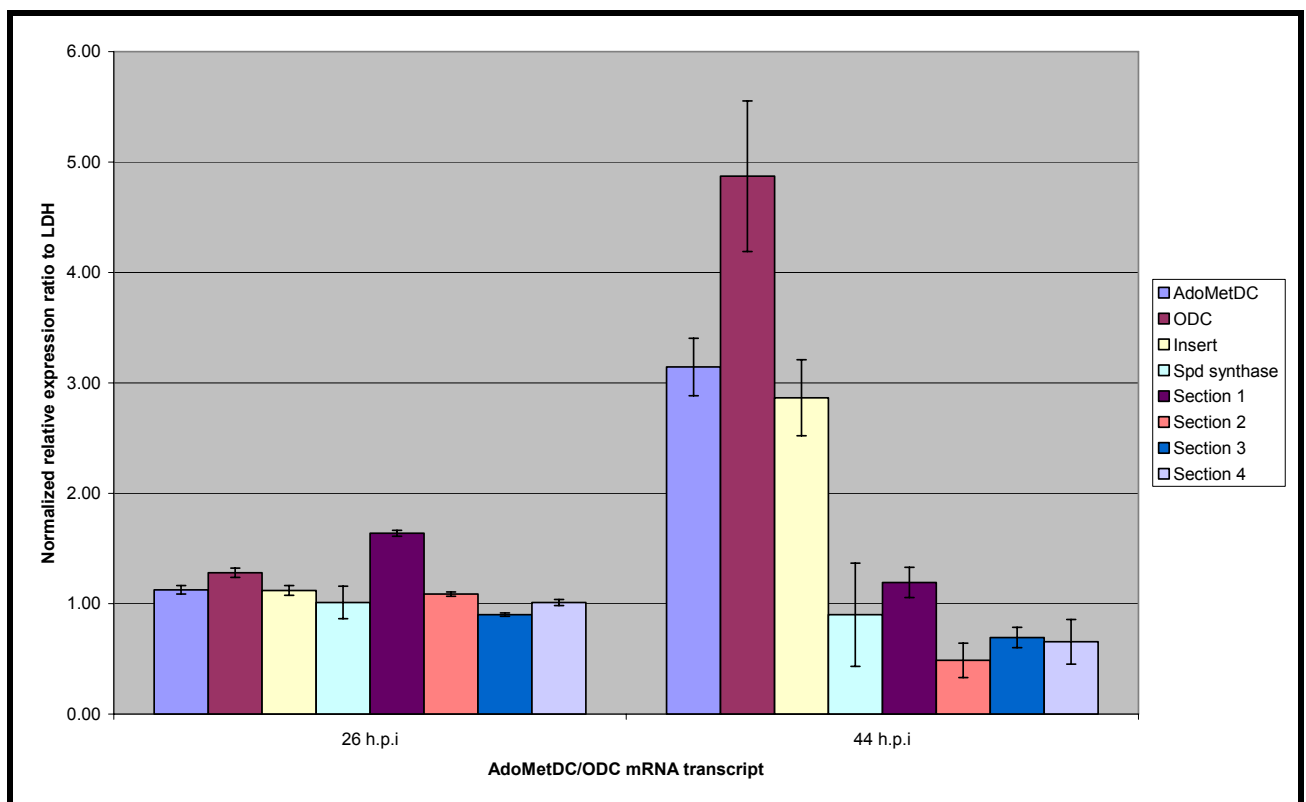


Figure 3.18: Average expression ratios of *P. falciparum* AdoMetDC/ODC transcripts after 6 (26 h.p.i harvested) and 24 hours incubation (44 h.p.i harvested) with double-stranded RNA, starting in the trophozoite stage.

Error bars indicate standard deviations. Double-stranded RNA treatments shown in right hand panel.

As is shown in Figure 3.18, the majority of double-stranded RNA treatments had minor effects on AdoMetDC/ODC transcript levels while only Section 3 double-stranded RNA caused a slight decrease in transcript levels of AdoMetDC/ODC at 26 h.p.i.

After 24 hours double-stranded RNA incubation (44 h.p.i), the AdoMetDC/ODC transcript production has come to a halt (refer to Figure 3.3(A)) and the long term effect of using longer double-stranded RNA sequences becomes more significant. At 44 h.p.i the untreated parasites have entered the schizont developmental stage while all the treated parasites had retarded development and parasite arrest appeared to have occurred in the trophozoite stage.

After 24 hours double-stranded RNA incubation, the short double-stranded RNA sequences designed to knock-down AdoMetDC/ODC transcripts, increased AdoMetDC/ODC transcript levels, except for the Insert which caused a slight decrease in transcript levels. The larger double-stranded RNA sequences (Section 2, 3 and 4) decreased AdoMetDC/ODC transcript levels. Assuming that double-stranded RNA was spontaneously taken up from the surrounding culture medium, this result at 44 h.p.i thus suggests that larger sections of double-stranded RNA are more effective in obtaining the desired knock-down results as compared to the shorter double-stranded RNA sequences.

Figure 3.19 below illustrates the transcript levels of Spermidine synthase after 6 and 24 hours double-stranded RNA incubation in the trophozoite stage.

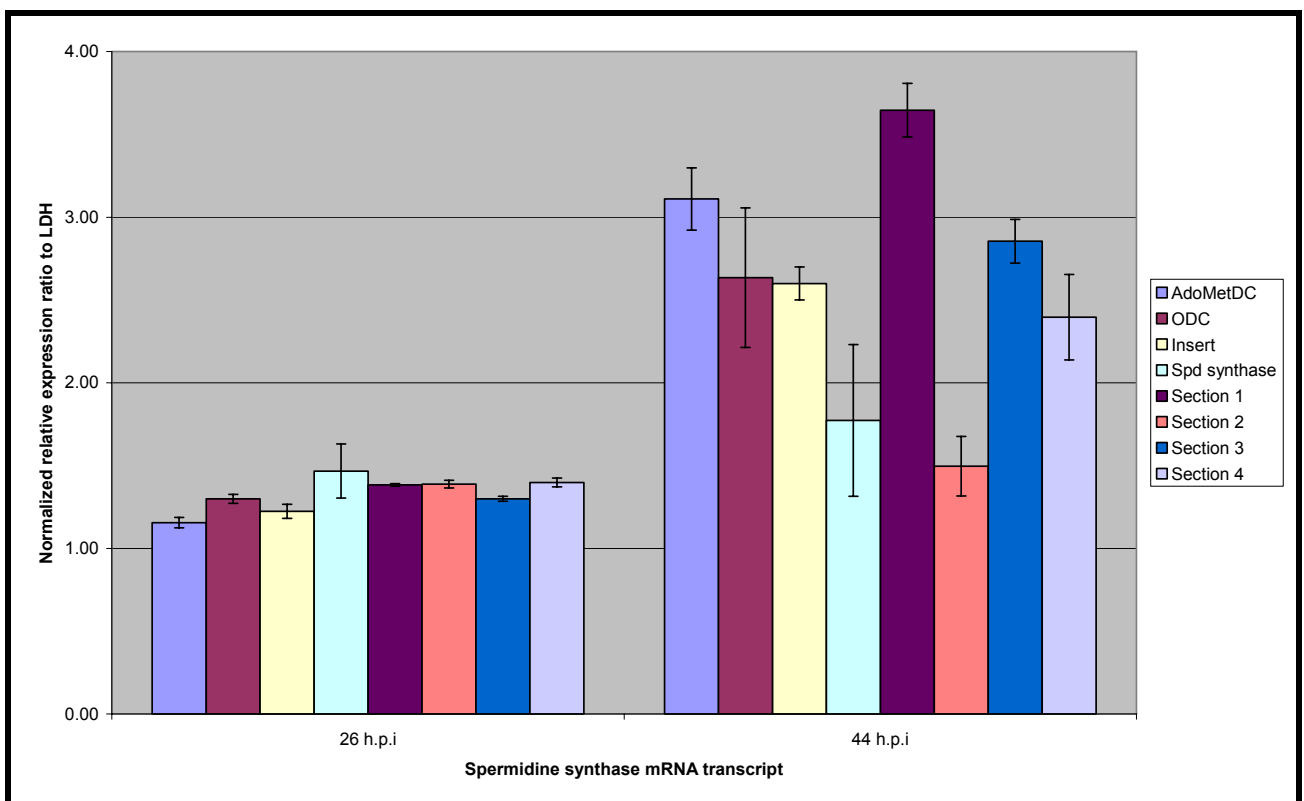


Figure 3.19: Average expression ratios of *P. falciparum* Spermidine synthase transcripts after 6 and 24 hours incubation with double-stranded RNA, starting in the trophozoite stage.

Error bars indicate standard deviations. Double-stranded RNA treatments shown in right hand panel.

At 26 h.p.i, Spermidine synthase transcript production is at a gradual decrease (refer to Figure 3.3 (A)) and none of the double-stranded RNA treatments, including double-stranded RNA from Spermidine synthase, had any specific effect on Spermidine synthase transcript levels. After 24 h.p.i however, once again a non-specific increase in Spermidine synthase transcript levels was observed. Morphologically, at 44 h.p.i, the treated parasites development were halted in the trophozoite stage and the parasites were clearly under stress, which could suggest that the transcript level increase observed for Spermidine synthase was as a result of a general stress response.

3.4 DISCUSSION

RNA interference in *P. falciparum* has been a controversial subject due to the lack of homologues to the major RNA interference components such as Dicer. Nonetheless, in light of several reports claiming the successful use of RNA interference silencing in malaria parasites, as well as the relative advantages afforded by RNA interference versus more conventional gene knock-out approaches, an RNA interference study was designed to knock-down two *P. falciparum* polyamine biosynthetic enzymes, AdoMetDC/ODC and Spermidine synthase, and determine the effect of gene knock-down on parasite survival, to introduce a new means of therapeutic intervention. Short (~120 nucleotide) and long (~980 nucleotide) double-stranded RNA sequences were designed to knock-down *P. falciparum* AdoMetDC/ODC and Spermidine synthase. Double-stranded RNA was introduced to the parasites via electroporation in the ring stage and simple incubation in the trophozoite stage. The effect of RNA interference on the transcript levels of AdoMetDC/ODC and Spermidine synthase was analysed 6 and 24 hours later

Figure 3.20 illustrate the targeted areas for double stranded RNA knock-down of *P. falciparum* AdoMetDC/ODC. AdoMetDC/ODC has five parasite specific inserts termed A1, A2, A3, O1 and O2 which are separated by a hinge region believed to be important for functional protein complex formation (Figure 3.20) (Birkholtz *et al.*, 2004; Williams *et al.*, 2007).

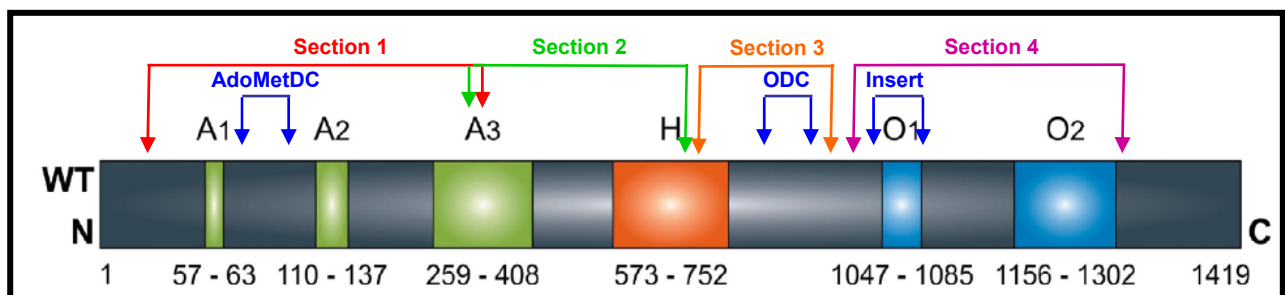


Figure 3.20: Parasite-specific inserts within the N- and C-terminal of the bifunctional AdoMetDC/ODC protein of the wild type *P. falciparum* parasite (Williams *et al.*, 2007)

Residue numbers are indicated for each insert position. Double stranded RNA sequence targets are indicated with arrows.

The nucleotide positions from where the double-stranded RNA sequences were designed consequentially indicates that Section 1 double-stranded RNA was aimed at targeting mRNA regions corresponding to A1, A2 and A3 of AdoMetDC. The Insert double stranded RNA was designed to target the O1 insert of ODC while Section 2 and 3 were designed to target the first and second half of the hinge region respectively. Section 4 was designed to target both insert O1 and O2 of ODC.

Parasites were treated in the ring stage and at 16 h.p.i, AdoMetDC/ODC transcript levels were decreased with all double-stranded RNA treatments, except for AdoMetDC and Section 1 double-stranded RNA. This would suggest that the Section 1 double-stranded RNA sequence is not effective at producing RNA interference effects. Spermidine synthase double-stranded RNA was designed to specifically knock-down Spermidine synthase and unless a feedback or compensatory mechanism exists, this double-stranded RNA treatment was expected to have no effect on AdoMetDC/ODC transcript levels. However, AdoMetDC/ODC transcript levels were decreased with Spermidine synthase double-stranded RNA treatment at 16 h.p.i, which raises the possibility that some feedback mechanism may exist. Assuming once again that the RNA interference effect was specific and successful at knocking down Spermidine synthase, the subsequent reduction of polyamines could have caused the decrease of AdoMetDC/ODC transcript levels. Previous studies resulting in ODC inhibition in *P. falciparum* revealed that ODC is inhibited by putrescine levels and that a feedback mechanism may exist (Muller *et al.*, 2008). At 34 h.p.i, the AdoMetDC/ODC transcript levels remained reduced for all double-stranded RNA treatments, except AdoMetDC, ODC and Insert double-stranded RNA. At 16 h.p.i and 34 h.p.i, double-stranded RNA treatments resulted in the non-specific increase of Spermidine synthase transcript, possibly indicative of a stress response.

Parasites were treated in the trophozoite stage and at 26 h.p.i, AdoMetDC/ODC and Spermidine synthase transcript levels were unaffected for all double-stranded RNA treatments except for Section 3, which caused a minor reduction of AdoMetDC/ODC transcript. After 24 hours incubation, at 44 h.p.i, it appeared as though the short double-stranded RNA sequences had lost their gene inhibitory effect while increased incubation time with the longer double-stranded RNA sequences resulted in a greater inhibitory effect on AdoMetDC/ODC transcript production, except for Section 1 which had no effect on AdoMetDC/ODC transcript levels. Spermidine synthase transcript levels at 44 h.p.i were once again increased as a result of non-specific stress response.

In the light of the current controversy surrounding RNA interference in *P. falciparum*, certain trends were observed and will therefore be discussed. With regards to AdoMetDC/ODC transcript levels, a greater inhibitory effect was observed with parasites treated in the ring stage, rather than the trophozoite stage. After 6 hours incubation in the trophozoite stage, both

AdoMetDC/ODC and Spermidine synthase transcript levels remained unchanged. Only after 24 hours incubation (44 h.p.h) did the inhibitory effect on AdoMetDC/ODC transcript levels become apparent. The main observation in this RNA interference study was the constant AdoMetDC/ODC inhibitory effect observed with Section 3 double-stranded RNA, regardless of the stage of RNA introduction or the incubation time. Section 3 was designed to knock-down an area that would be translated into part of the hinge region of the bifunctional AdoMetDC/ODC enzyme. This RNA interference study reveals that interference with this region of the transcript affects AdoMetDC/ODC transcripts adversely. The general trend for AdoMetDC/ODC thus far is the decrease of AdoMetDC/ODC transcript production with extended double-stranded RNA incubation time, when using larger double-stranded RNA sequences.

The results from this RNA interference study allow numerous observations to be analyzed for optimization of RNA interference in *P. falciparum*. Firstly, during increased incubation times, the shorter double-stranded RNA sequences tend to lose their gene inhibitory effect, while the longer double-stranded RNA sequences maintain their inhibitory effect. The decreased efficiency of short double-stranded RNA sequences to knock-down their target mRNA with extended incubation, observed in this study, may be as a result of double-stranded RNA dilution or degradation. In addition, the inhibitory effects of longer double-stranded RNA sequences become more evident with extended incubation, suggesting that longer double-stranded RNA sequences and extended double-stranded RNA incubation time will result in greater gene knock-down of the target gene (AdoMetDC/ODC). Since double-stranded RNA mechanism of action requires the cleavage of the long double-stranded RNA sequences into siRNA's by the RISC complex, assuming that a RISC complex exists in *P. falciparum*, it seems logical that longer double-stranded RNA sequences (1000 bp) will in turn provide a mixture of siRNA's, each directed at the same mRNA target for degradation and consequently have a greater knock-down effect. Also, RNA interference utilizes various cellular enzymes to degrade the targeted transcripts in a sequence-specific manner and thus, the double-stranded RNA length dependence of RNA interference could reflect that longer RNA sequences may enable more co-factors (such as Dicer, R2D2, Loquacious, Protein Kinase R Protein Activator (PACT) and HIV TAR RNA Binding Protein (TRBP)) to be recruited to degrade the target mRNA at multiple sites (Collins *et al.*, 2006). With regards to increasing the incubation time, Wanidworanun *et al.* (1999) used antisense technology to knock-down the aldolase gene in *P. falciparum* and their study found that at 24 hours incubation, no knock-down effect of the target gene was obtained, while increasing the incubation time to 72 hours resulted in a significant knock-down of aldolase (Wanidworanun *et al.*, 1999). Thus the delayed knock-down observed in this study for AdoMetDC/ODC using RNA interference could become even more evident if double-stranded RNA incubation times were extended.

Bosher *et al.* (1999) performed RNA interference studies in *C. elegans* and discovered that the length of the double-stranded RNA can affect the RNA interference efficiency (Bosher *et al.*, 1999). Longer double-stranded RNA's had a greater gene knock-down effect when compared to shorter sequences and furthermore, using shorter double-stranded RNA sequences in *C. elegans* proved effective only when the concentration of the short double-stranded RNA's were increased by up to 250 fold (Bosher *et al.*, 1999). In this RNA interference study, identical amounts (40 µg) of double-stranded RNA were introduced into *P. falciparum* culture, regardless of the length of the double-stranded RNA sequence. It could therefore be that a higher concentration of the shorter double-stranded RNA sequences, may have provided a more effective gene knock-down result for AdoMetDC/ODC, and more specifically for Spermidine synthase. Higher amounts of double-stranded RNA may be more effective in knocking down the target gene, however this could also counteract RNA-editing enzymes such as Adenosine deaminase acting on RNA (ADAR) (Brantl, 2002). ADAR's promiscuously deaminate adenosines present in long double-stranded RNA's prior to processing and in turn, change the RNA structure making a fraction of the double-stranded RNA sequences non-homologous to the target mRNA (Brantl, 2002). Adenosine deaminase (PF10_0289) has been identified in *P. falciparum* and since RNA interference is homology dependent, a single base pair mismatch between the siRNA and the target mRNA can reduce the silencing effect dramatically. Thus, the use of increased double-stranded RNA concentrations in RNA interference studies must be considered with caution.

It should also be considered that long double-stranded RNA sequences can activate the double-stranded RNA-dependent protein kinase response, which results in the phosphorylation of eIF2 α translation initiation factor in response to stress. Several protein kinases have been identified in *P. falciparum* and are important for cell cycle regulation, stress response and sexual differentiation which suggests that activation of such a stress response by long double-stranded RNA sequences could lead to cytostatic arrest (Kappes *et al.*, 1999). This therefore also suggests that the increased inhibition or transcript reduction observed with the longer double-stranded RNA could be as a result of a general stress response and not necessarily RNA interference.

The absence of a significant knock-down effect observed with parasites treated in the trophozoite stage may be due to a general lack of double-stranded RNA uptake by the parasite. Double-stranded RNA was simply added to the culture medium and was assumed to be taken up by the parasite. Sriwilaijaroen *et al.* (2009) performed double-stranded RNA interference on *P. falciparum* histone deacetylase (*PHDAC-1*) by treating parasites with double-stranded RNA in the ring stage and isolating RNA after 24 and 36 hours of incubation (Sriwilaijaroen *et al.*, 2009). In their study double-stranded RNA was added to the medium in increasing concentrations, without electroporation and revealed that gene knock-down was dose-

dependent, but only until a certain threshold, after which increased double-stranded RNA concentration did not increase the gene knock-down effect (Sriwilajaroen *et al.*, 2009). This result suggests that either the erythrocyte has a limited ability to take up double-stranded RNA or that the processing enzymes are limited. Previous RNA interference studies in *P. falciparum* claim that electroporation of 1 µg/µl of double-stranded RNA is sufficient for inhibition and that no inhibition will occur without electroporation (McRobert *et al.*, 2002) while other studies have claimed that adding double-stranded RNA directly to the culture medium at 25 µg/µl can inhibit parasite growth (Gissot *et al.*, 2005; Malhotra *et al.*, 2002). Electroporation may enhance the uptake and delivery of double-stranded RNA to the parasite by assisting passage through three membrane layers (erythrocyte membrane, parasitophorous vacuolar membrane, parasite plasma membrane) however, parasitized erythrocytes have been shown to permit the entry of oligonucleotides when added directly to the medium, whereas uninfected erythrocytes do not (Malhotra *et al.*, 2002; Pouvell *et al.*, 1991; Rappaport *et al.*, 1992). In addition, it was determined that approximately 0.1-0.15% of the double-stranded RNA present in the medium was taken up by the parasite (Malhotra *et al.*, 2002; Pouvell *et al.*, 1991; Rappaport *et al.*, 1992). Assuming that 0.15 % of the double-stranded RNA was taken up spontaneously by the *P. falciparum* parasites in this study, the question remains as to whether the double-stranded RNA concentrations were sufficient to cause gene knock-down after 6 and 24 hours. AdoMetDC/ODC transcript levels appeared to be decreased after 24 hours but Spermidine synthase transcript levels remained increased. Trophozoite parasites can not survive the harsh conditions of electroporation and thus, for future studies, it may be beneficial to use pre-electrophoresed erythrocytes since *P. falciparum* may be able to take up the double-stranded RNA spontaneously from the cytoplasm of pre-electrophoresed uninfected erythrocytes, as was done with plasmids (Deitsch *et al.*, 2001b; McRobert *et al.*, 2002).

Similar gene knock-down of ODC and Spermidine synthase by Xiao *et al.* (2009) in *T. brucei* resulted in cell cycle arrest, which was observed after double-stranded RNA for ODC and Spermidine synthase was introduced into the parasite culture (Xiao *et al.*, 2009). Although the polyamine biosynthetic pathway enzymes differ between *T. brucei* and *P. falciparum*, RNA interference trends may be similar and may aid in understanding the RNA interference effects observed in this study presented here with *P. falciparum*. RNA interference in *T. brucei* with 6 hours incubation with Spermidine synthase and ODC double-stranded RNA resulted in the depletion of both polyamines and trypanothione, which lead to cell growth arrest but did not assert any significant effect on the transcript levels of other polyamine pathway enzymes (Xiao *et al.*, 2009). An interesting finding was that the Spermidine synthase double-stranded RNA resulted in a 20% inhibition of Spermidine synthase after 2 days incubation while ODC double-stranded RNA inhibition led to ~90% reduction in ODC mRNA within 24 hours and resulted in almost complete depletion of putrescine (Xiao *et al.*, 2009). In the study presented here for *P. falciparum*, the effect of double-stranded RNA on Spermidine synthase do not seem evident

since the transcript levels of Spermidine synthase were not significantly knocked-down, even with increased incubation. The observation by Xiao *et al.* (2009) regarding the delayed knock-down of Spermidine synthase could suggest that extended incubation time, such as 48 hours, is required for a knock-down effect of Spermidine synthase to be observed in *P. falciparum*.

Considering the results obtained after double-stranded RNA treatment, several trends, especially those observed with ODC inhibition, remain similar when compared to literature. RNA interference studies and DFMO inhibition of ODC in *P. falciparum* prevented the parasites from developing past the trophozoite stage - a similar observation was made morphologically in this study using RNA interference (Heby *et al.*, 2003; Muller *et al.*, 2008; Sriwilaijaroen *et al.*, 2009). This therefore suggests that in this study some gene interference is occurring. Whether the mechanism behind this knock-down was as a result of RNA degradation or antisense remains to be elucidated. Since certain antisense RNA's have been found to have more than one mRNA target (Brantl, 2002), it remains plausible that certain transcript reductions, such as the Spermidine transcript decrease with Section 2 double-stranded RNA or the AdoMetDC/ODC transcript reduction with Spermidine synthase double-stranded RNA, are due to non-specific, antisense-mediated effects.

The origin of double-stranded RNA design can also prove problematic. Studies by Boshier *et al.* (1999) found that double-stranded RNA designed from intronic sequences were less potent in knocking down *C. elegans* genes than double-stranded RNA sequences designed from exonic sequences, which suggests that pre-mRNA may be protected against RNA interference or that RNA interference can occur in the nucleus but is predominantly active in the cytoplasm (Boshier *et al.*, 1999). The eight double-stranded RNA sequences designed in this study were designed from the exonic sequences of the genes under study and thus cytoplasmic RNA degradation was anticipated.

In this study, double-stranded RNA degradation targeting the mRNA region encoding the ODC domain of AdoMetDC/ODC resulted in a significant knock-down of AdoMetDC/ODC, suggesting that the double-stranded sequences corresponding to this region, may be more effective. In the study by Van Brummelen *et al.* (2009), AdoMetDC/ODC transcript production was inhibited with the use of several irreversible inhibitors and the down-stream reactions were analyzed (Van Brummelen *et al.*, 2009). As expected, they found that polyamine (putrescine) levels were diminished due to the proper functioning of AdoMetDC/ODC being abolished and the fold decrease in polyamines was identical to the fold decrease in transcript level (Van Brummelen *et al.*, 2009). Thus, the parasite seemed to respond to the decreasing transcript levels by decreasing its requirement for polyamines by the same fold, suggesting that this regulation occurs on both the transcriptome and proteome level. In this study, the mRNA transcripts of AdoMetDC/ODC were knocked-down and revealed that on the transcriptome level,

AdoMetDC/ODC transcript reduction lead to cytoostasis and it is assumed the parasite adjusted its polyamine requirement accordingly. Quantitative microarray and semi-quantitative proteomic datasets obtained from the various life cycle stages of the *P. falciparum* parasite failed to provide evidence of a strict correlation between mRNA and protein since it seems that mRNA can accumulate and the protein may only become transcribed later, suggesting a major role of post-transcriptional regulation of parasite genes (Le Roch *et al.*, 2004).

RNA interference was selected as the method of gene knock-down due to its advantages over other knock-down techniques, which include the low-cost and speed of the assay, as well as the fact that multiple genes can be analyzed simultaneously. Although the exact mechanism behind the knock-down of transcript levels observed in this study remains to be elucidated, several observations have suggested that gene inhibition was evident. RNA interference may be possible in *P. falciparum* however, due to the complexity of this parasite, certain optimizations and additional analysis may be required for future RNA interference attempts.

For future studies, it may be advantageous to include an additional harvesting time point, where parasites are treated at ~20 h.p.i and harvested in the next cycle (after incubating parasites with double-stranded RNA for ~30 or ~40 hours). This would allow analysis of the RNA interference effect in a new parasite cycle and in addition, the percentage parasitemia could be determined before and after double-stranded RNA treatment to determine the full effect of introducing double-stranded RNA into *P. falciparum* culture. This extended incubation time may also aid in specifically knocking down Spermidine synthase since this enzyme may require longer incubation times than AdoMetDC/ODC. It will be of interest to this study to confirm the observed results via either RNA dot blots or with Northern blot analysis where the mRNA can be detected with labelled antisense RNA probes. Western blots may also be incorporated to determine the protein levels and indicate the level at which these genes are regulated, while analysis of polyamine pools will contribute to understanding the effect of enzyme inhibition. The effect of double-stranded RNA type RNA interference can also be determined with subsequent enzyme activity assays of the enzymes in question. Previous co-inhibition studies of AdoMetDC/ODC by van Brummelen *et al.* (2009) resulted in the subsequent increase of degradation enzymes such as Ornithine aminotransferase (OAT) to counteract the ornithine accumulation. Thus, in addition to analyzing the mRNA transcript levels of the targeted genes (AdoMetDC/ODC and Spermidine synthase) after double-stranded RNA incubation, it would be interesting to analyze the transcript levels of other enzymes related to the polyamine biosynthetic pathway such as OAT. It would also be of considerable value to analyze the effect of antisense sequences on the transcript levels of Spermidine synthase and AdoMetDC/ODC, since the target specificity of antisense technology should assist in unravelling the mechanism behind the transcript knock-down observed here.

The regulatory switch that controls the key control point of *P. falciparum* ODC remains to be identified. The results of this study could ultimately be used to design more specific inhibitors and with additional information, such as the 3-dimensional structure of the enzymes, selective interference of *P. falciparum* essential genes may be possible using available knock-down techniques. This study therefore contributes to our understanding of *P. falciparum* polyamine enzymes and may give some insight into the regulatory control points in polyamine biosynthetic pathways, to ultimately aid in eradicating this parasite from the human host.

CHAPTER 4

CONCLUDING DISCUSSION

The malaria parasite *P. falciparum* has proven to be exceptionally proficient at manipulating the host resources in such a way to maintain a chronic infection. Due to the tight regulation and “just-in-time” expression of its genes, the mechanisms behind parasitic gene regulation have been identified as a likely Achilles heel for *P. falciparum*.

Gene regulation studies in *P. falciparum* are ill defined and since the elucidation of its mechanism of regulation could lead to the discovery of the ultimate means of controlling malaria, understanding the regulatory mechanism is of critical value. Few parasite-specific transcriptional factors and their regulatory sequences have been identified to date due to the AT-richness of the parasite genome and the nature of the techniques to study gene regulation have made this fairly challenging. The use of different algorithms during *in silico* searches have generated numerous potential *cis*-regulatory sequences, however various limitations have been identified in the consistency of the data generated (Horrocks *et al.*, 2009). As discussed in Chapter 1, gene regulation occurs at various levels: on the transcriptional level by the intricate interplay of proteins, also known as transcription factors, with *cis*-regulatory DNA elements such as enhancers or repressors (Kumar *et al.*, 2004; Meissner *et al.*, 2005), on the post-transcriptional level via mRNA decay (Meyer *et al.*, 2004; Parker *et al.*, 2004; Wilusz *et al.*, 2001), RNA interference (Valencia-Sanchez *et al.*, 2006) or non-coding RNA's (Li *et al.*, 2008), on the translational level via translational repression (Gebauer *et al.*, 2004) and epigenetically on the chromatin level (Rando *et al.*, 2007). The global aims of this study were to investigate two possible mechanisms of gene regulation at the level of transcription and post-transcription.

In Chapter 2, transcriptional mechanisms were investigated through verification of the robustness of *in silico* methods, to identify *cis*-regulatory sequences in the *P. falciparum* genome. In this chapter, the complexity of the DNA-protein interaction using *P. falciparum* derived proteins was illustrated using EMSA's. Molecular studies on *P. falciparum* clearly require specialized methods and protocols and the methods used in this study have been optimized to provide a stepping stone for future analysis. The *cis*-regulatory sequences may have a regulatory function and in addition, appear to share similar regulatory proteins. It is evident that both double- and single-stranded regulatory proteins are present in *P. falciparum* nuclear extract since definite shifts were observed under various scenarios. Among the five *cis*-regulatory sequences identified, Motif 2 was previously identified as SPE 1 and found to bind a nuclear factor (Voss *et al.*, 2003) which support the possible regulatory role of the remaining four motifs. The presence and importance of *cis*-regulatory sequences and regulatory proteins

have been illustrated in *P. falciparum* (Flueck *et al.*, 2008; Gissot *et al.*, 2005; Osta *et al.*, 2002; Voss *et al.*, 2003) and thus this study has contributed to the global requirement of understanding *P. falciparum* gene regulation. Although additional studies, to unravel the details regarding the DNA-protein interactions are crucial, the identity and characterization of these regulatory proteins could ultimately lead to an important discovery and design of new anti-malarials.

The results presented in Chapter 3 supports the possibility of the presence of post-transcriptional gene regulatory mechanisms like RNA interference machinery in *P. falciparum*. Authors have claimed that RNA interference is both possible and impossible in *P. falciparum* (Baum *et al.*, 2009; Kumar *et al.*, 2002; Malhotra *et al.*, 2002; Mcrobert *et al.*, 2002) while a definite antisense mechanism has been identified in this parasite (Barker *et al.*, 1996; Gardiner *et al.*, 2000; Ikemoto *et al.*, 1999; Noonpakdee *et al.*, 2003; Wanidworanun *et al.*, 1999). The successful knock-down of the biosynthetically important AdoMetDC/ODC and Spermidine synthase genes resulted in morphological changes similar to what was observed with drug inhibition studies of the same enzymes (Birkholtz *et al.*, 2004; Das *et al.*, 1995; Van Brummelen *et al.*, 2009; Whaun *et al.*, 1985). The knock-down however could have been as a result of other mechanisms other than RNA interference, such as antisense or a general stress response. Further insight into the mechanism of gene knock-down however is imperative to fully understand and appreciate the complexity of the malaria parasite within the human host. The main outcome in discovering the importance of AdoMetDC/ODC and Spermidine synthase for *P. falciparum* survival would lead to the development of more effective anti-malarial drugs, especially if enzyme inhibition can be combined with polyamine transport inhibition.

Gene regulation, whether it is transcriptional, post-transcriptional, translational or epigenetic, plays a major role in parasite survival. The research presented here has lent some insight into the possible mechanisms of gene regulation *P. falciparum* utilizes *in vitro* for survival. These results have introduced a new avenue of exploiting the parasite *P. falciparum* for complete eradication from the human host and further studies are imperative. The feasibility of identifying regulatory proteins have been illustrated and in addition, a quicker and less expensive means of knocking-down genes, crucial to the parasite for survival, have been identified. The results obtained in this study have contributed to the global challenge of unravelling the gene-regulatory pathways within *P. falciparum* and although it may be clear that a great deal of work remains to be done in both the EMSA and RNA interference studies, this research has initiated the flow of making even greater discoveries in *Plasmodium*, and these discoveries are within reasonable reach.

REFERENCES

- ABNIZOVA, I. & GILKS, W.R. Studying statistical properties of regulatory DNA sequences, and their use in predicting regulatory regions in the eukaryotic genomes. *Briefings in Bioinformatics* (2006) **7**, 48-54.
- ADISA, A., FRANKLAND, S., RUG, M., JACKSON, K., MAIER, A.G., WALSH, P., *et al.* Re-assessing the locations of components of the classical vesicle-mediated trafficking machinery in transfected *plasmodium falciparum*. *International Journal for Parasitology* (2007) **37**, 1127-1141.
- AHMED, H. (2005). *Principles and reactions of protein extraction, purification and characterization*.
- AIDE, P., BASSAT, Q. & ALONSO, P.L. Towards an effective malaria vaccine. *Archives of Disease in Childhood* (2007) **92**, 476-479.
- ASSARAF, Y.G., GOLENSER, J., SPIRA, D.T. & BACHRACH, U. Polyamine levels and the activity of their biosynthetic enzymes in human erythrocytes infected with the malarial parasite *plasmodium falciparum*. *Biochemical Journal* (1984) **222**, 815-819.
- BABITZKE, P., BAKER, C.S. & ROMEO, T. Regulation of translation initiation by rna binding proteins. *Annual Review of Microbiology* (2009) **63**, 27-44.
- BALAJI, S., MADAN BABU, M., LYER, L.M. & ARAVIND, L. Discovery of the principle specific transcription factors of apicomplexa and their implication for the evolution of the ap2-intergrase DNA binding domains. *Nucleic Acids Research* (2005) **33**, 3994-4006.
- BALINT, G.A. Artemisinin and its derivatives: An important new class of antimalarial agents. *Pharmacology and Therapeutics* (2001) **90**, 261-265.
- BARILLAS-MURY, C. & KUMAR, S. *Plasmodium*-mosquito interactions: A tale of dangerous liaisons. *Cellular Microbiology* (2005) **7**, 1539-1545.
- BARKER, R.H., METELEV, V., RAPAPORT, E. & ZAMECNIK, P. Inhibition of *plasmodium falciparum* malaria using antisense oligodeoxynucleotides. *Proceedings of the National Academy of Science of the USA* (1996) **93**, 514-518.
- BAUM, J., PAPENFUSS, A.T., MAIR, G.R., JANSE, C.J., VLACHOU\$, D., WATERS, A.P., *et al.* Molecular genetics and comparative genomics reveal rai is not functional in malaria parasites. *Nucleic Acids Research* (2009), 1-11.
- BIRKHOLTZ, L., VAN BRUMMELEN, A.C., CLARK, K., NIEMAND, J., MARECHAL, E., LLINAS, M., *et al.* Exploring functional genomics for drug target and therapeutics discovery in *plasmodia*. *Acta Tropica* (2008) **105**, 113-123.
- BIRKHOLTZ, L., WRENGER, C., JOUBERT, F., WELLS, G.A., WALTER, R.D. & LOUW, A.I. Parasite-specific inserts in the bifunctional s-adenosylmethionine decarboxylase/ornithine decarboxylase of *plasmodium falciparum* modulate catalytic activities and domain interactions. *The Biochemical Journal* (2004) **377**, 439-448.

- BLYTHE, J.E., SURENTERAN, T. & PREISER, P.R. Stevor-a multifunctional protein. *Molecular and Biochemical Parasitology* (2004) **134**, 11-15.
- BOSHER, J.M., DUFOURCQ, P., SOOKHAREEA, S. & LABOUESSE, M. Rna interference can target pre-mrna: Consequences for gene expression in a *caenorhabditis elegans* operon. *Genetics* (1999) **153**, 1245-1256.
- BOZDECH, Z., LLINAS, M., PULLIAM, B.L., WONG, E.D., ZHU, J. & DERISI, J.L. The transcriptome of the intra-erythrocytic developmental cycle of *plasmodium falciparum*. *Public Library of Science Biology* (2003) **1**, 085-100.
- BRAKS, J.A.M., MAIR, G.R., FRANKE-FAYARD, B., JANSE, C.J. & WATERS, A.P. A conserved u-rich rna region implicated in regulation of translation in *plasmodium* female gametocytes. *Nucleic Acids Research* (2007) **36**, 1176-1186.
- BRANTL, S. Antisense-rna regulation and rna interference. *Biochimica et Biophysica Acta* (2002) **1575**, 15-25.
- BURGER, P.B., BIRKHOLTZ, L., JOUBERT, F., HAIDER, N., WALTER, R.D. & LOUW, A.I. Structural and mechanistic insights into the action of *plasmodium falciparum* spermidine synthase. *Bio-organic and Medicinal Chemistry* (2007) **15**, 1628-1637.
- CALDERWOOD, M.S., GANNOUN-ZAKI, L., WELLEMS, T.E. & DEITSCH, K.W. *Plasmodium falciparum* var genes are regulated by two regions with separate promoters, one upstream of the coding region and a second within the intron. *The Journal of Biological Chemistry* (2003) **278**, 34125-34132.
- CARTHEW, R.W. Gene regulation by micromnas. *Current Opinion in Genetics and Development* (2006) **16**, 203-208.
- CHEUNG, P. & LAU, P. Epigenetic regulation by histone methylation and histone variants. *Molecular Endocrinology* (2005) **19**, 563-573.
- CLARK, K., DHOOGRA, M., LOUW, A.I. & BIRKHOLTZ, L. Transcriptional responses of *plasmodium falciparum* to a-difluoromethylornithine-induced polyamine depletion. *Biological Chemistry* (2008) **389**, 111-125.
- COLEMAN, B.I. & DURAISINGH, M.T. Transcriptional control and gene silencing in *plasmodium falciparum*. *Cellular Microbiology* (2008) **10**, 1935-1946.
- COLLINS, R.E. & CHENG, X. Structural and biochemical advances in mammalian rna. *Journal of Cellular Biochemistry* (2006) **99**, 1251-1266.
- COMEAX, C.A. & DURAISINGH, M.T. Unravelling a histone code for malaria virulence. *Molecular Microbiology* (2007) **66**, 1291-1295.
- COTTRELL, T.R. & DOERING, T.L. Silence of the strands: Rna interference in eukaryotic pathogens. *Trends in Microbiology* (2003) **11**, 37-43.
- CRABB, B.S. Transfection technology and the study of drug resistance in the malaria parasite *plasmodium falciparum*. *Drug Resistance Updates* (2002) **5**, 126-130.

- CUI, L., FAN, Q. & LI, J. The malaria parasite *plasmodium falciparum* encodes members of the puf rna-binding protein family with conserved rna binding activity. *Nucleic Acids Research* (2002) **30**, 4607-4617.
- DAS, B., GUPTA, R. & MADHUBALA, R. Combined action of inhibitors of polyamine biosynthetic pathway with a known antimalarial drug chloroquine on *plasmodium falciparum*. *Pharmacological Research* (1995) **31**, 189-193.
- DASARADHI, P.V.N., MOHMMED, A., KUMAR, A., HOSSAIN, M.J., BHATNAGAR, R.K., CHAUHAN, V.S., *et al.* A role of falcipain-2, principal cysteine proteases of *plasmodium falciparum* in merozoite egression. *Biochemical and Biophysical Research Communications* (2005) **336**, 1062-1068.
- DASGUPTA, R., KRAUSE-IHLE, T., BERGMANN, B., MULLER, I.B., KHOMUTOV, A.R., MULLER, S., *et al.* 3-aminooxy-1-aminopropane and derivatives have an antiproliferative effect on cultured *plasmodium falciparum* by decreasing intracellular polyamine concentrations. *Antimicrobial Agents and Chemotherapy* (2005) **49**, 2857-2864.
- DE, A., RAMESH, V., MAHADEVAN, S. & NAGARAJA, V. Mg²⁺ mediated sequence-specific binding of transcriptional activator protein c of bacteriophage mu to DNA. *Biochemistry* (1998) **37**, 3831-3838.
- DE SILVA, E.K., GEHRKE, A.R., OLSZEWSKI, K., LEO' N, I., CHAHAL, J.S., BULYK, M.L., *et al.* Specific DNA-binding by apicomplexan ap2 transcription factors. *Proceedings of the National Academy of Science of the USA* (2008) **105**, 8393-8398.
- DEEN, J.L., VON SEIDLEIN, L. & DONDORP, A. Therapy of uncomplicated malaria in children: A review of treatment principles, essential drugs and current recommendations. *Tropical Medicine and International Health* (2008) **13**, 1111-1130.
- DEITSCH, K.W., CALDERWOOD, M.S. & WELLEMS, T.E. Cooperative silencing elements in *var* genes. *Nature* (2001a) **412**, 875-876.
- DEITSCH, K.W., DEL PINAL, A. & WELLEMS, T.E. Intra-cluster recombination and *var* transcription switches in the antigenic variation of *plasmodium falciparum*. *Molecular and Biochemical Parasitology* (1999) **101**, 107-116.
- DEITSCH, K.W., DRISKILL, C.L. & WELLEMS, T.E. Transformation of malaria parasites by the spontaneous uptake and expression of DNA from human erythrocytes. *Nucleic Acids Research* (2001b) **29**, 850-853.
- DEITSCH, K.W. & HVIID, L. Variant surface antigens, virulence genes and the pathogenesis of malaria. *Trends in Parasitology* (2004) **20**, 562-566.
- DEITSCH, K.W., MOXON, E.R. & WELLEMS, T.E. Shared themes of antigenic variation and virulence in bacterial, protozoal and fungal infections. *Microbiology and Molecular Biology Reviews* (1997) **61**, 281-293.
- DHARMARAJ, S. (Applied Biosystems). *Rt-pcr -the basics*.

- DRABOVICH, A. & KRYLOV, S.N. Single-stranded DNA-binding protein facilitates gel-free analysis of polymerase chain reaction products in capillary electrophoresis. *Journal of Chromatography A* (2004) **1051**, 171-175.
- DUFFY, M.F. & THAM, W. Transcription and coregulation of multigene families in *plasmodium falciparum*. *Trends in Parasitology* (2007) **23**, 183-186.
- DURASINGH, M.T., VOSS, T.S., MARTY, A.J., DUFFY, M.F., GOOD, R.T., THOMPSON, J.K., *et al.* Heterochromatin silencing and locus repositioning linked to regulation of virulence genes in *plasmodium falciparum*. *Cell* (2005) **121**, 13-24.
- DURRE, P. (2005). *Handbook on clostridia*.
- DZIKOWSKI, R., TEMPLETON, T.J. & DEITSCH, K.W. Variant antigen gene expression in malaria. *Cellular Microbiology* (2006) **8**, 1371-1381.
- ELFORD, B.C. L-glutamine influx in malaria-infected erythrocytes: A target for antimalarials? *Parasitology Today* (1986) **2**.
- FERNANDEZ, V., HOMMEL, M., CHEN, Q., HAGBLOM, P. & WAHLGREN, M. Small, clonally variant antigens expressed on the surface of the *plasmodium falciparum*-infected erythrocyte are encoded by the rif gene family and are the target of human immune responses. *Journal of Experimental Medicine* (1999) **190**, 1393-1403.
- FIGUEIREDO, L.M. & SCHERF, A. *Plasmodium* telomeres and telomerase: The usual actors in an unusual scenario. *Chromosome Research* (2005) **13**, 517-524.
- FLICK, K. & CHEN, Q. *Var* genes, pfemp1 and the human host. *Molecular and Biochemical Parasitology* (2004) **134**, 3-9.
- FLUECK, C., NIEDERWIESER, I., MOES, S., JENOE, P. & VOSS, T.S. (2008). Identification of the first transcription factor of *var* genes. In *MAM conference*, Australia.
- FRANK, M. & DEITSCH, K.W. Activation, silencing and mutually exclusive expression within the *var* gene family of *plasmodium falciparum*. *International Journal for Parasitology* (2006a) **36**, 975-985.
- FRANK, M., DZIKOWSKI, R., COSTANTINI, D., AMULIC, B., BERDOUGO, E. & DEITSCH, K.W. Strict pairing of *var* promoters and introns is required for *var* gene silencing in the malaria parasite *plasmodium falciparum*. *The Journal of Biological Chemistry* (2006b) **281**, 9942-9952.
- FREITAS-JUNIOR, L.H., BOTTIUS, E., PIRRIT, L.A., DEITSCH, K.W., SCHEIDIG, C., GUINET, F., *et al.* Frequent ectopic recombination of virulence factor genes in telomeric chromosome clusters of *p.Falciparum*. *Nature* (2000) **407**, 1018-1022.
- FREITAS-JUNIOR, L.H., HERNANDEZ-RIVAS, R., RALPH, S.A., MONTIEL-CONDADO, D., RUVALCABA-SALAZAR, O.K., ROJAS-MEZA, A., *et al.* Telomeric heterochromatin propagation and histone acetylation control mutually exclusive expression of antigenic variation genes in malaria parasites. *Cell* (2005) **121**, 24-36.
- GALINSKI, M.R. & BARNWELL, J.W. Monkey malaria kills four humans. *Trends in Parasitology* (2009) **25**, 200-204.

- GANESAN, K., PONMEE, N., JIANG, L., FOWBLE, J.W., WHITE, J., KAMCHONWONGPAISAN, S., *et al.* A genetically hard-wired metabolic transcriptome in *plasmodium falciparum* fails to mount protective responses to lethal antifolates. *Public Library of Science: Pathogens* (2008) **4**, 1-13.
- GANNOUN-ZAKI, L.L., JOST, A., MU, M., DEITSCH, K.W. & WELLEMS, T.E. A silenced *plasmodium falciparum* var promoter can be activated *in vivo* through spontaneous deletion of a silencing element in the intron. *Eukaryotic Cell* (2005) **4**, 490-492.
- GARCIA-SANZ, J.A., MIKULITS, W., LIVINGSTONE, A., LEFKOVITS, I. & MULLNER, E.W. Translational control: A general mechanism for gene regulation during t cell activation. *The Federation of American Societies for Experimental Biology Journal* (1998) **12**, 299-306.
- GARDENER, M.J., HALL, N., FUNG, E., WHITE, O., BERRIMAN, M., HYMAN, R.W., *et al.* Genome sequence of the human malaria parasite *plasmodium falciparum*. *Nature* (2002) **419**, 498-511.
- GARDINER, D.L., HOLT, D.C., THOMAS, E.A., KEMP, D.J. & TRENHOLME, K.R. Inhibition of *plasmodium falciparum* clag9 gene function by antisense rna. *Molecular and Biochemical Parasitology* (2000) **110**, 33-41.
- GEBAUER, F. & HENTZE, M.W. Molecular mechanisms of translational control. *Nature Reviews* (2004) **5**, 827-835.
- GHOSH, A., EDWARDS, M.J. & JACOB-LORENA, M. The journey of the malaria parasite in the mosquito: Hopes for the new century. *Parasitology Today* (2000) **16**, 196-201.
- GISSOT, M., BRIQUET, S., REFOUR, P., BOSCHET, C. & VAQUERO, C. Pfyb, a *plasmodium falciparum* transcription factor, is required for intra-erythrocytic growth and controls key genes for cell cycle regulation. *Journal of Molecular Biology* (2005) **346**, 29-42.
- GREENWOOD, B.M., FIDOCK, D.A., KYLE, D.E., KAPPE, S.H.I., ALONSO, P.L., COLLINS, F.H., *et al.* Malaria: Progress, perils, and prospects for eradication. *The Journal of Clinical Investigation* (2008) **118**, 1266-1276.
- GRIFFITH, K.S., LEWIS, L.S., MALI, S. & PARISE, M.E. Treatment of malaria in the united states-a systematic review. *Journal of the American Medical Association* (2007) **297**, 2264-2277.
- GUERRA, C.A., GIKANDI, P.W., TATEM, A.J., NOOR, A.M., SMITH, D.L., HAY, S.I., *et al.* The limits and intensity of *plasmodium falciparum* transmission: Implications for malaria control and elimination worldwide. *Public Library of Science-Medicine* (2008) **5**, 0300-0311.
- GUNASEKERA, A., MYRICK, A., LE ROCH, K., WINZELER, E. & WIRTH, D.F. *Plasmodium falciparum*: Genome wide perturbations in transcript profiles among mixed stage cultures after chloroquine treatment. *Experimental Parasitology* (2007a) **117**, 87-92.
- GUNASEKERA, A., MYRICK, A., MILITELLO, K.T., SIMS, J., DONG, C.K., GIERAHN, T., *et al.* Regulatory motifs uncovered among gene expression clusters in *plasmodium falciparum*. *Molecular and Biochemical Parasitology* (2007b) **153**, 19-30.

- GUNASEKERA, A., PATANKAR, S., SCHUG, J., EISEN, G. & WIRTH, D.F. Drug-induced alterations in gene expression of the asexual blood forms of *plasmodium falciparum*. *Molecular Microbiology* (2003) **50**, 1229-1239.
- HAIDER, N., ESCHBACH, M.L., DE SOUZA DIAS, S., GILBERGER, T.W., WALTER, R.D. & LÿERSEN, K. The spermidine synthase of the malaria parasite *plasmodium falciparum*: Molecular and biochemical characterization of the polyamine synthesis enzyme. *Molecular and Biochemical Parasitology* (2005) **142**, 224-236.
- HAKIMI, M. & DEITSCH, K.W. Epigenetics in apicomplexa: Control of gene expression during cell cycle progression, differentiation and antigenic variation. *Current Opinion in Microbiology* (2007) **10**, 357-362.
- HALL, N., KARRAS, M., RAINE, J.D., CARLTON, J.M., KOOIJ, T.W.A., BERRIMAN, M., *et al.* A comprehensive survey of the *plasmodium* life cycle by genomic, transcriptomic and proteomic analyses. *Science* (2005) **307**, 82-86.
- HANNON, G.J. Rna interference. *Nature* (2002) **418**, 244-251.
- HEBY, O., ROBERTS, S.C. & ULLMAN, B. Polyamine biosynthetic enzymes as drug targets in parasitic protozoa. *Biochemical Society Transactions* (2003) **31**, 415-419.
- HEINTZMAN, N.D. & REN, B. The gateway to transcription: Identifying, characterizing and understanding promoters in the eukaryotic genome. *Cellular and Molecular Life Sciences* (2007) **64**, 386-400.
- HELLEMANS, J., MORTIER, G., DE PAEPA, A., SPELEMAN, F. & VANDESOMPELE, J. Qbase relative quantification framework and software for management and automated analysis of real-time quantitative pcr data. *Genome Biology* (2007) **8**, R19.1-14.
- HELLMAN, L.M. & FRIED, M.G. Electrophoretic mobility shift assay (emsa) for detecting protein-nucleic acid interactions. *Nature Protocols* (2007) **2**, 1849-1861.
- HORROCKS, P., WONG, E.D., RUSSELL, K. & EMES, R.D. Control of gene expression in *plasmodium falciparum* - ten years on. *Molecular and Biochemical Parasitology* (2009) **164**, 9-25.
- IKEMOTO, N., KIM, H.S., KANAZAKI, M., UENO, Y., SHUTO, S., MATSUDA, A., *et al.* Antisense oligodeoxynucleotides: Useful tool for search and assessment of new targets for anti-malarial drugs. *Nucleic Acid Symposium Series* (1999) **42**, 89-90.
- ISSAR, N., RALPH, S.A., MANCIO-SILVA, L., KEELING, C. & SCHERF, A. Differential sub-nuclear localisation of repressive and activating histone methyl modifications in *p. Falciparum*. *Microbes and Infection* (2009) **11**, 403-407.
- JÄNNE, O., BARDIN, C.W. & JACOB, S.T. DNA-dependent rna polymerases i and ii from kidney. Effect of polyamines on the in vitro transcription of DNA and chromatin. *Biochemistry* (1975) **14**, 3589-3597.
- JAZWINSKI, S.M. Participation of atp in the binding of a yeast replicative complex to DNA. *The Biochemical Journal* (1987) **246**, 213-219.

- JIANG, Y., ROBERTS, S.C., JARDIM, A., CARTER, N.S., SHIH, S., ARIYANAYAGAM, M., *et al.* Ornithine decarboxylase gene deletion mutants of *leishmania donovani*. *Journal of Biological Chemistry* (1999) **274**, 3781-3788.
- JINEK, M. & DOUDNA, J.A. A three-dimensional view of the molecular machinery of rna interference. *Nature* (2009) **457**, 405-412.
- JOANNIN, N., ABHIMAN, S., SONNHAMMER, E.L. & WAHLGREN, M. Sub-grouping and sub-functionalization of the rifin multi-copy protein family. *BMG Genomics* (2008) **9**.
- JOVANOVIC, M. & DYNAN, W.S. Terminal DNA structure and atp influence binding parameters of the DNA-dependent protein kinase at an early step prior to DNA synapsis. *Nucleic Acids Research* (2006) **34**, 1112-1120.
- KANG, S. & HONG, Y.S. Rna interference in infectious tropical diseases. *The Korean Journal of Parasitology* (2008) **46**, 1-15.
- KAPPES, B., DOERIG, C.D. & GRAESER, R. An overview of *plasmodium* protein kinases. *Parasitology Today* (1999) **15**, 449-454.
- KEYS, S., KRAEMER, S.M. & SMITH, J.D. Antigenic variation in *plasmodium falciparum*: Gene organization and regulation of the *var* multigene family. *Eukaryotic Cell* (2007) **6**, 1511-1520.
- KINNEY, J., LEIPPE, D., LEWIS, K., LYKE, B., MANDREKAR, M. & SHULTZ, J. The dnaquant™ DNA quantitation system for sensitive detection of double-stranded DNA. *Promega Corporation Notes* (1999) **73**.
- KIRK, K. Membrane transport in the malaria-infected erythrocyte. *Physiological Reviews* (2001) **81**, 495-537.
- KOCKEN, C.H., OZWARA, H., VAN DER WEL, A., BEETSMA, A.L., MWENDA, J.M. & THOMAS, A.W. *Plasmodium knowlesi* provides a rapid in vitro and in vivo transfection system that enables double-crossover gene knockout studies. *Infection and Immunity* (2002) **70**, 655-660.
- KOZAK, M. Regulation of translation via mrna structure in prokaryotes and eukaryotes. *Gene* (2005) **361**, 13-37.
- KRAEMER, S.M. & SMITH, J.D. A family affair: *Var* genes, pfemp1 binding, and malaria disease. *Current Opinion in Microbiology* (2006) **9**, 374-380.
- KUBISTA, M., ANDRADE, J.M., BENGTSSON, M., FOROOTAN, A., JONAK, J., LIND, K., *et al.* The real-time polymerase chain reaction. *Molecular Aspects of Medicine* (2006) **27**, 95-125.
- KUMAR, N., CHA, G., PINEDA, F., MACIEL, J., HADDAD, D., BHATTACHARYYA, M., *et al.* Molecular complexity of sexual development and gene regulation in *plasmodium falciparum*. *International Journal for Parasitology* (2004) **34**, 1451-1458.
- KUMAR, R., ADAMS, B., OLDENBURG, A., MUSIYENKO, A. & BARIK, S. Characterisation and expression of a pp1 serine/threonine protein phosphatase (pfpp1) from the malaria parasite, *plasmodium falciparum*: Demonstration of its essential role using rna interference. *Malaria Journal* (2002) **1**.

- LAROCHE, K., BERGERON, M.J., LECLERC, S. & GUÉRIN, S.L. Optimization of competitor poly(di-dc). Poly(di-dc) levels is advised in DNA-protein interaction studies involving enriched nuclear proteins. *Biotechniques* (1996) **20**, 439-444.
- LASONDER, E., ISHIHAMA, Y., ANDERSEN, J.S., VERMUNT, A.M.W., PAIN, A., SAUERWEIN, R.W., *et al.* Analysis of the *plasmodium falciparum* proteome by high-accuracy mass spectrometry. *Nature* (2002) **419**, 537-542.
- LAVAZEC, C., SANYAI, S. & TEMPLETON, T.J. Expression switching in the *stevor* and *pfmc-2tm* superfamilies in *plasmodium falciparum*. *Molecular Microbiology* (2007) **64**, 1621-1634.
- LAW, P.J., CLAUDEL-RENARD, C., JOUBERT, F., LOUW, A.I. & BERGER, D.K. Madiba: A web server toolkit for biological interpretation of *plasmodium* and plant gene clusters. *BMC Genomics* (2008) **9**, 1-11.
- LE ROCH, K.G., JOHNSON, J.R., FLORENS, L., ZHOU, Y., SANTROSYAN, A., GRAINGER, M., *et al.* Global analysis of transcript and protein levels across the *plasmodium falciparum* life cycle. *Genome Research* (2004) **14**, 2308-2318.
- LEFEVER, S., HELLEMANS, J., PATTYN, F., PRZYBYLSKI, D.R., TAYLOR, C., GEURTS, R., *et al.* Rdml: Structured language and reporting guidelines for real-time quantitative pcr data. *Nucleic Acids Research* (2009) **37**, 2065-2069.
- LEUNG, R.K.M. & WHITTAKER, P.A. Rna interference: From gene silencing to gene-specific therapeutics. *Pharmacology and Therapeutics* (2005) **107**.
- LI, F., SONBUCHNER, L., KYES, S., EPP, C. & DEITSCH, K.W. Nuclear non-coding rna's are transcribed from the centromeres of *plasmodium falciparum* and are associated with centromeric chromatin. *Journal of Biological Chemistry* (2008) **283**, 5692-5698.
- LI, W., MO, W., SHEN, D., SUN, L., WANG, J., LU, S., *et al.* Yeast model uncovers dual roles of mitochondria in the action of artemisinin. *Public Library of Science: Genetics* (2005) **1**, 329-334.
- LI, Y.L., YE, F., HUA, Y., LU, W.G. & XIE, X. Identification of suitable reference genes for gene expression studies of human serous ovarian cancer by real-time polymerase chain reaction. *Analytical Biochemistry* (2009) **394**, 110-116.
- LILLEY, D.M.J. (1995). DNA-protein structural interactions, pp. 1-48.
- LOIKKANEN, I. (2005). Polyamine homeostasis-cellular responses to perturbation of polyamine biosynthetic enzymes, University of Oulu.
- LOPEZ-RUBIO, J.J., RIVIERE, L. & SCHERF, A. Shared epigenetic mechanisms control virulence factors in protozoan parasites. *Current Opinion in Microbiology* (2007) **10**, 560-568.
- MACLEAN, N. (1989). *Genes and gene regulation*.
- MAIR, G., BRAKS, J.A.M., GARVER, L.S., WIEGAND, G.C.A.G., HALL, N., DIRKS, R.W., *et al.* Regulation of sexual development of *plasmodium* by translational repression. *Science* (2006) **313**, 667-669.

- MALHOTRA, P., DASARADHI, P.V.N., KUMAR, A., MOHMED, A., AGRAWAL, N., BHATNAGAR, R.K., *et al.* Double-stranded rna-mediated gene silencing of cysteine proteases (falcipain-1 and -2) of *plasmodium falciparum*. *Molecular Biology* (2002) **45**, 1245-1254.
- MAQUAT, L.E. Nonsense-mediated mrna decay: Splicing, translation and mrnp dynamics. *Nature Reviews* (2004) **5**, 89-99.
- MARTIN, R.E. & KIRK, K. Transport of the essential nutrient isoleucine in human erythrocytes infected with the malaria parasite *plasmodium falciparum*. *Blood* (2007) **109**, 2217-2224.
- MARTY, A.J., J.K., T., DUFFY, M.F., VOSS, T.S., COWMAN, A.F. & CRABB, B.S. Evidence that *plasmodium falciparum* chromosome end clusters are cross-linked by protein and are the sites of both virulence gene silencing and activation. *Molecular Microbiology* (2006) **62**, 72-83.
- MATTICK, J.S. Non-coding rna's: The architects of eukaryotic complexity. *European Molecular Biology Organization* (2001) **2**, 986-991.
- MCENTEE, K., WEINSTOCK, G.M. & LEHMAN, I.R. Binding of the reca protein of *escherichia coli* to single- and double-stranded DNA. *The Journal of Biological Chemistry* (1981) **256**, 8835-8844.
- MCRROBERT, L. & MCCONKEY, G.A. Rna interference (rna) inhibits growth of *plasmodium falciparum*. *Molecular and Biochemical Parasitology* (2002) **119**, 273-278.
- MEISSNER, M. & SOLDATI, D. The transcription machinery and the molecular toolbox to control gene expression in *toxoplasma gondii* and other protozoan parasites. *Microbes and Infection* (2005) **7**, 1376-1384.
- MENETSKI, J.P. & KOWALCZYKOWSKI, S.C. Interaction of reca protein with single-stranded DNA: Quantitative aspects of binding affinity modulation by nucleotide co-factors. *Journal of Molecular Biology* (1985) **181**, 281-295.
- MERRICK, C.J. & DURAISINGH, M. Heterochromatin-mediated control of virulence gene expression. *Molecular Microbiology* (2006) **62**, 612-620.
- MEYER, S., TEMME, C. & WAHLE, E. Messenger rna turnover in eukaryotes: Pathways and enzymes. *Critical Reviews in Biochemistry and Molecular Biology* (2004) **39**, 197-216.
- MILITELLO, K.T., DODGE, M., BETHKE, L. & WIRTH, D.F. Identification of regulatory elements in the *plasmodium falciparum* genome. *Molecular and Biochemical Parasitology* (2004) **134**, 75-88.
- MOSS, T. (2001). *Methods in molecular biology- DNA-protein interactions: Principles and protocols*, 2nd edition. Humana Press.
- MUKHERJEE, S., BERGER, M.F., JONA, G., WANG, X.S., MUZZEY, D., SNYDER, M., *et al.* Rapid analysis of the DNA-binding specificities of transcription factors with DNA microarrays. *Nature Genetics* (2004) **36**, 1331-1339.
- MULLER, I.B., DAS GUPTA, R., LUERSEN, K., WRENGER, C. & WALTER, R.D. Assessing the polyamine metabolism of *plasmodium falciparum* as chemotherapeutic target. *Molecular and Biochemical Parasitology* (2008) **160**, 1-7.

- NEIDLE, S. (2002). *Nucleic acid structure and recognition*. Oxford University Press.
- NEWBOLD, C.I. Antigenic variation in *plasmodium falciparum*: Mechanisms and consequences. *Current Opinion in Microbiology* (1999) **2**, 420-425.
- NEWBURY, S.F. Control of mrna stability in eukaryotes. *Biochemical Society Transactions* (2006) **34**, 30-34.
- NIMONKAR, A.V. & BOEHMER, P.E. The herpes simplex virus type-1 single-strand DNA-binding protein (icp8) promotes strand invasion. *Journal of Biological Chemistry* (2003) **278**, 9678-9682.
- NKRUMAH, L.J., RIEGELHAUPT, P.M., MOURA, P., JOHNSON, D.J., PATEL, J., HAYTON, K., *et al.* Probing the multifactorial basis of *plasmodium falciparum* quinine resistance: Evidence for a strain-specific contribution of the sodium-proton exchanger pfnhe. *Molecular and biochemical parasitology* (2009) **2**, 122-131.
- NOONPAKDEE, W., POTHIKASIKORN, J., NIMITSANTIWONG, W. & WILAIRAT, P. Inhibition of *plasmodium falciparum* proliferation in vitro by antisense oligodeoxynucleotides against malarial topoisomerase ii. *Biochemical and Biophysical Research Communications* (2003) **302**, 659-664.
- NZILA, A. Inhibitors of de novo folate enzymes in *plasmodium falciparum*. *Drug Discovery Today* (2006) **11**, 939-944.
- OAKLEY, M.S.M., KUMAR, S., ANANTHARAMAN, V., ZHENG, H., MAHAJAN, B., HAYNES, J.D., *et al.* Molecular factors and biochemical pathways induced by febrile temperature in intra-erythrocytic *plasmodium falciparum* parasites. *Infection and Immunity* (2007) **75**, 2012-2025.
- OLIVIERI, A., SILVESTRINI, F., SANCHEZ, M. & ALANO, P. A 140-bp at-rich sequence mediates positive and negative transcriptional control of a *plasmodium falciparum* developmentally regulated promoter. *International Journal for Parasitology* (2008) **38**, 299-312.
- OSTA, M., GANNOUN-ZAKI, L., BONNEFOY, S., ROY, C. & VIAL, H.J. A 24bp *cis*-acting element essential for the transcriptional activity of *plasmodium falciparum* cdp-diacylglycerol synthase gene promoter. *Molecular and Biochemical Parasitology* (2002) **121**, 87-98.
- PARKER, R. & SONG, H. The enzymes and control of eukaryotic mrna turnover. *Nature Structural and Molecular Biology* (2004) **11**, 121-127.
- POUVELL, B., SPIEGEL, R., HSIAO, L., HOWARD, R.J., THOMAS, R.L., THOMAS, A.P., *et al.* Direct access to serum macromolecules by intra-erythrocytic malaria parasites. *Nature* (1991) **353**, 73-75.
- RALPH, S.A., SCHEIDIG-BENATAR, C. & SCHERF, A. Antigenic variation in *plasmodium falciparum* is associated with movement of *var* loci between subnuclear locations. *Proceedings of the National Academy of Science of the USA* (2005a) **102**, 5414-5419.
- RALPH, S.A. & SCHERF, A. The epigenetic control of antigenic variation in *plasmodium falciparum*. *Current Opinion in Microbiology* (2005b) **8**, 434-440.

- RANDO, O.J. & AHMAD, K. Rules and regulation in the primary structure of chromatin. *Current Opinion in Microbiology* (2007) **19**, 250-256.
- RAPPAPORT, E., MISIURA, K., AGRAWAL, S. & ZAMECNIK, P. Antimalarial activities of oligonucleotide phosphorothioate in chloroquine-resistant *plasmodium falciparum*. *Proceedings of the National Academy of Science of the USA* (1992) **89**, 8577-8580.
- RASTI, N., WAHLGREN, M. & CHEN, Q. Molecular aspects of malaria pathogenesis. *FEMS Immunology and Medical Microbiology* (2004) **41**, 9-26.
- RAYBURN, E.R. & ZHANG, R. Antisense, rna, and gene silencing strategies for therapy: Mission possible or impossible? *Drug Discovery Today* (2008) **13**, 513-521.
- REGUERA, R.M., TEKWANI, B.L. & BALANA-FOUNCE, R. Polyamine transport in parasites: A potential target for new antiparasitic drug development. *Comparative Biochemistry and Physiology* (2005) **140**, 151-164.
- RHO, S., KIM, S.J., LEE, S.C., CHANG, J.H., KANG, H. & CHOI, J. Colorimetric detection of ssdna in a solution. *Current Applied Physics* (2009) **9**, 534-537.
- RIDLEY, R.G. To kill a parasite. *Nature* (2003) **424**, 887-889.
- ROBERTS, S.C., JIANG, Y., JARDIM, A., CARTER, N.S., HEBY, O. & ULLMAN, B. Genetic analysis of spermidine synthase from *leishmania donovani*. *Molecular and biochemical Parasitology* (2001) **115**, 217-226.
- ROBERTS, S.C., SCOTT, J., GASTEIER, J.E., JIANG, Y., BROOKS, B., JARDIM, A., *et al.* S-adenosylmethionine decarboxylase from *leishmania donovani*. Molecular, genetic, and biochemical characterization of null mutants and overproducers. *Journal of Biological Chemistry* (2002) **277**, 5902-5909.
- RUSSO, I., OKSMAN, A., VAUPEL, B. & GOLDBERG, D.E. A calpain unique to alveolates is essential in *plasmodium falciparum* and its knockdown reveals an involvement in pre-s-phase development. *Proceedings of the National Academy of Science of the USA* (2009) **106**, 1554-1559.
- RYCHLIK, W., SPENCER, W.J. & RHOADS, R.E. Optimization of the annealing temperature for DNA amplification in vitro. *Nucleic Acids Research* (1990) **18**, 6409-6412.
- SADHALE, P., VERMA, J. & NAOREM, A. Basal transcription machinery: Role in regulation of stress response in eukaryotes. *Journal of Biosciences* (2007) **32**, 569-578.
- SCHERF, A. A greedy promoter controls malarial var-iations. *Cell* (2006) **124**, 251-253.
- SCHERF, A., LOPEZ-RUBIO, J.J. & RIVIERE, L. Antigenic variation in *plasmodium falciparum*. *Annual Review of Microbiology* (2008) **62**, 445-470.
- SCHRODER, E., JONSSON, T. & POOLE, P. Hydroxyapatite chromatography: Altering the phosphate-dependent elution profile of protein as a function of ph. *Analytical Biochemistry* (2003) **313**, 176-178.
- SHERMAN, I.W., EDA, S. & WINOGRAD, E. Cytoadherence and sequestration in *plasmodium falciparum*: Defining the ties that bind. *Microbes and Infection* (2003) **5**, 897-909.

- SHOCK, J.L., FISCHER, K.F. & DERISI, J.L. Whole genome analysis of mRNA decay in *plasmodium falciparum* reveals a global lengthening of mRNA half-life during the intra-erythrocytic development cycle. *Genome Biology* (2007) **8**, R134.0-134.12.
- SIAU, A., TOURÉ, F.S., OUWE-MISSI-OUKEM-BOYER, O., CICÉRON, L., MAHMOUDI, N., VAQUERO, C., *et al.* Whole-transcriptome analysis of *plasmodium falciparum* field isolates: Identification of new pathogenicity factors. *Journal of Infectious Diseases* (2007) **196**, 1603-1612.
- SMALL, I. Rnai for revealing and engineering plant gene functions. *Current Opinion in Biotechnology* (2007) **18**, 148-153.
- SMITH, J.D., GAMAIN, B., BARUCH, D.I. & KYES, S. Decoding the language of *var* genes and *plasmodium falciparum* sequestration. *Trends in Parasitology* (2001) **17**, 538-545.
- SRIWILAJAROEN, N., BOONMA, S., ATTASART, P., POTHIKASIKORN, J., PANYIM, S. & NOONPAKDEE, W. Inhibition of *plasmodium falciparum* proliferation in vitro by double-stranded RNA directed against malaria histone deacetylase. *Biochemical and Biophysical Research Communications* (2009) **381**, 144–147.
- STARK, H.C., WEINBERGER, O. & WEINBERGER, J. Common double- and single-stranded DNA binding factor for a sterol regulatory element. *Proceedings of the National Academy of Science of the USA* (1992) **89**, 2180-2184.
- SWITZER, R.C., MERRILL, C.R. & SHIFRIN, S. A highly sensitive silver stain for detecting proteins and peptides in polyacrylamide gels. *Analytical Biochemistry* (1979) **98**, 231-237.
- THAM, W., PAYNE, P.D., BROWN, G.V. & ROGERSON, S.J. Identification of basic transcriptional elements required for *rif* gene transcription. *International Journal for Parasitology* (2007) **37**, 605-615.
- THELLIN, O., ZORZI, W., LAKAYE, B., DE BORMAN, B., COUMANS, B., HENNEN, G., *et al.* Housekeeping genes as internal standards: Use and limits. *Journal of Biotechnology* (1999) **75**, 291-295.
- THOMAS, T. & THOMAS, T.J. Polyamine metabolism and cancer. *Journal of Cellular and Molecular Medicine* (2003) **7**, 113-126.
- TOMPA, M., LI, N., BAILEY, T.L., CHURCH, G.M., DE MOOR, B., ESKIN, E., *et al.* Assessing computational tools for the discovery of transcription factor binding sites. *Nature Biotechnology* (2005) **23**, 137-144.
- TRAGER, W. & JENSEN, J.B. Human malaria parasites in continuous culture. *Science* (1976) **193**, 673-675.
- TRENHOLME, K.R. & GARDINER, D.L. A sticky problem in malaria. *Biologist* (2004) **51**, 37-40.
- TRIGLIA, T., WANG, P., SIMS, P.F., HYDE, J.E. & COWMAN, A.F. Allelic exchange at the endogenous genomic locus in *plasmodium falciparum* proves the role of dihydropteroate synthase in sulfadoxine-resistant malaria. *The EMBO Journal* (1998) **17**, 3807-3815.

- TUTEJA, R., PRADHAN, A. & SHARMA, S. *Plasmodium falciparum* signal peptidase is regulated by phosphorylation and required for intra-erythrocytic growth. *Molecular and Biochemical Parasitology* (2008) **157**, 137-147.
- ULLU, E., TSCHDI, C. & CHAKRABORTY, T. Rna interference in protozoan parasites. *Cellular Microbiology* (2004) **6**, 509-519.
- VALENCIA-SANCHEZ, M.A., LUI, J., HANNON, G.J. & PARKER, R. Control of translation and mrna degradation by mirnas and sirnas. *Genes and Development* (2006) **20**, 515-524.
- VAN BRUMMELEN, A.C., OLSZEWSKI, K.L., WILINSKI, D., LLINÁS, M., LOUW, A.I. & BIRKHOLTZ, L.M. Co-inhibition of *plasmodium falciparum* s-adenosylmethionine decarboxylase/ornithine decarboxylase reveals perturbation specific compensatory mechanisms by transcriptome, proteome and metabolome analysis. *Journal of Biological Chemistry* (2009) **284**, 4635-4646.
- VAN DEN HOFF, M.J.B., MOORMAN, A.F.M. & LAMERS, W.H. Electroporation in 'intracellular' buffer increases cell survival. *Nucleic Acids Research* (1992) **20**, 2902.
- VAN HOOF, A., FRISCHMEYER, P.A., DIETZ, H.C. & PARKER, R. Exosome-mediated recognition and degradation of mrnas lacking termination codon. *Science* (2002) **295**, 2262-2264.
- VOSS, T.S., HEALER, J., MARTY, A.J., DUFFY, M.F., THOMPSON, J.K., BEESON, J.G., *et al.* A *var* gene promoter controls allelic exclusion of virulence genes in *plasmodium falciparum* malaria. *Nature* (2006) **439**, 1004-1008.
- VOSS, T.S., KAESTLI, M., VOGEL, D., BOPP, S. & BECK, H.P. Identification of nuclear proteins that interact differentially with *plasmodium falciparum var* gene promoters. *Molecular Biology* (2003) **48**, 1593-1607.
- VOSS, T.S., MINI, T., JENOE, P. & BECK, H.P. *Plasmodium falciparum* possesses a cell-cycle regulated short-type replication protein a large subunit encoded by an unusual transcript. *Journal of Biological Chemistry* (2002) **277**, 17493-17501.
- VOSS, T.S., THOMPSON, J.K., WATERKYEN, J., FELGER, I., WEISS, N., COWMAN, A.F., *et al.* Genomic distribution and functional characterization of two distinct and conserved *plasmodium falciparum var* gene 5' flanking sequences. *Molecular and Biochemical Parasitology* (2000) **107**, 103 - 115.
- VOSS, T.S., TONKIN, C.J., MARTY, A.J., THOMPSON, J.K., HEALER, J., CRABB, B.S., *et al.* Alterations in local chromatin environment are involved in silencing and activation of subtelomeric *var* genes in *plasmodium falciparum*. *Molecular Microbiology* (2007) **66**, 139-150.
- WALHOUT, A.J.M. Unraveling transcription regulatory networks by protein-DNA and protein-protein interaction mapping. *Genome Research* (2006) **16**, 1445-1454.
- WALKER, J.M. (2002). *The protein protocols handbook*, 2nd edition. Humana Press.
- WALLER, K.L., MUHLE, R.A., URSOS, L.M., HORROCKS, P., VERDIER-PINARD, D., SIDHU, A.B.S., *et al.* Chloroquine resistance modulated in vitro by expression levels of the *plasmodium*

- falciparum* chloroquine resistance transporter*. *Journal of Biological Chemistry* (2003) **278**, 33593-33601.
- WANIDWORANUN, C., NAGEL, R.L. & SHEAR, H.L. Antisense oligonucleotides targeting malarial aldolase inhibit the asexual erythrocytic stages of *plasmodium falciparum*. *Molecular and Biochemical Parasitology* (1999) **102**, 91-101.
- WATERKEYN, J.G., CRABB, B.S. & COWMAN, A.F. Transfection of the human malaria parasite *plasmodium falciparum*. *International Journal for Parasitology* (1999) **29**, 945-955.
- WELLS, T.N.C., ALONSO, P.L. & GUTTERIDGE, W.E. New medicines to improve control and contribute to the eradication of malaria. *Nature Reviews: drug discovery* (2009) **8**, 879-891.
- WHAUN, J.M. & BROWN, N.D. Ornithine decarboxylase inhibition and the malaria-infected red cell: A model for polyamine metabolism and growth. *The Journal of Pharmacology and Experimental Therapeutics* (1985) **233**, 507-511.
- WILLERT, E.K. & PHILLIPS, M.A. Regulated expression of an essential allosteric activator of polyamine biosynthesis in african trypanosomes. *Public Library of Science - Pathogens* (2008) **4**, 1-12.
- WILLIAMS, M., LOUW, A.I. & BIRKHOLTZ, L. Deletion mutagenesis of large areas in *plasmodium falciparum* genes: A comparative study. *Malaria Journal* (2007) **6**, 1-9.
- WILUSZ, C.J., WORMINGTON, M. & PELTZ, S.W. The cap-to-tail guide to mrna turnover. *Nature Reviews* (2001) **2**, 237-246.
- WINTER, G., KAWAI, S., HAEGGSTRÖM, M., KANEKO, O., VON EULER, A., KAWAZU, S., *et al.* Surfin is a polymorphic antigen expressed on *plasmodium falciparum* merozoites and infected erythrocytes. *The Journal of Experimental Medicine* (2005) **201**, 1853-1863.
- WOODROW, C.J. & KRISHNA, S. Antimalarial drugs: Recent advances in molecular determinants of resistance and their clinical significance. *Cellular and Molecular Life Sciences* (2006) **63**, 1586-1596.
- WRENGER, C., LUERSEN, K., KRAUSE, T., MULLER, S. & WALTER, R.D. The *plasmodium falciparum* bifunctional ornithine decarboxylase, s-adenosylmethionine decarboxylase, enables a well balanced polyamine synthesis without domain-domain interaction. *The Journal of Biological Chemistry* (2001) **276**, 29651-29656.
- XIAO, Y., MCCLOSKEY, D.E. & PHILLIPS, M.A. Rna interference-mediated silencing of ornithine decarboxylase and spermidine synthase genes in *trypanosoma brucei* provides insight into regulation of polyamine biosynthesis. *Eukaryotic Cell* (2009) **8**, 747-755.
- YASGAN, O. & KREBS, J.E. Noncoding but nonexpendable: Transcriptional regulation by large noncoding rna in eukaryotes. *Biochemistry and Cell Biology* (2007) **85**, 484-496.
- YEKA, A., ACHAN, J., D'ALESSANDRO, U. & TALISUNA, A.O. Quinine monotherapy for treating uncomplicated malaria in the era of artemisinin-based combination therapy: An appropriate public health policy? *The Lancet infectious diseases* (2009) **9**, 448-452.

